Exploring the Interface between Endoplasmic Reticulum Stress and Oncolytic Adenoviruses



William Keith Taverner

Brasenose College

The University of Oxford

A thesis submitted for the degree of Doctor of Philosophy to the Department of Oncology, University of Oxford

Trinity Term 2019

Abstract

Oncolytic viruses represent an emerging approach to cancer therapy. However, better understanding of their interaction with the host cancer cell and approaches to enhance their efficacy are needed. Efficient protein folding is essential for normal cell function but is perturbed in many cancer types and in cells suffering viral infections, resulting in endoplasmic reticulum (ER) stress and the consequent induction of the unfolded protein response (UPR). However, the interactions between viral infection and UPR signalling are poorly understood and could potentially be exploited for enhancing therapeutic effect.

Here, we investigate the effect of chemically induced endoplasmic reticulum (ER) stress on the activity of the chimeric group B oncolytic adenovirus Enadenotucirev, its closely related parental virus Ad11p, and the archetypal group C wild-type adenovirus Ad5. We find that EnAd and Ad11p induce ER stress much more powerfully than Ad5 infection. We show that treatment of colorectal and ovarian cancer cell lines with thapsigargin or ionomycin caused an influx of Ca^{2+}, leading to an upregulation in E1A transcript and protein levels. Increased E1A protein levels, in turn, increased levels of expression of the E2B viral DNA polymerase, genome replication, late viral protein expression, infectious virus particle production and cell killing during Enadenotucirev and Ad11p but not Ad5 infection.

The engineering of an EnAd virus armed with the ability to genetically knockdown the target of thapsigargin inhibition however did not result in enhanced replication. We then show that the effect of thapsigargin and ionomycin treatment was not due to the induction of ER stress, but rather the influx of extracellular Ca^{2+} and consequent increase in protein kinase C activity.

These results underscore the importance of Ca^{2+} homeostasis during adenoviral infection, indicate a novel signalling pathway between protein kinase C and E1A, and raise the possibility of using Ca^{2+} flux-modulating agents in the manufacture and potentiation of oncolytic virotherapies.

Declaration of Authentication

The work presented in this thesis is wholly my own, any contributions made by others have been acknowledged accordingly. The content submitted here does not form part of another thesis in this or at any other university. This work was carried out under the supervision of Professor Leonard Seymour, Dr Janet Lei-Rossmann and Professor Tom Brown at the Department of Oncology, Medical Science Division, University of Oxford.

William K Taverner

Publication notes

The work presented in chapters three and five of this thesis was accepted for publication in *Molecular Therapy – Oncolytics* (Taverner et al., 2019).

- Taverner, W.K., E.J. Jacobus, J. Christianson, B. Champion, A.W. Paton, J.C. Paton, W. Su, R. Cawood, L.W. Seymour, and J. Lei-Rossmann. 2019. Calcium influx caused by ER stress inducers enhances oncolytic adenovirus Enadenotucirev replication and killing through PKCα activation. *Mol. Ther. - Oncolytics*. doi:10.1016/J.OMTO.2019.09.003.

Other contributions to published work over the course of this DPhil:

- Lei, J., E.J. Jacobus, W.K. Taverner, K.D. Fisher, S. Hemmi, K. West, L. Slater, F. Lilley, A. Brown, B. Champion, M.R. Duffy, and L.W. Seymour. 2018. Expression of human CD46 and trans-complementation by murine adenovirus 1 fails to allow productive infection by a group B oncolytic adenovirusin murine cancer cells. *J. Immunother. Cancer*. 6. doi:10.1186/s40425-018-0350-x.

- Dyer, A., R. Baugh, S.L. Chia, S. Frost, Iris, E.J. Jacobus, H. Khalique, T.D. Pokrovska, E.M. Scott, W.K. Taverner, L.W. Seymour, and J. Lei. 2019a. Turning cold tumours hot: oncolytic virotherapy gets up close and personal with other therapeutics at the 11th Oncolytic Virus Conference. *Cancer Gene Ther*. 26:59–73. doi:10.1038/s41417-018-0042-1.

- Scott, E.M., E.J. Jacobus, B. Lyons, S. Frost, J.D. Freedman, A. Dyer, H. Khalique, W.K. Taverner, A. Carr, B.R. Champion, K.D. Fisher, L.W. Seymour, and M.R. Duffy. 2019. Bi- and tri-valent T cell engagers deplete tumour-associated macrophages in cancer patient samples. *J. Immunother. Cancer*. 7:320. doi:10.1186/s40425-019-0807-6.

Acknowledgements

This DPhil has been a pleasure to undertake, and whilst it has been challenging at times, it has been made easier by the support of so many bright and talented people along the way. First and foremost, I must thank my supervisors for their mentorship over these four years. Janet Lei-Rossmann has been a superb supervisor and friend and has kept me on the right track throughout my project, working tirelessly to keep the lab in shape and making it a great place to work. I know she's an inspiration to not just myself but to many of us. Janet it has privilege to be your first DPhil student, thank you. To Professor Len Seymour I will always be grateful for giving me the opportunity to join the group, and for all the invaluable support and guidance along the way. To professor Tom Brown thank you for sharing your expertise, I learnt a lot during my brief stint in your group.

I also wish to thank Arthur Dyer for his herculean effort keeping the lab in order, and him and Egon Jacobus for teaching and helping me so much particularly at the beginning of my project, it has always been hugely appreciated. I am grateful to Dr John Christianson for the many interesting discussions and for informing my thinking regarding cell stress. Special mentions also to Dr Emma Fenech, Dr Arun Shivalingham and Weiheng Su for all their assistance. To Sally Frost, thank you for helping me out when I've needed it and for being such a great friend over the three years. The same goes for Ellie Scott and Richard Baugh (DB, Brucie, Deborah and Theo), Tzveta Pokrovska, Brian Lyons, Hena Khalique, Joshua Freedman, Flurin Caviezel, Amanda Chapman and all of Len's Angels past and present, thank you for your friendship and support. I am grateful of course to my family who have supported me in pursuing this DPhil. Thank you to my Dad for kindling in me a love of science, to my Mum for *everything*, and to Ben, Sophie and Dani.

Last but not least thank you to Anna, you make it all worthwhile.

Table of Contents

Abstract 3

Declaration of Authentication 5

Publication notes 6

Acknowledgements 7

Table of Contents 8

List of Abbreviations 15

1 Introduction 20

1.1 Cancer and its treatment 20

1.2 Oncolytic virotherapy 21

1.2.1 Introduction to oncolytic virotherapy 21

1.2.2 Rational design of oncolytic viruses 25

1.2.3 Directed evolution of oncolytic viruses 30

1.3 Oncolytic adenovirus 32

1.3.1 Structure 33

1.3.2 Life cycle 37

1.3.3 Enadenotucirev 42

1.4 Role of calcium signalling and protein kinase C 45

1.5 Oncolytic adenovirus and RNA interference 47

1.6 ER stress and the unfolded protein response. 51

1.6.1 Introduction to ER stress and UPR signalling 51

1.6.2 ER stress in cancer 56

1.6.3 ER stress during viral infections 58

1.6.4 ER stress in oncolytic virotherapy 59

1.7 Thesis overview and hypothesis 61

1.7.1 Overview 61

1.7.2 Hypothesis 63

2 Materials and Methods 64

2.1 Molecular Biology 64

2.1.1 Production of heat shock competent *E.coli* cells 64

2.1.2 Bacterial transformation 64

2.1.3 DNA purification and precipitation 65

2.1.4 DNA restriction digests 66

2.1.5 Polymerase chain reaction (PCR) amplification 66

2.1.6 Agarose gel electrophoresis 67

2.1.7 Quantification of purified DNA 67

2.1.8 DNA ligation 67

2.1.9 Gibson assembly 68

2.2 Cell Culture 69

2.2.1 Maintenance of cell lines 69

2.2.2 Cryopreservation of cells and cell recovery 70

2.2.3 DNA transfections 70

2.2.4 Virus infections 70

2.2.5 siRNA transfections 71

2.2.6 Production of lentiviral constructs 72

2.2.7 Generation of cell lines by lentivirus infection 72

2.3 RNA work 73

2.3.1 RNA extraction 73

2.3.2 Reverse transcription 73

2.3.3 Assessment of XBP1 splice status 74

2.4 Quantitative PCR 74

2.4.1 Quantification of viral genomes 74

2.4.2 Reverse transcription PCR 75

2.5 Evaluation of cell cytotoxicity 76

2.5.1 Cell killing xCELLigence assay 76

2.5.2 MTS assay 77

2.6 Western blotting 77

2.6.1 Sample preparation, PAGE and transfer to nitrocellulose membrane 77

2.6.2 Immunoblot and detection 78

2.7 Adenovirus production 80

2.7.1 Production of virus stocks 80

2.7.2 Production of Recombinant Engineered Adenoviruses 83

2.8 Measuring infectious virus particles by $TCID_{50}$ 86

2.9 Luciferase assay 87

2.10 Fluo-8 calcium flux assay 87

2.11 Flow cytometry 88

2.12 Celigo cell imaging 89

2.13 Statistics 91

3 Chemical induction of ER stress and adenoviral infection 92

3.1 Introduction 92

3.2 Chapter aims 94

3.3 Results 94

3.3.1 Measuring the induction of ER stress in cancer cell lines 94

3.3.2 Adenovirus infection induces significant ER stress 101

3.3.3 Thapsigargin treatment increases early and late viral protein expression in EnAd, Ad11p but not Ad5 infection 104

3.3.4 Thapsigargin treatment accelerates the onset of DNA replication in EnAd and Ad11p, but not Ad5 infection 108

3.3.5 Thapsigargin treatment boosts production of EnAd and Ad11p but not Ad5 infectious virus particles. 109

3.3.6 Thapsigargin treatment enhances oncolytic virus induced cell killing by EnAd and Ad11p but not Ad5. 110

3.3.7 Thapsigargin treatment increases EnAd E1A expression 112

3.3.8 Ad5 E1A protein levels are enhanced by thapsigargin and ionomycin .. 113

3.3.9 E1A overexpression does not enhance Ad5 activity in DLD-1 cells 115

3.3.10 UPR induction is not responsible for the accelerated onset of EnAd/Ad11p replication 116

3.4 Chapter conclusions 123

3.5 Chapter discussion 124

4 Targeted knockdown of SERCA2 channels by virally encoded shRNA 127

4.1 Introduction 127

4.2 Chapter aims 129

4.3 Results 130

4.3.1 siRNA knockdown of SERCA2 channels enhances EnAd activity in SK-OV-3 cells 130

4.3.2 Expression of a plasmid-encoded shRNA construct successfully knocks down SERCA2 protein 131

4.3.3 Engineering of an EnAd variant encoding an shRNA expression cassette for the targeted knockdown of SERCA2 135

4.3.4 EnAd_U6-sh1748 achieves SERCA2 knockdown during infection of SK-OV-3 cells 140

4.3.5 EnAd_U6-sh1748 does not display enhanced viral replication 141

4.3.6 EnAd_U6-sh1748 does not show increased virus particle production ... 142

4.3.7 EnAd_U6-sh1748 does not show increased cell killing 143

4.4 Chapter conclusions 145

4.5 Chapter discussion 145

5 Calcium influx enhances oncolytic adenovirus activity through activation of PKCα. 150

5.1 Introduction 150

5.2 Chapter aims 153

5.3 Results 154

5.3.1 Thapsigargin and ionomycin treatments induce calcium influx 154

5.3.2 NAADP regulated lysosomal calcium release is not important in adenoviral lysosomal escape 156

5.3.3 Extracellular calcium is instrumental in the enhancing effect of thapsigargin and ionomycin 158

5.3.4 Extracellular calcium influx drives upregulated E1A expression 159

5.3.5 Calcium influx occurs through store-operated calcium channels 162

5.3.6 Thapsigargin treatment induces PKC phosphorylation 164

5.3.7 PKC activity mediates enhanced EnAd activity 167

5.3.8 Knockdown of PKCα abrogates the enhancing effect of thapsigargin on virus activity. 170

5.4 Chapter conclusion 172

5.5 Chapter discussion 173

6 Final discussion 176

6.1 Overview of this thesis 176

6.2 Adenovirus-induced ER stress 178

6.3 Differences in response of EnAd/Ad11p and Ad5 to ER stress-inducing chemicals 181

6.4 Mechanism of enhancement of virus replication 184

6.5 Improving arming of EnAd with shRNA expression constructs 189

6.6 Concluding remarks 191

7 References 193

8 Appendices 238

8.1 Materials 238

8.2 Recombinant adenovirus 240

8.3 DNA sequences 241

List of Abbreviations

/: per

3’ or 5’: three or five prime end of a DNA/RNA molecule

µ: Micro

Ad: adenovirus

ADP: adenovirus death protein

AdPol: Adenovirus polymerase

AML: acute myeloid leukaemia

ANOVA: analysis of variance

ATF: activating transcription factor

BAPTA: 1,2-bis(o-aminophenoxy)ethane-N,N,N′,N′-tetraacetic acid

bp: basepair

BCA: bicinchoninic acid

CML: chronic myeloid leukaemia

Ca^{2+}: calcium

CAR: coxsackievirus and adenovirus receptor

CD: cluster of differentiation

cDNA: coding DNA

CHOP: CCAAT-enhancer-binding protein homologous protein

CI: cell index

CMV: cytomegalovirus

CPE: cytopathic effect

CRAC: calcium release activated channel

Da: daltons

DAG: diacylglycerol

DEPC: Diethyl pyrocarbonate

DMEM: Dulbecco's modified eagle medium

DMSO dimethyl Sulphoxide

DNA: deoxyribonucleic acid

ds: double stranded

E: early adenovirus gene

EnAd: enadenotucirev

EDTA: ethylenediamine tetra-acetic acid

EIF: Eukaryotic initiation factor

ER: endoplasmic reticulum

ERAD: endoplasmic reticulum

FBS: fetal bovine serum

FDA: food & drug administration

G: grams

GADD: growth arrest and DNA damage-inducible protein

GAPDH: Glyceraldehyde 3-phosphate dehydrogenase

GBF-1: Golgi-specific brefeldin A-resistance guanine nucleotide exchange factor

GCA: golgicide A

GFP: green fluorescent protein

GM-CSF: Granulocyte-macrophage colony-stimulating factor

GRP: glucose regulated protein

HEPES: 4-(2-hydroxyethyl)-1-piperazineethanesulfonic acid

HEK293: human embryonic kidney cells

HSV-1: Human herpes simplex virus type 1

HRP: horseradish peroxidase

IFN: interferon

IgG: immunoglobulin isotype G

Im: ionomycin

IP_3: inositol trisphosphate

IP_3R: inositol trisphosphate receptor

IRE1: inositol requiring enzyme 1

ITR: inverted terminal repeat

IV: intravenous

k: Kilo

kb: kilobase

L: late adenovirus gene

LAMP3: Lysosome-associated membrane glycoprotein 3

M: molar

MFI: median fluorescence intensity

MHC: major histocompatibility 1

miRNA: microRNA

miviRNA: virus associated RNA

MLP: major late promoter

mRNA: messenger RNA

mTOR: mammalian target of rapamycin

MTS: 3-(4,5-Dimethylthiazol-2-yl)-5-(3-carboxymethoxyphenyl)-2-(4-sulfophenyl)-2H-tetrazolium

N/A: not applicable

NDV: Newcastle disease virus

ng: nanograms

NF-κB: nuclear factor kappa-light-chain-enhancer of activated B cells

NT: non-target

OD: optical density

ORF: open reading frame

OV: oncolytic virus

PBS: phosphate buffered saline

PCR: polymerase chain reaction

PERK: PKR-like endoplasmic reticulum kinase

PGK: phosphoglycerate kinase

p.i.: post-infection

PKC: protein kinase C

PKR: protein kinase R

PMA: Phorbol myristate acetate

pRB: retinoblastoma protein

pTP: pre-terminal protein

RCF: relative centrifugal force

RGD: Arginylglycylaspartic acid

RIDD: regulated IRE1-dependent decay

RISC: RNA induced silencing complex

RNA: ribonucleic acid

RPM: revolutions per minute

RyRs: Ryanodine receptors

SA: splice acceptor

SDS: sodium dodecyl sulfate

SEM: standard error of mean

SERCA: sarco/endoplasmic reticulum calcium-ATPase

shRNA: small hairpin RNA

siRNA: small interfering RNA

SOC: Super Optimal broth with Catabolite repression

ss: single stranded

SubAB: subtilase cytotoxin

TBS: tris-buffered saline

TCID: tissue culture infection dose

TFB: transformation buffer

Tg: thapsigargin

Tm: tunicamycin

TP: terminal protein

TPC: two-pore channel

TPL: tripartite leader

T-Vec: talimogene laherparepvec

UPR: unfolded protein response

VPC: virus particles/cell

wt: wild-type

x: multiplied by

VA: virus associated

VEGF: vascular endothelial growth factor

VSV: vesicular stomatitis virus

WB: western blot

XBP1: x-box binding protein 1

1 Introduction

1.1 *Cancer and its treatment*

Cancer is the name given to a group of related diseases which are characterised by abnormal and uncontrolled cell division and a propensity to invade other tissues (Hanahan & Weinberg, 2011). A genetic disease, it is caused by mutations in the cell's DNA that compromise the control of processes regulating a number of cellular events including cell division and death. Cancer represents a major health burden, with the lifetime risk of developing cancer for people born in the United Kingdom after 1960 now at over 50% (Ahmad et al., 2015). Overall cancer incidence in the UK has risen by 12% since the 1990s (Cancer Research UK, 2019), and is expected to continue to rise over the course of the coming decades due to a growing and ageing population (Smittenaar et al., 2016). However, thanks to improvements in treatment and diagnosis, the overall incidence of mortality of cancer in the UK has dropped by 16% since the 1970s, with 10 year survival rates doubling from 24% to 50% (Cancer Research UK, 2019). However, metastatic cancer remains a great challenge for treatment, being incurable in many cases and accounting for over 90% of cancer related deaths (Gupta and Massagué, 2006).

Whilst surgical resection can effectively and sometimes curatively remove solid tumours, it is unable to deal with micro-metastatic sites. Radiation therapy faces similar limitations. Chemotherapy on the other hand can target diffuse metastatic sites due to its systemic delivery, however it is associated with severe side effects due to its lack of specificity (Park and Choi, 2016). Often treatment regimens will combine these approaches and produce modest effects, however in many cases disease relapse confounds long-term

survival. Many of the chemotherapeutic drugs still used today were discovered at a time when very little indeed was known about cancer biology, this fact is reflected in their lack of specificity and often insufferable adverse effects.

The unprecedented increase in our understanding of the cellular events that govern cancer pathogenesis that has occurred over the course of the last few decades has made possible an approach to cancer treatment based on targeting of dysfunctional cellular mechanisms. The identification of key molecular players that are deregulated in cancer has allowed them to be targeted, and in some types of cancer this has transformed treatment and survival. For example, the development of Imatinib for the treatment of chronic myeloid leukaemia (CML) and acute myeloid leukemia (AML) has drastically improved outcomes (Cohen et al., 2002; Iqbal and Iqbal, 2014). Unfortunately successes such as these have not been replicated in the treatment of more complex and heterogenic solid tumours where responses are transient and are inevitably followed by relapse (Engelman and Settleman, 2008).

1.2 *Oncolytic virotherapy*

1.2.1 Introduction to oncolytic virotherapy

Oncolytic virotherapy is an emerging approach to cancer treatment that aims to harness the cytotoxic properties of viruses to selectively infect and kill cancer cells whilst leaving normal cells unharmed (Russell et al., 2012). The killing of the cancer cell occurs through a process of oncolysis and leads to the release of progeny virus particles that may then go

on to infect neighbouring cancer cells and establish subsequent rounds of replication and killing (Figure 1.1).

Numerous wild-type viruses display inherent replication selectivity for cancer cells, the reason for this is thought to be based on a phenotypic overlap between tumour biology and preferred environments for viral replication. In this model the tumour cell provides a niche for viral replication in which many of the numerous hallmarks of viral replication, such as immune evasion, resistance to apoptosis and deregulated cell growth are already provided as a consequence of malignant transformation (Seymour and Fisher, 2016). For example, the oncolytic effect of Newcastle disease virus (NDV) is thought be based on its strong preference towards apoptosis resistant cells (Mansour et al., 2011).

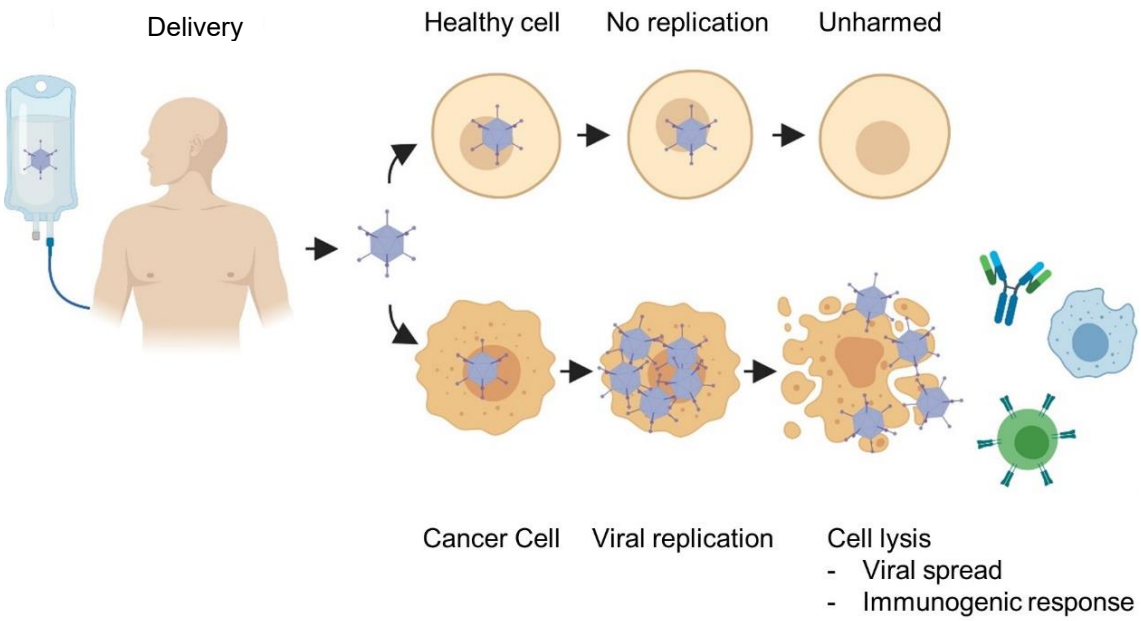


Figure 1.1. The principle of virotherapy. Following delivery, the oncolytic virus reaches and establishes an infection in the tumour. The virus is only able to replicate in transformed cells whilst replication does not occur in healthy cells. Viral replication culminates in lysis of the tumour cell, killing it and stimulating an immunogenic response against the tumour. Image created with Biorender.

Reovirus is another example of a naturally occurring virus with oncolytic properties (Duncan et al., 1978). The preference of reovirus replication for cancer cells is thought to be based on a combination of host factors that are deregulated in many cancer cells and act to enhance viral replication (Phillips et al., 2018). Most notably, deregulation of the protein kinase R (PKR) pathway, which normally detects double stranded RNA and phosphorylates eukaryotic initiation factor (EIF) EIF2α and thereby inhibits cap-dependent translation, is thought to facilitate reovirus activity. Originally this was linked to activation of the Ras pathway, which in many cancers enhances numerous aspects of reoviral replication, in part due to the inhibition by active Ras of PKR. This inhibition blocks the global downregulation of translation brought about by the PKR directed phosphorylation of EIF2α which in the absence of Ras activity, would frustrate reoviral replication (Strong et al., 1993, 1998). However, this model remains contentious since other investigators have not been able to find any predictive biomarkers for the sensitivity of cancer cells to reovirus replication from the analysis of the Ras signalling pathway (Twigger et al., 2012).

In the mid-1900s clinical trials were undertaken to investigate the possibility of using wild-type oncolytic viruses (OVs) as cancer therapies, most notably using adenovirus (Georgiades et al., 1959), West Nile (Southam and Moore, 1952), hepatitis (Hoster et al., 1949) and mumps viruses (Asada, 1974). These trials reported encouraging responses to the viral interventions, yet remissions were usually short lived and outcomes not always replicable (Kelly and Russell, 2007). In the years that followed, the field moved towards the engineering of viruses to optimise them for use as oncolytic agents (see section 1.2.2 Rational design of oncolytic viruses).

Since most naturally occurring candidate OVs do display some replication and cytotoxicity toward untransformed cells, much effort has focused on the design of

engineered OVs to improve specificity and oncolytic potential. Meanwhile the importance of the host immune system and the immune response to the infected tumour cell has been emphasised. Indeed, the ability of the oncolytic infection to promote immune mediated killing of the tumour cell has been touted as the principal mechanism of anti-tumour response and has become the focus of the field (Kaufman et al., 2015; de Graaf et al., 2018). It is thought that the lysis of the tumour cell by the virus can release tumour antigens and turn the tumour microenvironment, which is often an immunosuppressive environment, into a more immunogenically active one, leading to the destruction of the tumour by the immune system and a persistent anti-tumour vaccine effect (Twumasi-Boateng et al., 2018).

The rational design of oncolytic viruses was made possible by an increased understanding of both the relevant tumour biology and virology and was the catalyst for the completion of many clinical trials and the development of T-Vec (Talimogene Iahrparepvec), also known as Imlygic. T-Vec is an HSV-1 oncolytic virus engineered to express an immunomodulatory transgene, and the first oncolytic virus to be approved by the Food and Drug Administration (FDA) in the United States and by the European Medicines Agency (for further discussion of T-Vec please see section 1.2.2.2 Enhancing potency). The success of T-Vec, which showed acceptable response rates in clinical trials of patients with advanced metastatic melanoma (Andtbacka et al., 2015), demonstrates the potential of the oncolytic approach and is an encouraging result for the numerous other oncolytic agents currently involved in clinical trials, 49 of which are currently recruiting at the time of writing according to clinicaltrials.gov.

1.2.2 Rational design of oncolytic viruses

1.2.2.1 Optimising specificity

The growing understanding of tumour biology and of the virology of many of the most popular oncolytic viruses has led to an increased ability to rationally design viruses with optimised activity. The first and most important feature of any oncolytic virus is its ability to mediate lysis selectively towards cancer cells, with relatively limited toxicity towards non-transformed cells. Improving the specificity of candidate oncolytic viruses has been a topic of intense investigation. In many cases this strategy involves attenuating the virus in such a way that it is unable to replicate in normal cells but can respond to the phenotype of the cancer cell and undergo successful replication. This has been achieved by various approaches the most important of which are discussed below.

The intrinsic oncotropism of numerous wild-type viruses is thought to be in part explained by their preference towards cell surface receptors that are upregulated in cancer, which they use during the entry phase of infection. For example, adenoviral serotypes Ad5 and Ad11 use the coxsackie and adenovirus receptor (CAR) and the complement regulatory protein CD46 as their respective principal uptake receptors (Nemerow, 2002). Some group B adenoviruses, including Ad11, also use desmolglein-2 (Wang et al., 2011). Both CAR and CD46 receptors are upregulated in numerous cancers (Giaginis et al., 2008; Wunder et al., 2013; Thorsteinsson et al., 1998; Do et al., 2018). Retargeting of oncolytic viruses to enter cells via surface receptors that are differentially upregulated in cancers relative to untransformed cells is perhaps the simplest mode of improving virus targeting. Examples of this approach include the retargeting of Ad5 to the CD46 receptor (Do et al., 2018), of HSV to the Her2 receptor which is associated with breast and ovarian cancers

(Uchida et al., 2018), and of measles virus against the urokinase receptor, upregulated in numerous malignancies (Jing et al., 2009)

A second strategy is to use tumour-associated promoters and regulatory elements to drive essential viral genes to achieve tumour specific replication (Pesonen et al., 2012; Small et al., 2006; Pahl et al., 1996a). This has been best exemplified in adenovirus (Ko et al., 2005), and relies on cellular transcription factors and gene promoters which are deregulated in certain cancers to drive the replication of the virus. One such promoter is the prostate specific antigen (PSA) regulatory element which becomes overactive in prostate cancer leading to high levels of PSA expression (Stamey et al., 1987). An oncolytic adenovirus, CG7870, was designed to take advantage of this by placing its E1A and E2B genes (see section 1.3.1.1. Genome structure) under the control of the prostate specific rat probasin promoter and the PSA enhancer respectively, with the view to restrict viral replication to cells in which PSA expression levels were high, namely prostate cancer (Smal l et al., 2006; DeWeese et al., 2001; Rodriguez et al., 1997). In a further embodiment of this approach, in the design of oncolytic virus CG0070 the adenoviral E1A gene was placed under the control of the human telomerase reverse transcriptase (hTERT) promoter element (Ramesh et al., 2006), expression from which is also upregulated in many cancers (Jafri et al., 2016).

Thirdly, deletion of viral genes which can be trans-complemented by the tumour phenotype can improve OV specificity (Kirn, 2001; Senzer et al., 2009). The trans-complementation approach is exemplified by the development of the oncolytic adenovirus ONYX-015. Early during adenoviral infections, the virus expresses the E1B-55K protein which prevents apoptosis of the infected cell through its inhibitory association with p53 (Martin and Berk, 1998). This interaction formed the basis of a hypothesis in which the deletion of the E1B-55K gene would limit replication of the virus

to cells in which the p53 pathway was already dysregulated, which is frequently the case in human cancers (Miller and Koeffler, 1993). ONYX-015 showed enhanced specificity towards p53 mutated cancer cell lines compared to the wild-type Ad5 virus (Heise et al., 1997), and advanced to clinical trials where enhanced activity towards cancer cells over normal cells was also seen. Further study revealed that the cancer selectivity was not achieved through the mechanism originally hypothesised and was actually independent of p53 status (Rothmann et al., 1998). Instead more efficient export of late viral mRNAs in cancer cells accounted for its enhanced oncotropism (O'Shea et al., 2004). Nonetheless the development of ONYX-015 exemplifies how the attenuation of a virus can increase its therapeutic index as an anti-cancer agent. Adenovirus has also been attenuated by deletion of the E1A gene, whilst other viruses that have been modified by introducing genetic deletions include vaccinia virus (TK deletion) and HSV (ICP34.5 deletion) (Singh et al., 2012).

Lastly, the target sites for inhibitory microRNAs molecules that are specifically expressed in off-target tissues can be encoded within essential viral transcripts, to knockdown their expression and therefore limit viral replication in off-target sites (Cawood et al., 2009; Kelly and Russell, 2009).

1.2.2.2 Enhancing potency

Oncolytic viruses engineered to display attenuated replication in normal tissues and optimised replication in cancer cells have been in large part responsible for the exemplary safety record of oncolytic viruses in the clinic (Russell et al., 2012). However, the lacklustre anti-tumour potency of many of candidate OVs seen in clinical trials has led to a substantial effort being invested into improving this aspect of the therapy. The evident

genetic and phenotypic heterogeneity of human tumours make it difficult to envisage that any single OV could have the ability to infect and destroy disseminated disease in patients, thus combination therapies involving OVs have been of great interest.

The combination of OVs with independently administered small molecule drugs to improve anti-tumour effect has been demonstrated with some success. For instance, adenovirus, vesicular stomatitis virus (VSV), sindbis virus and Herpes simplex virus 1 (HSV-1) have all been synergistically combined with dimethyl fumarate, which potentiates their replication by reducing interferon (IFN) production through blockade of Nuclear Factor kappa-light-chain-enhancer of activated B cells (NF-κB) (Selman et al., 2018). VSV and HSV-1 have been successfully combined with histone deacetylase inhibitors (MacTavish et al., 2010) and the chemotherapeutic agent cyclophosphamide, respectively (Fulci et al., 2006). Anti-angiogenic therapies have also been used in combination with OVs, the anti-vascular endothelial growth factor (VEGF) antibody bevacizumab conferred improved virus spread in xenograft mouse tumour models (Tan et al., 2015). Notwithstanding the benefits of combining OVs with already approved drugs, foremost among them their already known safety profile, the focus of the field in recent years has been on a second approach of "arming" OVs with therapeutic transgenes.

The term "arming" refers to the inclusion of transgenes encoded within the viral genome for the intra-tumoural expression of biologics chosen for their ability to potentiate tumour cell killing directed by the virus, the immune response to the tumour, or both. For example, to enhance their cytotoxic potency, OVs can be armed with a transgene encoding an enzyme with the ability to convert a non-toxic pro-drug into a toxic drug at the tumour site. This approach has the potential to spread the cytotoxicity to include non-infected cells within the immediate vicinity of the infected cells, both increasing potency and also reaching any tumour cells that are intrinsically resistant to virus infection, whilst

in principle avoiding systemic toxicity. The most widely documented examples of this strategy are the HSV thymidine kinase gene which sensitises cells to Ganciclovir, and cytosine deaminase (CD), which renders cells sensitive to 5- fluorocytosine (Fillat et al., 2006).

In a second preferred approach, the OV encodes an immunomodulatory transgene intended to promote recognition of the tumour by the host's immune system, leading to the destruction of both infected cells and uninfected "bystander" tumour cells. This approach, often described as an "oncolytic vaccine", is particularly appealing since it may be able to overcome the limitation of poor delivery of OVs to tumours that is generally considered to be an important barrier to efficacy (Miller et al., 2014). OVs have been armed with an array of different immunomodulatory genetic payloads (Lichty et al., 2014; Keller and Bell, 2016; Raja et al., 2018) but the most successful to date has been the expression of GM-CSF from the herpes virus 1 (HSV-1) derived virus T-Vec.

HSV1 is a double stranded DNA virus which can infect skin and peripheral nerve cells, displaying lytic replication and causing blisters. In order to adapt HSV-1 for use as an OV, its propensity to infect these healthy cells was attenuated by removal of the neurovirulence protein, infected cell protein 34.5 (ICP 34.5) (Conry et al., 2018). In healthy cells, viral infection activates PKR which leads to the phosphorylation of EIF2α, limiting viral replication by downregulating protein translation and activating antiviral interferon responses (Williams, 1999). HSV-1 is able to replicate in some healthy cells however, due to the presence of the ICP 34.5 protein which directs dephosphorylation of EIF2α, blocking the effects of PKR activation. The removal of the ICP 34.5 protein therefore had the effect of attenuating viral replication in healthy cells with intact PKR responses, but not cancer cells in which the pathways that govern PKR activation are dysfunctional (Smith et al., 2006).

T-Vec was further improved by deletion of another gene, infected cell protein 47 (ICP47). ICP47 blocks the cell surface expression of major histocompatibility complex (MHC) 1 molecules to evade immune detection. Thus, its deletion had the dual effect of improving tumour cell surface antigen presentation and further improving safety by enhancing the immune detection of virally infected healthy cells. Finally, two copies of a transgene encoding human GM-CSF were inserted into the viral genome at the deleted ICP 34.5 site. GM-CSF expression promotes the accumulation of dendritic cells at sites of inflammation which enhances the antigen presentation function. This in turn contributes towards the enhanced cancer vaccine effect, with regression seen in non-injected tumours, and extended responses in patients.

Notably, in clinical trials the oncolytic vaccine effect was reported with apparent immune mediated destruction of non-infected metastatic sites (Andtbacka et al., 2015). The regulatory success of T-Vec is in no small part responsible for the surge of interest in oncolytic viruses as immunotherapies and consequently numerous trials are ongoing to investigate the effects of the inclusion of other immunomodulatory transgenes in the genomes of various OVs.

1.2.3 Directed evolution of oncolytic viruses

The rational design of OVs depends on an understanding of the tumour biology and virology that underpin the interactions between the cancer cell and virus within the body. The genetic and phenotypic heterogeneity of cancer is extraordinarily complex, indeed, the more we advance our understanding of the disease the more evident its complexity becomes. Moreover, our understanding of the virology of many candidate OVs is not complete, therefore it is not reasonable to expect that we will be able to rationally design

viruses with optimal activity as virotherapies. An intriguing alternative to rational design is to use bioselection to harness the power of natural selection to select for viruses with optimal activity in cancer cells. This approach circumvents the need for detailed mechanistic understandings of the tumour-virus interactions and can yield strongly potentiated new virus variants in a short space of time. Viruses are stringently selected for maximal proliferation in tumour cells under conditions promoting mutations or by using a genetically diverse starting pool and are subsequently negatively selected for replication in normal cells (Figure 1.2).

Enadenotucirev (EnAd) is an oncolytic adenovirus currently undergoing clinical trials which was produced by this method. The genetic complexity of the starting pool for the generation of EnAd was achieved by using an array of different adenoviral serotypes to co-infect HT-29 colon cancer cells. Recombination between homologous regions of the viral genomes produced a highly diverse virus library which was then exposed to stringent

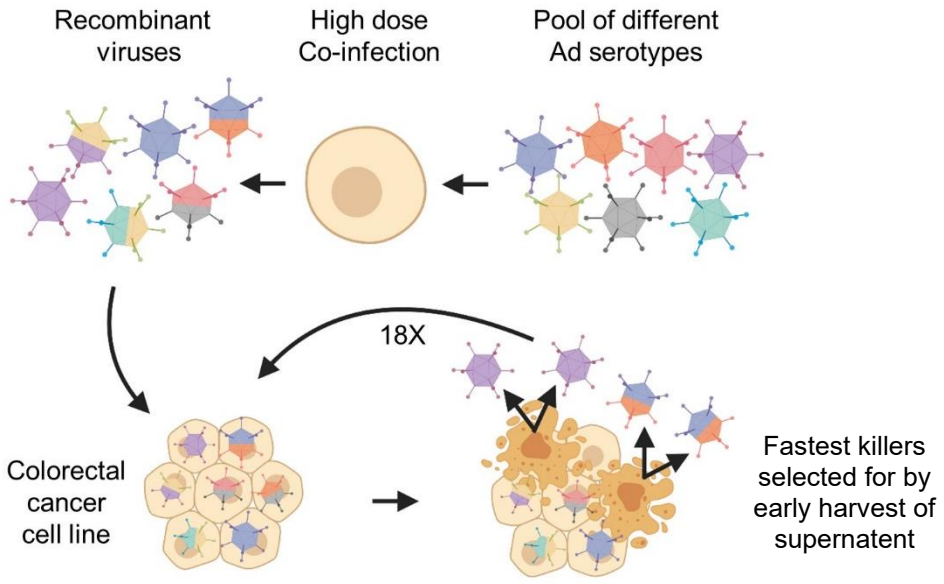


Figure 1.2. Generation of a new oncolytic virus through directed evolution. Recombinant viruses were generated by coinfection of cells with a diverse starting pool of viruses. Eighteen iterations of amplification, lysis and reinfection were carried out in a colorectal cancer cell line, collecting the supernatant of the infected cells at early time points to select for viruses which rapidly lyse the cancer cells. Image created using Biorender.

selection for rapid replication and early lysis of HT-29 colorectal cancer cells (Figure 1.2). Of the numerous viruses isolated at the end of the process, EnAd was the most attractive candidate for further development due to its high oncolytic potency against various cancer cell lines along with its apparent lack of activity in normal cells (Kuhn et al., 2008).

1.3 *Oncolytic adenovirus*

Despite the lack of pathogenicity of the most prevalent types of adenovirus, interest in adenoviruses within the field of basic virology has a long standing history, whilst their importance as an experimental system for the investigation of numerous fundamental biological processes cannot be overstated (San Martín, 2012). Adenovirus research has been of pivotal importance in the discovery of highly conserved eukaryotic processes including apoptosis and RNA splicing. Human adenovirus was first isolated from adenoid tissue over 65 years ago (Rowe et al., 1953), and since that time 68 types of human adenoviruses have been identified and classified into seven groups from A to G. Initially, this classification was based on hemagglutination and serum neutralisation reactions, but now adenoviruses are classified into types according to genomic sequencing and bioinformatic analysis (Ghebremedhin, 2014). Various characteristics have meant that adenoviruses have become the most widely used vector in cancer gene therapy. These include the relatively thorough understanding of adenovirus virology, their propensity to be grown to stocks of high titre and stability, their ability to infect both dividing and non-dividing cells, and their excellent safety and tolerability record (Wold and Toth, 2013). The majority of the literature describing the virology of human adenoviruses has been

conducted using species C viruses, most notably Ad5 and Ad2, and despite the substantial genetic heterogeneity between adenoviral species (Mei et al., 2003), these two virus are used as models for describing virology of human adenoviruses more widely.

1.3.1 Structure

1.3.1.1 Genome structure

Adenovirus has a double stranded DNA genome of approximately 36 kb, encoding over 40 proteins (Wold and Ison, 2013). The genes encoded are divided into early and late genes depending on whether they are expressed before or after DNA replication (Thomas and Mathews, 1980). The early regions E1A and E1B are the first to be expressed and function to optimise the cellular environment for viral replication (Frisch and Mymryk, 2002), whilst products from the E2 region direct DNA replication (Liu et al., 2003). The E4 and E3 proteins are involved in modulating host signalling and immune responses, respectively (Horwitz, 2004; Weitzman, 2005). The Major Late Promoter (MLP) is active after DNA replication and controls expression of the late protein products which primarily act as capsid proteins and are encoded in the L1-L5 genomic regions. The late products also include virus associated RNA products VA RNA I and II that are important for proper translation of the late genes, impede host interferon responses against the virus, and inhibit cellular micro-RNA processing (Thimmappaya et al., 1982; Hendrickx et al., 2014). At each of the very ends of the genome are the inverted terminal repeats (ITRs) from which DNA replication is initiated. Just downstream of the left ITR is a sequence important for the proper packaging of genomes into assembled virus particles during virus

assembly. The genome structure of adenovirus is schematically represented in Figure 1.3A.

1.3.1.2 Capsid structure

Adenoviruses are icosahedral, non-enveloped viruses with a protein shell surrounding a DNA-protein core complex. They have a mass of roughly 150 x10^6 Da, with the genome accounting for 22.6 x10^6 Da of this mass, encased in a capsid with a diameter of 914 Å (Stewart et al., 1991). Studies using electron microscopy (EM) and X-ray revealed the architecture of the capsid which is common amongst all adenoviruses. The capsid is made up of 240 minor surfaces, along with protruding fibre structures extending from 12 vertices (Valentine and Pereira, 1965). The component proteins consist of three major soluble antigens; the penton, hexon and fibre proteins. The three dimensional structure and positions of the component capsid proteins have been determined in detail by cryo-EM reconstruction (Liu et al., 2010). There are also four minor capsid proteins of smaller size named IIIa, VI, VIII and IX, these play a largely structural role and serve to stabilise the capsid structure and provide rigidity. Finally, four core proteins, V, VII, X and the terminal protein (TP) are packaged along with the viral DNA into the core of the capsid. The core proteins are involved in core condensation and binding of the DNA to the capsid structure (Rux and Burnett, 2004). In contrast to the outer capsid, the stoichiometry and structure of the four minor proteins making up the inner capsid and that of the core proteins has not been determined (Benevento et al., 2014). The capsid structure of adenovirus is schematically represented in Figure 1.3B.

The hexon protein is the most abundant of the structural proteins, accounting for 63% of the mass of the capsid. The molecular architecture of the hexon protein, with its

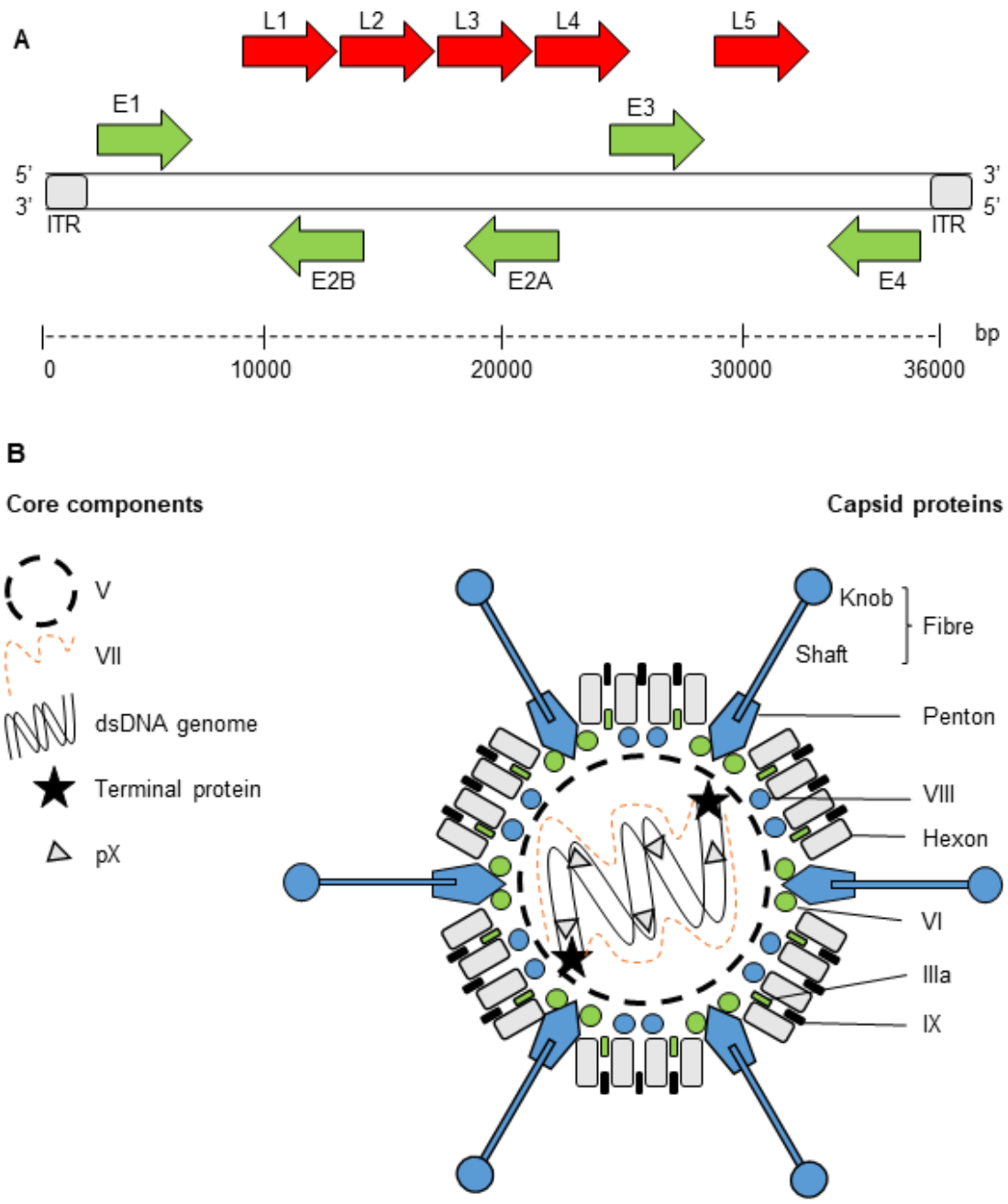


Figure 1.3. Adenovirus structure. A) The structure of the adenoviral genome is depicted, with early transcription units shown as green arrows and late units as red arrows. **B)** Schematic representation of a cross section of an adenoviral particle, showing the structural proteins and core.

interlocking trimeric topology, provides it with exceptional stability (Shortridge and Biddle, 1970). It has an evolutionarily conserved core region that is essential for proper formation of the capsid, whilst exposed loops at the top of the protein are hypervariable and differ substantially between serotypes. Due to the abundance of the hexon protein

and its exposed position on the capsid, it produces a strong host adaptive immune response (Crawford-Miksza and Schnurr, 1996), an important consideration for the use of adenoviral vectors in gene therapy and oncolytic applications. The penton complex, formed of the penton base and the fibre trimer, functions to seal the capsid at the 12 vertices. They are also responsible for attachment to the target cell, which occurs through an interaction between the fibre and a host cell receptor. Internalisation of the virus particle is triggered by an interaction between a conserved sequence within the variable region on the exterior of penton base and cell surface integrin molecules (Rux and Burnett, 2004).

The fibre protein which protrudes from each of the vertices of the capsid can be divided into three domains. The first is an N-terminal domain which connects the fibre to the rest of the capsid via the penton base, the second is the shaft domain which is made up of repeating motifs, and third is the globular C terminal knob domain which directs interactions with target cell receptors (Rux and Burnett, 2004; Zhang and Bergelson, 2005). The number of repeating motifs in the shaft region can vary from 6 to 22 resulting in a wide range in the length of fibre proteins between adenoviral serotypes (Green et al., 1983; Signas et al., 1985)

Minor protein IIIa is a 67 kDa monomeric elongated polypeptide that extends from the outer surface of the capsid to the inner surface. It is located underneath the penton base protein and peripentonal hexons (Liu et al., 2010). The IIIa protein interacts with various proteins including the penton-base monomer, an adjacent protein IIIa, and two peripentonal hexons. In this way it acts to bind the penton base to neighbouring peripentonal hexons (Liu et al., 2010). Although the role of protein IIIa is primarily a structural one, there is some evidence it may influence viral gene transcription late in infection (Molin et al., 2002).

The 22 kDa minor protein VI is located on the inner surface of the capsid, adjacent to the hexons, and connects the bases of neighbouring hexons (Liu et al., 2010). During endosomal escape protein VI induces a pH dependent disruption of the membrane (Wiethoff et al., 2005), and also plays a role in the nuclear import of newly synthesised hexon proteins.

Minor protein VIII is also situated on the inner surface of the capsid interacting with hexons. Each VIII monomer can be divided into three domains: head, neck, and body. Protein VIII is cleaved during viral maturation causing the middle section to be shed from the mature capsid. A total of four hexons interact with each VIII monomer, two via the body domain and one each via the neck and head domains. VIII also interacts with the IIIa protein via its body domain (Liu et al., 2010).

Minor protein IX is the smallest of the minor capsid proteins and alongside its structural role also has a DNA packaging function (Boulanger et al., 1979). Virus particles lacking the IX protein package wild-type genomes inefficiently and are not infective in plaque assays, whilst virus particles containing IX protein can successfully package genomes up to 105% the length of the wild-type genome (Ghosh-Choudhury et al., 1987). This has important implications for the therapeutic use of adenoviruses, into which therapeutic transgenes are often encoded (Vellinga et al., 2005).

1.3.2 Life cycle

The adenoviral life cycle has been the topic of intense research with a wealth of literature pertaining to the Ad5 and Ad2 serotypes. The life cycle can be conceptually divided into a number of stages: cell attachment and uptake, endosomal escape, nuclear import, early

gene expression, DNA replication, late gene expression, assembly and release. The typical lifecycle of adenovirus is depicted schematically in Figure 1.4.

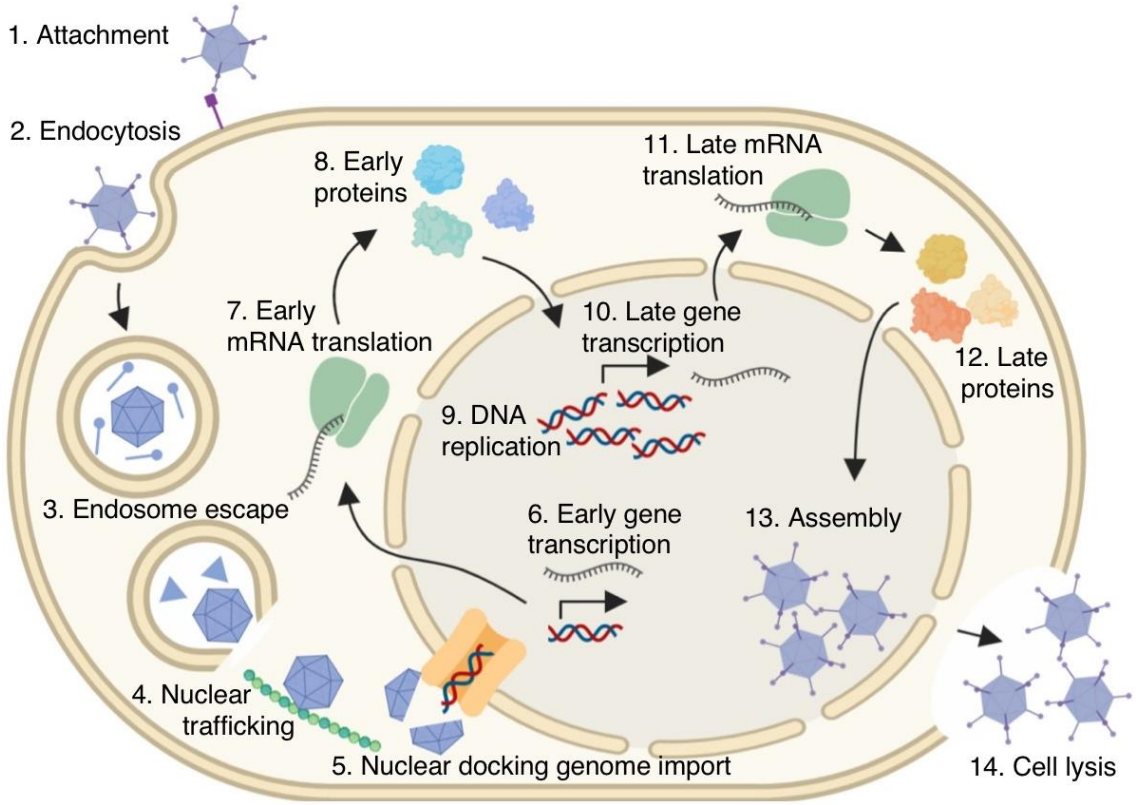


Figure 1.4. Adenovirus life cycle. The life cycle commences with the attachment of a viral particle to the cell through interactions between the fibre protein and cell surface receptors (1), attachment induces uptake of the virus into the cell through endocytosis (2). The virus begins to partially disassemble and escapes from the endosome into the cytosol (3) where it can then be trafficked along microtubules to the nucleus (4). The partially disassembled virus docks to the nuclear pore complex and the genome enters the nucleus (5). Upon entry of the viral genome into the nucleus the early viral mRNAs are transcribed (6) and exported to the cytosol for translation (7) to produce the early viral proteins (8). The early viral proteins are trafficked back to the nucleus to exert their functions including viral genome replication (9). After viral genome replication the late viral mRNAs are transcribed (10), exported to the cytosol for translation (11) to yield the late viral proteins (12). Late proteins are once again trafficked back into the nucleus where virus particles are assembled and accumulate (13) until the cell is lysed (14). Image created with Biorender.

1.3.2.1 Cell binding and entry

The initial binding of the adenoviral particle to the target cell occurs through an interaction between a conserved region of the globular knob domain of the fibre protein and its primary target receptor, which varies between adenoviral subgroups. The primary receptor for group A, C, E and F adenoviruses is the CAR receptor which is therefore the best studied (Zhang and Bergelson, 2005). Studies analysing the distribution of CAR mRNA in human tissues have found expression to be present in numerous human organs, including the liver. When delivered intravenously adenoviruses are strongly hepatotropic and are quickly taken up by the liver. Attempts to reduce this hepatotropism by impairing the binding interaction between the knob domain and the CAR receptor have not been useful *in vivo* (Alemany and Curiel, 2001). The CAR receptor has been reported to be downregulated in some cancers, and has been inversely associated with the progression of some tumours (Okegawa et al., 2001; Sachs et al., 2002; Zhang and Bergelson, 2005). Other receptors used by group C adenoviruses include the heparan sulfate glycosaminoglycans, the binding site for which is conserved among the fibre proteins of all group C adenoviruses.

Group B adenoviruses on the other hand do not bind CAR. This was first observed as the lack of competition for attachment between group B and group C viruses (Stevenson et al., 1995). Instead, group B adenoviruses use the CD46 receptor, a complement regulatory protein that is expressed on all nucleated human cells (Zhang and Bergelson, 2005). In contrast to the CAR receptor, CD46 expression is upregulated in many cancers and is associated with further progressed tumours (Niehans et al., 1996). This may make some group B viruses more inherently oncotropic and intrinsically more amenable for use as OVs than their group C counterparts. As already mentioned, group B adenoviruses also appear to use desmoglein-2 as an attachments receptor (Wang et al., 2011).

Once attachment has occurred, an interaction between the penton base, specifically on the RGD peptide, and integrin adhesion receptors, most importantly the vitronectin receptors αvβ3 and αvβ5, occurs (Wickham et al., 1994). This interaction induces a signalling pathway which brings about a cytoskeletal rearrangement which is needed to initialise the internalisation of the virus particle (Zhang and Bergelson, 2005). Internalisation usually takes place via clathrin- coated vesicles (Meier and Greber, 2003) but micropinocytosis has also been observed to be an uptake mechanism in group B adenoviral infections (Kalin et al., 2010).

1.3.2.2 Endosome escape and nuclear import.

Internalised Ad particles must escape the early endosomal compartment prior to degradation in lysosomes. The early events of capsid disassembly occur through a process that is independent of endosome acidification (Nakano et al., 2000). It remains contentious whether or not acidification of the endosomal compartment is involved in escape of the virus from the endosome (Nemerow and Stewart, 2016), however the most recent reports in this regard provided by Greber et al show that an acidic endosomal compartment is not a prerequisite for efficient viral membrane penetration in group B and C viruses (Suomalainen et al., 2013). The minor protein VI and viral protease together with the penton protein, play important roles in endosomal membrane disruption and escape (Wiethoff et al., 2005). There is some evidence that group B adenoviruses, due to their distinct receptor usage and internalisation pathway (Shayakhmetov et al., 2003), require a lower pH for endosome membrane disruption and thus progress further through the endocytic pathway into late endosomes than their group C counterparts before escaping (Miyazawa et al., 2001).

Once free of the endosome, the partially disassembled virus particle is trafficked towards the nucleus via interaction with microtubules (Suomalainen et al., 1999; Dales and Chardonnet, 1973) and docks via the hexon protein to the nuclear pore complex around 1 or 2 hours post-infection (Greber et al., 1997; Nemerow, 2002). The final stages of disassembly occur after docking when the capsid binds to kinesin-1 whose movement along microtubules leads to full capsid disassembly (Strunze et al., 2011). Viral DNA associated with protein VII is then imported through the nuclear pore complex by a poorly understood mechanism, with the outer coat proteins being left behind in the cytoplasm (Greber et al., 1993).

1.3.2.3 Early gene expression and DNA replication

Once the viral genome reaches the nucleus, the E1A gene is immediately transcribed, producing a single pre-mRNA that is alternatively spliced to yield the 12S and 13S E1A protein products. The E1A protein interacts with many important host factors to reprogram cellular gene transcription to optimise the cell for virus replication (Frisch and Mymryk, 2002). For example, E1A binds to the tumour suppressor pRb protein (Whyte et al., 1988; Egan et al., 1989) releasing the E2F transcription factor which promotes the expression of E2F dependent genes. E1A is also essential for the activation of transcription of the other early viral genes (Montell et al., 1982). The E2 transcription unit encodes three proteins needed for DNA replication, the E2B transcript produces the pre-terminal protein (pTP), the viral DNA polymerase (AdPol), and the E2A transcript produces the DNA binding protein (DBP). The AdPol and pTP proteins form a complex at the inverted terminal repeat sequences at the 5’ ends of the virus genome, where numerous interactions between the E2 proteins and other host factors orchestrate the protein primed initiation of DNA replication (Hoeben and Uil, 2013)..

1.3.2.4 Late gene expression, assembly and release

With the exception of the L1 (52/55K) product, late gene expression occurs exclusively after DNA replication (Paul Thomas and Mathews, 1980). The late proteins are under the control of the MLP and are transcribed as a single mRNA which is then alternatively spliced into multiple mRNAs (Berget et al., 1977), each containing a tripartite leader (TPL) sequence at the 5' end. The TPL has sequence complementarity with the ribosomal RNA, allowing ribosomes to be directly loaded onto late viral mRNAs, circumventing the need for the recruitment of the 5' cap complex. This enables late viral mRNAs to escape infection induced downregulation of 5' cap dependent translation, and affords them preferential translation (Ramke et al., 2017). Late viral proteins, which predominantly encode structural capsid proteins, are then transported back to the nucleus where they assemble into immature empty viral capsids that are then packaged with a copy of the genome (Ahi and Mittal, 2016). Successfully packaged virus particles then accumulate within the cell before its lysis through a process thought to involve the adenovirus death protein (ADP) (Tollefson et al., 1996). Group B adenoviruses including Ad11p lack the ADP gene, meaning the mechanism by which cell death is brought about must be distinct to that elicited by group C viruses. (Mei et al., 2003).

1.3.3 Enadenotucirev

EnAd is an oncolytic adenovirus generated by a process of bioselection described in section 2.2.4 and in Figure 1.2. Its genome is largely the same as that of Ad11p with 98.6 % sequence homology, but there are some important differences (Figure 1.5). EnAd has a near complete deletion of the E3 region, a partial 25 bp deletion mapping to E4 open reading frame (ORF) 4 in Ad5, and numerous mutations in E2B giving it an Ad3/Ad11p mosaic E2B region (Kuhn et al., 2008). It is thought that the mutations in the E2B region



Figure 1.5. Ad11p and EnAd genome structure. The genomes of Ad11p (top) and EnAd (bottom) are schematically displayed, with the differences indicated. These include numerous substitution mutation in the E2B region for the Ad3 E2B sequence, an almost complete deletion of the E3 region, and a smaller deletion in the E4 region mapping to E4 open reading frame 4.

may endow the viral polymerase with faster activity, perhaps by providing better interaction with the ITRs of Ad11p (Kuhn et al., 2008).

Ad5 and Ad11p share five common E3 proteins, although they are not well conserved. Ad11p has a further two E3 proteins (E3-20.3K and E3-20.6K) only found in group B viruses and that are of unknown function, but lacks the adenovirus death protein (Mei et al., 2003; Mei and Wadell, 1992). The large E3 deletion in EnAd leaves it with only three ORFs none of which have been characterised functionally. The E3 region is not essential for virus replication, but functions to modulate host immune responses, thus it may be that EnAd is attenuated in resisting host immunity, and this perhaps provides selectivity for tumour microenvironments with attenuated host immune function.

The E4ORF4 region has been studied in the context of Ad5 infection, but is also poorly conserved, sharing only 55.7% homology with the Ad11p sequence (Mei et al., 2003). During Ad5 infections at least, the E4ORF4 protein localised to the nucleus where it has a downregulating effect on E1A transactivation of the other early viral genes (Brestovitsky et al., 2011), affecting the switch between early and late gene expression.

E4ORF4 has also been implicated in the regulation of viral DNA replication (Medghalchi et al., 1997), to mimic growth signals to activate the mammalian target of rapamycin (mTOR) pathway and induce entry into the s-phase (O'Shea et al., 2005), and to interact with machinery regulating the alternative splicing of late vial mRNAs (Kanopka et al., 1998). It is not known if the E4ORF4 protein of Ad11p functions in a similar way, and it is further not known how the 25 bp deletion to E4ORF4 in EnAd affects its function compared to Ad11p. Aside from the effects this small deletion may have on the E4ORF4 protein, it may also have important ramifications for the splicing of downstream open reading frames such as E4ORF6. E4ORF6 has also had many functions attributed to it in the context of Ad5 infections and shares 68.8% homology with its counterpart in Ad11p (Mei et al., 2003). However, the proper expression of E4ORF6 depends upon the splicing events involving a splice acceptor site located in the E4ORF4 (Tigges and Raskas, 1984) region that may be disrupted in EnAd, and could have far reaching consequences for its life cycle.

Although the mechanisms are not yet fully understood, the genetic changes in the EnAd genome described above do seem to impart it with some properties that make it an attractive candidate oncolytic virus. When tested, EnAd was found to have higher oncolytic potency in various cancer cell lines compared to Ad11p, with very limited activity in non-transformed cells (Kuhn et al., 2008). Another difference is that EnAd directs killing of target cells through an oncosis related mechanism, characterised by the release of significant levels of inflammatory mediators that it is thought could promote an immune response against the tumour (Dyer et al., 2017). In clinical trials EnAd has been shown to reach the tumour following IV administration and to have a good safety and tolerability profile. These trials also revealed a fairly strong immune response to the tumour following EnAd replication (Machiels et al., 2019; Garcia-Carbonero et al., 2017).

1.4 *Role of calcium signalling and protein kinase C*

Cells must be able to adapt to changing environments and to do so they must be able to signal; therefore, they need a messenger whose concentration can vary with time. Calcium ions have been adopted by all life forms to fulfil this role, with subcellular stores of calcium creating steep gradients across membranes to provide rapid and precisely temporally controlled signalling that regulates almost all cellular events (Clapham, 2011). The principal cellular store of calcium is the endoplasmic reticulum (ER) and by extension the nuclear envelope, which together form a contiguous luminal space (Görlach et al., 2006). Acidic vesicles, the golgi and the mitochondria also represent significant pools of calcium (Clapham, 2011).

Since viruses rely on the hijacking of host cellular processes by extension they also rely on cellular calcium and calcium-dependent events, thus they have evolved mechanisms to manipulate a diverse range of calcium signals to their own advantage (Zhou et al., 2013). In the earliest stages of infection, extracellular calcium has been shown to be necessary for adenovirus uptake into cells (Wu et al., 2006; Greber et al., 1997). Protein VI from incoming virus particles is thought to increase influx of calcium into the cell by creating small plasma membrane lesions which enhance viral endocytosis and subsequently endosome escape (Luisoni et al., 2015). Furthermore, the ER/nuclear envelope calcium store is needed for import of the virus genome into the nucleus (Greber et al., 1997). Calcium flux and virus release are also closely associated. Verapamil, a calcium channel blocker, has been shown to enhance oncolytic adenovirus potency by increasing release and spread in mouse xenograft tumours (Gros et al., 2010). Gros et al. isolated a mutant Ad5 virus through a process of bioselection which had enhanced virus release and anti-tumour potency attributed to truncated E3-19K protein. The truncated

protein was redirected to the plasma membrane and thought to act as a viroporin to permeabilise the membrane and allow influx of extracellular calcium into the cell (Gros et al., 2008).

In order to respond to the signals generated by changes in calcium gradients, the cell expresses various effectors of calcium signalling. An important group of effectors are the protein kinase C (PKC) family of serine/threonine kinases. Ten different PKC isoforms have been characterised so far (Steinberg, 2008). These evolutionarily conserved kinases transduce a multitude of environmental cues into cellular actions, and regulate critical processes including cell-cycle progression, proliferation and differentiation, cell migration, cell survival and apoptosis, whilst their interaction with numerous transcription factor can have a profound impact on gene expression within cells (Garg et al., 2013; Isakov, 2018). The wide range of functions and processes affected by PKC signalling is reflected in the presence of multiple PKC isoforms. Unsurprisingly, deregulation of PKC has been implicated in a wide range of cancers. Different PKC isoforms have been shown to have both tumour-promoting and supressing effect, and be up- or down-regulated depending on the cancer type (Isakov, 2018), making PKC an attractive therapeutic target (Marengo et al., 2011).

The α, βI, βII and γ isoforms of PKC are known as classical isoforms, and are able to respond to and become activated by increases in cytosolic calcium thanks to a conserved calcium responsive C2 domain (Isakov, 2018). Very briefly, release of calcium ions from intracellular compartments leads to the cleavage of phosphatidylinositol 4, 5 bisphosphate (PIP_2) into 1,4,5-inositol trisphosphate (IP_3) and diacylglycerol (DAG). The ER localised IP3 receptor (IP3R), when bound by IP_3, brings about a more sustained rise in cytosolic calcium concentration by allowing the diffusion of calcium from the ER. Calcium may

then bind to the C2 domain of the classical PKC isoforms which then translocate to the plasma membrane and are activated by DAG (Clapham, 2011).

As major regulators of cell signalling, PKCs have a long association with virus infection, mostly at the level of viral endocytosis. It has been suggested that numerous viruses, including HSV, alphavirus, influenza, poxvirus, rhabdovirus and adenovirus require PKC activity for efficient internalisation (Sieczkarski and Whittaker, 2005). PKC activity is required for type 2 adenovirus infection, since in the presence of chemical inhibitors of PKC, adenovirus is unable to escape the endosome and accumulates in cytoplasmic vesicles in a manner indistinguishable from that which occurs when the actin cytoskeleton is disrupted (Nakano et al., 2000). PKC has also been suggested to act upstream of focal adhesion kinase cSrc, which is phosphorylated at the very early stages of adenoviral infection and mediates endocytosis of the virus particle. The same study found PKCα to be activated following infection of cells with adenovirus type 37, and that chemical inhibition of PKC reduced early viral gene expression (Yousuf et al., 2016).

1.5 *Oncolytic adenovirus and RNA interference*

As discussed in previous sections, the design of oncolytic viruses with strict tropism towards cancer cells has made them very safe and has allowed investigators to turn towards making them more efficacious. As we have seen, this increasingly involves "arming" the oncolytic virus with a transgene to be expressed within the tumour to aid the therapeutic outcome in some way. In adenovirus, there has been increasing interest in a manifestation of this approach in which the virus is armed with genetic material

allowing it to bring about the silencing of a target gene by taking advantage of the RNA interference (RNAi) pathway.

The RNAi pathway is a mechanism in eukaryotic cells that allows small double- stranded RNA (dsRNA) molecules to direct homology-dependent regulation of genes at the post-transcriptional level (Figure 1.6) (Svoboda, 2014). These dsRNAs, known as small interfering RNAs (siRNAs) are 21-22 nt long and have 2 nt long 3' overhangs through which they interact with the RNAi machinery. In mammalian cells, siRNAs can be produced endogenously by cleavage of a longer precursor dsRNA directed by the RNaseIII endonucleases Dicer, or alternatively they can be synthesised chemically and introduced into the cell exogenously (Svoboda, 2014). The siRNA is assembled with the RNA induced silencing complex (RISC), made up of the Argonaute (Ago) protein family members. Ago-2 has catalytic activity that cleaves the double-stranded siRNA, releasing what is known as the passenger strand, and activating the RISC complex which now contains a single-stranded guide RNA that is able to specifically pair with homologous sequences and achieve targeted gene silencing (Kim and Rossi, 2008).

Oncolytic adenovirus can be armed with the ability to express exogenous siRNAs within cells by encoding within its genome constructs to express a single-stranded RNA transcript which folds to form a hairpin structure known as a short hairpin RNA (shRNA). The shRNA expression construct usually consists of a target sequence, followed by a loop structure, followed by the antisense of the target sequence finally followed by a transcription termination signal (Moore et al., 2010). Upon expression, the shRNAs are then processed by the RNAi machinery, being cleaved by dicer, and the active strand guiding the RISC complex to the target transcript. Pol III promoters such as U6 and H1 have well characterised transcriptional start and termination sites, their small size allows them to be easily packaged into vectors, and they provide high levels of expression and

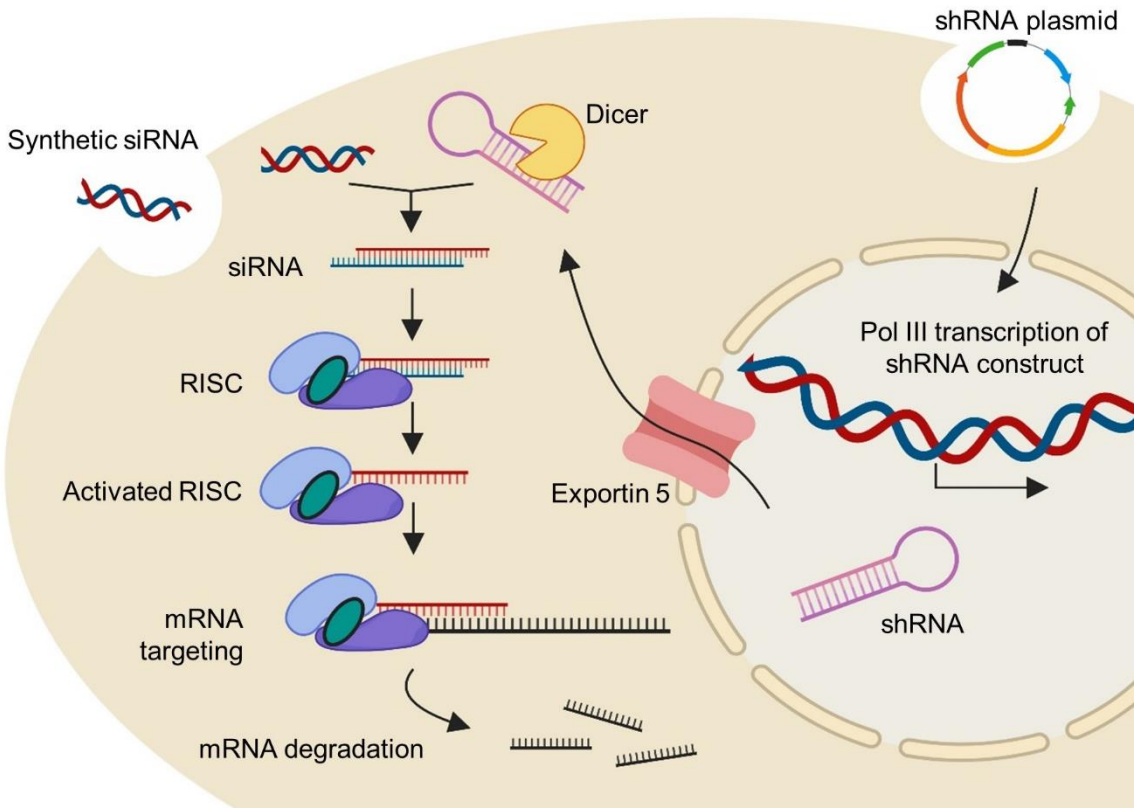


Figure 1.6. The RNA interference pathway. A plasmid encoding an shRNA expression construct can be transfected into the cell to direct the expression of an shRNA. The shRNA is exported from the nucleus via exportin 5 where it can be processed by Dicer to yield an active siRNA. Alternatively, chemically synthesised siRNAs can be directly introduced into the cell. The siRNA is loaded into the RISC complex, which cleaves and displaces one of the strands leaving only the guide strand in what is now the active RISC complex. The guide strand binds the target mRNA sequence through homologous base pairing. Perfect matching of the guide strand to the target induces the cleavage and hence knockdown of the target mRNA. Image created with Biorender.

gene silencing across multiple cell types. These features have made them the most widely used promoters for shRNA expression (Giering et al., 2008). However, in some scenarios the high levels of expression from Pol III promoters can cause cytotoxicity, whilst they also lack the spatio-temporal control necessary for some applications. To overcome these disadvantages, some have turned to embedding shRNA constructs in the sequence context of miRNAs using Pol II promoters with lower expression levels (Xia et al., 2002; Zeng et al., 2005) .

The RNAi pathway is highly conserved, and is often considered to have evolved in part as a mechanism of anti-viral defence (Obbard et al., 2009). Therefore, adenoviruses have evolved means to inhibit the pathway at various stages, for example, the interferon response evoked by adenovirus particles has been shown to inhibit dicer processing (Machitani et al., 2017). RNAi inhibition occurs primarily through the action of the virus associated RNAs I and II (VA RNA) (Lu and Cullen, 2004). Conversely the RNAi machinery can cleave VA RNAs, stopping them from blocking the action of PKR, which acts in the interferon response to block mRNA translation (Machitani et al., 2016). The RNAi machinery may also process VA RNA I and II to produce viral microRNAs (miviRNA), which it is suggested act to improve virus replication by regulating the expression of host genes (Aparicio et al., 2006).

Initially, it was thought that these interactions might make replicative virus infection and RNAi knockdown incompatible, however, despite these concerns adenovirus encoded shRNAs have been implemented with increasing success since their proof of principal report in 2004 (Carette et al., 2004). Here, Carette et al designed a replicating adenovirus armed with a U6 driven shRNA construct for the targeted silencing of a luciferase reporter gene. A549 lung cancer cells were infected with the shRNA armed adenovirus and subsequently transfected with the luciferase expressing plasmid. Luciferase signal from infected cells was approximately half that of uninfected cells 30 h post-infection (Carette et al., 2004).

In agreement with findings that suggested VA RNAs inhibit knockdown, their deletion from non-replicating adenoviruses improves knockdown (Machitani et al., 2013), but since VA RNAs are needed for efficient replication (Thimmappaya et al., 1982; Aparicio et al., 2006) this strategy has not been taken forward with regards to replicating oncolytic adenoviruses. The ability of replicating adenovirus to increase the copy number of

expression constructs in the target cell through replication is thought to be enough to achieve highly efficient knockdown in most cases. RNAi delivery by replicating adenoviruses, although now quite well characterised, has not been as of yet exploited to the degree one might expect. ShRNAs have been encoded in adenovirus to silence various target proteins, from cyclin-depend kinases to immunoregulatory proteins, which have been reviewed recently (Brachtlova and van Beusechem, 2018), and some of which are summarised in Table 1.1.

Table 1.1. Examples of shRNA armed replication competent adenoviruses

Target	Result	Reference
Luciferase	Proof of principal study showed efficient knockdown from shRNA encoded in replicating adenovirus	(Carette et al., 2004)
Apollon	Successful knockdown prevented tumour growth *in vitro/vivo*	(Chu et al., 2008)
TGF-β2	Enhanced GM-CSF mediated immune response	(Kim et al., 2017)
STAT3	Block SATA3 signalling, potentiate anti-tumour activity *in vitro/vivo*	(Han et al., 2009b)
K-Ras	10-fold increased activity in K-Ras mutated cells	(Zhang et al., 2006)
VEGF	Antiangiogenic effect *in vitro* and *in vivo*, and enhanced survival *in vivo*	(Yoo et al., 2007)
Dicer	Enhanced replication and tumour cell lysis	(Machitani et al., 2017a)

1.6 *ER stress and the unfolded protein response.*

1.6.1 Introduction to ER stress and UPR signalling

The ER is a dynamic tubular network which apart from being the main calcium storage site within the cell, is also the site in which many of the initial protein maturation steps

take place, and as such it plays a critical role in the proper folding of approximately 30% of cellular proteins (Görlach et al., 2006). External and internal factors that perturb the ER environment, including disruption of the calcium pool, inevitably impede protein folding, glycosylation and disulphide bond formation. These factors, as well as a fluctuating demand for ER processed protein production, can affect the fidelity and efficiency of the folding process and can lead to a deregulation of protein folding homeostasis. Consequently, an accumulation of unfolded protein in the lumen of the ER occurs in a condition known as ER stress (Ron and Walter, 2007). ER stress triggers the activation of an adaptive signalling response called the unfolded protein response (UPR).

Activation of UPR signalling attempts to restore protein folding homeostasis in a number of ways. Firstly, by degrading the improperly folded proteins in a process known as ER associated degradation (ERAD) (Ruggiano et al., 2014), by reducing the load of protein being folded in the ER through selective degradation of ER targeted mRNAs, and by bringing about a temporary global downregulation of protein translation (Harding et al., 1999). Secondly, by increasing the folding capacity of the ER, which is achieved by activating a transcriptional programme to upregulate genes encoding proteins involved in facilitating folding (Kozutsumi et al., 1988), and through expansion of the ER itself (Bommiasamy et al., 2009). And finally, in severe and chronic cases where normal function cannot be restored, the UPR can eliminate damaged cells by inducing apoptosis (Fribley et al., 2009).

The UPR response can be conceptually divided into three main signalling arms emanating from three principal ER stress sensing proteins which span the membrane of the ER (Figure 1.7). These ER stress sensing proteins are protein kinase RNA-like ER kinase (PERK), inositol-requiring protein 1 (IRE1) and activating transcription factor 6 (ATF6). In a simplified model for UPR activation, under normal conditions the luminal domains

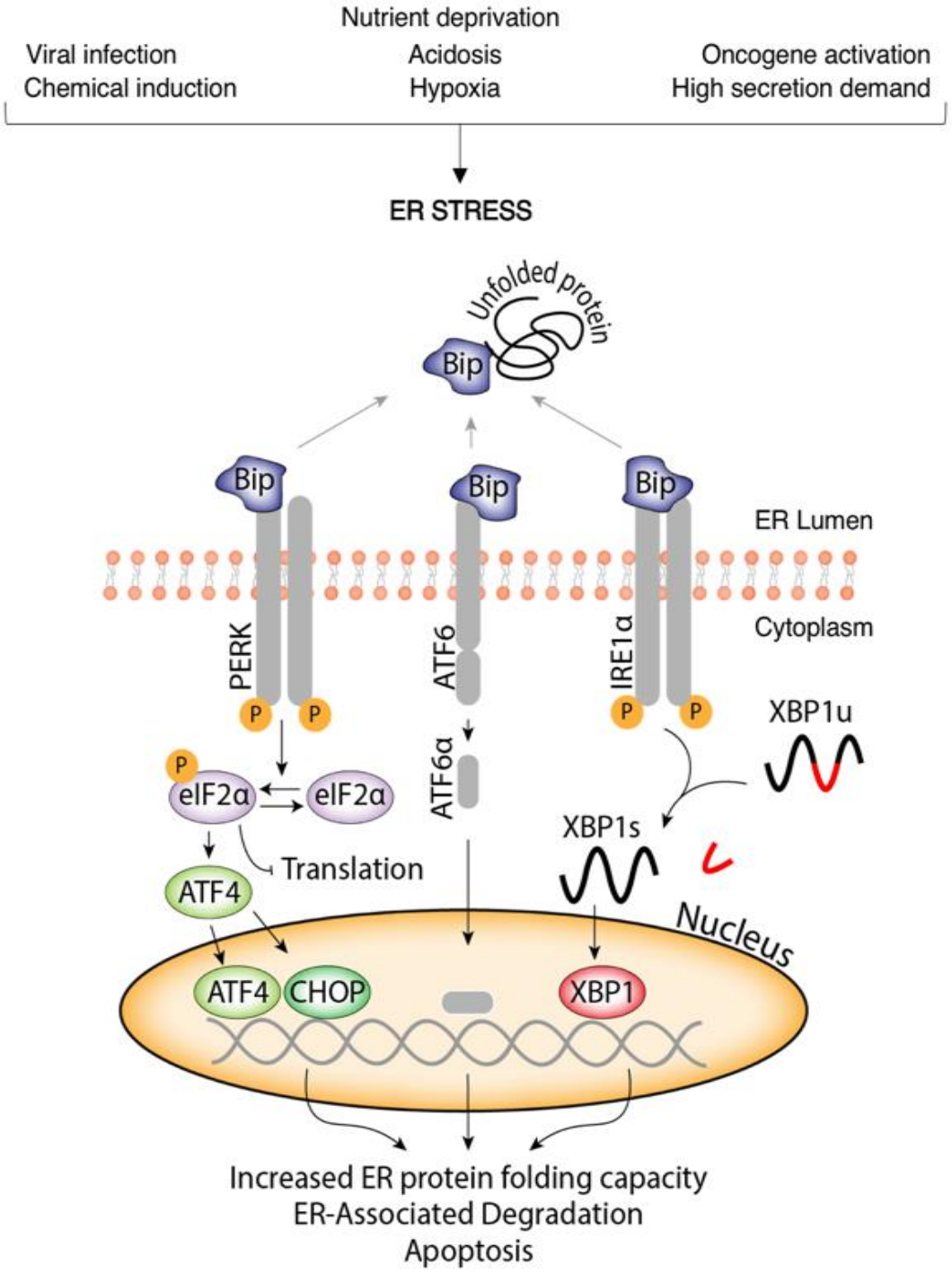


Figure 1.7. UPR signalling. Numerous extrinsic and extrinsic factors can perturb protein folding and lead to an accumulation of unfolded protein in the lumen of the ER. Unfolded protein competes for the binding of chaperone protein BiP, thereby releasing the ER stress sensing signal transducers PERK, ATF6 and IRE1α from the inhibitory binding of BiP. Free from BiP, the sensor proteins can activate their downstream signalling to bring about their effects in the cell.

of these proteins are bound by BiP (also known as GRP78) which prevents their activation. However, when ER stress occurs, BiP preferentially binds to the unfolded protein that begins to accumulate within the ER lumen, releasing the stress sensing proteins and allowing their self-dimerisation and activation (Marcu et al., 2002; Chuan Yin Liu et al., 2000; Bertolotti et al., 2000; Oikawa et al., 2009). In reality it is of course more complex. There is some evidence that the different arms of the UPR may be preferentially activated by different forms of ER stress, with the IRE1 and PERK responding more rapidly than ATF6 to calcium homeostasis disruption for example (DuRose et al., 2006). The response is also finely temporally controlled adding a further layer of complexity. IRE1 signalling seems to be diminished after prolonged ER stress whilst PERK signalling activity is sustained. This is thought to contribute towards the switch of the UPR from a pro-survival to pro-apoptotic response in cases of extended stress, by switching off the generally restorative effects of IRE1 signalling whilst maintaining some of the pro-apoptotic signals associated with PERK signalling (Lin et al., 2007).

1.6.1.1 PERK

The primary outcome of PERK activation is the attenuation of translation which is achieved by phosphorylation of eIF2α, consequently limiting the amount of eIF2–GTP–tRNA ternary complex available for translation initiation (Harding et al., 2000). This attenuation is transient, and in addition to reducing the protein folding load placed upon the UPR, it also encourages polysome dissociation, freeing up ribosomes for the translation of restorative mRNAs recently transcribed in response to the transcriptional programme directed by the UPR (Harding et al., 2000).

A growing number of select mRNAs are known to be able to escape this downregulation of translation, most notable among them is activating transcription factor 4 (ATF4) (Vattem and Wek, 2004). ATF4 is upregulated during ER stress and enhances expression of ER stress response genes to promote survival. One of these target genes is the growth arrest and DNA damage-inducible protein 34 (GADD34), which acts to dephosphorylate eIF2α and restore global translation (Wang and Kaufman, 2014). Conversely, ATF4 also upregulated the C/EBP homologous protein (CHOP) which plays a critical role in bringing about ER stress mediated apoptosis (Palam et al., 2011; Marciniak et al., 2004).

1.6.1.2 IRE1-XBP1

Activation of IRE1 occurs immediately upon induction ER stress (Han et al., 2009), stimulating its endonuclease activity and causing it to direct the cleavage of a 26 bp intron from the XBP1 mRNA transcript (Lee et al., 2002). This results in a frame shift allowing the translation of the active form of the XBP1 protein product known as spliced XBP1 (sXBP1). Upon localisation to the nucleus, sXBP1 contributes to the alleviation of ER stress by inducing the expression of target genes which increase rates of ERAD and enhance protein folding (Lin et al., 2007). In cases of chronic stress IRE1 activation is usually reduced (Han et al., 2009a), highlighting again the temporal regulation of the response. IRE1 directs the cleavage of many other mRNAs in addition to XBP1, in a process known as regulated IRE1-dependent degradation (RIDD). RIDD carries out the degradation of selected mRNAs target for the ER (Han et al., 2009a; Hollien and Weissman, 2006; Li et al., 2010), and that of some microRNAs too (Upton et al., 2012).

1.6.1.3 ATF6

When ER stress occurs and ATF6 is released from the inhibitory binding of BiP, ATF6 is trafficked to the golgi apparatus where it is further processed into its active form (Ye et al., 2000). In response to ER stress ATF6 directs a transcriptional programme to upregulate both genes that increase the protein folding capacity of the ER, and the XBP1 gene (Yoshida et al., 2001).

1.6.2 ER stress in cancer

As tumours proliferate, their demand for oxygen and other nutrients surpasses the supply provided by the local vasculature, and despite many cancers adapting to this challenge by inducing angiogenesis, invariably the cores of solid tumours are nutrient deprived and hypoxic (Chipurupalli et al., 2019). Hypoxia and nutrient depravation, as well as the high secretory demand and aberrant expression of oncogenes commonly associated with cancer cells, are all conditions that impede proper protein folding and are known to induce ER stress (Figure 1.7). Due to the inherent genomic instability of cancer cells, the UPR can become activated even in the absence of ER stress, that is to say in the absence of any accumulation of unfolded protein in the ER (Karali et al., 2014), through acquired mutations in key UPR signal transducers (Chevet et al., 2016).

ER stress is therefore increasingly being associated with numerous different cancers (summarised in table 1.2.), and activation of the UPR is increasingly being seen as a key enabler of the acquisition of numerous malignant characteristics (Urra et al., 2016). For example, the VEGF promoter has been shown to be regulated by the direct binding of ATF4, meaning expression is increased in cells experiencing ER stress, this in turn promotes survival of highly proliferative tumours (Wang et al., 2012; Pereira et al., 2014).

PERK-ATF4 signalling has also been suggested to be an important driver of cancer cell invasion, migration and metastasis, with lysosome associated membrane protein 3 (LAMP3), a target of ATF4 mediated transcriptional activation, being crucial for metastasis of hypoxic breast tumour cells (Mujcic et al., 2013). Many other associations between cancer and ER stress have been reported, with numerous UPR signalling components upregulated in various cancers, some of these have been summarised in table 1.2.

Table 1.2. Association of UPR and ER stress markers with cancer. Adapted from Yadav et al., 2014 (Yadav et al., 2014)

Cancer	Sample	ER stress association
Breast	Human breast cancer tissues	Elevated BiP expression
		Elevated sXBP1 mRNA
	Cell lines	Increased ATF4 expression in severe hypoxia
		BiP relocated to cell surface, exacerbating ER stress
Prostate	C4-2B cell line	BiP relocated to cell surface, exacerbating ER stress
Pancreatic	Human tumour xenograft mice	PERK promotes angiogenesis
Liver	Human hepatocellular carcinoma tissues and SMMC7721 cell line	Bip promotes invasion
Lymphoma	Patient	sXBP1 promotes proliferation in hypoxia
Brain, central nervous system	Human brain tumour specimens, various cell lines	Elevated levels of BiP
	Glioblastoma patient samples	Inhibiting IRE1α enhances oncolytic therapy
Colorectal	HT29 cells	Increased ATF4 expression in severe hypoxia
	Various human colon carcinoma cell lines	BiP relocated to cell surface, exacerbate ER stress and promote invasion
Ovarian	Patients	Elevated levels of BiP

1.6.3 ER stress during viral infections

Viral infection is one of the many extrinsic factors that can induce ER stress within a cell (Figure 1.7) (Zhang and Wang, 2012). Viruses hijack the cellular protein synthesis machinery for the production of their own proteins, and in doing so impart a large protein folding burden on the cell, leading to an overwhelming build-up of misfolded protein (Zhang and Wang, 2012). Additionally, some viruses encode pore like proteins which can act to permeabilise membranes and disrupt the ER calcium pool (Tian et al., 1995; Gros et al., 2008). It seems that the UPR has evolved alongside viruses in part as a defence mechanism. PERK mediated inhibition of translation, ERAD and RIDD (Bhattacharyya, 2014) degradation of viral mRNAs and proteins as well as interferon responses activated by the UPR can all act to frustrate viral replication (Galluzzi et al., 2017). On the other hand, the UPR can be manipulated by viruses which can activate specific arms of the response at particular stages of infection to optimise cellular conditions for virus replication. For example dengue virus activates PERK signalling early in infection but then supresses PERK and activates IRE1 and ATF6 signalling at later stages of infection (Peña and Harris, 2011). A non-exhaustive list of reports of viruses either inducing ER stress, upregulating UPR components or mediating the UPR response in some way is shown in table 1.3.

Given the wealth of research into the life cycle of human adenoviruses, their pre-eminence as vectors for gene therapy and their mounting therapeutic relevance as oncolytic agents, very little is known about their propensity to induce ER stress or to modulate UPR signalling. One report found that expression of the E1B 55K and E4ORF6 proteins was necessary to limit phosphorylation of eIF2α at the late stages of infection, though this was through inhibition of protein kinase R (PKR) activity rather than of PERK activity (Spurgeon and Ornelles, 2009). Transcription factor NF-κB, which is often

activated in response to ER stress and PERK signalling (Deng et al., 2004) has also been found to be activated by build-up of adenovirus E3/19K protein in the ER, but this was attributed to a mechanism associated with calcium release and independent of classical UPR signalling.

Table 1.3. Reported interactions between the UPR and virus infections. Adapted from (He et al., 2006) and (Asha et al., 2018).

Virus	Reported site of interaction
Cytomegalovirus	XBP1, ATF4, ATF6
Herpes simplex virus 1	PERK
Hepatitis B virus	BIP
Papillomavirus	GADD34
Vaccinia virus	PERK
Hepatitis C virus	BiP, PERK and XBP1
Japanese encephalitis virus	BiP and CHOP
Influenza A virus	BiP
Respiratory syncytial virus	BiP
Vesicular stomatitis virus	BiP and PERK
Epstein-Barr virus	ATF6
Hepatitis E Virus	IRE1
Dengue Virus	ATF6, IRE1 and PERK
Cytomegalovirus	IRE1 and PERK

1.6.4 ER stress in oncolytic virotherapy

Numerous investigators have reported important implications of ER stress and the UPR for oncolytic virotherapy. The question as to whether ER stress and the UPR should be inhibited or induced in order to enhance oncolytic potency seems to depend on the virus and cell type in question.

Mahoney et al used an siRNA screening approach to knockdown many cellular genes in order to identify which of these might play important roles in modulating the replication

of oncolytic rhabdovirus (Mahoney et al., 2011). Bioinformatic analysis of their results revealed that many of the genes which when knocked down enhanced oncolysis were in fact genes with functions in the UPR signalling pathway. In particular, knockdown of ATF6 and of IRE1 (and therefore inhibition of XBP1 splicing) were found to dramatically sensitise cells from patient samples and mouse tumour models to oncolysis (Mahoney et al., 2011). On the other hand, induction of ER stress and UPR signalling by treatment with ER stress inducing chemical bortezomib has been reported to act synergistically with HSV-1, increasing its replication and antitumour effect in glioma mouse xenograft models (Yoo et al., 2014). The synergistic effect of bortezomib has also been observed during infections with the reovirus based oncolytic agent Reolysin, which is currently under clinical development (Kelly et al., 2012).

There is very little literature on the relationship between adenovirus and ER stress, but currently it seems that adenovirus might benefit from chemical induction of the UPR. Greber and colleagues found that chemical inhibition or genetic knockdown of Golgi-specific brefeldin A-resistant guanine nucleotide exchange factor 1 (GBF-1) stimulated Ad5 replication (Prasad et al., 2014). Blockade of GBF-1 by treatment with golgicide A (GCA) induced ER stress by disruption of ER-to-Golgi apparatus and intra-Golgi apparatus membrane transport. Treatment of A549 lung cancer cells with GCA enhanced the post-entry steps of infection, increasing the levels of early and late gene expression and the titre of infectious virus particles. The treatment also acted synergistically with the Ad5 virus to increase cancer cell killing. Importantly, these effects seemed to be dependent on IRE1 mediated XBP1 splicing, since addition of 4μ8C, an inhibitor of IRE1, ablated the GCA induced boost to infection that had been observed (Prasad et al., 2014). These effects are probably cell type and virus species dependent, but they demonstrate

the possibility of enhancing oncolytic adenovirus therapies by manipulation of ER stress and the UPR.

It is clear that a better understanding of the interactions between oncolytic viruses and their host cancer cell will aid in designing better oncolytic therapies in the future, and interactions with the UPR are no exception to this. Some important benefits have already been seen in preclinical investigations and indicate that modulation of the UPR may represent an important opportunity for enhancing oncolytic therapies. This is particularly the case for adenoviruses, where relatively little is known about such interactions and further work to elucidate them is certainly warranted.

1.7 *Thesis overview and hypothesis*

1.7.1 Overview

Oncolytic viruses hold much promise for the treatment of cancer and some patients are already seeing benefits from their development. However, with response rates in phase II trials ranging from 30% to 70% (Mahoney et al., 2011), strategies to potentiate oncolytic viruses or sensitise cancer cells to their killing will be important if wider cohorts of patients are to benefit. The design of improved oncolytic agents impinges on our understanding of the tumour and virus biology, and how they interact with one another. It is becoming ever clearer that ER stress and activation of UPR signalling is tightly associated with the progression of many tumours, as well as many viral infections. Whilst the response of viruses to induction of ER stress is far from uniform, there is growing appreciation of the mechanisms by which viruses induce and manipulate these signalling

events to their own advantage. The improved understanding of these considerations has led to considerable success in optimising oncolytic therapies by manipulating the UPR, but this approach is relatively unexplored in the context of adenovirus.

Therefore, the overarching aim of this thesis is to examine the relationship between the adenovirus life cycle and induction of ER stress and the UPR. This is done primarily using the group B adenovirus Enadenotucirev, however the parental virus Ad11p and group C Ad5 are also used and provide useful insights and comparisons. The aim is also to explore whether approaches to manipulate the UPR might represent a viable strategy for the potentiation of oncolytic adenoviruses therapeutically. To test this, chemical inducers of ER stress are used in combination with the viruses, as well as the engineering of an armed virus to bring about RNAi mediated knockdown of a target gene in an attempt to induce ER stress. The mechanisms which mediate the effects observed are explored in detail by numerous experimental approaches.

1.7.2 Hypothesis

1. Adenovirus infection induces ER stress in its infected host cell

2. Chemical induction of ER stress and UPR signalling will potentiate EnAd oncolytic activity

3. EnAd can be armed with the ability to knockdown a target protein to induce ER stress and enhance its activity.

In the final chapter, based on the interpretation of the evidence presented in the previous two chapters, a new hypothesis is proposed:

4. Potentiation of adenovirus replication by treatment with ER stress inducing chemicals is due to calcium flux modulation, rather than UPR signalling

2 Materials and Methods

2.1 *Molecular Biology*

2.1.1 Production of heat shock competent *E.coli* cells

For plasmid amplification, XL10 Gold Ultra-competent Escherichia coli (*E.coli*) bacteria were used. Stock batches of competent cells were prepared from fresh aliquots of XL10 cells (Stratagene, USA). A frozen aliquot was used to inoculate 3 mL of 2YT media and cultured at 37°C using an orbital incubator (SI-300R, Medline Scientific, UK). This culture (along with all further cultures at 37°C) were incubated with 200 RPM agitation. Once an optical density (OD) of 0.3 at 550 nm had been reached, the 3 mL culture was added to a fresh 200 mL culture of prewarmed 2YT media and incubated until the OD550 reached 0.480. Cultures were then kept on ice for 5 minutes and subsequently pelleted by centrifugation at 4°C for 20 minutes. Cells were then resuspended in 80 mL sterile transformation buffer I (TFBI; see Materials for recipe) and kept on ice for 5 minutes. Bacterial cells were pelleted again, resuspended in 8 mL transformation buffer II (TFBII; see Materials for recipe) and incubated on ice for 15 minutes. Aliquots of 100 µL of competent cells were transferred into pre-chilled microcentrifuge tubes, frozen on dry ice and transferred to -80°C for long term storage.

2.1.2 Bacterial transformation

Recombinant plasmid DNA was amplified by transformation into competent *E. coli* cells. For transformation, an aliquot of competent *E. coli* cells was thawed on ice. Plasmid DNA (10 to 100 ng) was then added and cells were incubated on ice for a further 20 minutes.

Cells were heat-shocked by transferring tubes to a water bath at 42°C for 30 seconds after which the tube was placed back on ice. Up to 500 µl of Super Optimal broth with Catabolite repression (SOC) (Thermo Fischer, UK) was added to each tube and incubated at 37°C with agitation for 45 minutes. Samples were then spread on to LB agar (1.5% agar) plates supplemented with the relevant antibiotic for selection (50 µg/mL ampicillin or 50 µg/mL kanamycin) and incubated at 37°C overnight for outgrowth and isolation of individual bacterial colonies. Individual colonies were picked and used to inoculate a culture of Luria Bertani (LB) broth (20 g/L) which were grown overnight at 37°C with shaking (200 rpm) in an orbital incubator (SI-300R, Medline Scientific, UK).

2.1.3 DNA purification and precipitation

Plasmid DNA was purified from mini-prep cultures of bacterial cells using QIAprep Spin Miniprep Kit (Qiagen, UK). For purification from maxi-prep cultures using the Qiagen High Speed Maxi-prep kit (Qiagen, UK). Following plasmid purification, plasmid clones were screened by diagnostic restriction digest and resolved by agarose gel electrophoresis. Plasmids were further validated at the sequence level by Sanger sequencing (Eurofins Genomics, Luxemburg). For molecular engineering applications using PCR amplification or digestions, the desired DNA fragments were visualised by agarose gel electrophoresis. The band was then excised from the gel and purified using the QIAquick Gel Extraction Kit (Qiagen, UK). Commercial column-based purification kits are unsuitable for the purification of very large DNA fragments (> 20 kb), such as whole adenovirus genomes. For the purification of large fragments, DNA was precipitated using isopropanol. An equal volume of isopropanol was added to the DNA solution, mixed thoroughly, and incubated for 60 minutes at -80 °C. The DNA was pelleted by centrifugation for 30 minutes at 15,000 g at 4°C, and the supernatant removed

by pipetting. The DNA pellet was air-dried and resuspended in nuclease-free water (Thermo Fisher, UK) before use in downstream applications.

2.1.4 DNA restriction digests

Restriction endonucleases were used to generate diagnostic digestion patterns for validation of plasmid DNA, or to produce DNA with overhanging 'sticky' ends for molecular engineering and ligation into vectors with complementary overhanging ends or in Gibson assembly reactions. All digestion reactions were performed according to manufacturer's instructions (New England Biolabs, UK). In short, up to 5 µg DNA, 2 µL enzyme and an appropriate buffer solution were combined in a 100 µL reaction volume and incubated at 37°C for 3 hours.

2.1.5 Polymerase chain reaction (PCR) amplification

PCR amplifications were performed with 10 ng of the relevant DNA template, custom synthesised primers (Thermo Fischer, UK) at a concentration of 10 µM, and Phusion DNA polymerase Master Mix (Life Technologies, UK) according to manufacturer's instructions. In summary, this involved an initial denaturation step (98°C for 30 seconds), followed by 25 iterative cycles of denaturation (98°C for 10 seconds), annealing (temperature calculated based on annealing temperature of primers, 10 seconds), and extension (72°C for 15 seconds/kb), and ending with a final extension step (72°C for 10 seconds). Upon completion, PCR reactions were kept at 4°C for short term storage. PCR reactions were performed using a PTC-225 Peltier Thermal Cycler DNA Engine Tetrad (MJ Research, USA).

2.1.6 Agarose gel electrophoresis

Agarose gel electrophoresis enabled visualisation of DNA from purified plasmids, validation of plasmids by inspection of diagnostic digest pattern, fragments from restriction digests or PCR reactions, and splicing patterns of RNA transcripts. The size of any given band was estimated by comparison to a commercially available molecular weight marker (Generuler 1kb, Thermo Fischer, UK). DNA was resolved by size on 1% (w/v, unless otherwise stated) agarose gels containing 1X Gel Red nucleic acid stain (Biotium, UK) in 1 × TAE buffer (composition provide in Materials). Following loading of DNA into wells, gel electrophoresis was initiated (10 volts per cm gel length, 30 – 120 minutes) in DNA electrophoresis gel tanks (Bio-Rad Laboratories Ltd, UK). For the excision of bands for downstream purification, bands were visualised under blue light using Dark Reader transilluminator (GRI, UK). For all other applications, DNA was visualised under ultraviolet light using a fluorescent imaging system (AlphaImager, Alpha Innotech Corportation, USA).

2.1.7 Quantification of purified DNA

DNA concentration was determined using a Nanodrop spectrophotometer (Thermo Scientific, UK). The Nanodrop was blanked using the solution in which the DNA was suspended (either nuclease free water, or elution buffer from the relevant kit) prior to loading and measurement of the sample.

2.1.8 DNA ligation

Insert and vector DNA underwent single or double restriction endonuclease digest in order to generate compatible and complementary overhanging DNA ends for subsequent

ligation of the insert into the vector. The digested insert was purified by gel extraction from an excised agarose using QIAquick gel extraction kit (QIAGEN, UK). To reduce the number of vector re-ligations, and therefore the number of false positive colonies, the vector was dephosphorylated by treatment with 2 µL of calf intestinal alkaline phosphatase (CIAP, Invitrogen, USA) for 2 hours at 37°C, and DNA purified as above. All purified DNA was eluted in nuclease-free water. Ligation reactions were performed using T4 DNA Ligase (New England Biolabs, UK), with a ratio of vector:insert ratio of 1:3, according to manufacturer's instructions.

2.1.9 Gibson assembly

Gibson assembly enables the ligation of numerous DNA molecules in a single reaction providing that the molecules to be assembled have 20-40 bp of overlapping sequence homology with their adjacent fragment. Suitable fragments containing the required homologous flanking sequence were generated by PCR amplification or by annealing complementary oligonucleotides, and DNA was purified as described above. Gibson assembly reactions were performed using NEBuilder HiFi DNA Assembly Master Mix (New England Biolabs, UK). Briefly, 10 µl of the 2x HiFi master mix was combined with 10 µl of solution containing 100 ng of plasmid DNA and a three-fold molar excess of fragments. The reaction was then incubated at 50°C for 15 minutes before transformation into competent *E. coli*.

2.2 *Cell Culture*

2.2.1 Maintenance of cell lines

Cell lines were cultured in the Dulbecco's Modified Eagle's Medium (DMEM) with high glucose (Sigma Aldrich, UK) and maintained at 37°C in a humidified incubator with 5% CO_2. Growth medium was supplemented with 10% fetal bovine serum (FBS, Gibco, UK). DMEM supplemented with 10% FBS is known herein as complete culture medium. For sub-culturing, cells were washed with phosphate buffered saline (PBS), treated with 0.05% trypsin (Sigma-Aldrich, UK) and incubated at 37°C until cells detached from the culture flask. Complete culture medium was added to the cells to neutralise the trypsin. Cell clumps were disaggregated by pipetting and subsequently passaged or plated for experiments. When cells were to be seeded into microplates, they were counted using a haemocytometer and the appropriate number of cells were diluted into an appropriate volume of growth medium. Cells were then added to the wells of the microplate. All cell lines were authenticated by short tandem repeat (STR) profiling (CRUK Cambridge Institute, Cambridge) and routinely tested for mycoplasma using MycoAlert™ Mycoplasma Detection Kit (Lonza, Switzerland). Details of cell lines used in this thesis are provided in table 2.1.

Table 2.1. Details of cell lines used in this thesis.

Cell line	Source	Description	Culture medium
SK-OV-3	ATCC, USA	Human adenocarcinoma cells derived from ovaries	DMEM + 10% FBS
DLD-1	ATCC, USA	Human adenocarcinoma cells derived from colon	DMEM + 10% FBS
A549	ATCC, USA	Human carcinoma cells derived from lung	DMEM + 10% FBS
293T	ATCC, USA	A subclone of the 293 cell line containing the SV40 large T antigen	DMEM + 10% FBS
HEK293A	ATCC, USA	An adherent subclone of the 293 cell line, derived from human embryonic kidney cells transformed with adenoviral E1A gene.	DMEM + 10% FBS
HT-29	ATCC, USA	Human adenocarcinoma cells derived from colon	DMEM + 10% FBS

2.2.2 Cryopreservation of cells and cell recovery

To prepare cells for cryopreservation, cells were resuspended in freezing medium (FBS + 10% DMSO) to protect cells from the formation of crystals. Cryovials were used to store 1 mL of cell suspension and were placed at -80°C in freezing containers. When cryopreserved cells were to be recovered for use, frozen vials were thawed at 37°C in a water bath with gentle agitation. Once thawed, cells were transferred to a 15-mL falcon tube. Pre-warmed culture medium was added, and cells were pelleted by centrifugation for 5 minutes at 350g. Cells were then resuspended in fresh growth medium and transferred into a culture flask for culturing.

2.2.3 DNA transfections

DNA transfections were performed using Lipofectamine 2000 (Life Technologies, UK) transfection reagent following the manufacturer's instructions. Briefly, DNA and lipofectamine were added separately to OptiMEM (Life Technologies, UK) and incubated at room temperature for 5 minutes. The two suspensions were then combined and incubated at room temperature for a further 20 minutes. A ratio of 1 µg DNA to 3 µl of lipofectamine was used. The mixture was then added dropwise onto cells in microplate wells, culture flasks or plates. After 6 hours, the culture media was replaced with fresh complete culture medium.

2.2.4 Virus infections

Infections were carried out in complete culture medium at a dose of 100 virus particles per cell (VPC) unless otherwise stated. Cells were exposed to the infection media for two

hours, unless otherwise stated, after which time infection media was replaced with DMEM supplemented with 2% FBS.

2.2.5 siRNA transfections

siRNA transfections were performed with Lipofectamine 2000 (Life Technologies, UK) transfection reagent following the manufacturer's instructions. Cells were seeded in 24-well plates to achieve approximately 40% confluency. The following day, each well was transfected with 40 pMol of siRNA as follows: 40 pMol of siRNA was added in 50 µl of OptiMEM (Life Technologies, UK) using 1 µl of Lipofectamine 2000 suspended in 50 µl OptiMEM (prepared separately). Mixtures were incubated at room temperature for 5 minutes and then combined. Complexation was allowed to occur for 20 minutes before the mixture was applied to cells dropwise by pipetting. At 6 hours post-transfection, the media was replaced with fresh complete culture medium. Silencer Select ® siRNAs were purchased from Thermo Fischer UK. Sequences are provided in Table 2.2.

Table 2.2. Details of siRNAs used in this thesis

Target	Assay ID	Sense	Antisense
SERCA2	s1746	CCACAAGUCUAAAAUCGUATT	UACGAUUUUAGACUUGUGGGA
SERCA2	s1747	GAUCAUGUCUGUCAUUCGATT	UCGAAUGACAGACAUGAUCTT
SERCA2	s1748	CAACUGGAGUUAACACCGATT	UCGGUGUUAACUCCAGUUGCT
PKCα	s11094	GGCUGUACUUCGUCAUGGATT	UCCAUGACGAAGUACAGCCGA
No target	#2	N/A	N/A

2.2.6 Production of lentiviral constructs

Recombinant lentivirus was used for the generation of stably transduced cell lines expressing a gene of interest. The pCAX-F-XBP1delDBD-venus plasmid was a kind gift from Professor Masayuki Miura (University of Tokyo). The pCAX-FXBP1delDBD plasmid was digested with KpnI and NheI restriction enzymes and the XBP1-Venus fusion fragment (approximately 1000 bp) was purified by gel extraction (Figure 3.3B). This fragment was ligated into a third-generation lentiviral expression vector (pSF-Lenti) digested with the same restriction enzymes to generate pSF-Lenti-XBP1-Venus, which also contained a puromycin resistance gene driven by the phosphoglycerate kinase 1 (PGK) promoter. Recombinant plasmids were screened for correct insertion of the transgene by diagnostic enzymatic digestion and sanger sequencing. Lentiviruses were generated by cotransfection of 293T cells with pSF-Lenti-XBP1-Venus alongside three packaging plasmids (pSF-CMV-HIV-Rev, pSF-CMV-VSVG, and pSF-CMV-HIV-Gag-Pol, Oxford Genetics, UK) using Lipofectamine 2000. Cell supernatants were harvested 48 hours post-transfection and passed through a 0.45 μm filter to clear cellular debris. Supernatant containing lentivirus was then aliquoted and stored at -80°C for future use.

2.2.7 Generation of cell lines by lentivirus infection

Lentiviral infections were performed by serially diluting the lentivirus onto A549 cells in 6-well plate format (2×10^5 cells/well). To enhance the efficiency of infection, polybrene (Sigma Aldrich, UK) was added to the lentivirus-containing media to a final concentration of 4 μg/mL. Polybrene is a polycation that reduces the charge repulsion between the membrane of the cell and the lentivirus. Infected plates were then incubated under cell culture conditions for 24 hours, at which point the infection media was replaced with complete culture medium with puromycin antibiotic for selection. The appropriate

concentration of puromycin had been pre-determined to be 2 µg/ml by setting up a dose response kill curve. Over the following two weeks, successfully transduced cells formed colonies. Surviving colonies were then pooled and reseeded at serial dilution in fresh media supplemented with 2 µg/mL puromycin in order to isolate individual cell clones. Individual clones were isolated and expanded.

2.3 *RNA work*

2.3.1 RNA extraction

Cells were seeded in microplate wells to 70-80% confluence and the following day treated as indicated. At the indicated time points, cells were washed in PBS and then harvested in 350 µl RLT buffer (Qiagen, UK, # 79216) supplemented with 10% β-mercaptoethanol (Sigma Aldrich, UK, #M6250) by scraping the cells from the well. Samples were stored at -80°C until RNA extraction was performed using the RNeasy mini kit (Qiagen, UK, # 74104) with on-column DNA digestion following manufacturer's instructions. RNA content was measured on a NanoDrop Microvolume Spectrophotometer (ThermoFischer, UK).

2.3.2 Reverse transcription

To quantify cellular mRNA, 800 ng total RNA was reverse transcribed into cDNA using the QuantiTect Reverse Transcription Kit (Qiagen, UK, # 205310) following the manufacturer's instructions. In short, 800 ng RNA was combined with 2 µl gDNA Wipeout buffer in a 14 µl reaction and incubated at 42°C for 2 minutes. RNA was then

reverse transcribed into cDNA in a 20 µl reaction by adding random primers, buffer and an RNA-dependent DNA polymerase with RNase H activity to degrade the RNA in the DNA:RNA duplex. This reaction mixture was incubated at 45°C for 15 minutes.

2.3.3 Assessment of XBP1 splice status

Spliced and unspliced XBP1 was amplified using 5 µl of the reverse transcription reaction and primers 5′-TTACGAGAGAAAACTCATGGCC-3′ and 5′-GGGTCCAAGTTGTCCAGAATGC-3′ (Mendez et al., 2015). The polymerase chain reaction product was resolved on a 2.5% agarose gel, revealing amplicons for the XBP1 full-length product (289 bp) and spliced product (263 bp). A third band was also often observed which is generated by the annealing of a spliced strand with an unspliced strand to generate a hybrid band that migrates more slowly through the gel. This hybrid band is often reported in the literature (Shang and Lehrman, 2004).

2.4 *Quantitative PCR*

2.4.1 Quantification of viral genomes

EnAd, Ad11p and Ad5 genomes were measured by quantitative PCR (qPCR). Cells were seeded in microplates and the following day infected and treated as appropriate. At the designated time points, cells were scraped from the wells in their supernatants and transferred into microcentrifuge tubes. DNA extraction was carried out using the PureLink Genomic DNA Purification Kit (Life Technologies, UK, #K182001) following the manufacturers protocol. The eluted DNA was diluted 1000-fold in diethyl

pyrocarbonate (DEPC)-treated nuclease free water, and 5 µl of this was used in a 20 µl qPCR reaction. The reaction consisted of 2x qPCRBIO Probe Mix Hi Rox (PCR Biosystems, UK), and 10 µM each of forward and reverse primers and hexon probe (Table 2.3). Cycling conditions were as follows: one cycle at 95°C for 2 min, followed by 40 cycles at 95°C for 5 s and 60°C for 30 s. C_T values from known quantities of virus particles were used to calculate a standard curve.

Table 2.3. Primers and probes used for qPCR detection of viral genomes

Virus	Target	Oligo	Sequence (5'-3')
EnAd/Ad11p	Hexon	Fwd primer	TACATGCACATCGCCGGA
		Rev primer	CGGGCGAACTGCACC
		Probe	[6FAM] CCGGACTCAGGTA 3'CTCCGAAGCA TCCT [TAM]
Ad5	Fibre	Fwd primer	TGGCTGTTAAAGGCAGTTTGG
		Rev primer	GCACTCCATTTTCGTCAAATCTT
		Probe	[6FAM] TCCAATATCTGGAACAGTTCAAAG TGCTCATCT [TAM]

2.4.2 Reverse transcription PCR

EnAd E1A and E2B mRNA levels were measured by RT-qPCR. Total RNA was extracted, and cDNA generated as described in section 2.3.1 of this thesis. mRNA copies were quantified in a 20 µl qPCR reaction consisting of 2x qPCRBIO Probe Mix Hi-Rox (PCR Biosystems, UK), and 10 µM each of forward primer, reverse primer, and probe (Table 2.4). Cycling conditions were as follows: one cycle at 95°C for 2 min, followed by 40 cycles at 95°C for 5 s and 60°C for 30 s. C_T values from known copy numbers of each gene were used to calculate a standard curve.

Table 2.4. Primers and probes used for qPCR quantification of EnAd transcripts.

Target	Oligo	Sequence (5'-3')
E1A	Fwd primer	CCATCTCCTGATTCTACTACC
	Rev primer	CCGTGTACTCAAGTCCAA
	Probe	[6FAM] TAAGCCTGGGAAACGTCCAGCAGT [BHQ1]
E2B	Fwd primer	CTCTTCAATGATGTTACTTTCG
	Rev primer	GTAGCGAAGCGTGAGTAAG
	Probe	[6FAM] AGGCTCCCTGTTCCCAGAGTTGGA [BHQ1]

2.5 *Evaluation of cell cytotoxicity*

2.5.1 Cell killing xCELLigence assay

Viability of cells following infection with adenoviruses was tracked using xCELLigence RTCA technology (ACEA Biosciences). In this system, specialised E-plates (ACEA Biosciences) with electrodes embedded at the base of the well are used. The electrodes measure an electrical current that flows through the culture medium between the electrodes. In the absence of cells, the current flows freely. When cells are present, they impede the current, and thus by measuring the magnitude of the impedance a cell index (CI) score is calculated that relates to the number of cells adhering to the well surface and the nature of this adherence, allowing cytotoxicity of the cell monolayer to be tracked. The cell viability assay was performed according to manufacturer's instructions. Briefly, target cells were seeded in the specialised E-plates and incubated at 37°C in a humidified chamber for 24 hours. Cells were infected with virus for two hours and then subsequently infection media was substituted for treatment media. Cell index values were monitored every 15 minutes for the duration of the experiment.

2.5.2 MTS assay

Cell viability was determined using CellTiter 96 Aqueous One Solution Cell Proliferation Assay (Promega, UK, G3582). The assay measured the ability of cells to reduce a tetrazolium compound into a coloured formazan product, which only occurs in metabolically active cells. In brief, 20,000 cells were seeded in 96-well plate format and the following day treated with various compounds. Treatments were carried out using complete culture medium After the indicated time, the supernatant was replaced with 80 µl PBS and 20 µl of MTS reagent. Plates were incubated at 37°C in a humidified chamber for 1–2 hours to allow the reaction to occur. Absorbance was measured at 490 nm using a POLARstar Omega plate reader spectrophotometer (BMG Labtech). A blank measurement (media only, no cells) was subtracted from all other measurements, and values were expressed as a percentage of the untreated cell absorbance value.

2.6 *Western blotting*

2.6.1 Sample preparation, PAGE and transfer to nitrocellulose membrane

Protein expression in cells was analysed by western blotting. Cells were harvested by removing the supernatant from cell cultures and rinsing gently with PBS. Cells were lysed by adding Pierce RIPA lysis and extraction buffer (Thermo Fischer, UK, #89901), supplemented with 1 x Halt™ protease and phosphatase inhibitor single-use cocktail (Thermo Fischer, UK, #78442) protease inhibitor directly to the cell monolayer and incubating at room temperature for 5 minutes. Lysates were scraped and transferred into 1.5 mL Eppendorf tubes and incubated with 2.5 U Benzonase for 30 minutes at room temperature. Lysate concentrations were measured by the QuantiPro BCA Assay Kit

(Sigma-Aldrich, UK, QPBCA-1KT). Samples containing 30 µg of each protein lysate in 1x Laemmli sample buffer were heated at 95°C for 5 minutes. Proteins were separated on a 4-20% Mini-PROTEAN TGX Precast Protein Gel (Bio-Rad, UK) in Tris-glycine running buffer with : sodium dodecyl sulfate (SDS) (see Materials for composition) and transferred onto a 0.2 µm nitrocellulose membrane using the wet blot method in transfer buffer (see Materials for composition).

2.6.2 Immunoblot and detection

After transfer of protein to membranes, membranes were washed in TBST (Tris-buffered saline with 0.05% Tween-20, Sigma Aldrich, UK). Non-specific binding blocked by incubation with 5% skimmed milk powder (Sigma Aldrich, UK, 1153630500) in TBST with constant agitation on a benchtop tube roller at room temperature for two hours. Membranes were then incubated with the appropriate primary antibody at the appropriate dilution in 5% milk in TBST overnight at 4ºC. The next day, membranes were washed three times in TBST for five minutes. Next, membranes were incubated with the appropriate secondary antibody at the appropriate concentration in 5% milk TBST with constant agitation for two hours. Details of all antibodies used are provided in Table 2.5.

Membranes were again washed for five minutes three times in TBST. Membranes were incubated with SuperSignal West Dura Extended Duration Substrate (Thermo Fisher, UK, #34075) and bands detected using the Gel Doc system (Bio-rad). Quantification of blots was performed by densitometry using ImageLab software. Intensity volume of the bands was normalised to its relevant loading control. Values were divided by the value of the untreated control band to give relative fold change values which are displayed on blot figures.

Table 2.5. List of antibodies used in western blotting

Antibody	Species/isotype	Clone	Dilution	Company
Direct-Blot™ HRP anti-DYKDDDDK Tag	Rat IgG2a, λ	L5	1:5000	Biolegend
Anti-β-Actin−Horseradish peroxidase	Mouse, IgG1	AC 15	1:50000	Sigma Aldrich
Phospho-PKC (pan) (βII Ser660)	Rabbit, IgG	N/A	1:1000	Cell Signaling Technology
Phospho-PKCα/β II (Thr638/641)	Rabbit, IgG	N/A	1:1000	Cell Signaling Technology
Phospho-PKD/PKCμ (Ser916)	Rabbit, IgG	N/A	1:1000	Cell Signaling Technology
PKD/PKCμ (D4J1N)	Rabbit, IgG	N/A	1:1000	Cell Signaling Technology
Phospho-PKCδ (Thr505)	Rabbit, IgG	N/A	1:1000	Cell Signaling Technology
Phospho-PKCδ/θ (Ser643/676)	Rabbit, IgG	N/A	1:1000	Cell Signaling Technology
Phospho-PKCθ (Thr538)	Rabbit, IgG	N/A	1:1000	Cell Signaling Technology
Phospho-PKCζ/λ (Thr410/403)	Rabbit, IgG	N/A	1:1000	Cell Signaling Technology
PKCα	Rabbit, IgG	N/A	1:1000	Cell Signaling Technology
Anti-mouse IgG HRP-linked	Horse, IgG	N/A	1:2000	Cell Signaling Technology
Anti-rabbit IgG HRP-linked	Goat, IgG	N/A	1:3000	Cell Signaling Technology
SERCA2	Rabbit	N/A	1:2000	Cell Signaling Technology
BiP	Mouse, IgG2a	40/BiP	1:5000	BD
Adenovirus -2/5 E1A (13S)	Rabbit, IgG2a	M73	1:2000	Santa Cruz Biotechnologies
Anti-adenovirus (ab36851)	Goat, IgG	N/A	1:20000	Abcam

2.7 *Adenovirus production*

2.7.1 Production of virus stocks

2.7.1.1 Virus amplification

To amplify virus to create high yield stocks of EnAd, EnAd-CMV-GFP, EnAd-SA-GFP, Ad11p, Ad5 and Ad5-CMV-GFP, a 10-layer HyperFlask (Corning, USA) was seeded with HEK293A cells. Once confluent, cells were infected 100 VPC with each of the viruses. Once cytopathic effect (CPE) was observed, cells were detached by gentle agitation and collected from the flask, pelleted and resuspended in 10 mL of the supernatant and stored at -80°C until virus purification by caesium chloride (CsCl) gradient banding.

2.7.1.2 Virus purification by caesium chloride gradients

Complete virus particles were purified by ultracentrifugation over a CsCl gradient, with viral particles forming distinct bands based on their size and density. For purification, adenovirus-infected cells harvested from hyperflasks were subjected to three rounds of freeze-thawing in liquid nitrogen and a 37°C water bath, releasing the virus from the cells. In order to remove cellular debris, the lysate was centrifuged at 500 g for 15 minutes at 4°C. The pellet was discarded and the supernatant containing the free virus particles was collected. The supernatants were applied to discontinuous CsCl gradients in centrifugation tubes (Figure 2.1A). The gradient was constructed by underlaying 2 mL of CsCl (ρ = 1.45) underneath 3 mL of CsCl (ρ = 1.32), on top of which 2 mL of 40% glycerol was carefully added. Then the supernatant containing the free virus particles was

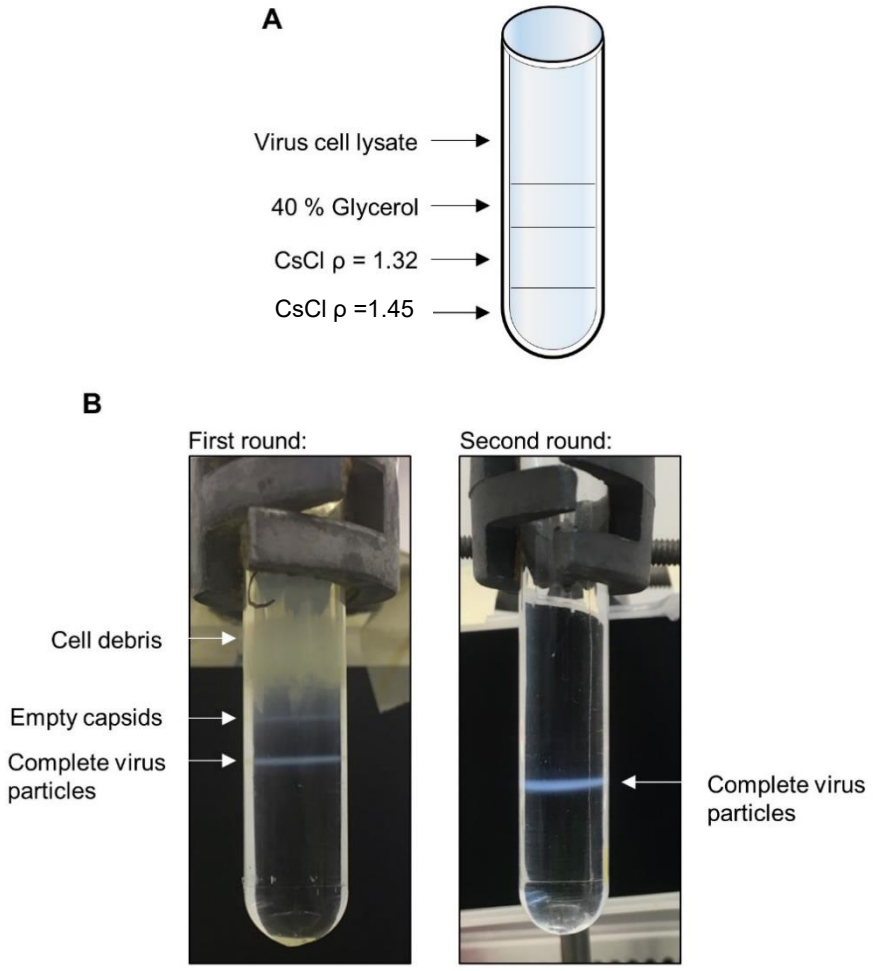


Figure 2.1 Purification of virus stocks by caesium chloride (CsCl) gradient banding. A) Diagram representing the CsCl gradient constructed in an ultracentrifuge tube for virus purification**.** Two mL of CsCl ρ = 1.45 was underlayed beneath 3 mL of CsCl ρ = 1.32, followed by an overlay of two mL 40% glycerol. Then the virus lysate supernatant is added on top of the glycerol. **B)** Representative images of CsCl banded virus preparations after ultracentirugation. Two rounds of purification were carried out for each adenovirus. The left image shows the tube following the first round of banding using the crude cell lysate preparation, and therefore cellular protein and lipid is visible in a diffuse band towards the top of the tube. Below this two more distinct bands are present. The lower larger band corresponds to complete virus particles (at the (CsCl(ρ1.45): CsCl(ρ1.32) interface), whilst the upper band is formed by the empty viral particles (at the CsCl(ρ1.32):glycerol interface). The right shows a sample after extraction of the lower band, dialysis, benzonase treatment and the second round of banding. The remaining band corresponds to intact virus particles.

added on top of the glycerol layer. Recipes for the above can be found in the materials section.

Tubes were then centrifuged at 25,000 rpm at 10°C for 120 minutes, in a Beckman L8-70M Ultracentrifuge with SW40TI rotor. Once centrifugation was complete, two discrete

bands were apparent – the lower band consisting of complete virus particles packaged with genomes, and the upper band containing viral particles void of complete genomes. To harvest the complete virus particles only, the centrifuge tube was punctured under the lower band with an 18G needle and the lower band collected into a syringe. (Figure 2.1.B).

The CsCl was then removed by dialysing twice in PBS at 4°C, and subsequently once in PBS supplemented with 4-(2-hydroxyethyl)-1-piperazineethanesulfonic acid (HEPES). Dialysis was performed using 3-15 mL Slide-A-Lyzer Dialysis cassettes (Thermo Fisher, UK). Virus was then recovered from the cassette, and contaminating unpackaged DNA was degraded by addition of $MgCl_2$ and Benzonase DNA nuclease (EMD Millipore, USA) for 30 minutes at room temperature. Subsequently, another iteration of banding by CsCl gradient was performed as described, and dialysis was performed in PBS using 0.5-3 mL Slide-A-Lyzer Dialysis cassette (Thermo Fisher, UK). Following the final dialysis step, glycerol was added to a final concentration of 40% to recovered virus to act as a cryoprotectant. Aliquots of virus stock were stored at -80°C for future use.

2.7.1.3 dsDNA measurement for adenovirus titre quantitation

The PicoGreen dsDNA assay (Invitrogen, UK) was used in order to measure the DNA concentrations of the purified adenovirus stocks. The assay uses a nucleic acid probe that fluoresces upon binding to dsDNA. Samples of virus stock were diluted in 1×TE buffer with 0.5% SDS and incubated at 56°C for 30 minutes to degrade the viral protein capsids and release the encased genomes. dsDNA was then quantified following the manufacturer's instructions using a standard curve generated by serial dilution of

bacteriophage lambda DNA. Virus particle concentration was calculated for each sample based on 1 μg DNA being equal to 2.7×10^{10} adenovirus particles. Stocks were also titred by the 50% tissue culture infection dose ($TCID_{50}$) method (see section 2.8.) and a VP to $TCID_{50}$ ratio was calculated (Table 2.6.).

Table 2.6. Purified virus stock titres

Virus	VP/mL	$TCID_{50}$/mL	VP:$TCID_{50}$ Ratio
EnAd	2.73E+11	1.58E+10	17.3
EnAd-CMV-GFP	2.94E+11	3.96E+10	7.4
EnAd-SA-GFP	1.35E+11	1.00E+10	13.5
Ad11p	6.41E+11	3.16E+10	20.3
Ad5	1.37E+12	1.26E+11	10.9
Ad5-CMV-GFP	4.04E+11	2.51E+10	16.1

2.7.2 Production of Recombinant Engineered Adenoviruses

2.7.2.1 Virus cloning strategy

Recombinant shRNA expressing EnAd viruses were generated using the Colo2.4 cloning vector (Figure 2.2) containing the EnAd genome. shRNA constructs were inserted immediately downstream of the fibre gene into the EnAd backbone by Gibson assembly. The shRNAs were driven by a U6 promoter sequence and were followed by a T_5 transcription termination sequence (Appendix 1).

The EnAd-FLAG-E1A virus was engineered by Dr Egon Jacobus. Briefly, an *Ndel* flanked 6.6 kbp fragment of the EnAd genome containing the E1A region was amplified by PCR from the ColoAd2.4 plasmid (Figure 2.2) and cloned by sticky ended ligation

into a pSF shuttle plasmid backbone. A double stranded insert encoding the Flag-tag and appropriate homology arms was used for the 3' specific insertion of the Flag-tag at the C terminus of E1A. The modified fragment now containing the flag tagged E1A was amplified from the shuttle plasmid by PCR using primers to introduce homology arms with complementarity to ColoAd2.4. The resulting amplicon was inserted by Gibson assembly into an *NdeI* linearised ColoAd2.4 plasmid. Virus was then rescued, amplified and purified as described below.

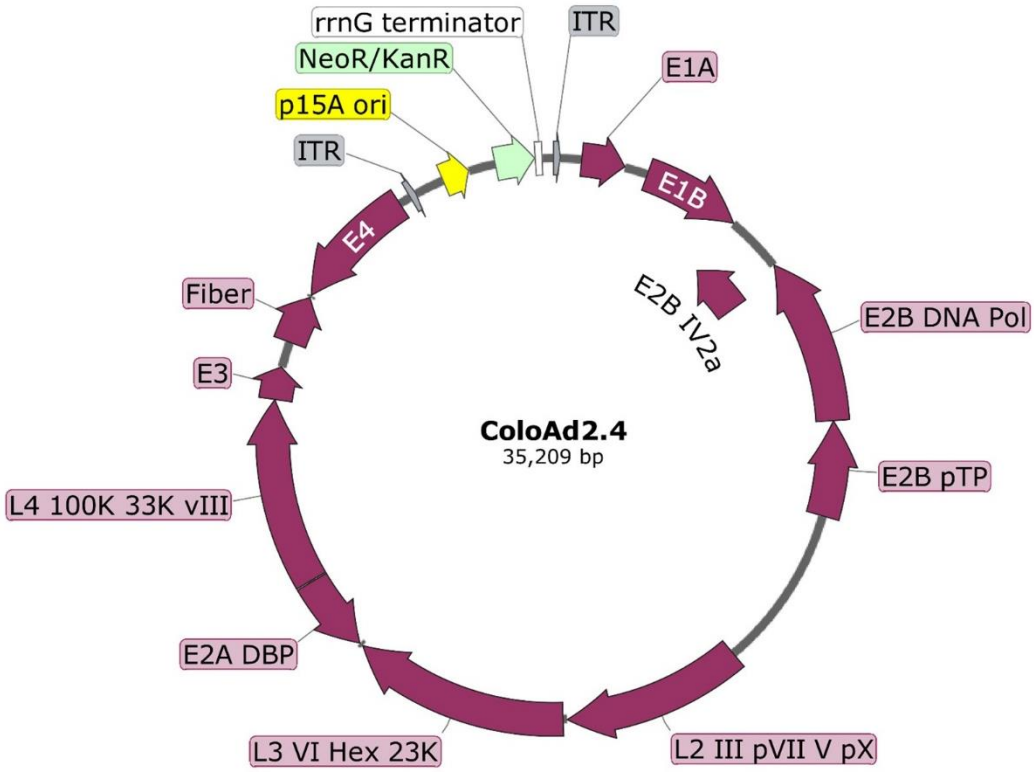


Figure 2.2. Plasmid map of ColoAd2.4 vector. Map of the ColoAd2.4 vector containing the EnAd genome used for engineering recombinant viruses. Transgene shRNA expression cassettes were inserted downstream of the fibre gene. In addition to the viral genome, the plasmid also encodes the genes necessary for plasmid propagation in bacteria and virus production in mammalian HEK293A cells. p15A ori, origin of replication; KanR, Kanamycin resistance; ITR, inverted terminal repeat; E, early; L, late; Hex, hexon

2.7.2.2 Virus rescue and amplification

The modified ColoAd2.4 plasmids encoding the EnAd genome and shRNA expression constructs were linearised by restriction digestion with endonuclease enzyme AscI, which also removes non-viral DNA sequence needed for propagation of the plasmid. Digested DNA was purified by isopropanol precipitation and resuspended in nuclease-free water. HEK293A cells were grown in T25 culture flasks and transfected with 5 µg of linearised DNA using Lipofectamine 2000 transfection reagent (Thermo Fischer, UK) at 80-90% confluency. After 6 hours, the transfection mix was replaced with DMEM supplemented with 2% FBS and flasks incubated at 37°C in humidified chambers until CPE was observed. When extensive CPE was observed, cells were pelleted, and the virus was harvested by three freeze-thaw cycles.

2.7.2.3 Plaque purification

Single viral clones were isolated by serially diluting harvested lysate and re-infecting A549 cells in a plaque assay. To do this, A549 cells were seeded to confluency in 6-well plates. The following day, harvested virus underwent ten-fold serial dilution. For each well, plating medium was replaced by 500 µl of virus dilutions of 10^{-3} to 10^{-8}, with one well remaining uninfected as a negative control. After six hours, infectious media was removed, cells were rinsed in PBS and then overlaid with DMEM containing 0.8 % agarose and 2% FBS. Plates were incubated at room temperature for 15 minutes to allow the agarose to set before incubating the plates at 37°C. When plaques formed and were clearly visible approximately seven days post-infection, the plaque was picked using a sterile pipette tip and used to infect new A549 cells in a T25 flask. When substantial CPE was observed, the process was repeated twice more. Stocks of clonally selected viruses were generated by infecting a larger T175 flask of A549 cells. When CPE was observed,

viruses were harvested from cells by freeze-thaw cycles. Cell debris was removed by centrifugation and the lysate aliquoted and stored at -80°C for future use.

2.8 *Measuring infectious virus particles by $TCID_{50}$*

Quantification of infectious virus particles was performed by the $TCID_{50}$ method. To measure the effect of different treatments of infectious virus particle production in DLD-1 and SK-OV-3 cells, cells were seeded at 50,000 cells per well in a 24-well plate and incubated overnight to adhere. They were then infected in triplicate and, where indicated, subsequently exposed to drug treatments. At the indicated time points, cells were scraped and the sample including supernatant was stored at -20°C until analysis. Samples were subjected to three rounds of freeze-thawing to encourage cell lysis and release of cell associated virus particles. A549 cells were seeded at 20,000 cells per well in 96-well plates in complete culture medium to achieve a 100% confluent cell monolayer. The following day harvested samples were thawed and 10-fold serial dilutions were made using DMEM supplemented with 2% FBS as the diluent ranging from 10^{-3} to 10^{-12}. A549 cells were infected with 200 µl of diluted virus with 10 replicates per dilution. A group of cells acting as a negative control received media known to be free of virus. Cells were incubated for 5 days then scored for the presence of viral plaques by visual inspection using a Zeiss Axiovert 25 microscope. From this scoring, the $TCID_{50}$ was calculated using the KARBER statistical method:

$$\text{Titre } (TCID_{50}/mL) = 10^{\,1 + D\,(S - 0.5)}$$

$$D = \log(d);\ d = \text{dilution factor}$$

$$S = \text{sum of the ratios of wells with CPE to CPE-free wells}$$

2.9 *Luciferase assay*

Cells were plated in 24 well microplates and the following day infected with Ad5-E1A-Luc virus. Two hours after infection, infectious media was replaced with treatment media. Twelve hours after initial infection, cells were lysed in 100 µl passive lysis buffer (Promega, UK, #E1941), scraped and underwent 3 rounds of freeze thaw to encourage cell lysis. Cell debris was removed by centrifugation in a V-bottom plate. Luciferase activity was measured using the Promega luciferase assay system (Promega, UK, #E1500) following the manufacturer's instructions. Briefly, 20 µl of sample was dispensed into wells of a white 96 well microplate, 100 µl of luciferase assay reagent was added to each well. Light produced by each well was quantified by measuring the plate using a POLARstar Omega plate reader spectrophotometer (BMG Labtech). The same samples total protein content was measured in a BCA assay, and used to normalise the luciferase signal to control for cell number.

2.10 *Fluo-8 calcium flux assay*

Cells were seeded in black 96 well microplates in normal DMEM supplemented with 10% FBS. The next day calcium flux was assayed using the Abcam calcium flux no wash fluo-8 kit (Abcam, UK, #ab112129) following the manufacturer's instructions. Briefly, media was removed from the wells and cells were washed with calcium free DMEM. Fluo-8 loading solution was then applied to the well and cells were incubated at 37ºC for 30 minutes, followed by a 30-minute incubation at room temperature. The fluo-8 loading

solution was then removed, and cells were washed with calcium free DMEM, before calcium free DMEM supplemented with 2% dialysed calcium free FBS was added to wells. Fluorescence was then monitored at excitation 490 nm and an emission 525 nm using a POLARstar omega plate reader (BMG Labtech, UK). Baseline fluorescence was measured continuously for 5 minutes, at which point a drug or vehicle control was added using the microplate reader's integrated autoinjectors to achieve the indicated final concentration on cells. After this first injection fluorescence was monitored for a further five minutes at which point calcium was injected back into the medium using the autoinjectors. Fluoresce was measured for a further final five minutes.

2.11 *Flow cytometry*

Cells were harvested form microplates by trypsinisation. Trypsin was neutralised by addition of complete culture medium, and cells were transferred into a V-bottom 96-well plate. Cells were washed with PBS, and then fixed by incubation for 15 minutes in 4% paraformaldehyde (PFA) in PBS at room temperature. After fixation, cells were washed again in PBS and resuspended in MACS buffer (see Materials for composition). Samples were stored at 4^{o}C for no more than a week until analysis. Flow cytometry was performed on an Attune NxT Flow Cytometer (ThermoFisher, UK). Data analysis was carried out using FlowJo software (FlowJo LLC, UK). Forward scatter (FSC-A) area was plotted against side scatter area (SSC-A) and gating was used to exclude cell debris. Of the remaining "Live" population, the height and area of the forward scatter was plotted to exclude doublets. The resulting "single cells" population was plotted as a histogram to display the event count along the y-axis and the fluorescent signal in the BL1-A channel

(excitation with 488 nm laser and detection using bandpass filter 530 ± 30 nm) along the x-axis. An appropriate gate was drawn to create two populations of cells, one positive and one negative for GFP expression (Figure 2.3). The proportion of cells in the positive gate for BL1-A signal and the median fluorescence intensity (MFI) was used to compare levels of fluorescent signal between treatment groups.

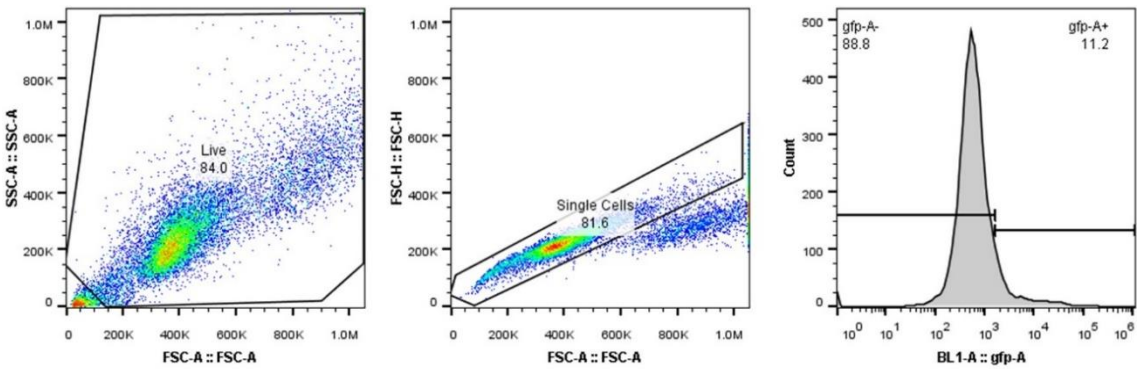


Figure 2.3. Flow cytometry gating strategy. Cells were harvested from plates by trypsinisation and run on an Attune flow cytometer. Cell debris was excluded by plotting FSC-A versus SSC-A (left). Doublet cells were excluded by plotting FSC-H against FSC-A (middle). Fluorescence was then displayed by plotting the BL1-A signal against cell count. A gate was set to create a positive and negative cell population (right).

2.12 *Celigo cell imaging*

Cells were plated in standard microplates and infected with the indicated virus and dose as described. At the appropriate time points, infected cells were imaged using the Celigo image cytometer (Nexcelom Biosciences, UK). The Celigo cytometer captures many images per well and stiches them together to create an image of the entire well in both channels. The images were then analysed by the Celigo software using the confluence ratio program. This program runs an image analysis algorithm to delineate cells within

the image so that the user can optimise parameters to get the most accurate cell detection (Figure 2.4). The total surface area of the cell monolayer in the bright field channel, and the surface area of the fluorescent cells in the fluorescent channel was then calculated (Figure 2.4). The surface area in the fluorescent channel was divided by that of the bright field channel to yield a percentage of cells positive for GFP expression. This ratio was then converted into a percentage.

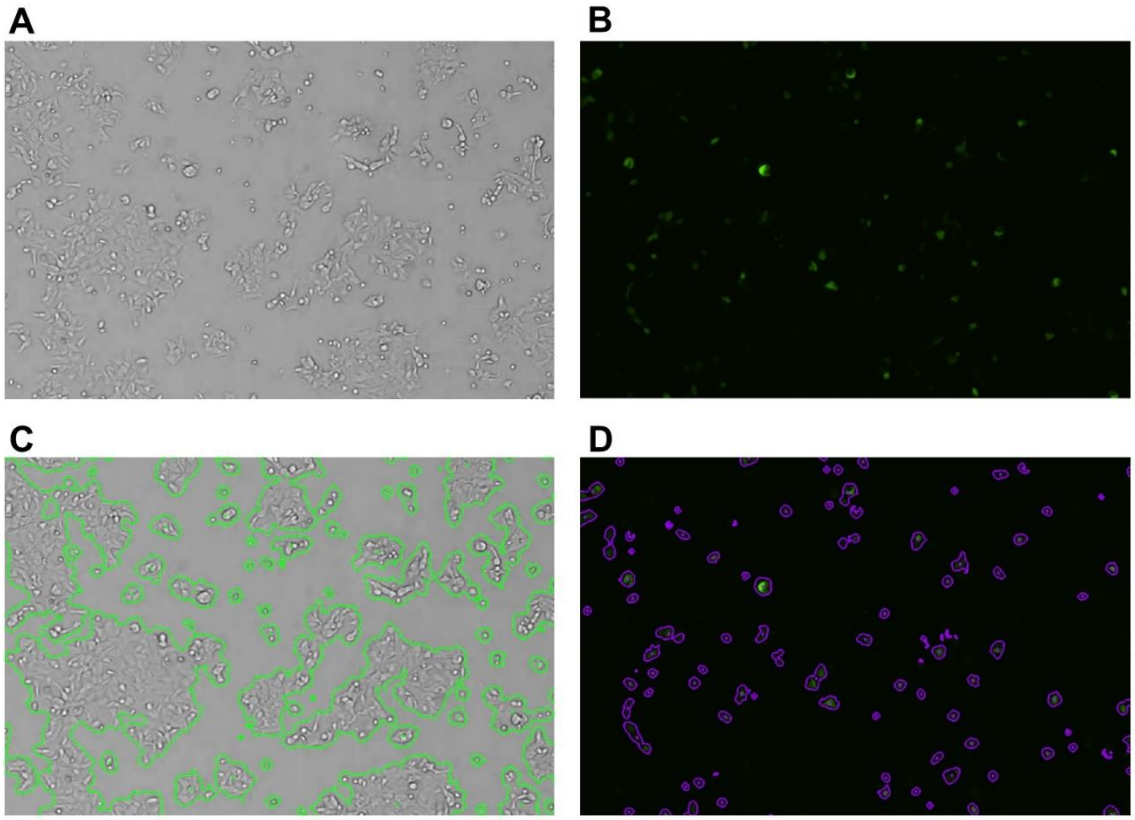


Figure 2.4. Celigo imaging and analysis. The Celigo cytometer takes images in brightfield **(A)** and fluorescent channels **(B).** The analysis parameters of the confluence ratio program are then optimised to achieve accurate cell detection. In the brightfield image, the program draws green lines around all areas in which cells are detected **(C)** allowing it to calculate total cell monolayer surface area. In the fluorescent channel, the program draws lines around fluorescent cells **(D)** and calculates the total area for fluorescent cells. These two areas are used to estimate a percentage of cells displaying GFP expression.

2.13 *Statistics*

Various statistical analyses were employed to evaluate whether differences between datasets were significant. When comparing two datasets, a Student's two-tailed t-test was used. Where more than two groups were compared, one-way Analysis of Variance (ANOVA) test was used with Tukey's post-hoc analysis. For grouped datasets, two-way ANOVA test was used with Bonferroni post-hoc analysis. All data is presented alongside bars indicating ± standard error in the mean (SEM). The significant levels used were $p = 0.01 - 0.05$ (*), $0.001 – 0.01$ (**), ≤ 0.001 (***). All experiments were performed in triplicate, unless otherwise stated.

3 Chemical induction of ER stress and adenoviral infection

3.1 *Introduction*

Conditions of cell stress are common in many highly proliferative solid (Déry et al., 2013; Davies et al., 2008; Tseng et al., 2013; Gupta et al., 2009; Su et al., 2010; Li et al., 2013b; Delie et al., 2012) and blood (Boelens et al., 2013; Masouleh et al., 2014) cancers, with any of several intrinsic and extrinsic factors contributing to their occurrence. ER stress occurs when protein folding homeostasis within the ER is perturbed and unfolded protein begins to accumulate, this triggers a set of adaptive signalling responses, known together as the UPR, which attempt to restore normal function (Figure 1.7). The adaptive UPR plays a role in the acquisition of numerous malignant characteristics which conspire to allow tumour progression (Urra et al., 2016).

It is now well established that ER stress can also be induced by viral infections (Table 1.3.). Adenoviral infections have been shown to modulate cellular stress responses primarily by stopping the shutdown of protein translation through inhibition of PKR, and the consequent block to phosphorylation of its downstream target EIF2α (McKenna et al., 2006). Yet the role of adenoviral infection in *inducing* ER stress is less clear. Whilst Pahl et al. found that overload of the ER with the E3-19K protein did lead to activation of NF-κB, this occurred through a new ER-nuclear pathway distinct from classical UPR signalling. (Pahl et al., 1996; Spurgeon and Ornelles, 2009; Mathews and Shenk, 1991). The propensity of adenoviral infections to induce the UPR pathway as classically described is still an open question.

Oncolytic virotherapies exploit differences between transformed and untransformed cells to achieve their specificity, making the higher levels of ER stress in many tumours therapeutically interesting. There are numerous examples of the induction of ER stress being used to sensitise cancer cells to destruction by oncolytic viruses (Prasad et al., 2014; Yoo et al., 2014; Roulstone et al., 2015; Workenhe and Mossman, 2014; Carew et al., 2013; Mahoney et al., 2011). Of particular relevance is the observation that induction of IRE1 signalling using the Golgi-disrupting chemical GCA enhanced oncolytic killing of A549 lung cancer cells by Ad5 (Prasad et al., 2014). There is little other evidence to suggest a synergistic effect between adenovirus infection and ER stress inducers, particularly for group B adenoviruses such as Ad11p and the clinical candidate EnAd.

In this chapter, we sought to investigate the proclivity of Ad5, Ad11p and EnAd to induce ER stress by monitoring IRE1 signalling, using levels of XBP1 splicing as a read out. To this end, we created a reporter cell line to provide a fluorescent read out for XBP1 splicing. Splicing of the XBP1 transcript in these cells brings a sequence encoding a fluorescent venus fusion protein into frame. We also use expression levels of the ER chaperone BiP as a marker of UPR activation. To better understand the relationship between induced ER stress, UPR signalling and adenoviral infection, and to explore whether any therapeutically useful synergistic effect might exist, we measured various parameters of viral replication in the presence of four ER stress-inducing compounds: thapsigargin, ionomycin, tunicamycin and subtilase cytotoxin (SubAB). Thapsigargin is a small molecule inhibitor that irreversibly inhibits the sarco/endoplasmic reticulum Ca^{2+}-ATPase (SERCA). SERCA is a calcium pump that is responsible for actively pumping calcium into the ER, thus its inhibition by thapsigargin causes a depletion of the ER calcium pool. Ionomycin is an ionophore that facilitates the movement of Ca^{2+} across membranes and therefore acts on all calcium pools. Tunicamycin blocks N-linked

glycosylation in the ER, whilst SubAB very specifically cleaves BiP, releasing the ER stress sensing molecules IRE1, PERK and ATF6 from its inhibitory binding.

3.2 *Chapter aims*

1. Generate a reporter cell line to measure ER stress in real time.

2. Assess levels of UPR induction during adenoviral infection

3. Investigate possible synergy between ER stressors and adenovirus

3.3 *Results*

3.3.1 Measuring the induction of ER stress in cancer cell lines

The IRE1 signalling arm is the most highly conserved arm of the UPR. Upon induction by ER stress, the endonuclease activity of IRE1 is activated, leading it to degrade many ER-targeted mRNAs. Among its targets is the XBP1 transcript. IRE1 directs the splicing of the unspliced XBP1 transcript (XBP1(u)), excising a 26 bp intron and causing a frameshift to yield the spliced transcript (XBP1(s)). This ER stress-induced splicing event can be exploited using a fluorescent reporter as a means to track ER stress induction in cells over time (Iwawaki et al., 2004). Here, we used a system in which the protein coding sequence of a yellow fluorescent protein, venus, is placed downstream and in a different coding frame relative to the XBP1 splice site (Figure 3.1). If XBP1 remains unspliced,

the venus coding sequence remains out of frame and no functional venus protein is expressed (Iwawaki et al., 2004). ER stress activates XBP1 splicing and removal of a 26 bp intron, bringing the venus reporter sequence into-frame with the XBP1 protein and

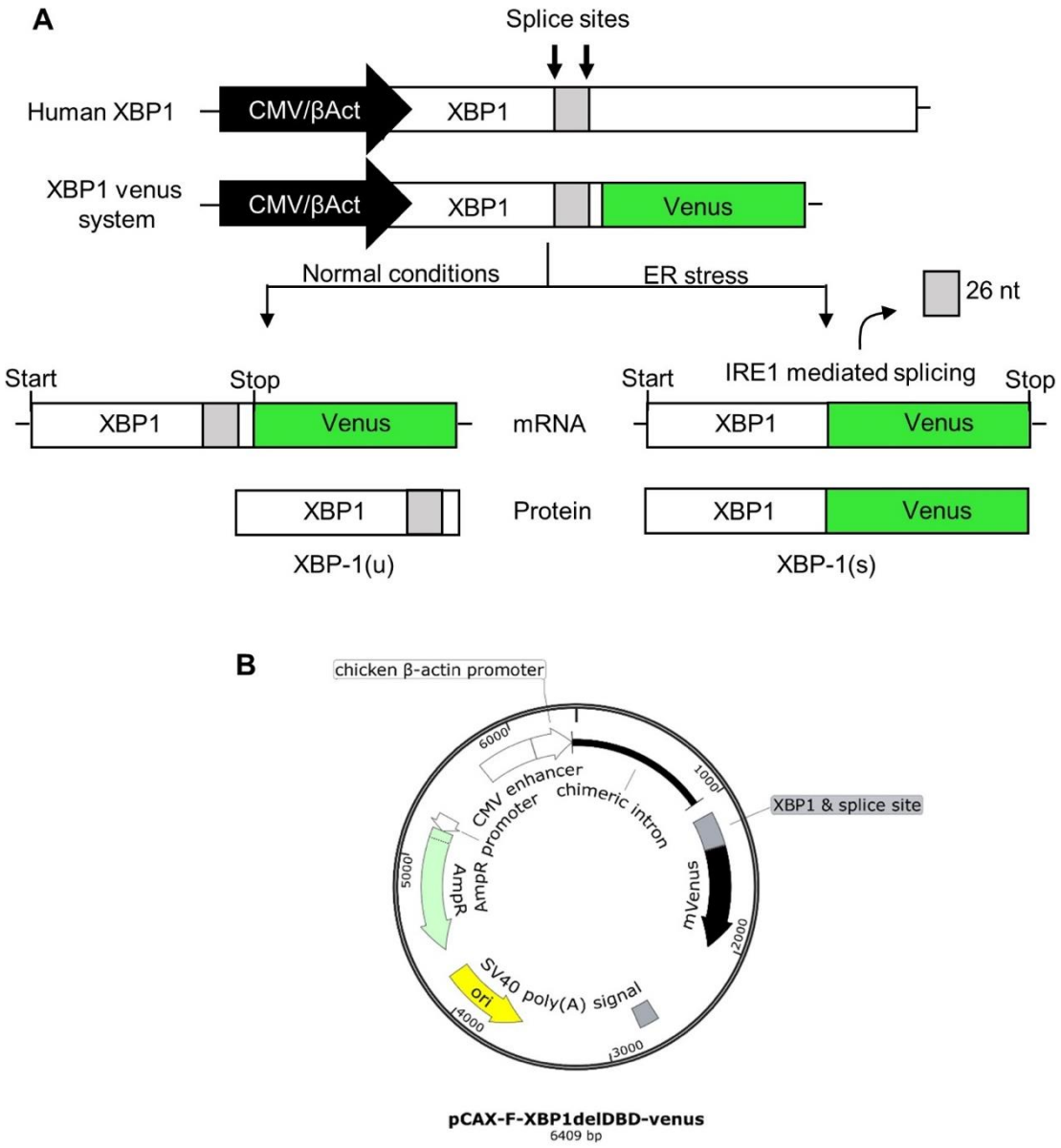


Figure 3.1. The XBP1-Venus ER stress fluorescent reporter system. A) Schematic representation of the XBP1-Venus reporter system adapted from Iwawaki et al., 2014. The venus fluorescent protein coding sequence is fused downstream of the XBP1 sequence and splice site. When ER stress occurs, IRE1 mediates the cleavage of the XBP1 transcript, removing a 26 bp intron, bringing the coding sequence of the venus fluorescent reporter into frame and removing the stop codon which is present before the venus sequence in the absence of splicing. Therefore, fluorescent protein is only produced in the presence of ER stress. **B)** Map of the original pCax-F-XBP1delDBD-venus received from the Miura lab

leading to the expression of a fluorescent XBP1-Venus fusion protein that can be observed by fluorescent microscopy or flow cytometry (Figure 3.1A).

The system was first tested in A549 cells by transient lipofectamine transfection of cells with pCAX-F-XBP1delDBD-Venus plasmid (Figure 3.1B). Twenty-four hours post-transfection cells were treated with either the ER stress-inducing drug thapsigargin or vehicle control DMSO. Cells were then harvested and fixed at indicated time points before analysis by flow cytometry. From 20 h post-treatment onwards, a significantly higher proportion of cells were positive for venus expression when transfected cells were treated with thapsigargin compared to cells treated with DMSO (Figure 3.2A). The median florescence intensity (MFI) was also significantly higher in the transfected thapsigargin-treated cells compared to DMSO-treated cells (Figure 3.2B). These results

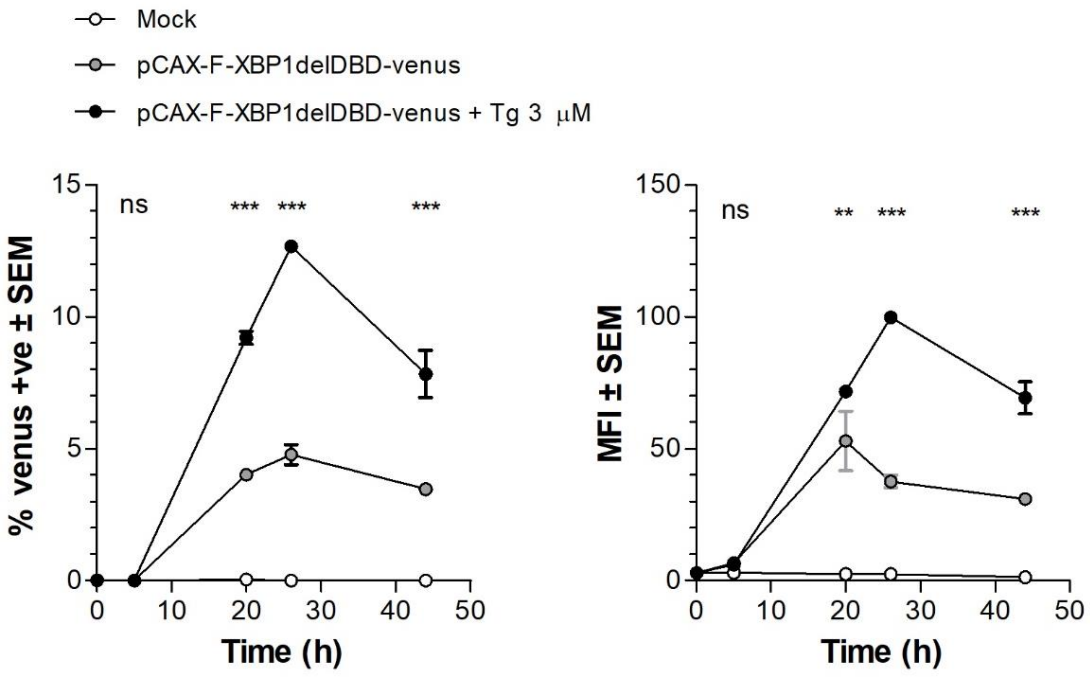


Figure 3.2. The XBP1-Venus ER stress fluorescent reporter system. A549 cells were transfected with the pCax-F-XBP1delDBD-Venus plasmid and treated with thapsigargin (Tg) 24 hours post-transfection. At the indicated times post-treatment cells were harvested and fluorescence measured by flow cytometry. The percentage of cells falling in the positive gate of venus expression **(A)** is shown, as well as the median fluorescent intensity (MFI) of the total cell population **(B)**. The mean of three replicates is plotted, significance between the transfected samples was assessed by two-way ANOVA, ** $p \leq 0.01$, *** $p \leq 0.001$, ns: not significant.

confirmed the utility of the reporter system for providing a read out of ER stress induction in cells over time.

Since plasmid transfection results in only transient expression of the reporter system, we sought to stably express the reporter construct from the genome of the A549 cells by lentiviral transduction. To achieve this, the XBP1-Venus sequence from the pCAX-F-XBP1delDBD-Venus plasmid was excised and ligated into the third-generation lentiviral genome pSF_Lenti by restriction enzyme cloning (Figure 3.3A, B). The genome was packaged into VSVG-pseudotyped lentiviruses using plasmids expressing HIV PolGag

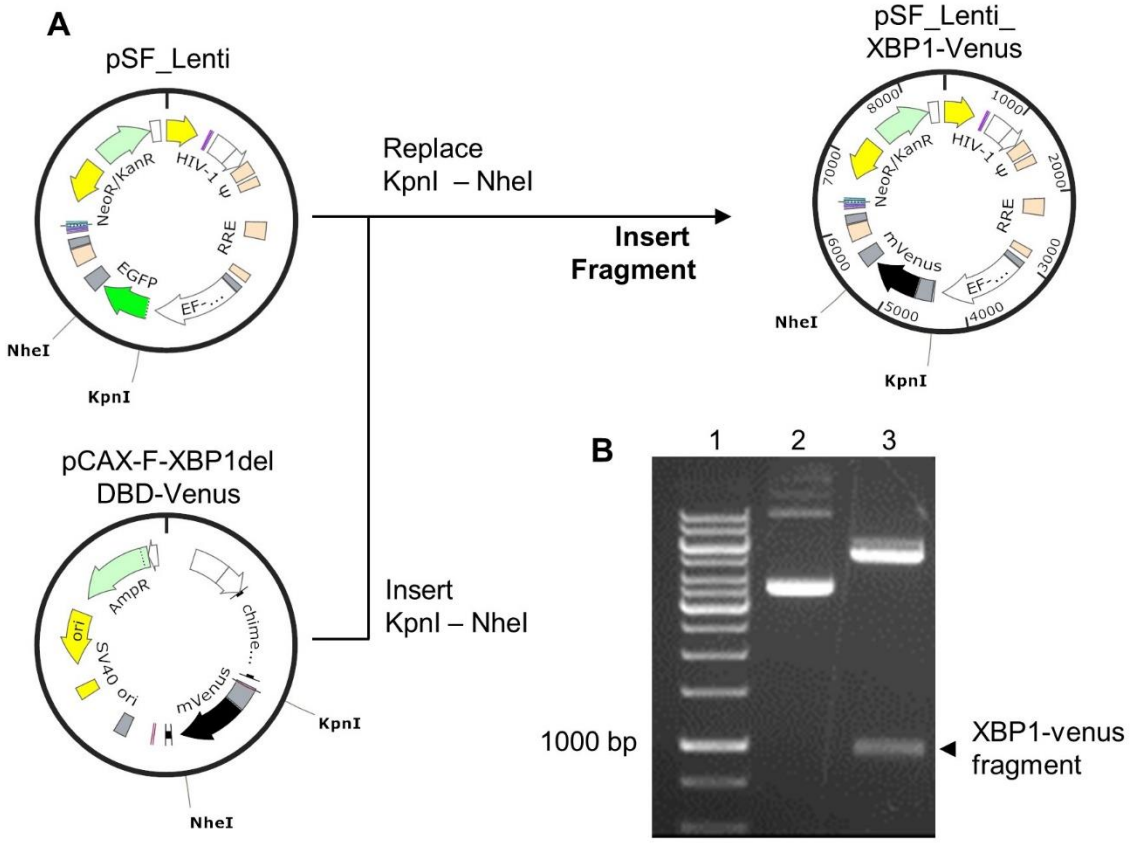


Figure 3.3. Construction of a lentiviral plasmid to generate a cell line stably expressing the XBP1-venus system. **A)** Schematic representation of the cloning strategy employed to create the pSF_Lenti_XBP1-Venus plasmid. **B)** Image of an agarose gel used to resolve the product of a digest reaction of plasmid pCax-F-XBP1delDBD-Venus using restriction enzymes *NheI* and *KpnI*. The XBP1-Venus fragment is visible as a band of roughly 1000 bp. 1: Generuler 1Kb, 2: undigested pCax-F-XBP1delDBD-Venus, 3: pCax-F-XBP1delDBD-Venus digested with *KpnI* and *NheI*

and Rev, and VSV-G. Successfully transduced A549 cells were selected using puromycin and underwent clonal expansion.

These A549-Venus cells were tested for their response to ER stress induction by treatment with thapsigargin. Cells were exposed to the indicated drugs and analysed by flow cytometry 24 h post-treatment. Thapsigargin induced a significant three-fold increase in the proportion of venus-positive cells and in the MFI signal of the cells (Figure 3.4A, B). When treatment media included 4μ8C (an inhibitor of IRE1 and therefore of XBP1 splicing) alongside thapsigargin, the proportion of venus positive cells and the MFI signal was significantly reduced compared to when thapsigargin treatment was used alone, but was still significantly higher than when cells were treated with vehicle control DMSO

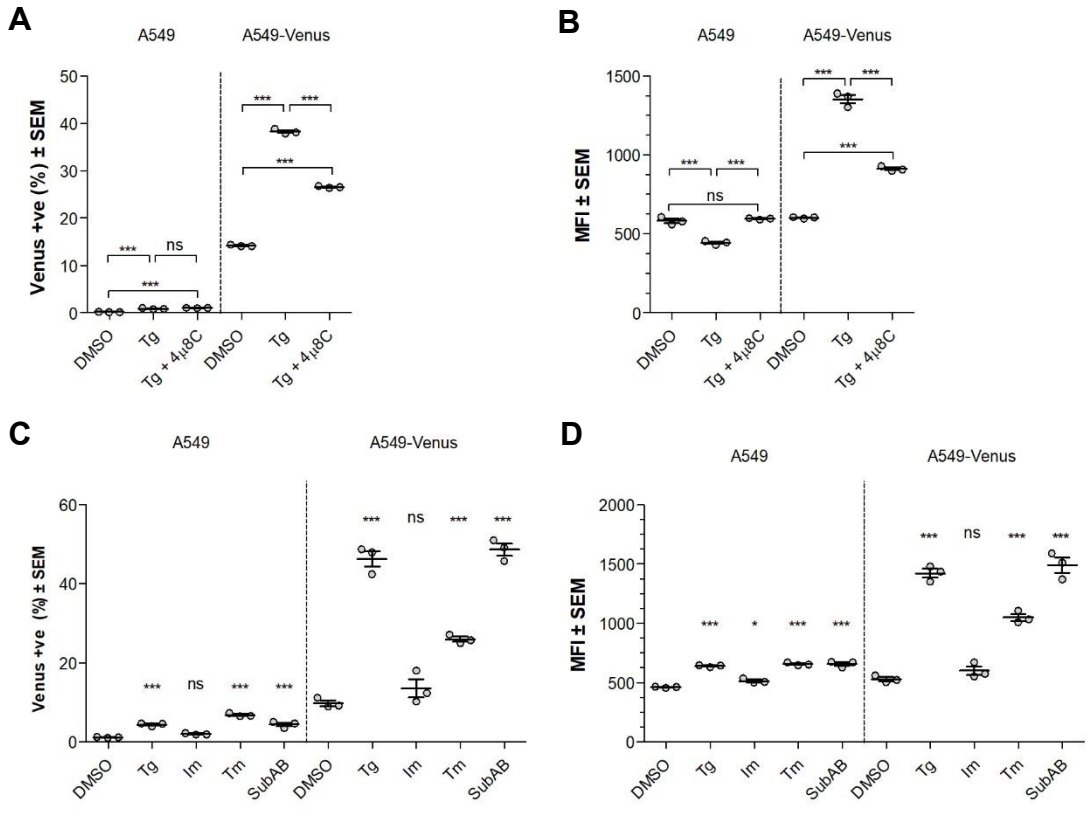


Figure 3.4. Validation of the A549-Venus cell line as a tool to monitor ER stress in cells. A549-Venus or parental control A549 cells were exposed to indicated chemicals or vehicle control DMSO. Fluorescence was measured by flow cytometry 48 hours after treatment. The percentage of cells positive for fluorescent signal **(A, C)** and the median fluorescent intensity of the signal **(B, D)** is displayed. Significance was assessed by one-way ANOVA *** $p \leq 0.001$, ns: non-significant. Thapsigargin (Tg, 0.1 μM), ionomycin (Im, 1.25 μM), tunicamycin (Tm, 1μg/mL), Subtilase cytotoxin (SubAB, 0.5 μg/mL).

(Figure 3.4.A, B). When parental control A549 cells lacking the integrated reporter system were used, treatments did significantly alter the proportion of cells positive for fluorescent signal, however these extremely small changes are likely to be slight changes in autofluorescence due to cytotoxicity of the treatments (Steinkamp and Stewart, 1986), and would not have any impact on the changes measured when using the reporter cells (Figure 3.4A, B).

Having validated the ability of the A549-Venus cell line to respond to ER stress using thapsigargin, which is a widely used ER stress-inducing agent, other chemical treatments were tested for their propensity to induce ER stress. A549-Venus cells and parental A549 cells were treated with thapsigargin, ionomycin, tunicamycin and SubAB (Figure 3.4C, D). At 48 h post-treatment, fluorescence was measured by flow cytometry. Thapsigargin, tunicamycin and SubAB all induced significant increases in venus fluorescence, whilst treatment with ionomycin did not. The treatments had very little to no effect on fluorescent signal levels in parental A549 cells, again the small shifts in fluorescence observed likely to be due to changes in auto-fluorescence (Figure 3.4C, D).

To further assess ER stress induction following chemical treatment of cancer cell lines with ER stress-inducing drugs, expression levels of BiP/GRP78, a key UPR marker protein, were measured by western blot. BiP is a chaperone protein found within the lumen of the ER whose inhibitory binding to the luminal domains of the ER stress sensing UPR signal transducers IRE1, ATF6 and PERK keeps UPR signalling switched off under normal conditions. BiP is upregulated under conditions of ER stress and its protein level can serve as an indicator of the level of ER stress in cells. SK-OV-3 ovarian cancer and DLD-1 colorectal cancer cells were treated with thapsigargin, ionomycin, tunicamycin or vehicle control DMSO and harvested at the indicated time points post-treatment. Western blotting revealed that all of the treatments except the vehicle control led to some

upregulation of BiP. At the concentrations used, thapsigargin and ionomycin upregulated BiP to very similar extents in SK-OV-3 cells, but thapsigargin had a slightly more potent upregulating effect in DLD-1 cells. In both cell lines, tunicamycin brought about a more powerful and rapid upregulation of BiP than the other two treatments (Figure 3.5A, B).

In a third approach for measuring ER stress induction, XBP1 splicing levels were measured by RT-PCR by directly isolating RNA from cells following treatment with various ER stress-inducing chemicals. Isolated RNA was reverse transcribed to cDNA and PCR used to amplify both the spliced and unspliced forms of XBP1. The bands for each of the XBP1 splice variants can then be resolved by running the samples on a 2.5% agarose gel, allowing direct visual inspection of XBP1 splicing patterns. Using this approach, we found that ionomycin did not induce visible levels of XBP1 splicing, thapsigargin induced modest levels of XBP1 splicing, and tunicamycin and SubAB induced the most potent levels of XBP1 splicing. Inclusion of the IRE1 inhibitor 4μ8C in the treatment media blocked XBP1 splicing in all samples, regardless of the addition of

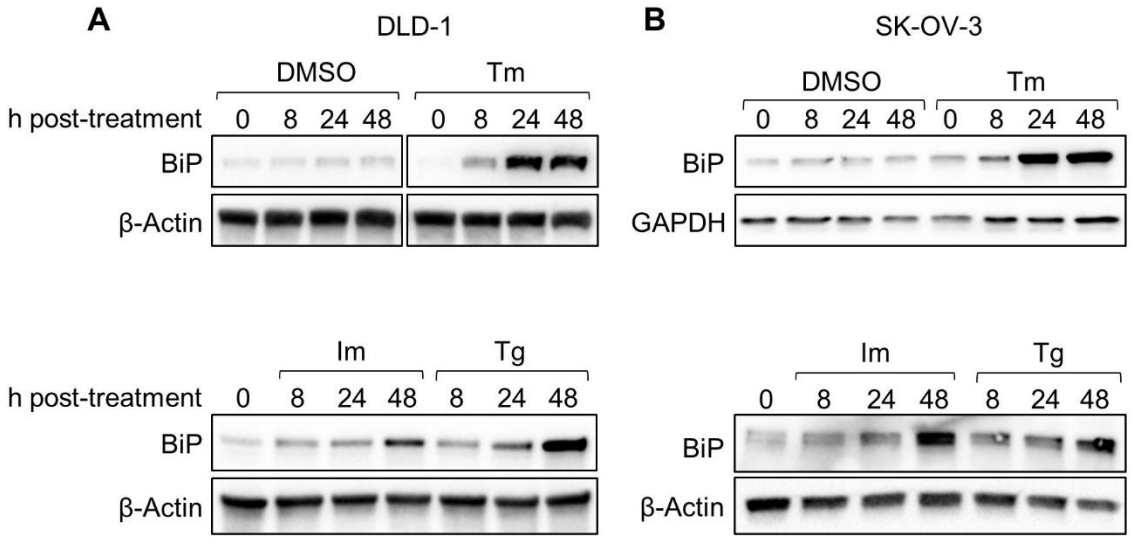


Figure 3.5. Detection of BiP expression to measure ER stress induction. A) DLD-1 or B) SK-OV-3 cells were exposed to the following treatments: vehicle control DMSO, tunicamycin (Tm, 1 μg/mL), ionomycin (Im, 1.25 μM) or thapsigargin **(**Tg, 0.1 μM). At the indicated time points post-treatment cells lysates were collected and levels of BiP expression were probed by western blotting. GAPDH or β-Actin was used as a loading control.

any ER stress-inducing drugs. These results were consistent in both DLD-1 and SK-OV-3 cells (Figure 3.6).

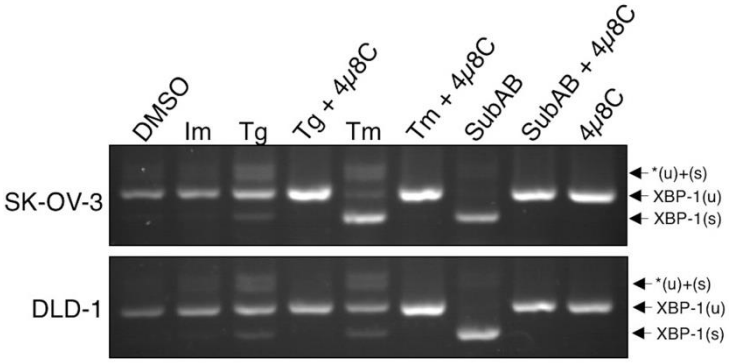


Figure 3.6. Treatments induce XBP1 splicing to varying extents. SK-OV-3 or DLD-1 cells treated with the indicated chemical for 12 h before harvesting for total RNA extraction. A set of primers was used to amplify both the spliced and unspliced XBP1 transcripts, which were resolved on a 2.5% agarose gel. XBP1(u) was observed at 283 bp; XBP1(s) at 257 bp. A third band was also detected, this is a hybrid band with one of the DNA strands being unspliced and the other the spliced one. Its detection in this assay is frequently reported in the literature (Shang and Lehrman, 2004).

3.3.2 Adenovirus infection induces significant ER stress

Having confirmed that the fluorescent signal from A549-Venus cells could be used to measure IRE1 induced XBP1 splicing and therefore ER stress induction, we used this cell line to track the induction of ER stress in cells infected with oncolytic adenovirus EnAd, Ad11p and Ad5. A549-Venus and parental control A549 cells were infected with each virus. At 48 h post-infection (p.i.), fluorescence was measured by flow cytometry. EnAd and Ad11p infection caused a significant roughly 6-fold increase in the proportion of cells positive for venus expression (Figure 3.7A) and in the median level of fluorescent signal (Figure 3.7B). Ad5 infection also caused a significant increase in the percentage of venus positive cells, but this increase was significantly smaller than those observed when cells were infected with either of the group B adenoviruses, at approximately 2-fold (Figure 3.7A). Ad5 infection did not induce any change to the MFI recorded (Figure 3.7B).

Thapsigargin was used as a positive control for ER stress induction in the experiment and induced a significant approximately 3-fold increase in both MFI and in the percentage of venus positive cells (Figure 3.7A, B).

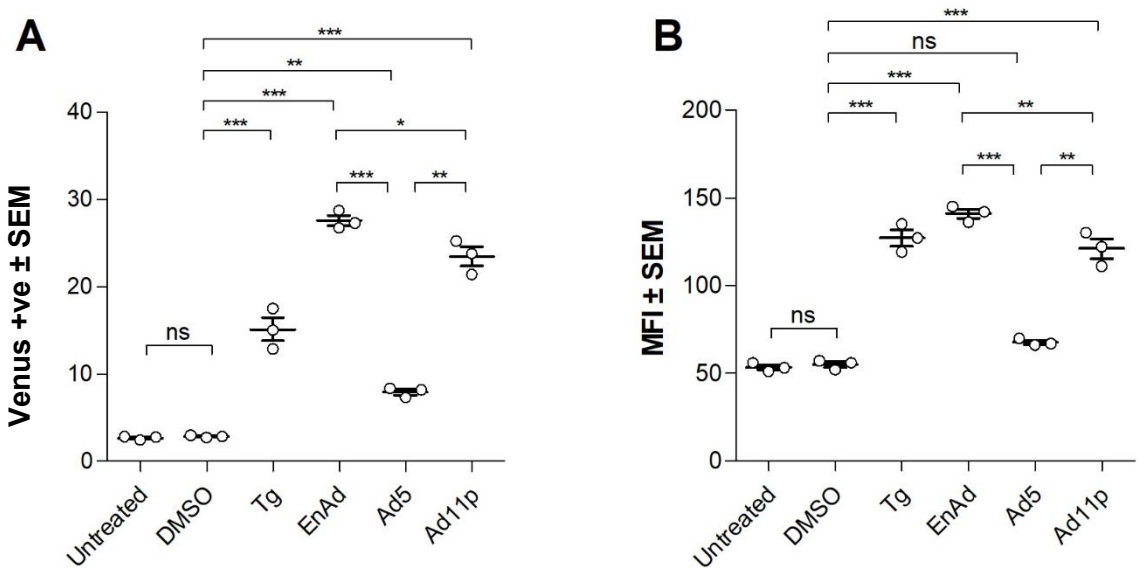


Figure 3.7. EnAd and Ad11p infection induces ER stress in A549 cells. A549-Venus cells were infected with the indicated virus at a dose of 3 $TCID_{50}$/mL or treated with thapsigargin (Tg, 0.1 µM) as a positive control for ER stress induction. Fluorescent signal was measured 48 hours post-infection/treatment by flow cytometry. Percentage of cells falling in the positive gate for venus expression **(A)** and the median fluorescent intensity **(B)** are shown. The significance of the difference compared to the DMSO control samples was assessed by one-way ANOVA, *** $p \leq 0.001$, ** $p \leq 0.01$, ns: non-significant.

In a separate experiment cells were infected with increasing virus doses of EnAd or Ad5. At 48 h p.i. fluorescence was measured by flow cytometry. EnAd infection was found to induce ER stress in a dose-dependent manner, with higher virus doses inducing greater levels of venus expression (Figure 3.8A, B). At the highest infectious dose, the MFI and the percentage of cells positive for venus expression was four times that of uninfected cells (Figure 3.8B). These levels of ER stress induction are comparable to levels in cells treated with thapsigargin, the positive control for ER stress induction. Ad5 infection did not result in ER stress induction to the same extent. Ad5 infection did cause a statistically

significant increase in the percentage of venus positive cells, but MFI was only significantly increased at the highest dose (Figure 3.8A, B). In the parental control A549 cells a very small (but statistically significant) increase in fluorescence was observed upon thapsigargin treatment (Figure 3.8C, D).

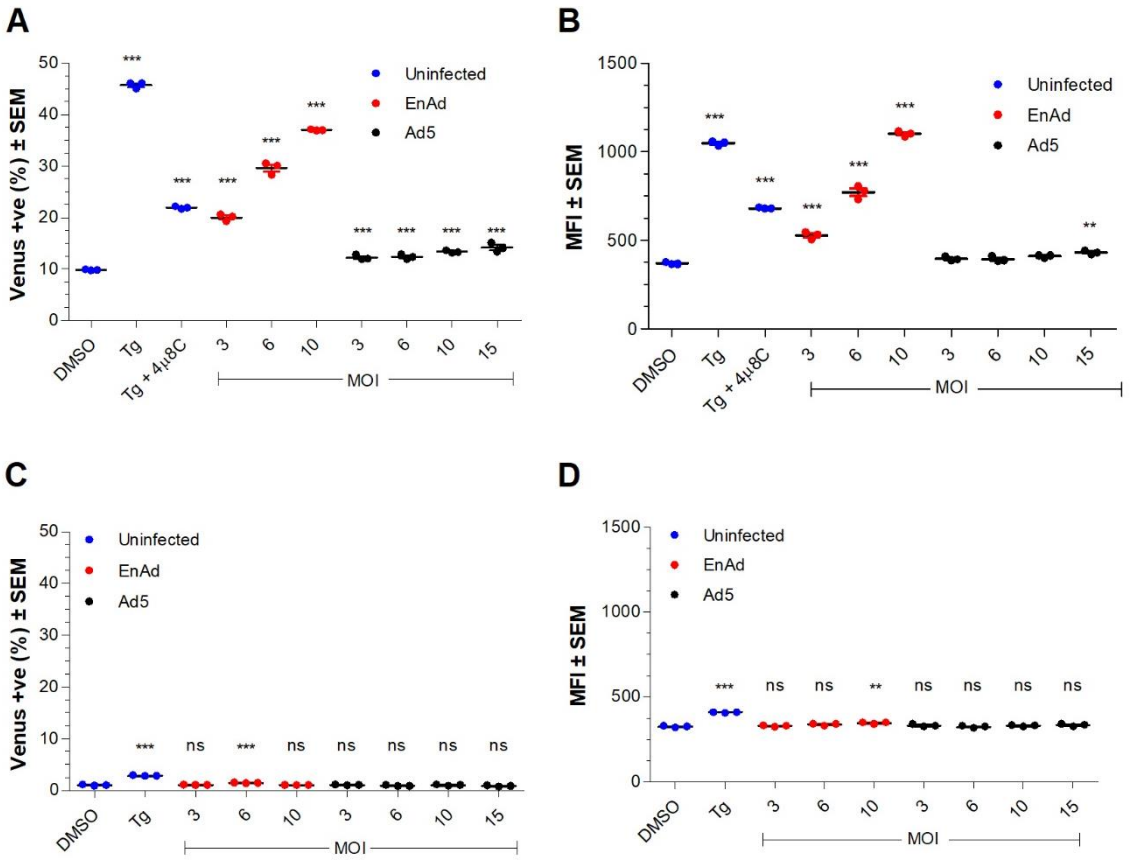


Figure 3.8. EnAd induces ER stress in A549 cells in a dose dependent manner. A549-Venus cells **(A, B)** and parental control A549 cells **(C, D)** were infected with increasing dosages of EnAd or Ad5, or treated with thapsigargin (Tg, 0.1 μM) as a positive control for ER stress induction. Fluorescent signal was measured 48 h post-infection/treatment by flow cytometry. Percentage of cells falling in the positive gate for venus expression (A, C) and the median fluorescent intensity (B, D) are shown. The significance of the difference compared to the DMSO control samples was assessed by one-way ANOVA, *** $p \leq 0.001$, ** $p \leq 0.01$, ns: non-significant.

3.3.3 Thapsigargin treatment increases early and late viral protein expression in EnAd, Ad11p but not Ad5 infection

Our results above suggest a major interaction between adenoviruses and responses to ER stress, particularly with EnAd. We sought to investigate the effect of inducing ER stress on the virus replication cycle in cells. Initially, we chose to evaluate the expression of early and late viral gene expression under ER stress versus normal conditions using reporter viruses harbouring GFP transgenes. In EnAd, GFP expression was driven by either the CMV immediate-early promoter (EnAd-CMV-GFP) or the adenovirus major late promoter (MLP) via a splice acceptor (SA) site (EnAd-SA-GFP) (Marino et al., 2017).

In Ad5, GFP expression was driven by the CMV promoter, the expression cassette for which was inserted into the E3 region, yielding an E3 deleted replicating Ad5-CMV-GFP virus (Taverner et al., 2019). Details and schematics of all recombinant virus genomes are provided in section 8.2 of the appendices on recombinant viruses. CMV-driven transgenes are expressed immediately upon arrival to the nucleus, thus providing an indirect readout for early viral gene expression. The MLP drives expression alongside the viral late genes, linking transgene expression to the viral replication cycle. We infected SK-OV-3 and DLD-1 cells with the reporter viruses EnAd-SA-GFP, EnAd-CMV-GFP or Ad5-CMV-GFP and subsequently treated them with ER-inducing chemicals. GFP expression in cells was quantified at 72 and 24 h p.i., respectively, by imaging the plates on a Celigo imaging cytometer (Figure 3.9).

We tested the effect of thapsigargin, ionomycin, and tunicamycin on virus activity. In SK-OV-3, thapsigargin and ionomycin treatment increased the percentage of cells expressing GFP measured three days p.i. EnAd-encoded reporter expression increased by approximately 7- and 47-fold with thapsigargin and ionomycin treatment, respectively,

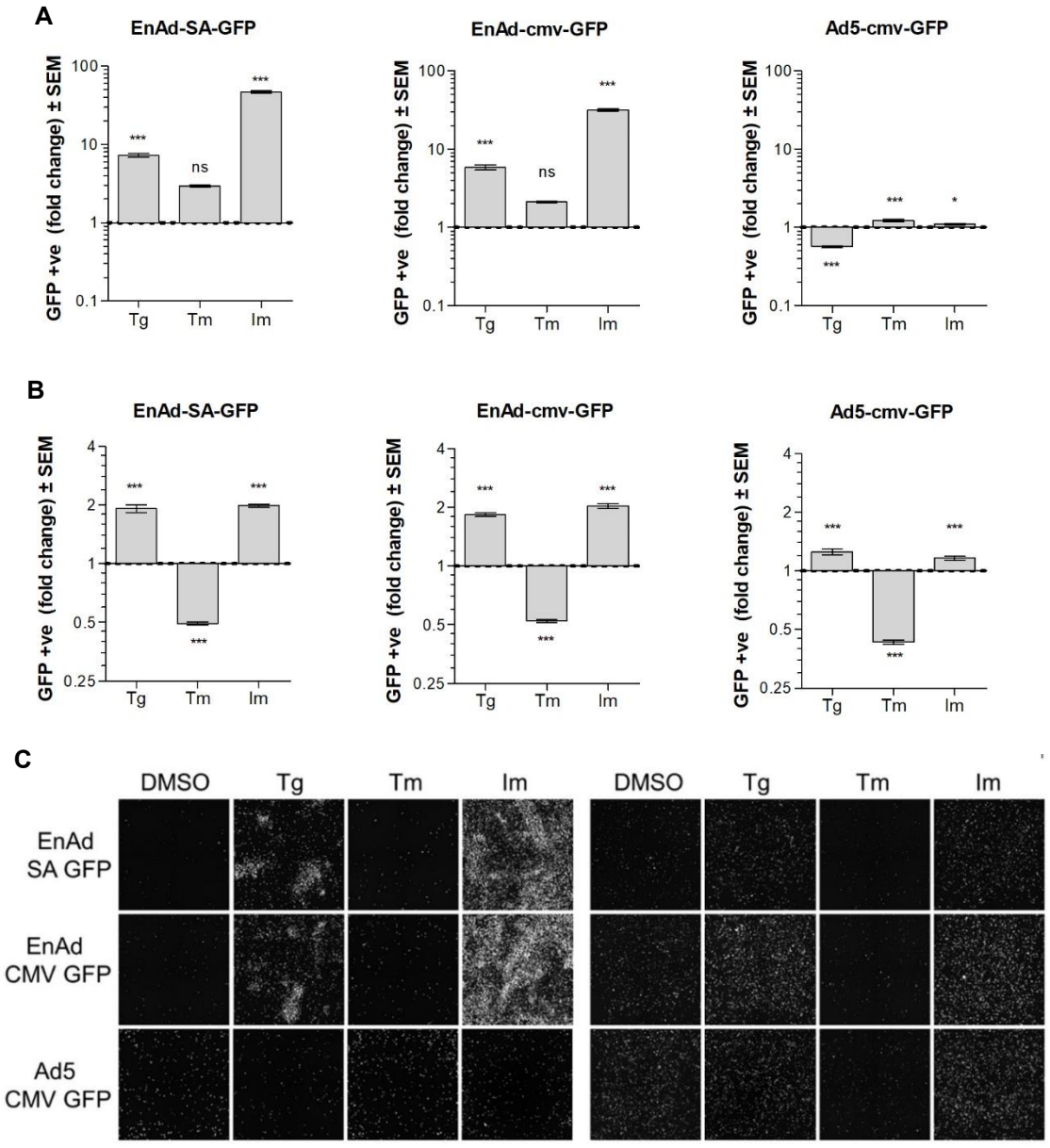


Figure 3.9. Effect of ER stress inducing chemicals on EnAd and Ad5 transgene expression SK-OV-3 ovarian cancer cells **(A)** or DLD-1 colorectal cancer cells **(B)** were plated in a 96-well plate, infected with EnAd-SA-GFP, EnAd-CMV-GFP, or Ad5-CMV-GFP at 100 VPC and subsequently treated with thapsigargin (Tg, 0.1 µM), ionomycin (Im, 1.25 µM) or tunicamycin (Tm, 1 µg/mL). Cells were imaged on a Celigo image cytometer and GFP expression quantified at 72 h (A) or 24 h (B) post-infection. Data represent average fold-change in the percentage of GFP-positive cells from 60 replicates relative to DMSO vehicle control-treated cells. Broken line represents ± SEM of the DMSO control. Significance was evaluated using one-way ANOVA. *, $p \leq 0.05$; **, $p \leq 0.01$; ***, $p \leq 0.001$; ns, non-significant. **(C)** Representative images from the Celigo cytometer of virus-encoded GFP expression for the conditions in A and B. Absolute levels of % positive GFP cells in vehicle control treated cells were 0.5, 0.8 and 6 in SK-OV-3 cells and 11, 17 and 31 in DLD-1 cells for EnAd-SA-GFP, EnAd-CMV-GFP and Ad5-CMV-GFP respectively.

whilst tunicamycin treatment had no significant effect, regardless of the promoter driving GFP expression. GFP levels in Ad5-CMV-GFP-infected and treated cells were not substantially different compared to untreated cells, with fold changes of 0.5, 1.2 and 1.1 for thapsigargin, tunicamycin and ionomycin, respectively (Figure 3.9A).

A very similar pattern of effects was observed in DLD-1 cells, though the fold-changes, although significant, were more modest, probably reflecting this cell line's inherently greater permissivity to adenoviral infection and therefore saturation of their ability for transgene expression and virus production. The proportion of EnAd-SA-GFP- and EnAd-CMV-GFP- infected cells expressing GFP doubled following treatment with thapsigargin or ionomycin, whilst treatment with tunicamycin caused a 0.5-fold reduction. There was almost no change in GFP expression in Ad5-CMV-GFP-infected cells when treated with thapsigargin or ionomycin (1.25- and 1.16-fold, respectively), whilst treatment with tunicamycin reduced reporter expression by approximately half, similar to EnAd-infected cells (Figure 3.9B). The effects of the drugs on reporter expression can also be seen in the images taken by the Celigo cytometer which are provided in Figure 3.9C.

To test whether enhancement of EnAd transgene expression by thapsigargin treatment is applicable to other cell types, we also used A549 lung cancer cells and colorectal cancer HT-29 cells. In both cases, thapsigargin treatment led to a significant increase in the proportion of cells expressing GFP 24 h post-treatment in infected cells but not uninfected control cells (Figure 3.10A). The effect was no longer present at 40 h p.i. however, and GFP expression in A549 cells was decreased significantly at this time-point, most likely due to virus induced cell killing (Figure 3.10B).

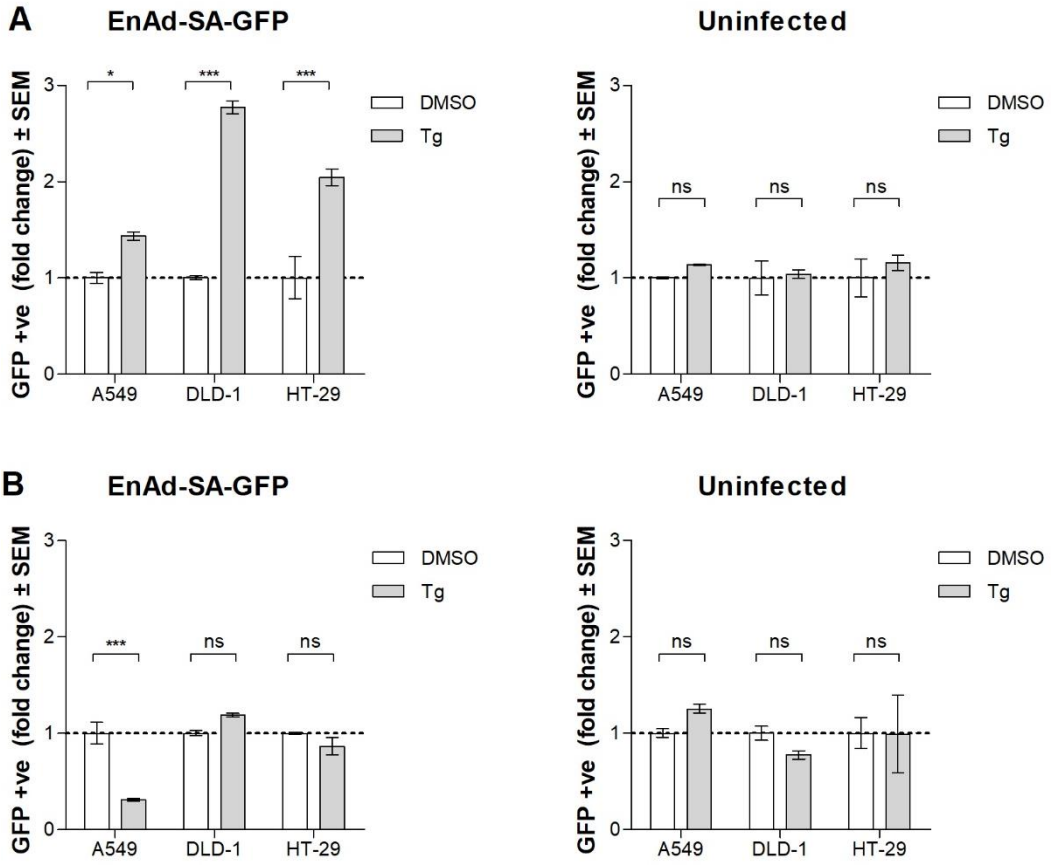


Figure 3.10 Thapsigargin treatment enhances EnAd activity in various cell lines. A549, DLD-1 or HT-29 cells were infected with EnAd-SA-GFP at a dose of 100 VPC and subsequently exposed to thapsigargin treatment (Tg, 0.1 μM) or vehicle control DMSO. GFP expression was measured by flow cytometry at 24 hours (A) or 48 hours (B) post-infection. The mean fold change of the percentage of cells falling in the positive gate for GFP expression relative to the DMSO treated group is displayed. All groups were measured in triplicate. Significance was assessed by two way ANOVA, * $p \leq 0.05$; **, $p \leq 0.01$; ***, $p \leq 0.001$; ns, non-significant.

3.3.4 Thapsigargin treatment accelerates the onset of DNA replication in EnAd and Ad11p, but not Ad5 infection

To further study the ER stressor-induced significant increase in virus activity, as measured by reporter expression in different cell lines observed above, we next determined whether any significant change in rates of viral DNA replication could be induced by treatment of cells with thapsigargin. DLD-1 or SK-OV-3 cells were infected with EnAd, Ad11p or Ad5 and subsequently exposed to medium supplemented with 0.1 µM thapsigargin. At 72 or 24 h p.i. for SK-OV-3 and DLD-1 cells, respectively, cells and supernatants were harvested together, and the number of viral genomes was measured by qPCR. We found that thapsigargin treatment increased the number of EnAd and Ad11p genomes six-fold in infected DLD-1 cells (Figure 3.11A). In SK-OV-3 cells, we observed a nine-fold increase in EnAd and a four-fold increase in and Ad11p genome copy number in infected cells treated with thapsigargin (Figure 3.11B). No significant difference in genome copy number was observed with Ad5 genomes in either cell line with or without treatment (Figure 3.11A, B).

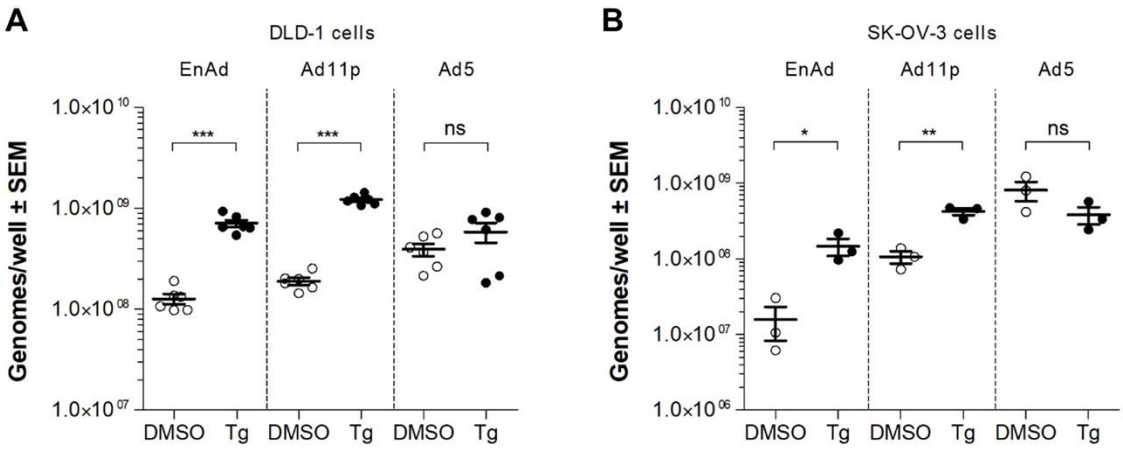


Figure 3.11. Thapsigargin treatment enhances viral DNA replication during EnAd and Ad11p but not of Ad5 infections. QPCR of viral genomes in (A) DLD-1 cells 24 h post-infection and (B) SK-OV-3 cells 72 h post-infection, in the presence and absence of thapsigargin (Tg, 0.1 µM) or vehicle control DMSO. Cells were infected at 100 VPC. Significance was evaluated by two-tailed t-test. *, $p \leq 0.05$; **, $p \leq 0.01$; ***, $p \leq 0.001$; ns, non-significant.

3.3.5 Thapsigargin treatment boosts production of EnAd and Ad11p but not Ad5 infectious virus particles.

Increases in levels of reporter protein production and genome replication observed in thapsigargin-treated cells compared to control treated cells strongly suggest an enhancement to viral DNA replication. To measure whether these enhancements to virus encoded reporter protein and DNA replication translated into a higher output of infectious virus particles, we quantified the number of infectious virus particles produced from EnAd, Ad11p and Ad5-infected DLD-1 and SK-OV-3 cells at 24 and 72 h p.i., respectively. Cells were infected with virus and subsequently treated with thapsigargin. At the appropriate time p.i., cells and supernatants were harvested for quantification of infectious particles by the $TCID_{50}$ method. In DLD-1 cells, we observed a statistically significant three-fold increase in EnAd and a four-fold increase in Ad11p infectious particle numbers upon thapsigargin treatment, whilst Ad5 levels remained unchanged (Figure 3.12A). In SK-OV-3 cells, the number of progeny EnAd particles increased 13--fold and Ad11p particles, 30-fold 72 h p.i. Ad5 infectious particle levels again remained unresponsive to thapsigargin treatment (Figure 3.12B).

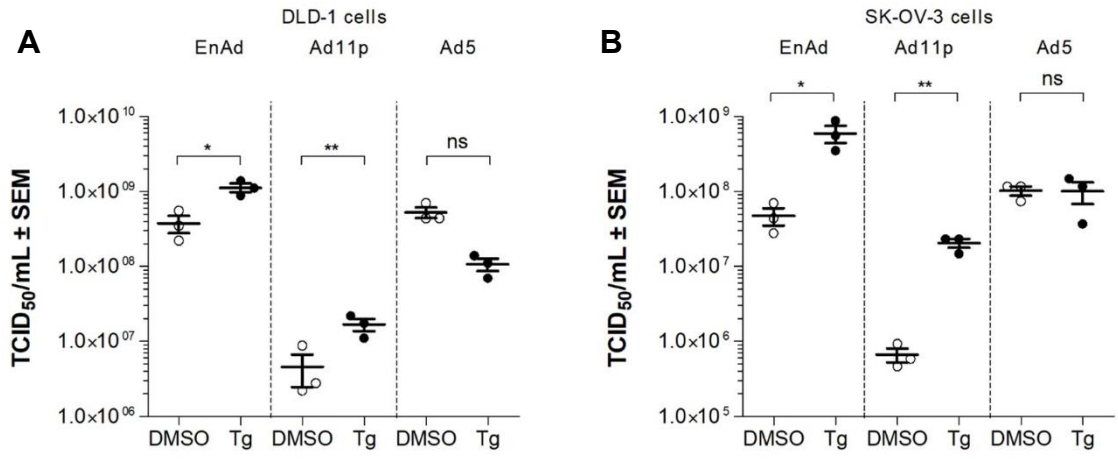


Figure 3.12. Thapsigargin treatment enhances infectious virus particle production during EnAd and Ad11p but not of Ad5 infections. $TCID_{50}$ measurement of infectious virus particles produced in **(A)** DLD-1 cells 24 h p.i. and **(B)** SK-OV-3 cells 72 h p.i.. Significance was evaluated by two-tailed t-test. *, $p \leq 0.05$; **, $p \leq 0.01$; ***, $p \leq 0.001$; ns, non-significant.

3.3.6 Thapsigargin treatment enhances oncolytic virus induced cell killing by EnAd and Ad11p but not Ad5.

Since one of the primary therapeutic aims of oncolytic viruses is to induce cell killing through cancer cell lysis, we measured whether thapsigargin treatment of target cells would have a synergistic effect with virus infection to increase killing. We employed the xCELLigence system, which allows real-time label-free recording of cell impedance measurements, also known as the cell index (CI). CI is a function of cell morphological parameters, such as cell adhesion, cytotoxicity and proliferation. Monitoring changes in this measurement over time provides a useful means to track virus-induced cytotoxicity and cell killing.

In uninfected DLD-1 cells, very little to no cytotoxic effect was observed when cells were treated with thapsigargin (Figure 3.13A). Untreated cells infected with EnAd, Ad11p or Ad5 began to show signs of cytotoxicity at between one, two and two days p.i., respectively. Thapsigargin treatment of target cells prompted earlier cell killing by EnAd and Ad11p. Cell killing was also faster in these samples, indicated by the more vertiginous decline in CI and the earlier time point at which a CI of 0 is reached. This effect was not seen with Ad5-infected cells (Figure 3.13A).

Compared to DLD-1, SK-OV-3 do show substantial cytotoxicity to thapsigargin alone, though we note that the course of the assay is much longer in this case, since SK-OV-3 cells are inherently far more resistant to adenovirus infection (Figure 3.13B). Initially, thapsigargin is more toxic than the viral infection in SK-OV-3 cells. At 72 h p.i., when protein levels, genome and infectious virus particle numbers were measured, thapsigargin-treated cells have a CI comparable to that of untreated cells. In treated SK-

OV-3 cells, there is a divergence of the CI between infected and uninfected samples at roughly between four and five days post-infection the context of Ad11p and EnAd infections. At this time, the CI of uninfected, treated cells begins to plateau, whilst the CI of treated cells infected with EnAd or Ad11p continues to decline. This sustained decline in CI is not seen in treated cells infected with Ad5. Virus-induced cytotoxicity, which occurs in addition to thapsigargin-induced toxicity in EnAd and Ad11p-infected cells, occurs earlier than virus-induced cytotoxicity in untreated cells (Figure 3.13B).

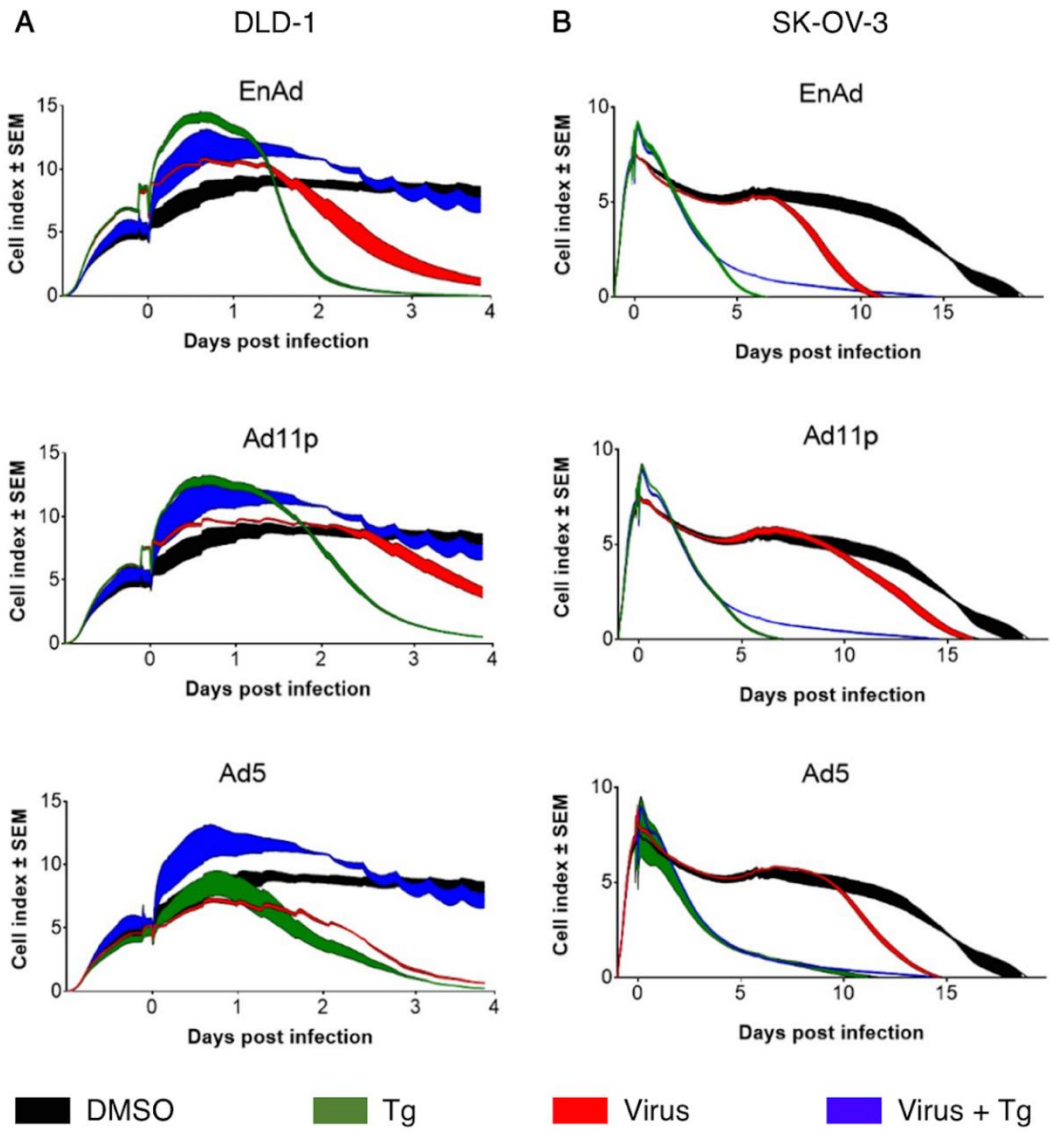


Figure 3.13. Thapsigargin treatment enhances killing in EnAd, Ad11p but not Ad5 infections. Virus killing of (A) DLD-1 cells or (B) SK-OV-3 cells was monitored by xCELLigence in the presence or absence of thapsigargin (Tg, 0.1 µM) after infection with EnAd, Ad11p or Ad5 virus. Impedance was measured every 10 minutes. Data show the mean of four replicates ± SEM. An infectious dose of 100 VPC was used in all experiments.

3.3.7 Thapsigargin treatment increases EnAd E1A expression

As thapsigargin was added two hours p.i. during which time the virus attaches to cells and is internalised, in all experiments, we excluded the possibility that the treatment effect was mediated through increased rates of attachment and entry. Instead, we chose to examine expression of the earliest viral genes in the presence and absence of thapsigargin. The immediate early adenovirus gene E1A is the very first viral gene to be expressed following adenoviral infection. E1A is the master regulator of expression of the other viral genes and mediates many important interactions in the cell, both with viral and host factors. EnAd E1A transcript levels were measured by qPCR at 2, 4, 6, and 9 h p.i. in DLD-1 cells and subsequent treatment with thapsigargin or vehicle control DMSO. A significant three-fold increase in E1A mRNA copy number was recorded at six and nine h p.i (Figure 3.14A).

To determine whether increased levels of E1A transcripts translated into higher levels of E1A protein, cells were infected with an EnAd variant modified to encode a Flag tag on its E1A protein (see appendices section 8.2). This enables detection of EnAd E1A protein, for which there are no commercially available antibodies, to be detected using an anti-Flag antibody by western blot. DLD-1 cells were infected with EnAd-Flag-E1A. Flag-E1A levels were assessed 12 h p.i. A substantial increase in Flag-E1A was observed when cells were treated with thapsigargin following infection, suggesting that the treatment enhanced E1A protein levels by increasing transcription of the E1A gene (Figure 3.14B). We also measured mRNA copies of the early gene E2B, the viral DNA polymerase whose regulation is dependent on E1A expression. A significant increase in E2B mRNA levels was observed at 9 h p.i. with an expected time lag compared to E1A expression (Figure 3.14C). The observation that an E1A-dependent gene was also upregulated by the

treatment further supports the observation that E1A levels increased with treatment by thapsigargin.

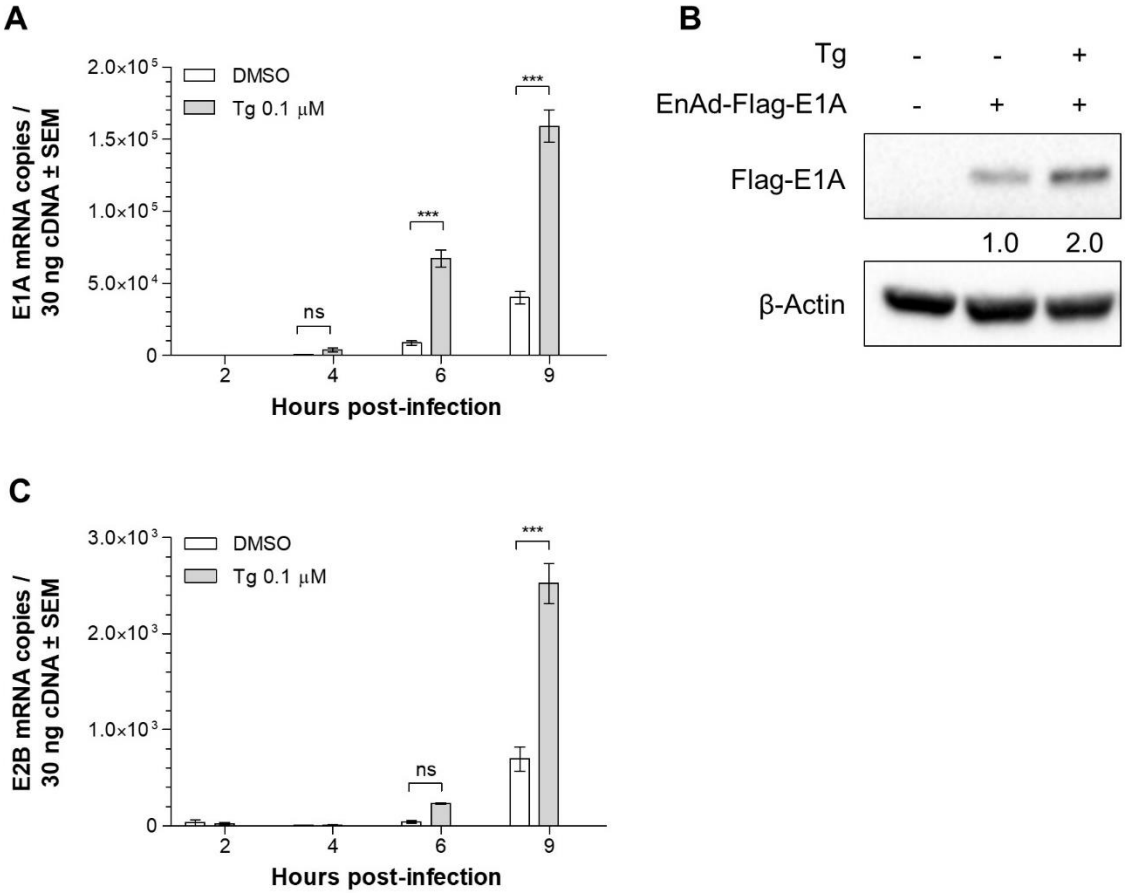


Figure 3.14. Thapsigargin treatment enhances early viral gene mRNA and protein levels. A) Quantification of EnAd mRNA levels of E1A by RT-qPCR. Data represents the mean of three biological replicates each an average of three technical replicates. **B)** Western blot of Flag-E1A 50 kDa protein levels in DLD-1 cells 12 h post-infection with EnAd-Flag-E1A (3 PFU/cell). Numbers indicate average normalised fold upregulation relative to DMSO control of three independent replicate experiments. C) Quantification of EnAd mRNA levels of E2B by RT-qPCR. Data represents the mean of three biological replicates each an average of three technical replicates Significance was assessed by two-way ANOVA using Bonferroni post-test. ***, $p \leq 0.001$; ns, non-significant.

3.3.8 Ad5 E1A protein levels are enhanced by thapsigargin and ionomycin

Since we observed marked differences between the behaviour of the group C adenovirus Ad5 and the group B adenoviruses Ad11p and EnAd in the presence of thapsigargin, we

sought to assess whether these differences were due to an inability of the treatment to increase E1A protein levels in the context of Ad5 infection. To this end, cells were infected with Ad5 virus and subsequently treated with the ER stress-inducing chemicals thapsigargin, ionomycin or tunicamycin. After 12 hours, cells were harvested and E1A protein was probed for by western blot. A small upregulation of E1A levels was observed when cells were treated with thapsigargin or ionomycin, while tunicamycin seemed to have no effect (Figure 3.15A).

To corroborate these findings, we used another experimental approach to measure Ad5 E1A levels. Ad5-E1A-Luc is an Ad5 virus engineered to express an E1A-luciferase fusion protein, thus allowing quantification of E1A levels in a luciferase-based reporter assay (Cawood et al., 2009). In this experiment, cells were infected with Ad5-E1A-Luc and subsequently treated with thapsigargin or ionomycin. After 12 hours, cells were harvested and lysed to measure luciferase activity. We found that luciferase activity was significantly higher in samples from cells treated with thapsigargin or ionomycin

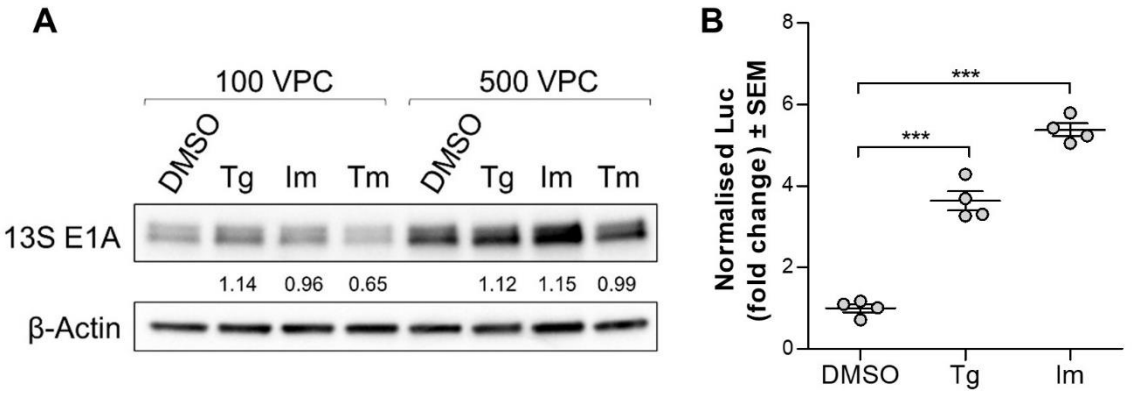


Figure 3.15. Thapsigargin treatment enhances early viral gene E1A expression in Ad5 infections. A) Western blot of E1A levels 12 hours post-infection of DLD-1 cells with Ad5 at doses of either 100 or 500 VPC. Following infection cells were exposed to treatments of thapsigargin (Tg, 0.1 μM), ionomycin (Im, 1.25 μM) or tunicamycin (Tm, 1 μg/mL). Using densitometry analysis, protein bands were normalised to their respective loading control band, and band signal relative to the DMSO control in each group is indicated. **B)** DLD-1 cells were infected with Ad5-E1A-Luc (3 PFU/cell) and treated with thapsigargin (Tg, 0.1 μM) or ionomycin (Im, 1.25 μM). Cells were lysed to measure luciferase activity (Luc) at 12 hours post-infection. Significance was assessed by one-way ANOVA. ***, $p \leq 0.001$; ns, non-significant.

following infection (Figure 3.15B). These were substantial increases of approximately four- and six-fold, respectively. Together with our results from western blotting, the data suggest that the thapsigargin and ionomycin enhance E1A protein expression levels during Ad5 infection, and that differences between the response to thapsigargin and ionomycin by Ad11p/EnAd and Ad5 do not stem from differences in E1A protein expression.

3.3.9 E1A overexpression does not enhance Ad5 activity in DLD-1 cells

The results presented so far regarding Ad5 infection show that whilst thapsigargin treatment does upregulate E1A expression levels, this does not seem to translate into increased viral replication, protein production, viral particle production or killing. These results would suggest that E1A levels are not a limiting factor to Ad5 replication in the early stages of infection. To test this reasoning further, we transfected DLD-1 cells with a plasmid encoding a construct for the expression of the Ad5 E1A gene (pE1A). Alternatively, as a control for transfection, cells were transfected with a luciferase expression plasmid (pLuc). E1A levels were measured by western blot at 24 hours post-transfection, confirming strong expression of Ad5 E1A in cells transfected with pE1A, with no signal observed in cells transfected with pLuc control plasmid (Figure 3.16A).

When cells were infected with Ad5-CMV-GFP 24 h post-transfection with either plasmid and imaged 24 hours post-infection, there was no difference in the proportion of cells positive for GFP expression between cells transfected with pE1A compared to those transfected with pLuc (Figure 3.16B). These results support the notion that E1A levels are not limiting to Ad5 infection in DLD-1 cells.

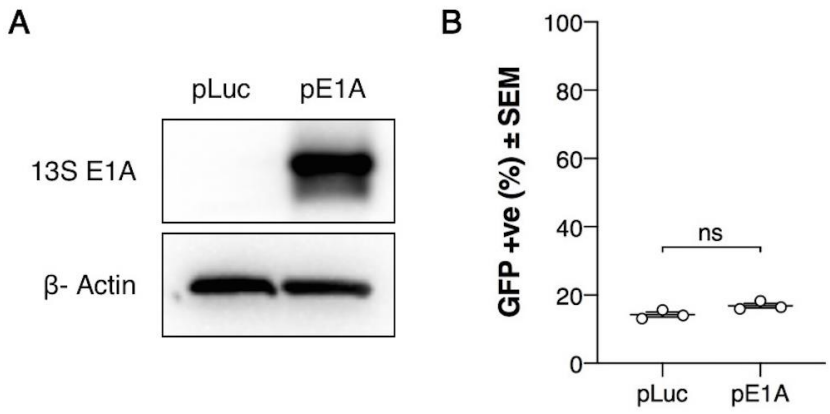


Figure 3.16. Overexpression of E1A does not increase Ad5 activity in DLD-1 cells. **A)** DLD-1 cells were transfected with either a plasmid expressing the Ad5 E1A gene (pE1A), or a control plasmid expressing luciferase (pLuc). Cells were harvested and Ad5 E1A content measured by western blot 24 h post-transfection, β- Actin was used as a loading control. **B)** DLD-1 cells were transfected with plasmids expressing Ad5 E1A or luciferase, 24 h post-transfection cells were infected with Ad5-CMV-GFP at 100 VPC, 24 h post-infection the proportion of cells positive for GFP expression was quantified by imaging on the celigo imaging cytometer. Significance was assessed by student's t-test, ns: non-significant. Bars represent ± SEM.

3.3.10 UPR induction is not responsible for the accelerated onset of EnAd/Ad11p replication

In the experiments described so far in this chapter, we aimed to explore the relationship between ER stress and oncolytic adenoviral infection. We performed experiments using a variety of chemical agents which induce ER stress to varying extents, namely thapsigargin, ionomycin and tunicamycin, and found that a subset of these, thapsigargin and ionomycin, induced a dramatic increase in numerous parameters of virus replication in EnAd and Ad11p infected cells. We originally hypothesised that the mechanism by which treatment with the chemical ER stressors could be acting to enhance E1A mRNA levels could be via downstream signalling molecules activated upon UPR induction.

To test whether UPR induction is an important mediator of the enhancing effect of thapsigargin treatment to virus activity, we infected DLD-1 and SK-OV-3 cells with the reporter viruses EnAd-CMV-GFP, EnAd-SA-GFP or Ad5-CMV-GFP, and then exposed

them to treatment with 4μ8C, an inhibitor of IRE1-mediated UPR signalling, in the presence and absence of thapsigargin. In all cases, blockade of IRE1 signalling by treatment with 4μ8C had a negative effect on virus activity. This negative effect was somewhat relieved by treatment with thapsigargin. The effect was consistent in both DLD-1 cells (Figure 3.17A) and SK-OV-3 cells (Figure 3.17B).

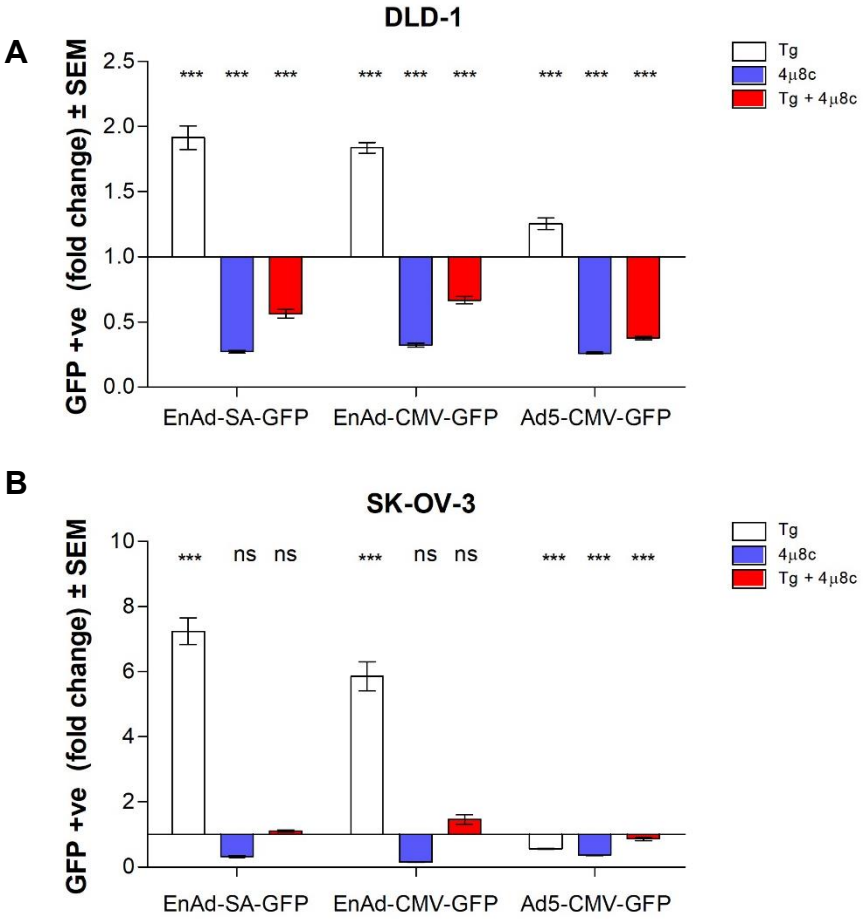


Figure 3.17. The thapsigargin effect is not mediated by IRE1 signalling. DLD-1 cells (A) or SK-OV-3 cells (B) were plated in a 96-well plate, infected with EnAd-SA-GFP, EnAd-CMV-GFP, or Ad5-CMV-GFP (all infections at a dose of 100 VPC) and treated with vehicle control DMSO, Tg (0.1 μM), and or IRE1 inhibitor 4μ8C (100 μM). Cells were imaged on a Celigo image cytometer and GFP expression quantified at 24 h (A) or 72 h (B) Significance was assessed by one-way ANOVA. ***, $p \leq 0.001$; ns, non-significant.

The ability of thapsigargin to relieve the repression to virus activity of 4μ8C treatment was not due to restoration of IRE1 activity in the presence of 4μ8C, as no splicing of XBP1 was observed when we previously treated cells with thapsigargin and 4μ8C in combination (Figure 3.6). These results suggest that IRE1 signalling may well play an important role in viral infection, as its loss impacts virus activity negatively, however thapsigargin appears to act through a different pathway. It is important to consider that small molecule inhibitors such as 4μ8C may have off-target effects and we cannot be absolutely certain from the data presented here that the loss of IRE1 signalling is responsible for the observed downregulation in virus activity.

To further support our observations with 4μ8C, EnAd E1A protein levels were examined by western blot using the EnAd-Flag-E1A virus. As previously observed, Flag-E1A expression levels increased in the presence of thapsigargin and substantially decreased in the presence of 4μ8C (Figure 3.18A). Treatment with both thapsigargin and 4μ8C resulted a level of expression similar to that in untreated cells (Figure 3.18A). These results correlate well with results obtained using fluorescent reporter viruses described in Figure 3.17.

As EnAd E1A protein levels were negatively affected by inhibition of IRE1 signalling, we explored whether this was caused by lower E1A mRNA levels. DLD-1 cells were infected with EnAd and subsequently treated with vehicle control or thapsigargin in the presence and absence of 4μ8C. As previously observed, thapsigargin treatment induced a significant increase in E1A mRNA levels. However, inhibition of IRE1 by 4μ8C treatment had no effect on E1A mRNA levels and failed to ablate the enhancement to E1A levels provided by thapsigargin treatment (Figure 3.18B). Taken together, these results indicate that thapsigargin does not increase E1A transcript levels through modulation of IRE1 signalling, as E1A transcript levels still increased in the presence of

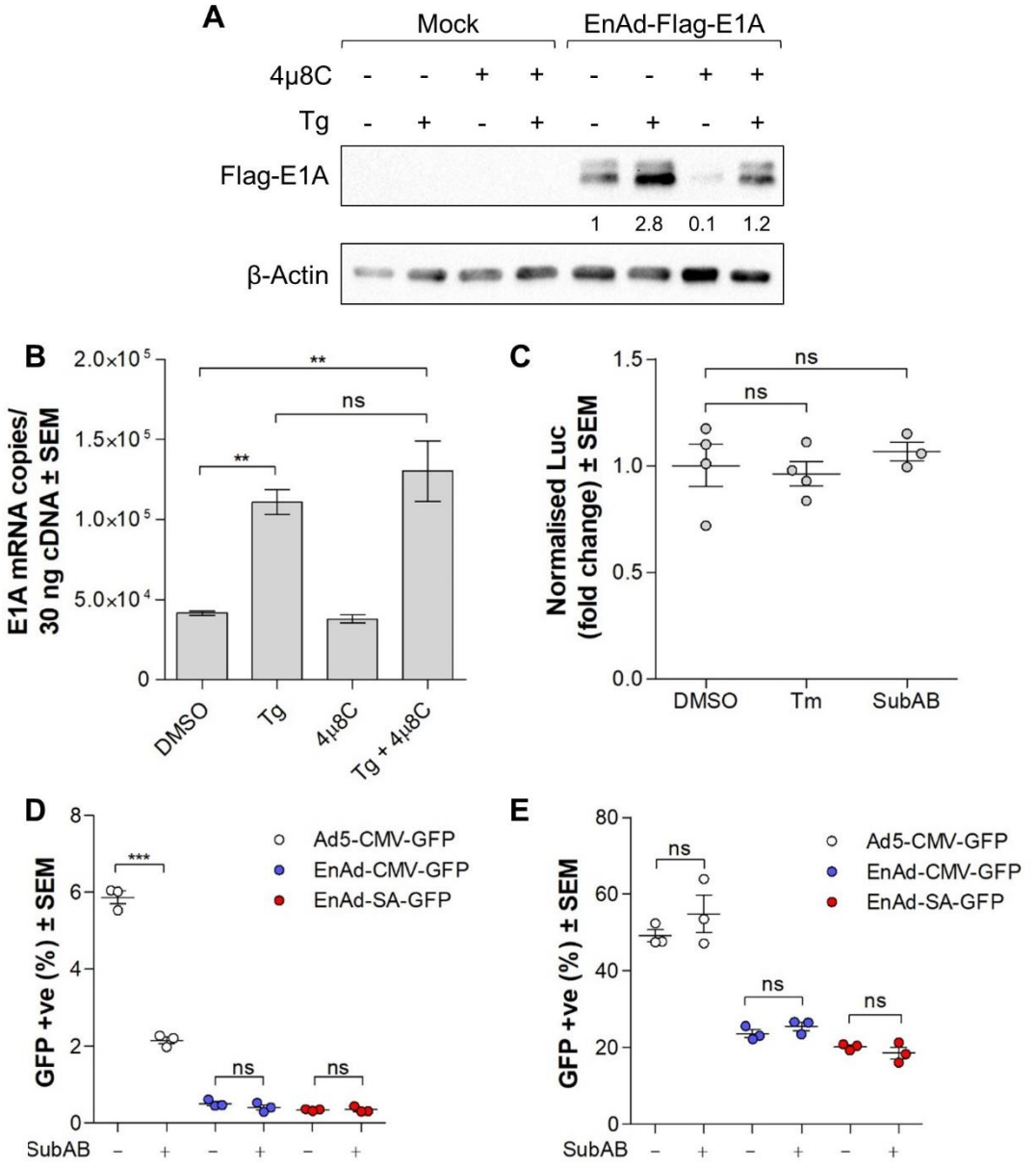


Figure 3.18. UPR induction is not responsible for the increase in early viral gene expression or virus activity. A) Western blot of Flag-E1A protein levels in DLD-1 cells 12 h post-infection with EnAd-Flag-E1A (multiplicity of infection, 3). Densitometry analysis was used to normalise each band to its loading control band, and band signal relative to the untreated control is indicated. **B)** RT-qPCR quantification of EnAd E1A mRNA in DLD-1 cells 9 h post-infection. The mean of three replicates is plotted. **C)** Quantification of E1A-Luc reporter protein levels in DLD-1 cells 12 h post-infection with Ad5-E1A-Luc. **D-E)** SK-OV-3 (D) and DLD-1 (E) were infected with EnAd-CMV-GFP, EnAd-SA-GFP, or Ad5-CMV-GFP and subsequently treated with SubAB. Data show the percentage of GFP-positive cells 72 h (D) and 24 h post-infection (E), as quantified by Celigo. Significance was assessed by one-way ANOVA; ***, $p \leq 0.001$; **, $p \leq 0.01$; ns, non-significant. The following concentrations were used: Tg (0.1 µM), Tm (1 µG/mL), SubAB (0.5 µg/mL), and 4µ8C (100 µM).

IRE1 signalling must play an important role in E1A translation however, since the addition of 4μ8C in the treatment media severely reduced E1A-Flag signal levels.

We wanted to know whether the more potent inducers of ER stress, tunicamycin and SubAB, could upregulate the expression of Ad5 E1A in the luciferase-based assay, as shown with thapsigargin and ionomycin above (Figure 3.15B). DLD-1 cells were infected with Ad5-E1A-Luc at a dose of 3 plaque forming units (PFU) per cell and subsequently exposed to treatments of either tunicamycin or SubAB. Neither treatment resulted in an increase in luciferase signal at 12 hours p.i. (Figure 3.18C).

In a further experiment, we examined the ability of SubAB to increase GFP expression from reporter viruses. SubAB is a highly specific and potent inducer of ER stress and the UPR. During normal conditions BiP is responsible for maintaining the inactive state of all three arms of UPR signalling through its inhibitory binding. Thus, the cleavage of BiP by SubAB in the lumen of the ER leads to the activation of all three arms of UPR signalling. Therefore, if UPR induction is responsible for the enhancement to virus activity seen when cells are treated with thapsigargin or ionomycin, SubAB too should have a positive effect on virus activity. DLD-1 and SK-OV-3 cells were infected with EnAd-SA-GFP, EnAd-CMV-GFP or Ad5-CMV-GFP and subsequently treated with SubAB. SK-OV-3 cells were imaged 72 hrs and DLD-1 cells at 24 hours post-infection on the Celigo imaging cytometer. SubAB treatment had no effect on the proportion of GFP-positive cells except in Ad5 infection of SK-OV-3 cells, where the addition of SubAB caused a marked decrease in GFP expression (Figure 3.18D, E).

In a final experiment, small molecule inhibitors specifically targeting all three arms of UPR signalling, IRE1, PERK and ATF6 were used. DLD-1 cells were infected with EnAd-SA-GFP and treated with combinations of thapsigargin, IRE1 inhibitor 4μ8C,

PERK inhibitor GSK 2656157 or ATF6 inhibitor Ceapin-A7. 4μ8C and GSK 2656157 did not ablate thapsigargin-mediated enhancement, whilst inhibition of ATF6 by Ceapin-A7 surprisingly did (Figure 3.19). However, in light of the other data presented in this chapter, it seems unlikely that ATF6 signalling mediates the enhancing effect to virus activity we have described, as we would have expected that tunicamycin and SubAB also increase virus activity.

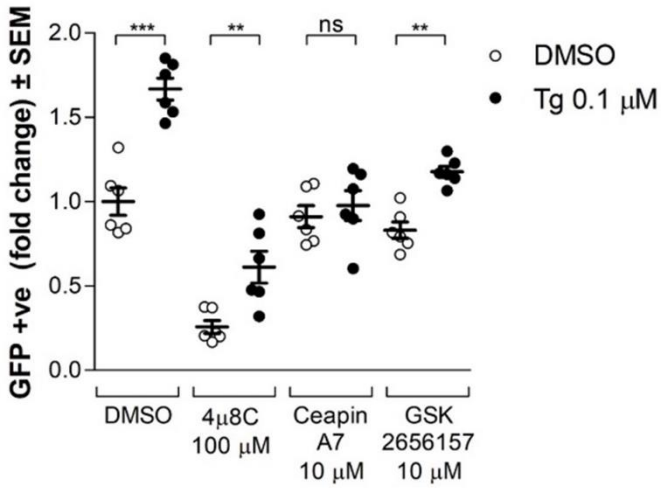


Figure 3.19. Impact of UPR signalling inhibitors on the effect of thapsigargin treatment on virus activity. DLD-1 cells were infected with EnAd-SA-GFP (100 VPC) and subsequently exposed to treatments at indicated concentrations. At 24 h post-infection, the proportion of GFP-positive cells was analysed by Celigo. Significance was assessed by one-way ANOVA. **, $p \leq 0.01$; ***, $p \leq 0.001$; ns, not significant.

We show above that tunicamycin and SubAB are more powerful inducers of ER stress than thapsigargin or ionomycin, as they cause greater XBP1 splicing (Figure 3.6) and bring about a faster and more powerful upregulation of the UPR marker BiP (Figure 3.5). These results, combined with lack of response of EnAd activity to tunicamycin (Figure 3.9A-C) or SubAB treatment (Figure 3.18D-E), show that the strongest UPR inducers, tunicamycin and SubAB, had the weakest effects on adenoviral activity. Meanwhile, thapsigargin and ionomycin, which induced UPR signalling more modestly, had

consistently strong effects in enhancing virus activity. These results highlight a reverse correlation between the strength of UPR induction and enhancement of adenovirus activity, and strongly suggest that induction of the UPR is not the determining factor mediating enhancement of virus activity observed upon treatment with thapsigargin or ionomycin.

3.4 *Chapter conclusions*

1. EnAd induces ER stress more quickly and potently than Ad5

2. A subset of ER stress-inducing chemicals, thapsigargin and ionomycin, increase EnAd and Ad11p but not Ad5 activity

3. Thapsigargin treatment upregulates EnAd and Ad5 E1A protein levels

4. Elevated E1A drives increased DNA replication, infectious virus particle production and cell killing in EnAd- and Ad11p- but not Ad5-infected cells.

5. Thapsigargin-induced upregulation of E1A and virus activity is not mediated through UPR signalling

3.5 *Chapter discussion*

Viruses can induce ER stress by various means, most directly by overloading the ER with viral proteins. The mechanism by which this might occur seems rather intuitive when considering enveloped viruses whose membrane spanning glycoproteins necessitate processing and transport through the secretory pathway and thus their overexpression may be inherently ER stress causing. For example, the HA glycoporotein of influenza virus requires N-glycosylation which takes place in the ER, and overload of the ER with this protein during infection causes ER stress (Frabutt et al., 2017). However, since adenoviruses are non-enveloped, for the most part their structural proteins do not require membrane spanning ability. With the exception of the Ad5 and Ad2 fibre protein (Cauet et al., 2005), glycosylation of adenoviral structural proteins is much less common (Murray et al., 2006). Therefore, there is no reason why their functionality should necessarily depend on processing in the secretory pathway, and hence the mechanism by which they may cause ER stress is not quite as straightforward to conceptualise.

The E3 transcription unit does encode proteins with membrane spanning ability, with variable coding capacity between virus groups (Wilson-Rawls et al., 1994). These proteins localise to the ER, potentially allowing the virus to induce ER stress by ER protein overload. However, we have found that EnAd, which has a near complete deletion of the E3 region, rather than Ad5, which has intact E3 protein expression, induces ER stress more potently. To our knowledge, this is the first report of induction of UPR through IRE1 signalling by an adenovirus. Our results suggest that an alternative mechanism to ER protein overload might be responsible for inducing ER stress.

From a set of chemical ER stress inducers, we identified two which significantly enhanced EnAd activity in a range of cancer cell lines (Figure 3.9). Thapsigargin and ionomycin both cause ER stress by modulating the flux of calcium across membranes (Prostko et al., 1995), an important cofactor for the ER folding environment. Further investigations showed that the treatments enhanced EnAd activity by upregulating levels of E1A transcription (Figure 3.14). Surprisingly, although thapsigargin increased E1A levels in both EnAd and Ad5 infection, this increase in E1A improved DNA replication, infectious virus particle production and cell killing only in cells infected by EnAd, but not Ad5 (Figures 3.11 to 3.13). It is difficult to speculate about the reason for the discrepancy in the response to thapsigargin treatment between EnAd and Ad5. Since the viruses share relatively low sequence homology (54 %) (Stone et al., 2003), any number of genetic differences could account for this difference in behaviour. We can reason however, that E1A seems to be a limiting factor to EnAd DNA replication at early time points during infection in the cell lines used, and that conversely this does not seem to be the case during Ad5 infections. Our observation that expression of E1A from a plasmid in DLD-1 cells prior to infection did not increase Ad5-CMV-GFP activity also supports this model (Figure 3.16). Although E1A is the main driver of expression of the viral DNA polymerase E2B, it is not the sole determining factor, with other viral and host cell-specific factors also playing a role. Therefore, a direct correlation between E1A expression levels and viral replication is unlikely.

These results are interesting from a basic virology perspective but may also be of value in the potentiation of therapeutically active oncolytic adenovirus. Although thapsigargin is highly toxic and has no therapeutic index *in vivo,* use of thapsigargin pro-drugs for the treatment of prostate cancer have attracted considerable interest (Denmeade et al., 2003), raising the possibility of combination therapies alongside an oncolytic virus. Importantly,

our data also strongly suggest that the enhancement of virus activity by thapsigargin or ionomycin is not dependent on UPR signalling. Instead alternative mechanistic explanations are explored in the final chapter of this thesis. Indeed, more detailed understanding of the underlying mechanism would be useful if this seemingly useful combination between the group B adenoviruses and thapsigargin were to be exploited therapeutically.

4 Targeted knockdown of SERCA2 channels by virally encoded shRNA

4.1 *Introduction*

Oncolytic adenoviruses can be armed with a range of transgenes to be expressed intratumourally to enhance the oncolytic potency of the virus, modulate the local immune response to the tumour, or modify the tumour microenvironment in a therapeutically beneficial manner. There has been substantial interest in approaches which combine gene repression with oncolytic therapies relying on the identification of cellular factors that hamper the efficacy of the virus. RNAi is the most widely used method to achieve reliable knockdown of a target gene within cells and has been exploited for the optimisation of oncolytic therapies.

Genetic constructs directing the expression of shRNAs within cells can be encoded in the viral genome to bring about knockdown of a target gene in infected cells. Conveniently, shRNAs can be easily designed from siRNA sequences that have been previously synthesised and validated for efficient knockdown (Barøy et al., 2010). The promoter used to drive the transcription of the construct can vary. Pol III promoters such as U6 and H1 have well characterised transcriptional start and termination sites, their small size allows them to be easily packaged into vectors, and they provide high levels of expression and gene silencing across multiple cell types (Giering et al., 2008). These features have made them the most widely used promoters for shRNA expression.

The arming of oncolytic adenovirus with shRNA expression constructs for the targeted knockdown of inhibitory cellular proteins has been demonstrated many times (Brachtlova and van Beusechem, 2018). The construction of an adenovirus with shRNAs targeting the cyclin dependent kinase inhibitor p21 is a good example. Briefly, it had been observed that cell cycle inhibition at the G1 checkpoint was inhibitory to adenoviral replication. Experiments showed that elevated expression of the major cyclin-dependent kinase inhibitor $p21^{WAF1/CIP1}$ inhibited adenovirus replication (Höti et al., 2006) whilst another study showed that its knockout enhanced replication (Shiina et al., 2009). On the basis of these findings, an Ad5 virus was constructed armed with shRNA expression constructs to mediate the targeted knockdown of $p21^{WAF1/CIP1}$. This recombinant virus showed increased replication and cancer cell killing both *in vitro* and *in vivo* (Höti et al., 2010).

In Chapter 3, we observed significant potentiation of EnAd infection in the presence of thapsigargin, an inhibitor of SERCA channels. In this chapter, we explore the potential for arming EnAd with shRNA constructs for the knockdown of SERCA proteins as a strategy to enhance EnAd replication in cancer cells. Three genes encode three highly conserved SERCA paralogs: SERCA1, SERCA2 and SERCA3, alternative splicing gives rise to numerous further isoforms from each gene (Brini et al., 2012). Of the SERCA genes, SERCA1 expression is confined to skeletal muscle (Zhao et al., 2015). SERCA2 is expressed ubiquitously, producing four isoforms (SERCA2 a, b, c and d). Of these, the SERCA2b isoform has an essential housekeeping role whilst the others are only expressed in muscle, heart and neuronal cells (Vangheluwe et al., 2005). The least well characterised is SERCA3 which is expressed at variable levels in numerous cell types (Martin et al., 2002). Since SERCA2 is the most widely expressed form, and because we were unable to detect the SERCA 1 or 3 proteins in our cell lines (data not shown), we decided to target the SERCA2 protein for genetic knockdown using synthetic siRNAs.

In a proof-of-concept experiment, we observed enhanced EnAd activity when the SERCA2 channels were knocked down in cells by transfection of siRNA molecules. These results incentivised us to design shRNA expression constructs, which were first validated for effective knockdown of SERCA2 by their expression from shuttle plasmids. The constructs were then incorporated into the genome of EnAd by molecular cloning followed by virus rescue. The insertion of the constructs into engineered EnAd viruses was again validated and the knockdown of SERCA2 protein in DLD-1 and SK-OV-3 cells was assessed during infection. We also characterised the replication kinetics of the engineered and unmodified viruses in both cell lines.

4.2 *Chapter aims*

1. Validate the knockdown of SERCA2 gene using synthetic siRNAs

2. Design shRNA expression constructs for targeted knockdown of the SERCA2 gene

3. Engineer an oncolytic adenovirus armed with an shRNA construct to direct knockdown of SERCA2

4. Assess whether shRNA mediated knockdown of SERCA2 by the engineered oncolytic adenovirus confers enhanced replication and cancer cell killing

4.3 *Results*

4.3.1 siRNA knockdown of SERCA2 channels enhances EnAd activity in SK-OV-3 cells

In an approach aimed to harness the powerful effect of thapsigargin and ionomycin treatment on viral replication described in chapter 3, in this chapter we explore whether the virus can be equipped with its own means to bring about this same effect and thus enhance its replication, bypassing the need for chemical intervention. To investigate whether using RNA interference for the targeted knockdown of the SERCA2 channels might mimic the enhanced virus activity phenotype observed with thapsigargin treatment, we first transfected SK-OV-3 cells with one of three siRNAs all targeting the SERCA2 gene, or with a non-target siRNA, and assayed for protein knockdown by western blot three-days post-transfection. Whilst transfection with the non-target siRNA had no impact on SERCA2 channel levels (Figure 4.1A), transfection with any of the three targeted siRNA molecules lead to a dramatic depletion of SERCA2 protein levels in cells (Figure 4.A).

After validating that siRNA could be used for the knockdown of the SERCA2 channels, the siRNAs were used to knockdown SERCA2 protein in target cells that were subsequently infected with EnAd-SA-GFP to assess the impact on viral activity. GFP expression was quantified using the Celigo cytometer 72 h post-infection. The non-target siRNA had no effect on virus activity, whilst transfection with the SERCA2-targeted siRNAs lead to a roughly 10% increase in the percentage of GFP-positive cells (Figure 4.B).

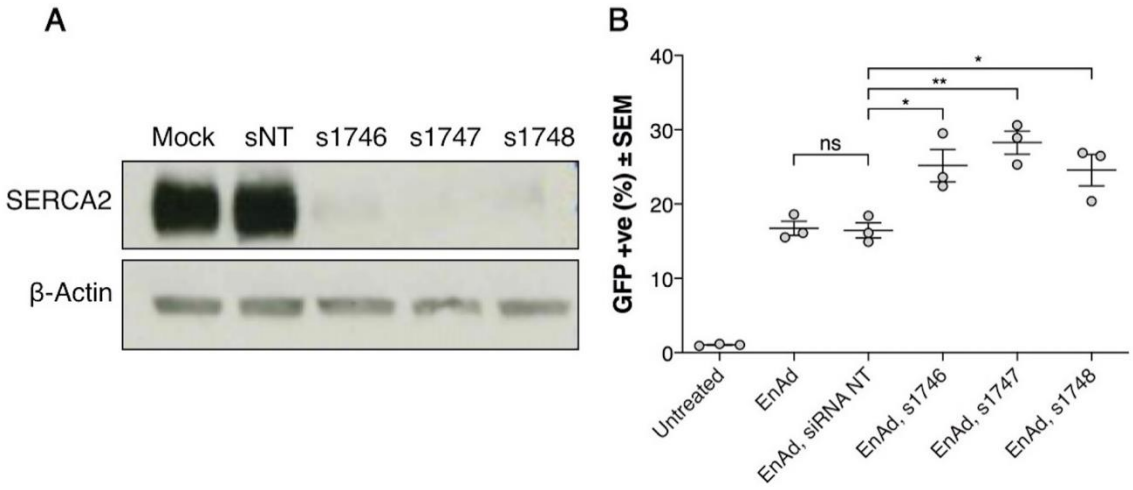


Figure 4.1. Genetic knockdown of SERCA2 channels enhances virus activity in SK-OV-3 cells. SK-OV-3 cells were transfected with one of three siRNAs targeting the SERCA2 transcript, or with a non-target negative control siRNA (sNT). A) Cell lysates were collected at 72 hours post-transfection and western blotting was used to measure levels of SERCA2 protein. β-Actin was used as a loading control. B) At 72 hours post-transfection SK-OV-3 cells were infected with 100 VPC EnAd-SA-GFP for two hours. Three days post-infection the proportion of cells positive for GFP expression was quantified by imaging in the Celigo cytometer. Significance was assessed by one way ANOVA, *** $p \leq 0.0001$, ** $p \leq 0.001$, * $p \leq 0.05$, ns: non-significant.

4.3.2 Expression of a plasmid-encoded shRNA construct successfully knocks down SERCA2 protein

Whilst siRNA transfection is a useful means to achieve transient knockdown of a target protein, shRNA expression constructs must be designed in order to be encoded in the EnAd genome to achieve the same function. Each of the three siRNAs tested produced effective knockdown and had very similar effects on virus activity (Figure 4.1B). Since no one particular siRNA offered a clear advantage over the others, we chose to use the s1748 sequence in further experiments simply due to the fact that we had already purchased a greater stock of this siRNA. An shRNA construct for the knockdown of SERCA2 was designed directly from the sequence of siRNA s1748. This was achieved by placing a loop sequence between the sense and antisense sequences of the s1748, and a T_5 termination signal immediately downstream. These shRNA sequences were

synthesised as forward and reverse strand oligos. The oligos were annealed to produce a double-stranded product containing sticky ends with complementarity ready for ligation into a vector downstream of a U6 promoter (Figure 4.2). Since the sequence of the non-target negative control siRNA is proprietary information owned by Thermo Fischer, a different negative control sequence was chosen. A previously used and published non-target shRNA sequence was used instead (Bryant et al., 2010) (Figure 4.2).

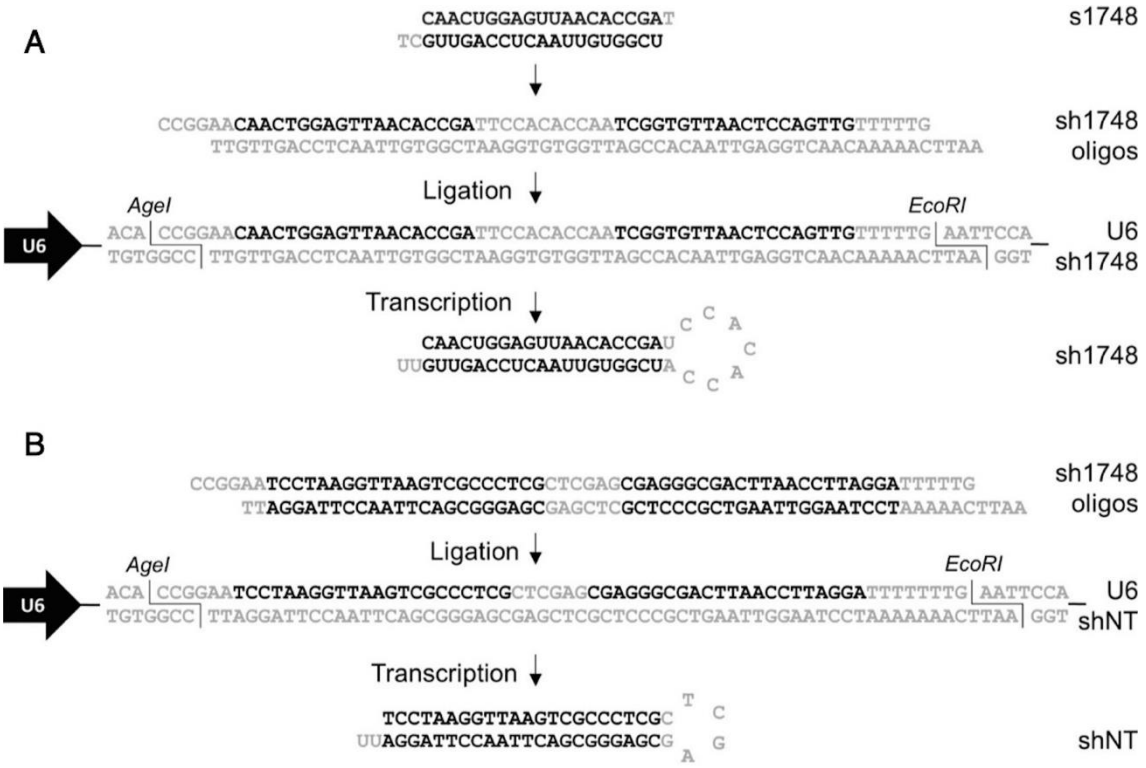


Figure 4.2. Design and construction of shRNA expression cassettes from siRNA sequence. A) The siRNA to shRNA conversion is shown for siRNA s1748. The siRNA is shown at the very top (s1748). Oligos containing the 19-nt target sequence displayed in black, a 7-nt loop sequence, a 19-nt sequence complementary to the target sequence also in black, and a T5 termination signal were annealed. The reverse oligo is shown as the bottom strand. Annealing of the forward and reverse oligos produces sh1748 oligo, with a 5' overhang of the top strand compatible with the end produced by DNA digestion using restriction enzyme AgeI, and a bottom strand 5' overhang compatible with the end produced by EcoRI digest. B) A previously published non-target shRNA sequence was used to construct the shRNA NT, following the same procedure as in (A).

Before insertion of the shRNA constructs into an appropriate shuttle vector, the shRNA sequences that were predicted to be transcribed from the shRNA expression constructs were subjected to *in silico* folding by inputting the sequences into the mFold web tool (Zuker, 2003). The secondary structure of the RNA molecules predicted by mFold were as expected for shRNA expression. (Figure 4.3A). The shRNA sequences were ligated into the U6-Stuffer shuttle plasmid, which encodes the U6 promoter, an RNA polymerase III promoter which is widely used for the expression of shRNAs (Ma et al., 2014). Directly downstream of the U6 promoter lies a large "stuffer" β-Gal sequence. The purpose of the stuffer sequence was to facilitate the resolution of undigested, single-

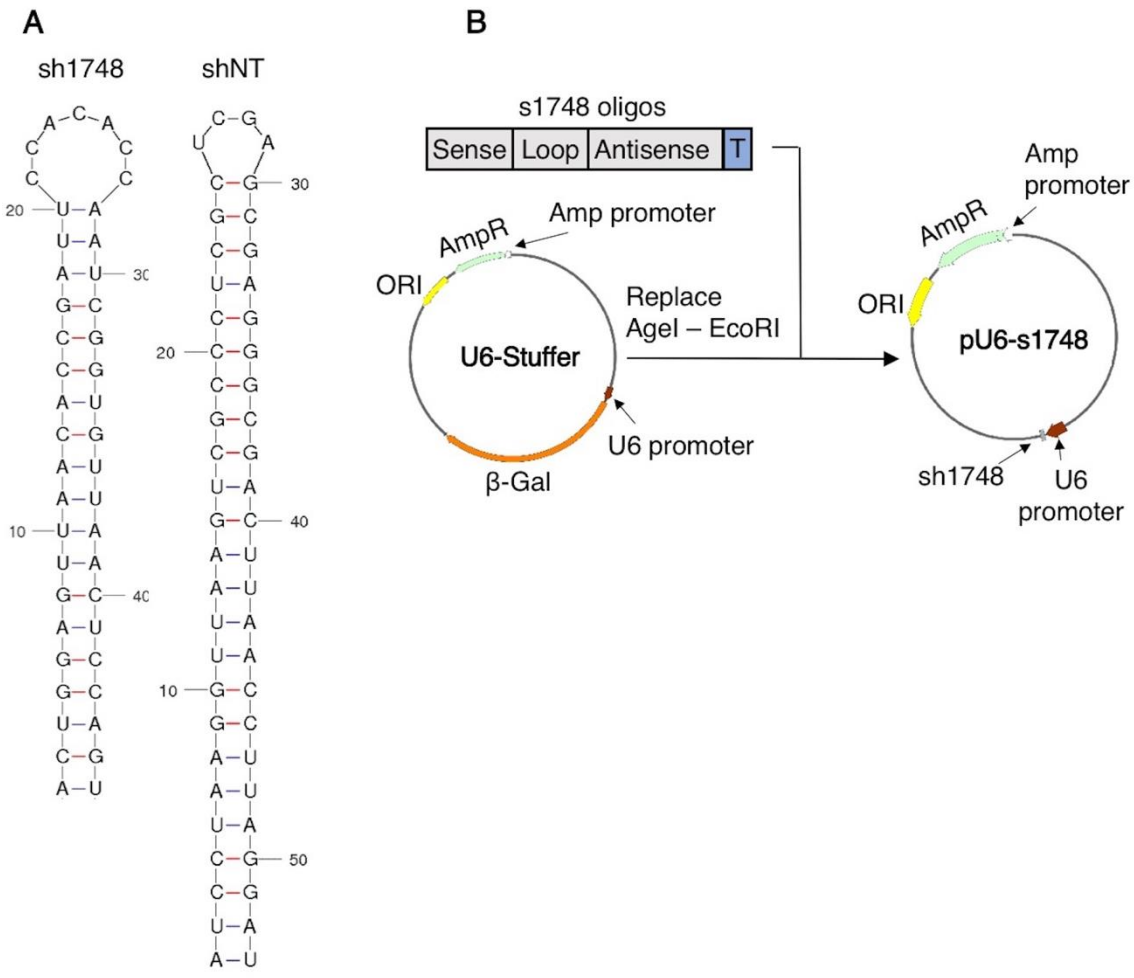


Figure 4.3. Simulated shRNA folding and the cloning strategy. A) In-silico folding of shRNA sequences was carried out using mFold. **B)** The overhanging ends produced by annealing the oligos facilitate ligation into the U6-stuffer plasmid which had also been digested with AgeI and EcoRI enzymes, to produce the pU6-s1748 plasmid.

digested and double digested plasmid by agarose gel electrophoresis following digestion by restriction enzymes, allowing purification of the double-digested product with very little or no contaminating single-digested DNA. This approach bypasses the need for dephosphorylation of the vector and allows unmodified annealed oligos with no 5' phosphate group to be directly ligated into the vector. The stuffer sequence was removed by digestion with endonucleases AgeI and EcoRI. The annealed oligo inserts were then ligated into the vector downstream of the U6 promoter, generating the pU6-sh1748 and pU6-shNT plasmids encoding the SERCA2 knockdown sh1748 and non-target shNT shRNA constructs, respectively (Figure 4.3B). Successful ligation products were selected on ampicillin-supplemented agar plates and sequence verified by Sanger sequencing.

Variable amounts of pU6-sh1748 and pU6-shNT plasmids were transfected into SK-OV-3 cells (Figure 4.4A) and DLD-1 cells (Figure 4.4B). The range of the amount of plasmid transfected was different between cell lines, with DLD-1 cells requiring more plasmid to achieve knockdown. These ranges were determined empirically in optimisation experiments, and may reflect the differences in transfection efficiency, cell number, SERCA2 expression and turnover, or likely a combination of all of these factors. At three days post-transfection, levels of SERCA2 protein were assessed by western blotting, revealing a marked decrease in expression levels when cells were transfected with increasing amounts of pU6-sh1748 but not when transfected with pU6-shNT. These results validate the design of the shRNA constructs and demonstrate that SERCA2 channel knockdown could be achieved using an shRNA encoded in pU6-sh1748.

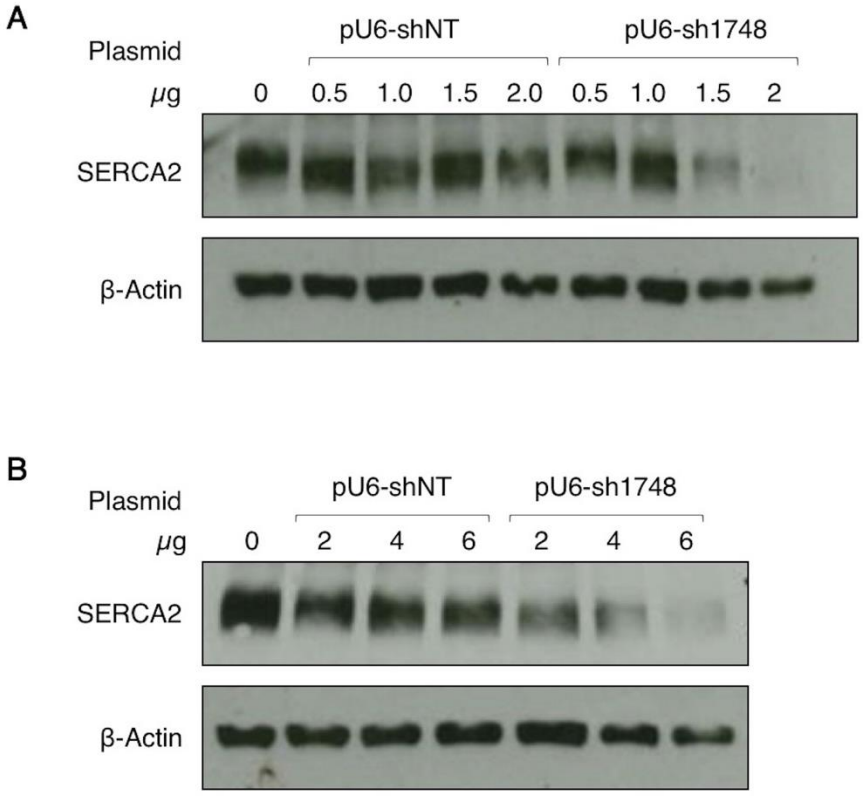


Figure 4.4. Successful knockdown of SERCA2 achieved by pU6-s1748 plasmid. A) SK-OV-3 cells or **B)** DLD-1 cells were transfected with the indicated amounts of either the pU6-shNT or pU6-sh1748 plasmids encoding the scramble control or SERCA2 targeted shRNAs respectively. At 72 hours post-transfection cell lysates were collected and analysed by western blot for SERCA2 protein levels. β-Actin was used as a loading control.

4.3.3 Engineering of an EnAd variant encoding an shRNA expression cassette for the targeted knockdown of SERCA2

Now that the shRNA expression constructs for the knockdown of the SERCA2 channels had been encoded at the DNA level, they were incorporated into the viral genome of EnAd with the aim of achieving knockdown of the SERCA2 channels in infected cells (Figure 4.5A). The U6-shRNA sequences were amplified from pU6-sh1748 and pU6-shNT by PCR (Figure 4.5B) and inserted into SbfI- and AsiSI-digested ColoAd2.4 plasmid (Figure 2.2) by Gibson assembly, directly downstream of the fibre site, generating plasmids ColoAd2.4_U6-sh1748 and ColoAd2.4_U6-shNT.

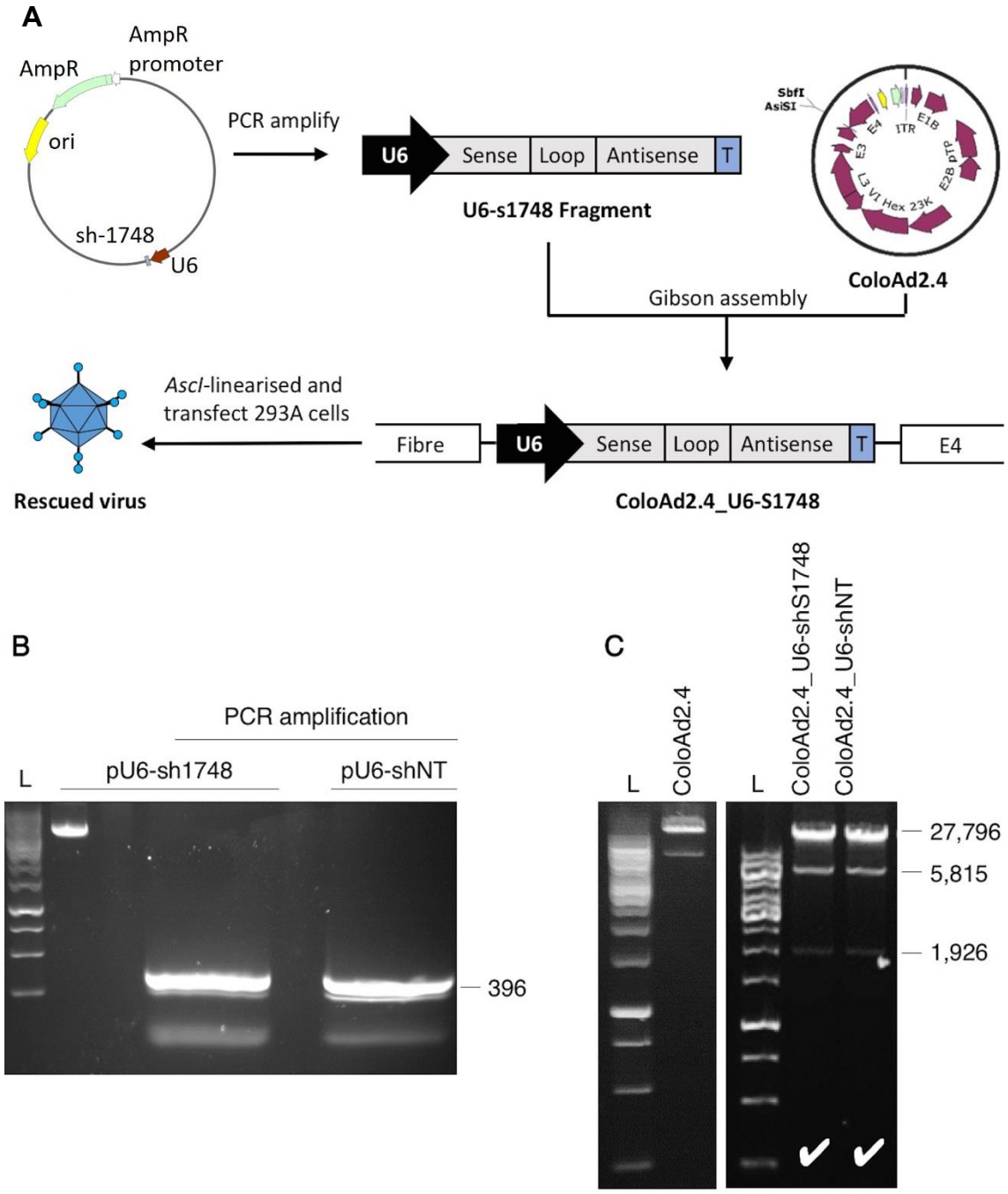


Figure 4.5. Engineering of shRNA armed adenovirus. A) Schematic representation of the cloning strategy to transfer the shRNA expression construct from the pU6-shRNA plasmid into the ColoAd2.4 plasmid and subsequent rescue of the virus. **B)** The 396 bp U6-shS1748 and U6-shNT expression constructs were amplified by PCR from the pU6-shS1748 and pU6-shNT plasmids. L, Generuler 1 Kb ladder. **C)** Recombinant plasmids generated by Gibson assembly of the PCR fragments generated in B into linearised ColoAd2.4 plasmid were screened for correct insertion of the shRNA expression construct by digest with EcoRI. Correct insertion is demonstrated by the presence of a 1,926 bp band and are indicated by a tick.

Correct insertion of the U6 shRNA constructs was validated by diagnostic restriction digest using EcoRI (Figure 4.5C). Unmodified ColoAd2.4 plasmid generates two restriction bands, whereas ColoAd2.4 with an U6-shRNA insert generates three bands. The sequences of the plasmids were validated by Sanger sequencing.

The ColoAd2.4_U6-S1748 and ColoAd2.4_U6-NT plasmids were linearised by digestion with AsiSI. The linearised recombinant viral genomes were transfected into HEK293A cells. Successful virus replication resulted in cytopathic effect and formation of plaques in a monolayer of HEK293A cells. At an advanced stage of cytopathic effect, supernatants were harvested and serially diluted in a plaque assay in order to isolate individual viral clones. Serially diluted supernatants were used to infect A549 cells which were then overlaid with agarose. On day seven post-infection, plaques beneath the agarose were evident (Figure 4.6). Plaques were picked using sterile pipette tips and used to infect fresh HEK293A cells to amplify the selected clone in a subsequent round of infection. Three rounds of plaque purification were performed in total.

After the third round of plaque purification, a T175 flask of A549 cells was infected. To check that the viral progeny produced encoded the intended shRNA expression construct, when significant cytopathic effect was observed 5 µl of the virus containing supernatant was collected and used to perform a PCR reaction using primers to amplify across the transgene insertion site. Resolution of the PCR product by gel electrophoresis generated the expected amplification products of 516 bp for EnAd_U6-S1748 and EnAd_U6-NT, and ~1800 bp for EnAd-CMV-GFP which had been used as a control (Figure 4.7A). Sanger sequencing of the PCR amplicons confirmed that the viral clones contained inserts of the correct DNA sequence encoding the shRNA expression constructs (Figure 4.7B).

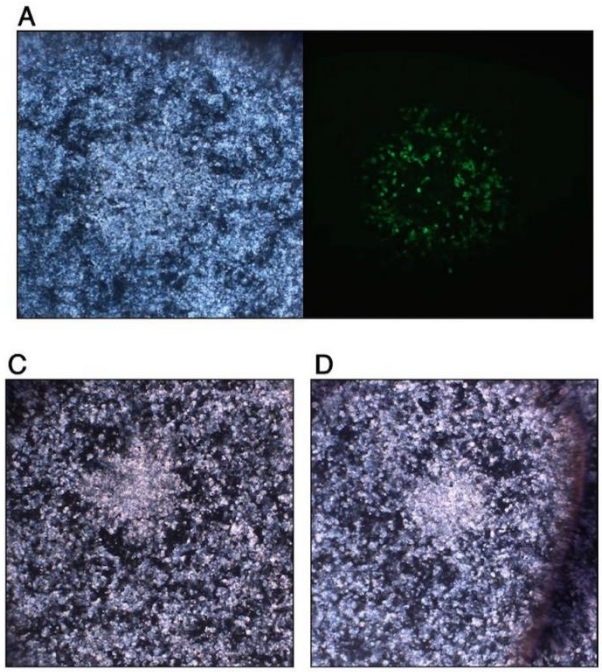


Figure 4.6. Plaque purification of individual viral clones. Plaque assays were performed by serially diluting recued virus onto A549 cells and overlaying with agar. On day 7 post-infection, plaques were imaged by fluorescence microscopy, picked, and transferred onto fresh HEK293A cells for further rounds of infection and purification. **A)** Example plaque from cells which had been infected with EnAd-CMV-GFP virus. Image of the plaque in brightfield (left). The image of the same plaque in the fluorescent channel (right) shows that the plaque is produced from viral infection. **B, C)** Individual plaques on A549 monolayer produced by infecting with **s**erially diluted supernatants from cells transfected with the ColoAd2.4_U6-sh1748 (B) or ColoAd2.4_U6-shNT (C).

Infected A549 cells from the T175 flask were harvested and an aliquot was analysed for the presence of viral capsid proteins. Western blotting confirmed that viral capsid proteins were being expressed at normal levels by EnAd_U6-sh1748 and EnAd_U6-shNT (Figure 4.7C). A virus stock for each recombinant virus and unmodified EnAd was then generated by subjecting the rest of the cells to three rounds of freeze-thawing to encourage cell lysis and release of virus particles. Cell debris was removed by centrifugation and lysates aliquoted and stored at -80^{o}C. Viral lysates were titred by $TCID_{50}$ serial titration (Figure 4.7D). We assessed the replication of the viruses using crude cell lysates because we wanted to first verify that the modified viruses replicated normally and to assess whether

they would merit extensive use and further study before carrying out expensive and time-consuming caesium chloride banding purification.

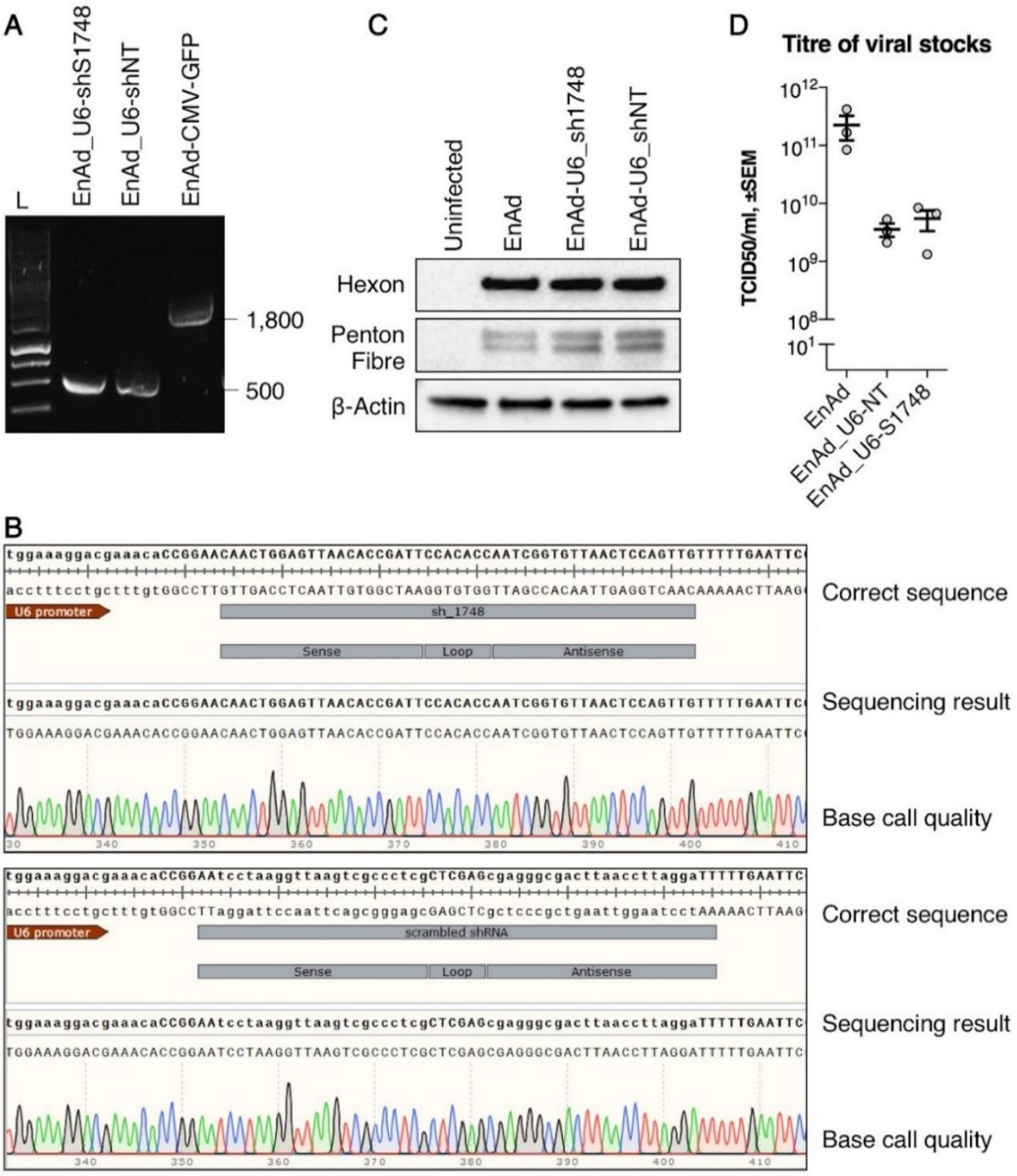


Figure 4.7. Validation of the engineered shRNA armed adenoviruses. To create equivalent stocks of the engineered virus and of unmodified EnAd, A549 cells were infected with EnAd or with virus which has been rescued by transfection of linearised coloAd2.4_U6-shNT, or coloAd2.4_U6-sh1748 plasmid into cells. When cytopathic effect was observed the following experiments were performed. **A)** 5 µl of supernatant was used in a PCR reaction using primers to amplify the transgene insertion in the EnAd genome. The PCR reaction product was resolved on a 1% agarose gel, revealing inserts of correct lengths corresponding to the U6-shRNA expression constructs or the CMV-GFP expression construct. **B)** PCR amplicons generated in A were sent for Sanger sequencing. Results from the shRNA expression construct are shown. **C)** Cells were harvested and a sample of them were analysed by western blot for adenoviral capsid proteins. β-Actin was used as a loading control. **D)** The rest of the harvested cells were used to make a stock of virus. This viral stock was titred by the $TCID_{50}$ method.

4.3.4 EnAd_U6-sh1748 achieves SERCA2 knockdown during infection of SK-OV-3 cells

Once we had generated validated stocks of EnAd_U6-sh1748 and EnAd_U6-shNT, we assessed their ability to direct the knockdown of the target protein SERCA2 over the course of an infection. Whilst EnAd and EnAd_U6-shNT infections should in principle have no effect on SERCA2 protein levels, we expected EnAd_U6-sh1748 to knockdown SERCA2 protein expression via its encoded shRNA construct targeted against the SERCA2 mRNA sequence.

EnAd, EnAd_U6-S1748 or EnAd_U6-NT were used to infect DLD-1 or SK-OV-3 cells at a dose of 3 or 10 $TCID_{50}$/cell, respectively (Figure 4.8). A higher infectious dose was used when infecting SK-OV-3 cells due to their inherent resistance to infection. Cells

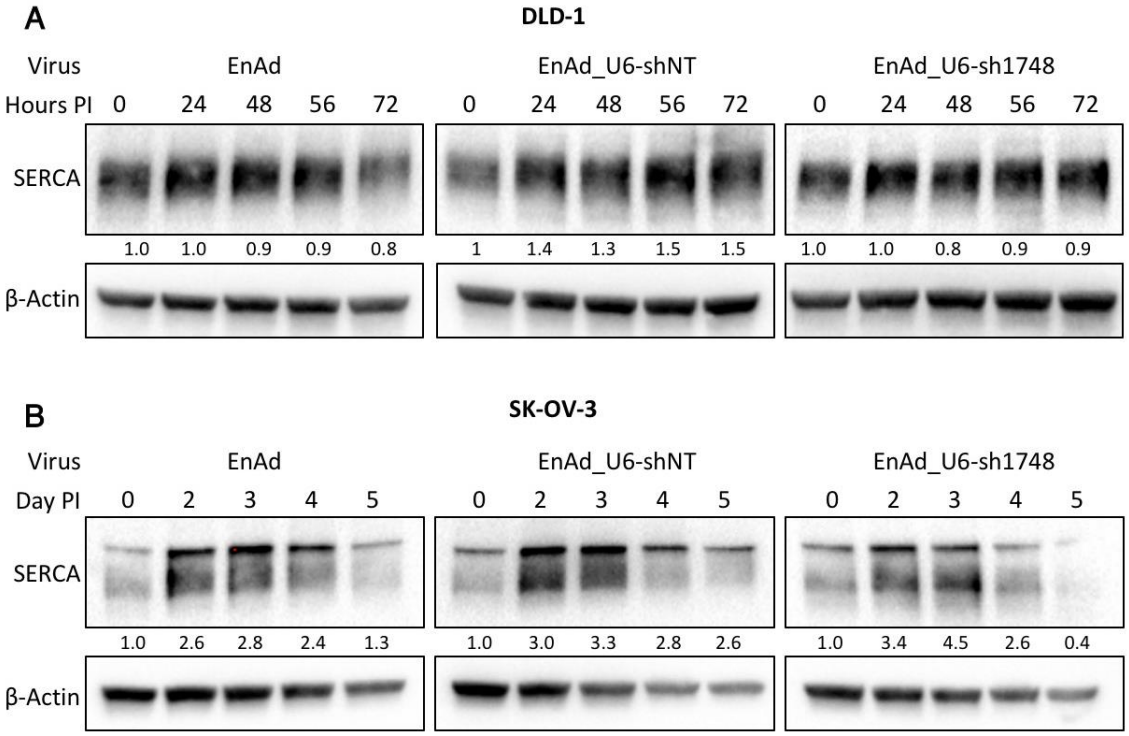


Figure 4.8. Targeted knockdown of SERCA2 can be achieved by adenovirally delivered shRNA. Unmodified EnAd, EnAd_U6-sh1748 or EnAd_U6-shNT were used to infect **A)** DLD-1 cells at a dose of 10 $TCID_{50}$ /cell or **B)** SK-OV-3cells at a dose of 3 $TCID_{50}$ /cell. Cells were harvested at the indicated times post-infection and the level of SERCA2 protein were measured by western blotting. β-Actin was used as a loading control. Densitometry analysis was used to normalise each band to its loading control band, and to provide a quantification value relative to the uninfected control in each group (day p.i. 0).

were then harvested at various time points over the course of the infection and cell lysates were probed for SERCA2 protein by western blotting. In DLD-1 cells, no substantial knockdown of SERCA2 occurred in cells infected with any of the three viruses (Figure 4.8A). In SK-OV-3 cells however SERCA2 protein levels increased initially at days 2, 3 and 4 post-infection with each of the three viruses. On the fifth day post-infection however, only in cells infected with EnAd_U6-sh1748 were SERCA2 levels reduced to levels lower than those observed before infection (Figure 4.8B).

4.3.5 EnAd_U6-sh1748 does not display enhanced viral replication

We assessed whether the inclusion of the shRNA expression constructs into the EnAd viral genome had translated into accelerated viral DNA replication as we had observed previously in cells treated with thapsigargin (Figure 3.9). Cells were infected with either EnAd, EnAd_U6-shS1748 or EnAd_U6-shNT at a dose of 3 $TCID_{50}$/cell (for DLD-1 cells) or 10 $TCID_{50}$/cell (for SK-OV-3 cells). Infected cells were harvested at various time points post-infection and viral genomes were quantified by qPCR. Initial rates of viral genome replication were very similar among the three viruses. However, a significant

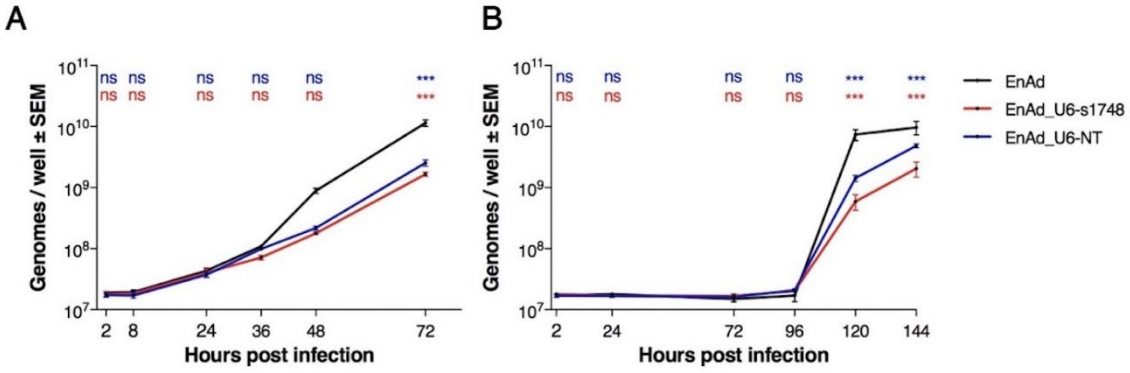


Figure 4.9. Viral genome production of engineered EnAd viruses. EnAd, EnAd_U6-shNT or EnAd_U6-sh1748 were used to infect A) DLD-1 cells at a dose of 3 TCID50/cell or B) SK-OV-3 cells at a dose of 10 TCID50/cell. Cells and supernatants were harvested at the indicated time points and viral genomes quantified by qPCR. Significance between the engineered and unmodified EnAd virus at each time point was assessed by two-way ANOVA. *** $p \leq 0.0001$, ** $p \leq 0.001$, * $p \leq 0.05$, ns: non-significant.

increase in the number of viral genomes measured in cells infected with EnAd compared to those infected with the modified viruses became apparent over time. In DLD-1 cells at 72 hours post-infection, the number of viral genomes in EnAd-infected cells was ten-fold higher than the number of viral genomes in cells infected with either of the two modified viruses (Figure 4.9A). Similar results were obtained in SK-OV-3, with EnAd producing a significantly higher number of viral genomes than either of the two engineered viruses from 120 hours post-infection onwards (Figure 4.9B).

4.3.6 EnAd_U6-sh1748 does not show increased virus particle production

We quantified the number of infectious virus particles produced by the engineered viruses in a $TCID_{50}$ experiment. SK-OV-3 and DLD-1 cells were harvested at five- and two-days post infection respectively. We found that the modified viruses EnAd_U6-s1748 and EnAd_U6-NT produced similar titres of progeny virus, but that these levels were

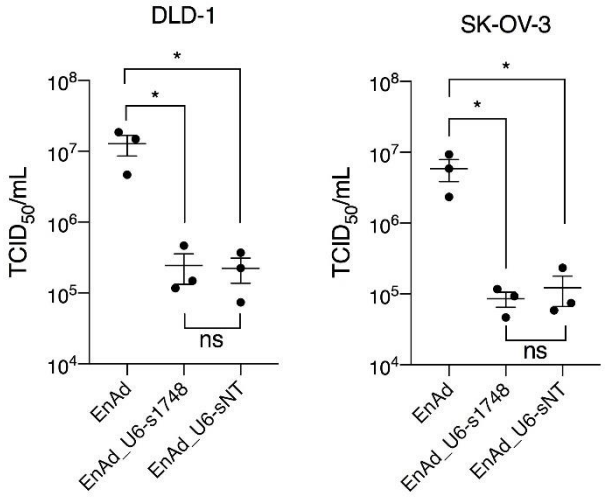


Figure 4.10. Infectious particle production is reduced in modified viruses. DLD-1 or SK-OV-3 cells were infected with viruses at a dose of 3 or 5 TCID50/cell respectively. DLD-1 cells were harvested at 2 days post-infection, and SK-OV-3 cells at 5 days post-infection. Infectious particle titre was then quantified by the $TCID_{50}$ method. Bars represent ± standard error of the mean. Significance was tested by one-way ANOVA. *** $p \leq 0.0001$, ** $p \leq 0.001$, * $p \leq 0.05$, ns: non-significant.

significantly below the levels produced by unmodified EnAd virus in each cell type (Figure 4.10).

4.3.7 EnAd_U6-sh1748 does not show increased cell killing

Previous experiments combining EnAd with thapsigargin, an inhibitor of SERCA channels (Figure 3.9), and experiments in which we had knocked down SERCA2 with siRNAs (Figure 4.1) strongly suggested it may be possible to potentiate cell killing by arming EnAd with ability to inhibit SERCA2 function by shRNA mediate knockdown. To investigate the effect of arming EnAd with SERCA2-specific shRNAs on cell killing, cells were infected with EnAd, EnAd_U6-sh1748 or EnAd_U6-shNT, at a dose of 3 or 10 $TCID_{50}$/cell for DLD-1 and SK-OV-3 cells, respectively. Cell death was monitored by the xCELLigence system, which measures electrical impedance to provide a read-out of cell viability. Cells were seeded to confluency and therefore show a rapid increase in cell index as cells adhered to the plate, reaching a plateau once all cells have attached to the surface of the well. In uninfected samples the signal remains stable for several days until cells begin to die due to over-confluence and nutrient deprivation (Figure 4.11).

Using DLD-1 cells, which are highly permissive to EnAd infection, virus-induced cytopathic effect becomes apparent quite rapidly, at just after 24 h post-infection. This is seen as a decrease in the cell index in infected cells. The onset of this cytopathic effect occurs at approximately the same time for all three viruses used, though cultures of cells infected with unmodified EnAd reach a cell index of 0 slightly earlier, indicating complete destruction of the monolayer (Figure 4.11A).

The effects were more dramatic in SK-OV-3 cells, as they are intrinsically more resistant to EnAd infection, and virally induced cytopathic effect does not occur until between

four- and five-days post-infection in EnAd-infected cells. Cell killing then ensues rapidly, with complete monolayer destruction by eight days post-seeding. Cultures infected with EnAd_U6-sh1748 and EnAd_U6-shNT, however, displayed substantially slower killing. Whilst cytopathic effect in these samples began at roughly the same time as in cells infected with unmodified EnAd, killing was slower taking approximately 2 days longer to reach a CI of near zero (Figure 5.11B).

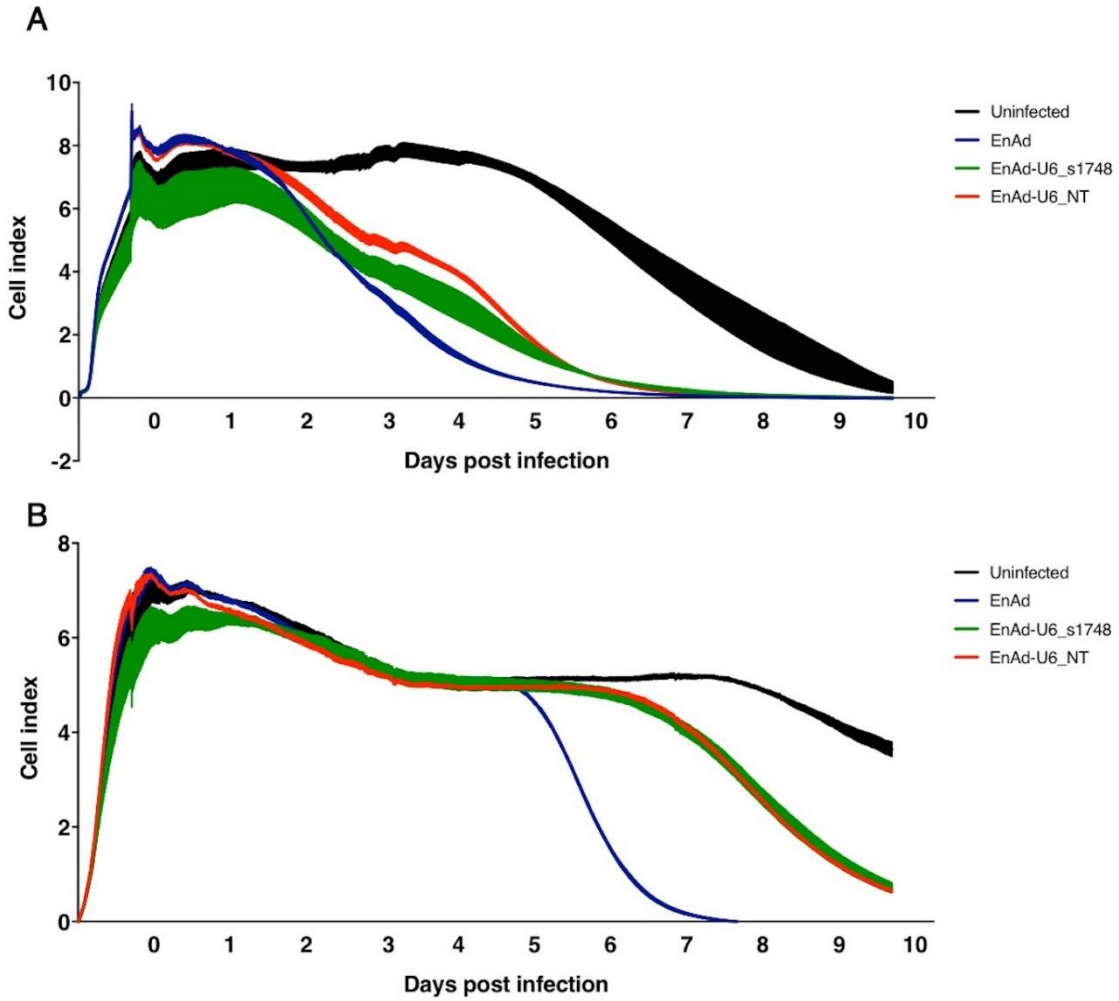


Figure 4.11. Arming EnAd with shRNA expression constructs for SERCA2 knockdown does not enhance killing. EnAd, EnAd_U6-shNT, EnAd_U6-sh1748 were used to infect (A) DLD-1 cells at a dose of 3 TCID50 /cell or (B) SK-OV-3 cell at a dose of 10 TCID50 /cell. Virus induced cell killing was monitored by xCELLigence. Impedance was measured every 10 minutes. Data show the mean of four replicates, weight of the line indicates ± SEM.

4.4 *Chapter conclusions*

1. shRNAs can be designed from siRNA sequences for the targeted knockdown the SERCA2 channel protein

2. EnAd armed with shRNA expression constructs can mediate knockdown of a target gene during infection

3. EnAd armed with shRNA for the targeted knockdown of SERCA2 did not result in accelerated replication kinetics, infectious particle production or enhanced killing

4.5 *Chapter discussion*

Building on our observations presented in chapter 3 that show that inhibition of the SERCA channels by treatment of cells with thapsigargin enhances EnAd activity, we devised a strategy to arm EnAd with its own means of bring about this effect. Adenovirally encoded shRNAs represents an attractive way to direct the knockdown of a target gene in infected cells. In this chapter, we designed a U6 Pol III promoter-driven shRNA expression construct from the sequence of a commercially available and validated siRNA. These shRNAs were expressed within cells from shuttle plasmids pU6-sh1748 and pU6-shNT, demonstrating targeted shRNA mediated knockdown of the SERCA2 channel proteins in DLD-1 and SK-OV-3 cells (Figure 4.4.A, B). We molecularly cloned these shRNA constructs into the genome of the oncolytic adenovirus EnAd (Figure 4.5,

4.6. and 4.7). However, when the engineered viruses EnAd_U6-sh1748 and EnAd_U6-shNT were used to infect cells, knockdown of SERCA2 was achieved only in SK-OV-3 cells.

The efficiency and speed of the knockdown of a target protein depends not only on the levels of expression of the shRNA molecule but also on the turnover of the target protein. SERCA2 is a stable, long-lived protein with a half-life of approximately three days (Andersson et al., 2009), potentially explaining why knockdown is not visible before five days post-infection in SK-OV-3 cells with EnAd_U6-sh1748. However, cultures of DLD-1 cells, which are highly permissive to EnAd replication, are almost completely lysed by three days post-infection; by five days post-infection, there are no cells remaining (Figure 4.11). Therefore, the kinetics of EnAd replication and SERCA knockdown in DLD-1 cells and other cell lines which are highly permissive to EnAd replication may be incompatible with EnAd-encoded shRNA strategies, since the cells are killed too quickly for knockdown to be measured. Conversely, in SK-OV-3 cells, far more time elapses between initial infection and cell lysis, providing a longer time window in which to measure knockdown. shRNAs are often chosen over siRNAs for the knockdown of proteins with longer half-lives, since their expression is stable and more persistent than siRNAs from a transient transfection. However, in the context of a replicating lytic viral infection time is limited, thus targeting proteins with shorter half-lives may be more sensible as knockdown will occur more quickly. Clearly a balance must be struck, between the half-life of the target protein and the replication cycle of the virus.

We had hypothesised that an enhancement to viral replication similar to that observed upon treatment with thapsigargin might be achievable by inhibiting the SERCA2 channels through RNA interference. However, the results presented in this chapter indicate that in SK-OV-3 cells, where knockdown of SERCA2 was observed by infection

of cells with EnAd_U6-sh1748, kinetics of viral replication were not enhanced compared to EnAd_U6-shNT. When compared to the parental virus EnAd, the modified viruses both displayed reduced viral genome replication and infectious virus particle production. One explanation for the lack of an enhancing effect might be timing. Thapsigargin will begin to exert its effects as soon as it binds to its target which will occur very quickly after application of thapsigargin supplemented medium to cells. This contrasts with the days needed to achieve any appreciable knockdown using the shRNAs. Perhaps the opportunity to induce an increase in virus activity is confined to early time points during the virus life cycle before shRNA mediated knockdown has any effect. This might be likely if the effect is to enhance E1A as we observed in the previous chapter, since E1A expression is needed for the transactivation of the other viral genes at early time points (Berk, 1986). In fact, inclusion of the shRNA expression constructs in the viral genome actually hindered rather than enhanced viral replication in SK-OV-3 cells. Since both EnAd_U6-sh1748 and EnAd_U6-shNT had attenuated replication in target cells compared to the parental EnAd virus, the reason for the hindrance to replication must be independent of any specific effect on the SERCA2 protein, and rather be due to some relationship between the virus infection and the RNA interference pathway in cells, or an effect of inclusion of the transgene into the viral genome

The interactions between adenovirus replication and the RNAi pathway are complex. RNAi is often considered to be a cellular defence mechanism against viral infections, and thus viruses have evolved various ways of inhibiting the pathway (Cullen, 2002). Particularly, the virus associated RNAs (VA RNA) I and II have been shown to inhibit the RNAi pathway at various levels. VA RNA I and II compete against host miRNA precursor molecules for nuclear export, processing by dicer, and incorporation into the RISC complex. They also directly downregulate dicer by inhibition of dicer mRNA

nuclear export (Bennasser et al., 2011). Consequently, deletion of the VA RNA genes can result in improved knockdown efficiency when using non-replicating adenoviral vectors (Machitani et al., 2013), but since the VA RNA sequences are needed for efficient translations of late viral RNAs (Thimmappaya et al., 1982), this is not a suitable strategy when considering replication competent vectors.

One point to consider is that any additional sequence added to the genome will impart a small burden on the virus, as a longer genome will by its very nature require more time to replicate. However, the shRNA expression constructs are extremely short at only 310 bases and should have no effect in this regard. Although there are many examples in the literature of adenoviruses armed with shRNAs that function to enhance their replication (Shiina et al., 2009), these are almost without exception based on Ad5 vectors. This is undoubtedly due to the popularity of Ad5 as a vector and the lack of molecular tools for modification of less commonly used group B viruses, but nonetheless, we were unable to find any example of a group B adenovirus engineered to express shRNA constructs. It is possible that EnAd, or group B viruses in general, are less amenable to use as replication competent vectors for shRNA expression, though there is currently no evidence to support this, and it remains unclear why in our case inclusion of shRNA constructs was prejudicial to replication.

In light of what we now know, it may have been a better approach to mimic the action of ionomycin, by encoding some protein to directly promote the release of calcium from the ER. However, well characterised ER located calcium release channel proteins such as the inositol 1,4,5-trisphosphate receptor (IP_3R) and ryanodine receptors (RyRs) are extremely large multimeric proteins, consisting of approximately 5,000 amino acids in length (Van Petegem, 2012), and would not be amenable to encoding in adenovirus. Other strategies to take advantage of the replication enhancing effects observed in chapter three surely

exist, and a better mechanistic understanding of the effect would allow it to be exploited more efficiently. Therefore, the following and final experimental chapter of this thesis attempts to explain why the virus responds positively to only a subset of the ER stress inducers used and involves a more detailed look at the mechanism behind the virus enhancing effects observed.

5 Calcium influx enhances oncolytic adenovirus activity through activation of PKCα.

5.1 *Introduction*

The ER calcium concentration is critical for the proper functioning of resident ER chaperone proteins (Corbett et al., 1999), and directly affects translation initiation and protein synthesis (Görlach et al., 2006). Thapsigargin and ionomycin induce ER stress primarily by depleting the ER of its calcium pool, compromising its ability to fold proteins. However, ER calcium depletion and the consequent rise in cytosolic calcium have many implications for the cell beyond ER stress, and the availability of calcium ions impacts almost every aspect of cell biology. Since calcium flux modulation is the primary effect of thapsigargin and ionomycin, the two treatments that had the greatest effect on adenovirus activity (described in chapter 3), this chapter investigates whether this could be the means by which virus activity was enhanced, rather than by UPR signalling as originally hypothesised.

During adenoviral infections, numerous lines of evidence suggest that disruption of calcium pools can enhance the spread of oncolytic adenovirus both *in vitro* and *in vivo* (Gros et al., 2010, 2008). Previous work with EnAd has described an influx of extracellular calcium late during infection associated with the process of oncolysis (Dyer et al., 2017). Importantly, the effect we described in the first experimental chapter of this thesis is one of enhancing viral replication, and thus must be a separate process to those previously described effects in the cited studies, which specifically pertain to viral spread.

Adenoviruses are first internalised into the cell via a process of endocytosis after having bound to cell surface receptors. This means that the virus particles follow the endosomal route towards acidic compartments and must escape the endosome after endocytosis in order to access the cell and reach the cytoplasm. A number of studies have demonstrated an important link between calcium stores and virus entry, including a role for nicotinic acid adenine dinucleotide phosphate (NAADP)mediated calcium release through two-pore channels (TPC) from endosomes in the endosomal escape of Ebola virus (Wu et al., 2006; Cheshenko et al., 2007; Bozym et al., 2010; Sakurai et al., 2015). In Ebola, blockade of NAADP regulated calcium release by treatment of cells with small molecule TPC inhibitor Ned-19 blocked infection, suggesting that calcium release regulated by NAADP was critical for infection (Sakurai et al., 2015). This has also been found to be the case for a form of coronavirus, as knockdown of TPCs impaired infectivity (Gunaratne et al., 2018). Indeed, calcium flux through endo/lysosome localised TPC channels has many important implications for the morphology, trafficking and maturation of these intracellular acidic compartments (Gunaratne et al., 2018).

An increase in the number of infectious viral particles reaching the nucleus of the cell could account for the effect we observed in Chapter 3; however, this seems unlikely due to the timing of the treatments which took place after a window of infection in which most infectious particles should have already reached the nucleus (Greber et al., 1997). Instead, we focused our attention on searching for a cellular effector of calcium signalling that might act either directly or indirectly to regulate transcription in favour of adenoviral replication upon treatment with thapsigargin.

Fundamentally, intracellular calcium signalling is initiated by release of calcium from an intracellular store. The most important calcium store is the ER, and, by extension the nuclear envelope, which forms a contiguous luminal space with the ER. These organelles

harbour a calcium concentration four orders of magnitude higher than that in the cytoplasm (Bagur and Hajnóczky, 2017). More recently, acidic vesicles such as endosomes and lysosomes have emerged as sites for calcium storage with implications for calcium signalling (Patel and Docampo, 2010).

The PKC family of protein kinases are among the most important calcium signal transducers and have been implicated in viral infections as already discussed. Importantly, treatment with PMA, an activator of PKC, has been reported to accelerate the onset of transcription of the early adenoviral genes (Carter et al., 1984). A further study identified a PMA responsive sequence within the promoter region of the gene and suggested, though with limited evidence in the form of southwestern blotting, that the responsiveness was due to the binding of unknown protein complexes to a region of the adenoviral E1A enhancer region (Gai and James, 2002).

In this chapter, we investigate how manipulation of calcium pools within intracellular calcium stores might affect infection. We measure how thapsigargin and ionomycin treatments mobilise calcium, acting to modulate the flux of calcium from both the extracellular pool and from intracellular calcium stores. We show that extracellular influx of calcium is critical in mediating the enhancing effect of these treatments to virus activity, and that this is achieved through the PKCα isoform.

5.2 *Chapter aims*

1. Describe the effects of thapsigargin and ionomycin treatments on cytosolic calcium levels.

2. Determine whether calcium flux modulation plays a role in the effect of thapsigargin on virus activity.

3. Identify the mechanism by which thapsigargin enhances virus activity.

5.3 *Results*

5.3.1 Thapsigargin and ionomycin treatments induce calcium influx

The results presented in Chapter 3 suggest that the induction of the UPR was not responsible for the upregulation of virus activity in cells upon treatment with thapsigargin or ionomycin. Both treatments interfere with calcium modulation in cells. Therefore, we monitored cytoplasmic calcium levels in DLD-1 cells under different conditions and upon treatment with either thapsigargin or ionomycin. To do so, cells were loaded with a cell permeable calcium-sensitive dye (Fluo-8, Abcam, UK #ab112129). Fluo-8 has lipophilic blocking groups which are cleaved by esterases upon entry into the cytoplasm, this imparts a negative charge on the dye which keeps it inside the cell. When bound by calcium the fluorescence of Fluo-8 is greatly increased, allowing cytosolic calcium levels to be monitored over time.

Fluorescence from cells was recorded over time using a plate reader to track changes in cytosolic calcium (Figure 5.1A). To distinguish between extracellular and intracellular sources of calcium, dye-loaded cells were initially maintained in calcium-free media supplemented with 2% dialysed calcium-free FBS. After 5 minutes of continuous measurements, thapsigargin, ionomycin or DMSO was injected into the appropriate wells of the plate (Figure 5.1A). Ionomycin induced the largest increase in cytosolic calcium, followed by thapsigargin, with DMSO having a very minor effect (Figure 5.1B). As at the time of treatment injection the cells were being maintained in calcium-free media, the source of the small spike in cytosolic calcium must have been intracellular calcium stores. Measurements proceeded for a further five minutes before re-introducing calcium into the media. In all treatment groups, this sudden rise in the extracellular concentration of calcium produced a spike in fluorescence. However, this spike in cytosolic calcium was

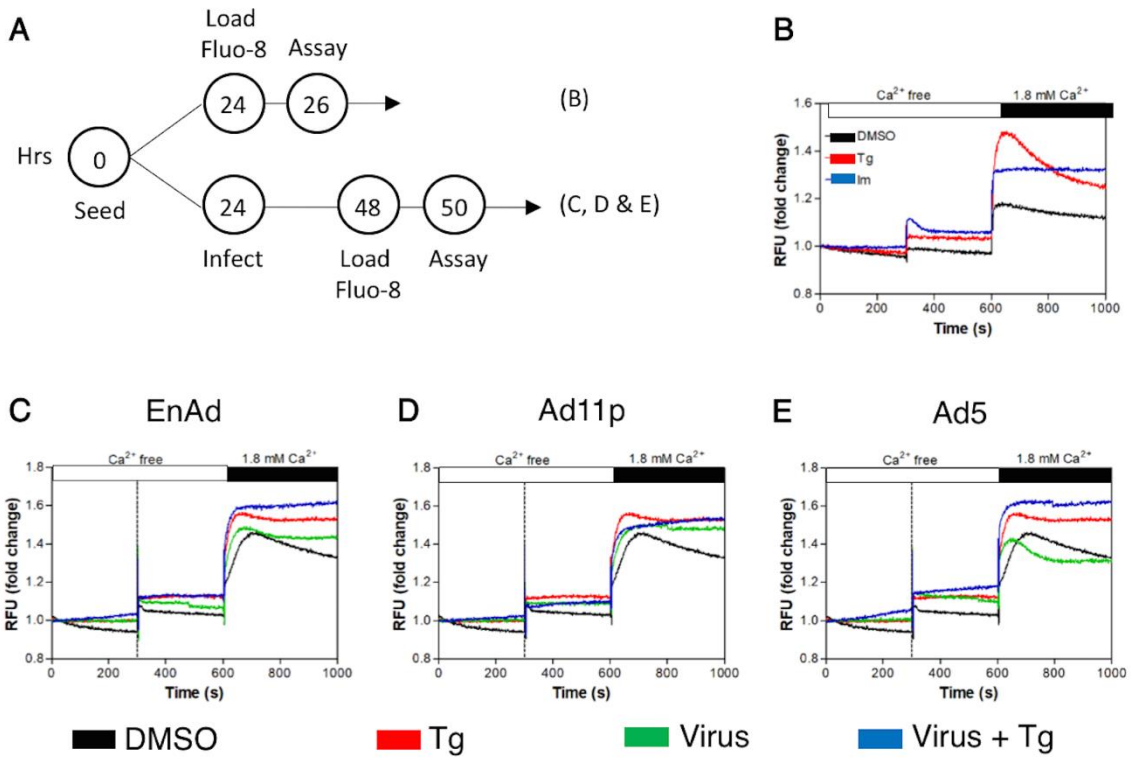


Figure 5.1. Effect of thapsigargin treatment on cytosolic calcium levels. A) Schematic representation of the workflow of each experiment, showing that cells were either infected or not, prior to loading with calcium sensitive dye (Fluo-8). **B)** Cytosolic calcium levels were measured in DLD-1 cells using Fluo-8, with fluorescence monitored over time in calcium free media. At 300 seconds, DMSO (black) thapsigargin (red) or ionomycin (blue) was injected into the well. At 600 seconds extracellular calcium levels were restored by injection of calcium into the well to a final concentration of 1.8 mM. **C-E)** Cytosolic calcium levels were measured in infected DLD-1 cells using Fluo-8 dye, with fluorescence monitored over time in calcium free media. Cells were either uninfected or infected with 100 VPC of either EnAd (C), Ad11p (D) or Ad5 (E). Infected and uninfected cells were then treated with either thapsigargin or vehicle control DMSO. In all cases DMSO or thapsigargin was injected into wells at 300 seconds, whilst calcium was injected back into the media after 600 seconds. Line colour denotes treatment group, black: uninfected + DMSO, red: uninfected + thapsigargin, green: infected + DMSO, blue: infected + thapsigargin. One representative experiment is shown. Thapsigargin (Tg 0.1 μM), Ionomycin (Im 1.25 μM).

greater and more sustained in cells that had been previously treated with one of the drugs (Figure 5.1B). These results indicate that, whilst the treatments do act on the intracellular calcium stores, the predominant effect was to increase calcium uptake from the extracellular environment.

We then went on to investigate whether adenoviral infection caused any great change to the effect of these drugs on calcium flux. DLD-1 cells were infected with the indicated

virus 24 hours before they were loaded with Fluo-8. Cells infected with EnAd and Ad11p, but not Ad5, showed increased calcium levels compared to uninfected cells by the end of the experiment after calcium had been added back to the medium (Figure 5.1C-E). This suggests that viral infection may have caused damage to the plasma membrane or had other cytotoxic effects. EnAd and Ad11p replicate more quickly than Ad5 (Dyer et al., 2017), and it is possible that these effects might be correlated to their faster replication rate. However, the effect of thapsigargin on calcium was not substantially affected by the presence of the virus, with thapsigargin treatment still causing a small increase in cytosolic calcium by depletion of the intracellular stores and a more substantial increase in the presence of extracellular calcium in both infected and infected samples (Figure 5.1C-E).

5.3.2 NAADP regulated lysosomal calcium release is not important in adenoviral lysosomal escape

There is some evidence that ER calcium depletion can lead to activation of NAADP regulated calcium release (Ronco et al., 2015; Morgan et al., 2013), we postulate that this pathway could also be important in adenoviral endosome escape. In order to test whether thapsigargin and ionomycin treatments mediate their effects by bringing about an increase in nicotinic acid adenine dinucleotide phosphate (NAADP) -dependent endosomal calcium release, we blocked calcium release using small molecule drug Ned-19 at varying concentrations in the treatment media. We found that blockade of NAADP-dependent calcium release by Ned-19 had no effect on the enhancement to virus activity provided by thapsigargin (Figure 5.2A) or ionomycin (Figure 5.2B). These results suggest that NAADP-dependent calcium release from acidic compartments in the cell, such as

endosomes and lysosomes, are not involved during adenoviral infection, contrasting with the literature reports relating to Ebola and coronavirus virus infection.

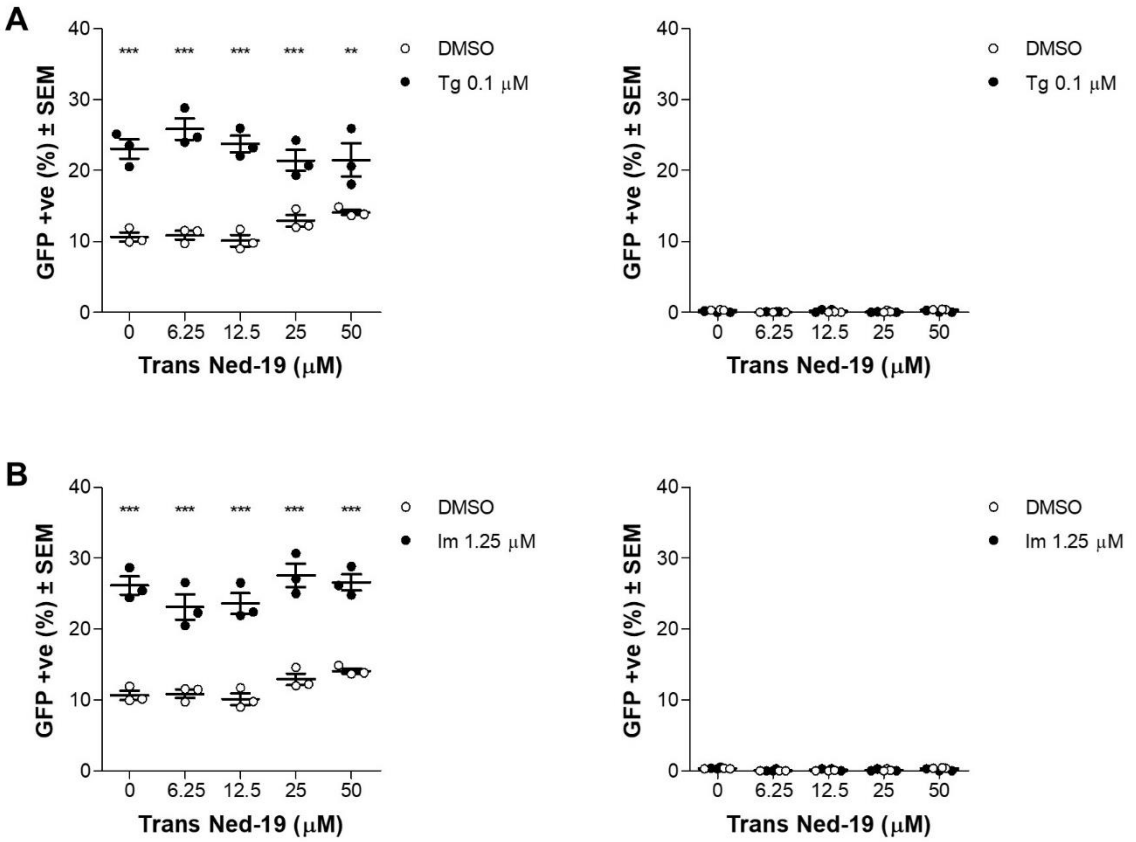


Figure 5.1. NAADP regulated lysosomal calcium release does not mediate enhanced virus activity. DLD-1 cells were infected with 100 VPC EnAd-SA-GFP (left) or were uninfected (right). After a 2-hour period of infection, infectious media was removed and cells were treated with **A)** thapsigargin (Tg 0.1 μM) or **B)** ionomycin (Im 1.25 μM) alongside increasing concentrations of Trans-Ned 19. Twenty-four hours post-infection, percentage of the cell monolayer showing GFP expression was quantified by Celigo imaging. Significance was assessed by two-way ANOVA, *** $p \leq 0.0001$, ** $p \leq 0.001$.

5.3.3 Extracellular calcium is instrumental in the enhancing effect of thapsigargin and ionomycin

Since we had observed that thapsigargin and ionomycin treatments had a substantial effect on the mobilisation of calcium within intracellular calcium stores and of calcium within the extracellular environments, we sought to investigate the effect of removing extracellular calcium from the medium on the virus infection. When calcium was depleted from the infection media by chelation with 1,2-bis(o-aminophenoxy)ethane-N,N,N′,N′-tetraacetic acid (BAPTA), infection was severely compromised, even in the presence of thapsigargin or ionomycin (Figure 5.3A). These results concur with previous findings that extracellular calcium is required for viral uptake and penetration (Greber et al., 1997).

To look more closely at how the presence of extracellular calcium might impact on the enhancing effect of thapsigargin or ionomycin treatment on virus activity, we infected cells with EnAd-SA-GFP and subsequently exposed the cells to medium containing variable concentrations of calcium in the presence or absence of thapsigargin and ionomycin. The medium was not exchanged for calcium-free medium supplemented with different concentrations of calcium until after a two-hour window of infection, excluding the possibly that changes in calcium conditions might have an effect on the earliest events of virus attachment and uptake. We found that the thapsigargin- or ionomycin-driven increase in EnAd activity was dose-dependent on extracellular calcium. Indeed, the enhancing effects of thapsigargin and ionomycin were lost altogether below an extracellular calcium concentration of 0.2 mM (Figure 5.3B, C).

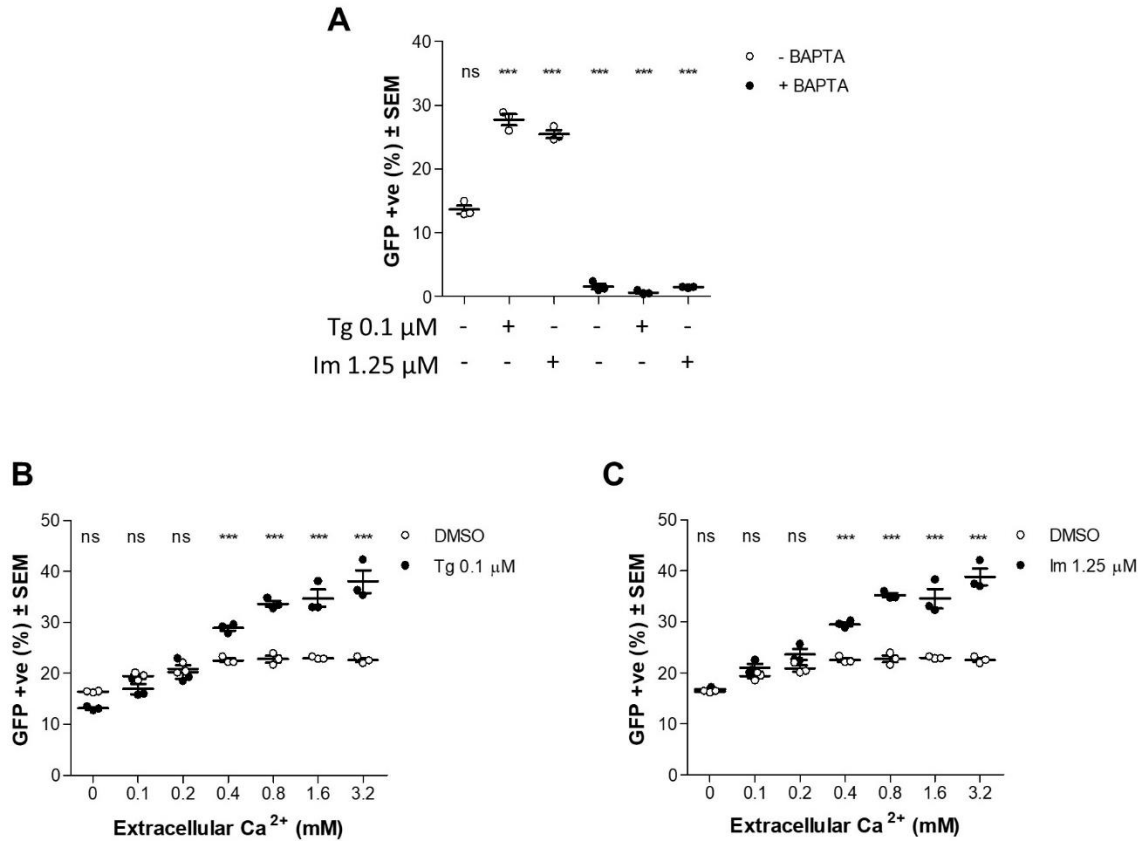


Figure 5.2. Extracellular calcium is critical in mediating the enhancing effect to virus activity. A) DLD-1 cells were infected for two hours with EnAd-SA-GFP (100 VPC) using infectious media supplemented with BAPTA (10 μM). After a two hour of incubation with infectious media cells were exposed to thapsigargin, ionomycin or vehicle control DMSO. Cells were imaged by Celigo 24 h post-infection. **B-C)** DLD-1 cells were infected with EnAd-SA-GFP (100 VPC) in complete culture medium for 2 hours, then treated with thapsigargin (B), ionomycin (C) or vehicle control DMSO. Treatment media contained variable concentrations of calcium and was supplemented with 2% dialysed (calcium free) FBS. Cells were imaged by Celigo 24 hours post-infection**.** Statistical significance of differences in GFP expression levels relative to the DMSO control group were assessed by one-way ANOVA (A) or two-way ANOVA (B, C). *** $p \leq 0.0001$, ** $p \leq 0.001$, * $p \leq 0.05$, ns: non-significant. Thapsigargin (Tg, 0.1 μM), ionomycin (Im, 1.25 μM).

5.3.4 Extracellular calcium influx drives upregulated E1A expression

Previous experiments had shown that thapsigargin and ionomycin treatments gave rise to an increase in late viral protein expression (Figure 3.9), genome replication (Figure 3.11), infectious particle production (Figure 3.12) and cell killing (Figure 3.13). We had further shown that this enhancement in virus replication was due to an upregulation of the E1A

protein (Figure 3.14). We measured E1A levels in cells treated with ionomycin or thapsigargin in the presence and absence of extracellular calcium. In all experiments, E1A levels were measured at 12 hours post-infection.

To test whether influx of extracellular calcium was driving the increase in E1A expression, DLD-1 cells were infected with EnAd-Flag-E1A virus in normal infection media. After two hours, the infectious media was swapped for treatment media either with normal levels of calcium or lacking calcium. In both cases, the medium was supplemented with 2% dialysed calcium free FBS. Western blot analysis revealed that, as before, a substantial increase in E1A levels was seen when cells were maintained in normal culture medium supplemented with thapsigargin or ionomycin, and that this enhancement was calcium-dependent (Figure 5.4A).

A very similar experiment was performed with Ad5, with the inclusion of the ER stress inducer tunicamycin as one of the treatments. DLD-1 cells were infected with wild-type Ad5 virus, treated with the indicated chemicals in the presence or absence of calcium and harvested 12 hours post-infection. Western blotting with an antibody specific to the Ad5 E1A protein again showed that thapsigargin and ionomycin treatments were able to drive enhanced E1A expression, but only in the presence of calcium in the culture medium. This was surprising since it suggests that the same mechanism may be responsible for the thapsigargin induced increase in EnAd and Ad5 E1A protein levels, yet as already described, Ad5 did not respond to increased E1A levels with enhanced replication, as was the case for EnAd. Tunicamycin had no discernible effect on E1A levels regardless of the presence of calcium, again highlighting the importance of calcium flux modulation, rather than UPR signalling, in mediating the effect on E1A expression and virus infection (Figure 5.4B).

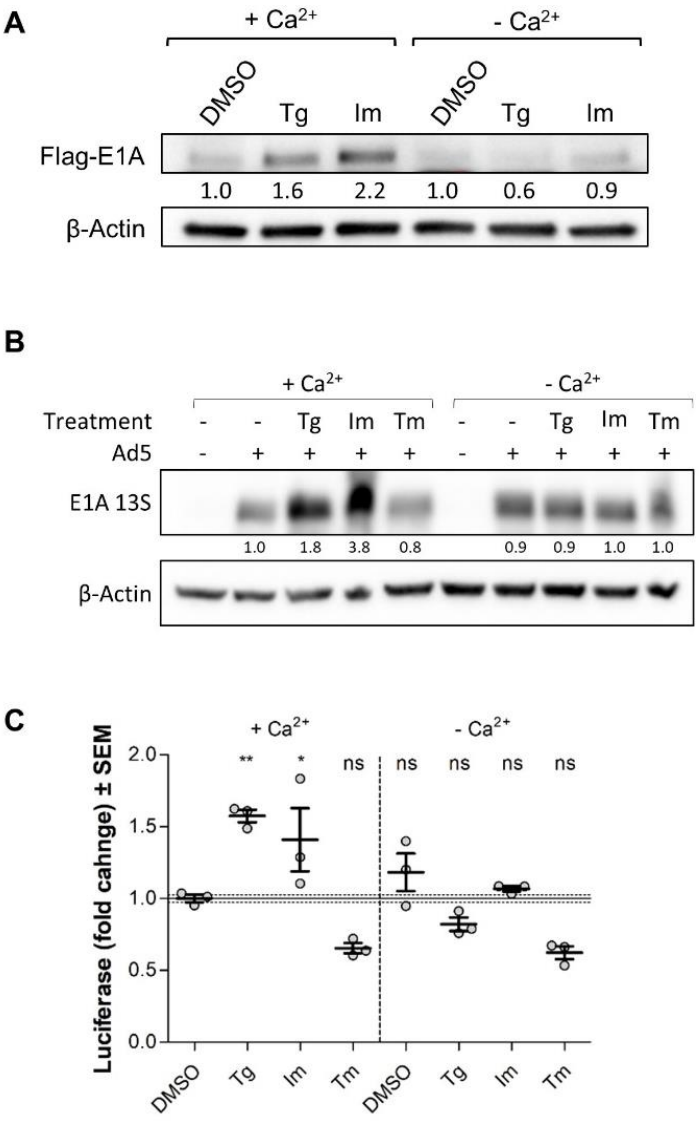


Figure 5.3. Thapsigargin treatment upregulated E1A expression by inducing extracellular calcium influx. A-B) Western blot of E1A levels in DLD-1 cells 12 hours post-infection with (A) EnAd-Flag-E1A (MOI 3) or (B) wild-type Ad5 (100 VPC). Following infection in complete culture media, cells were treated with either Tg, Im or Tm as indicated in the presence or absence of extracellular calcium. Band densitometries were normalised to loading controls, with numbers representing fold-change relative to DMSO control within the relevant calcium environment. **C)** E1A-Luc levels were measured in DLD-1 cells 12 hours post-infection with Ad5-E1A-Luc (3 PFU/cell). Cells were treated with either Tg, Im or Tm in the presence and absence of extracellular calcium. Statistical significance of differences in luciferase activity relative to the DMSO control group were assessed by one-way ANOVA, ** $p \leq 0.01$, * $p \leq 0.05$, ns: non-significant. Thapsigargin (Tg, 0.1 μM), ionomycin (Im, 1.25 μM), tunicamycin (Tm, 1 μg/mL).

To further support these results, we carried out the same experiment using a luciferase-based assay. Here, DLD-1 cells were infected with Ad5-E1A-Luc, subsequently treated with the indicated chemicals in the presence or absence of calcium and harvested 12 hours

post-infection. Quantification of luciferase reporter activity supported the data generated by western blotting, and showed that thapsigargin and ionomycin substantially and statistically significantly upregulated E1A levels roughly 1.5-fold, but only in the presence of calcium. No increase was seen in the absence of calcium. In agreement with previous results, tunicamycin had no significant effect on E1A levels irrespective of extracellular calcium levels (Figure 5.4C). These results demonstrate that the influx of calcium brought about by treatment of the cells with ionomycin or thapsigargin is the driver of E1A upregulation and ultimately enhancement to viral parameters described in Chapter 3.

5.3.5 Calcium influx occurs through store-operated calcium channels

Thapsigargin is a specific inhibitor of the SERCA channels, which are localised to the sarco/endoplasmic reticulum, whilst ionomycin is a calcium ionophore that increases the permeability of calcium across membranes, acting predominantly on calcium pools within intracellular stores rather than at the plasma membrane (Morgan and Jacob, 1994). Therefore, it was not immediately obvious how these two drugs were acting to increase calcium flux across the plasma membrane. This is especially the case for thapsigargin and particularly at the restrained concentrations used, as it acts very specifically against ER-localised SERCA channels. However, signalling networks between the plasma membrane and intracellular calcium stores exist, allowing communication between the two so that calcium can be replenished by opening of calcium release-activated calcium (CRAC) channels, also known as store-operated calcium channels.

Depletion of the ER calcium store can induce CRAC channel opening, leading to increased levels of calcium uptake from the extracellular environment (Prakriya, 2009;

Morgan and Jacob, 1994; Dedkova et al., 2000). We reasoned that both ionomycin and thapsigargin treatments would induce influx of extracellular calcium and the consequent rise in cytosolic calcium levels by activating the CRAC channels, and that this could be the relevant pathway for calcium flux and elevated viral E1A protein expression.

We infected DLD-1 cells with EnAd-SA-GFP, and subsequently treated them with thapsigargin or ionomycin in the presence of increasing dosages of BTP2, a potent inhibitor of plasma membrane CRAC channels. GFP expression was measured 24 hours post-infection. We found that BTP2 reduced the enhancing effect of thapsigargin (Figure 5.5A) and ionomycin (Figure 5.5B) treatment in a dose-dependent manner. To verify that the applied dosages of BTP2 did indeed block calcium influx caused by thapsigargin and ionomycin, we measured the change in cytosolic calcium levels of DLD-1 cells treated with thapsigargin in the presence or absence of BTP2. This was done in uninfected cells and cells infected with EnAd two hours prior to loading with the calcium-sensitive dye. We observed an increase in cytosolic calcium levels following treatment of cells with thapsigargin in both the uninfected (Figure 5.5C) and infected cells (Figure 5.5D). The presence of BTP2 reduced this increase substantially also in both cases.

These results demonstrate that cytosolic calcium levels rise due to the influx of calcium through store-operated calcium channels that open in response to depletion of the ER. This occurs upon treatment of EnAd infected cells, leading to increased E1A expression levels and viral replication.

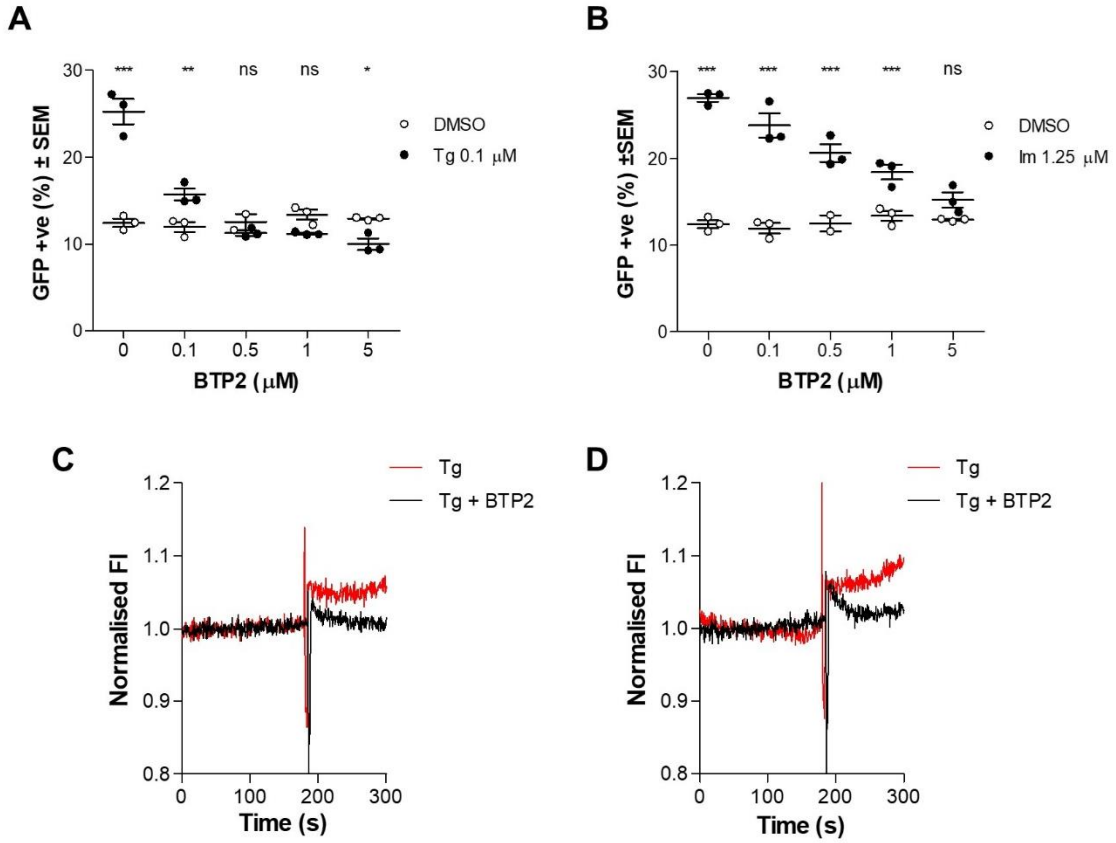


Figure 5.4. Inhibition of CRAC channels ablates the enhancing effect of thapsigargin and ionomycin by blocking extracellular calcium influx. **A-B)** DLD-1 cells were infected with EnAd-SA-GFP in the presence or absence of CRAC channel inhibitor BTP2 (5 μM). Cells were subsequently exposed to thapsigargin (A) or ionomycin (B) and imaged by Celigo 24 hours post-infection. Significance of differences in GFP expression levels relative to the DMSO control group were assessed by two-way ANOVA ***, $p \leq 0.001$; **, $p \leq 0.01$; * $p \leq 0.05$; ns, non-significant. **C-D)** Cytosolic calcium levels in uninfected DLD-1 cells (C) and in cells that had been infected with 100 VPC EnAd 2 hours previously (D) were measured by loading cells with Fluo-8 dye and monitoring normalised fluorescence intensity (FI) over time in complete growth media. Drug treatments were injected into wells at 3 minutes, one representative experiment is shown. Thapsigargin (Tg, 0.1 μM), ionomycin (Im, 1.25 μM), BTP2 (5 μM).

5.3.6 Thapsigargin treatment induces PKC phosphorylation

To explore the relationship between raised cytosolic calcium levels and E1A upregulation, we considered calcium-dependent host factors that might be involved in regulation of E1A expression. One such factor widely known to be activated in response to calcium increase is protein kinase C (PKC). The PKC family of kinases are important cellular signal transducers. Of the numerous PKC isoforms, the α, βI, βII, and γ isoforms require Ca^{2+} for activation whilst isoforms δ, ε, η, μ and θ are not sensitive to Ca^{2+} (Larsen

et al., 2000; Newton, 1995). We stimulated DLD-1 cells with thapsigargin or, as a positive control for PKC activation, phorbol myristate acetate (PMA) for 30 minutes. Western blotting was then performed using an antibody with pan-specificity to the phosphorylated forms only of PKC isoforms α, βI, βII, δ, ε, η and θ. An increase in levels of phosphorylated PKC, indicating PKC activation, was observed following treatment of DLD-1 cells with thapsigargin or PMA (Figure 5.6A).

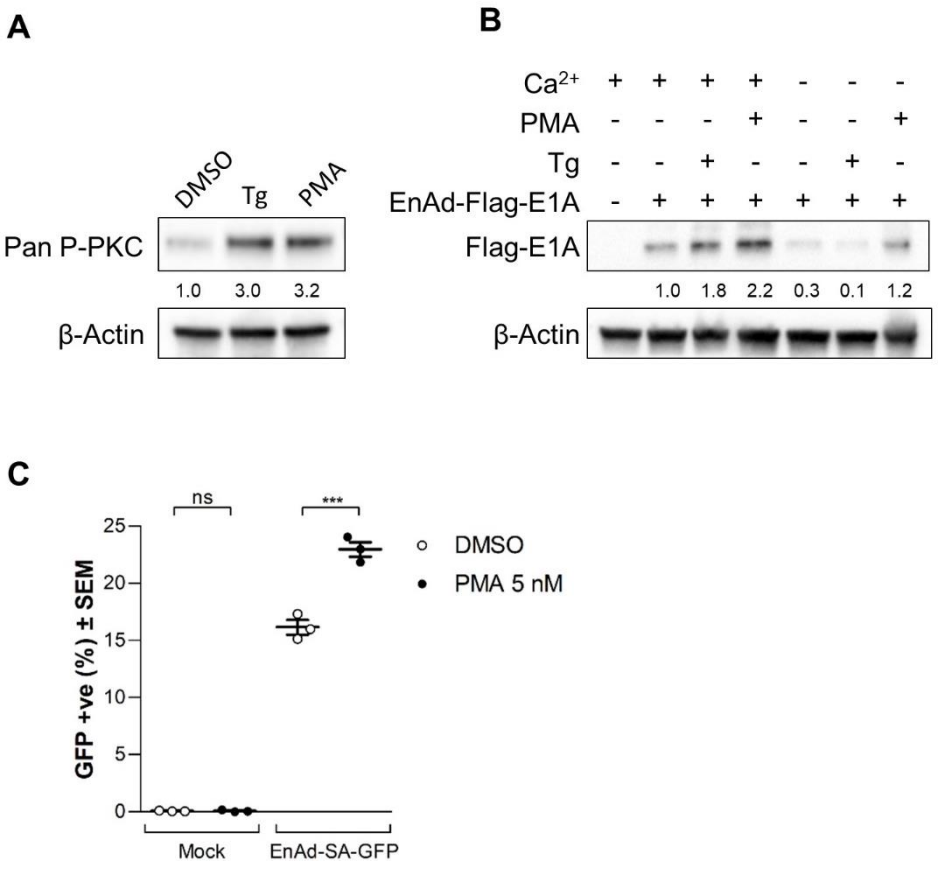


Figure 5.5. Thapsigargin and PMA both activate PKC, upregulating E1A and virus activity. **A)** Western blot of phosphorylated PKC in DLD-1 cells after 30 minutes of stimulation with thapsigargin, PMA or vehicle control DMSO. **B)** Cells were infected with EnAd-Flag-E1A at a dose of 3 PFU/cell and subsequently exposed to thapsigargin or PMA in the presence or absence of extracellular calcium. At 12 hours post-infection, cell lysates were probed for Flag-E1A expression using an anti-Flag antibody via western blot. Densitometry analysis was used to normalise bands to loading control, and quantification relative to the infected untreated sample in the relevant calcium environment is displayed. **C)** DLD-1 cells were infected with EnAd-SA-GFP at 100 VPC and subsequently treated with vehicle control DMSO or PMA, 24 hours post-infection GFP expression was quantified by Celigo imaging. Significance of differences in GFP expression levels relative to the DMSO control group were assessed by one-way ANOVA ***, $p \leq 0.001$; ns, non-significant. Thapsigargin (Tg, 0.1 μM), PMA (5 nM), Ca^{2+} (1.8 mM).

We assessed the ability of PMA stimulation of DLD-1 cells to enhance E1A expression during EnAd infections by western blotting. EnAd-Flag-E1A-infected cells stimulated with PMA or with thapsigargin had enhanced levels of Flag-E1A signal at 12 hours post-infection. When extracellular calcium was removed, levels of E1A fell substantially and could not be rescued by thapsigargin treatment. PMA restored E1A expression to the level of infected, untreated cells, even in the absence of extracellular calcium (Figure 5.6B).

DLD-1 cells were infected with EnAd-SA-GFP and subsequently treated with PMA or vehicle control DMSO. GFP expression was measured by the Celigo cytometer. PMA treatment increased the proportion of EnAd-SA-GFP-infected cells expressing major late promoter-driven GFP at 24 hours post-infection in DLD-1 cells (Figure 5.6C). In addition to blotting for phosphorylated PKC using the antibody with pan-phospho-PKC specificity, we also used antibodies with discriminatory specificity towards the phosphorylated forms of isoforms α/β II, δ, μ, and θ (Figure 5.7). Since non-classical PKC isoforms are not responsive to fluctuations in intracellular calcium, as expected these revealed no great increase in levels of phosphorylation after exposure of cells to thapsigargin.

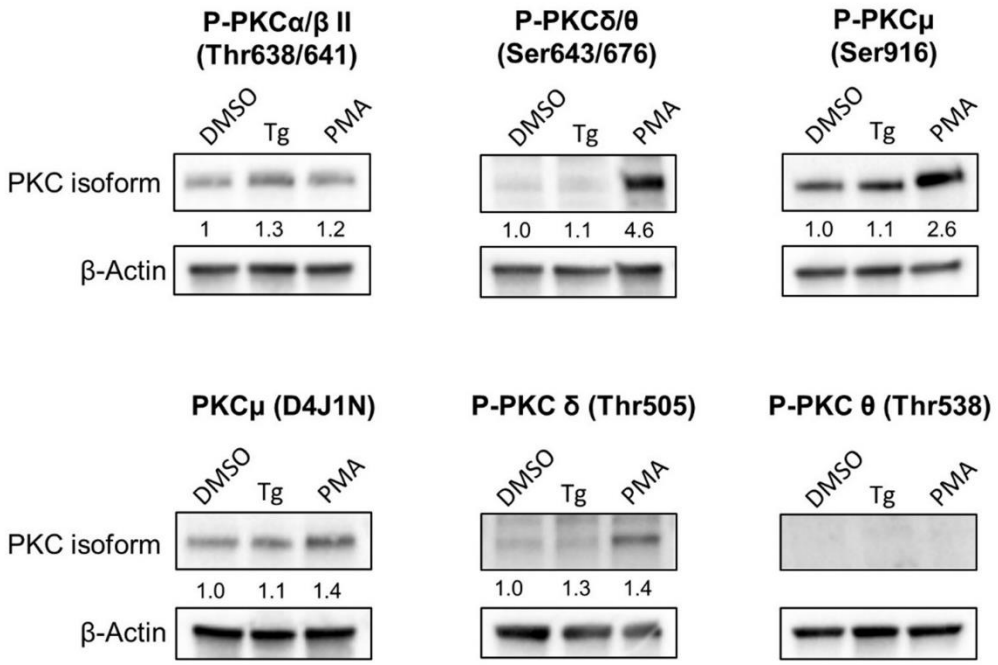


Figure 5.6. PKC and phospho-PKC isoform levels. Western blot of DLD-1 cells exposed to treatment with 0.1 μM thapsigargin or 5 nM PMA for 30 minutes. Numbers indicate the normalised fold-change in band volume intensity relative to the DMSO-treated sample.

5.3.7 PKC activity mediates enhanced EnAd activity

We tested whether increased PKC activity was responsible for enhancing virus activity by including small molecule PKC inhibitors in the treatment media. DLD-1 cells were infected with EnAd-SA-GFP and subsequently treated with thapsigargin alongside variable concentrations of PKC inhibitors Enzastaurin, GF-109203X, Gö-6976 and Gö-6983. Of the inhibitors, GF-109203X, Gö-6976 and Enzastaurin show selectivity towards calcium-responsive classical PKC isoforms, whilst Gö-6983 has a broad spectrum of inhibition. After 24 hours, GFP expression in cells was quantified by the Celigo imaging cytometer. PKC blockade by the inhibitors abrogated the enhancing effect of thapsigargin treatment on virus activity (Figure 5.8A-D).

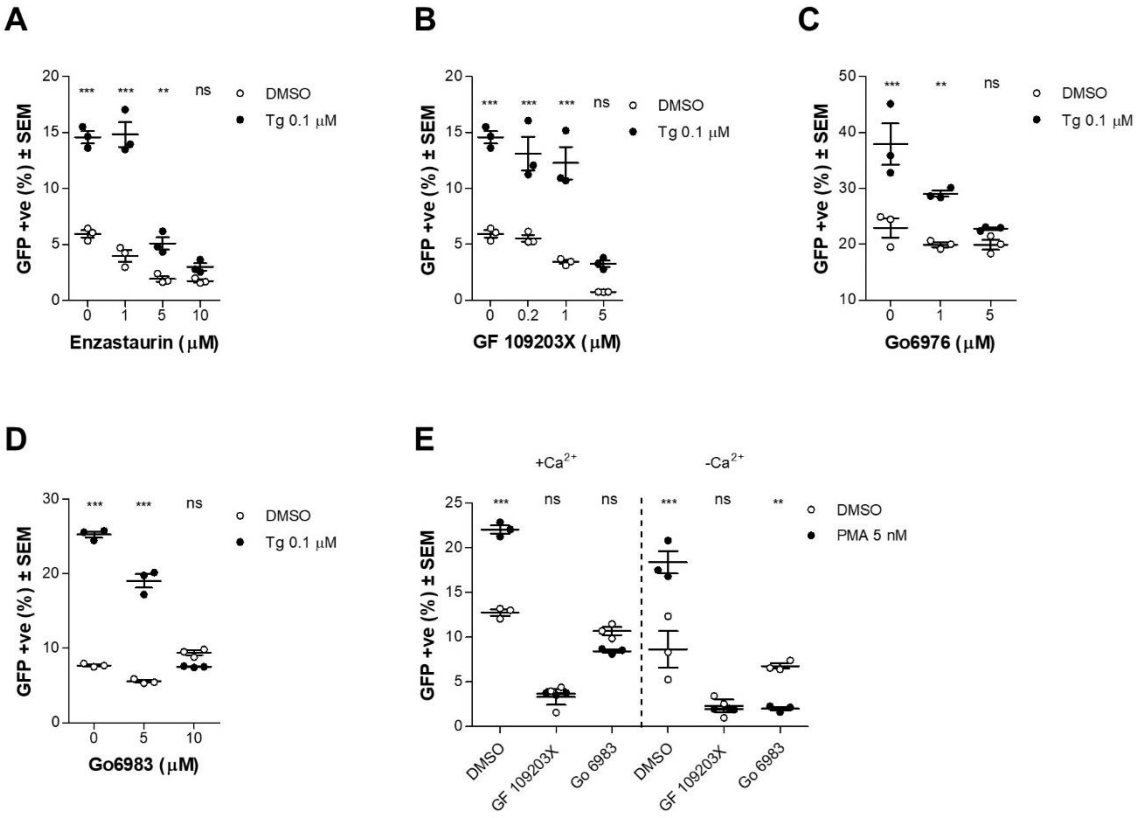


Figure 5.7. Inhibition of PKC ablates the enhancing effect of thapsigargin treatment to virus activity. A-D) DLD-1 cells were infected with 100 VPC EnAd-SA-GFP and subsequently exposed to thapsigargin alongside and various PKC inhibitors at increasing concentrations. Cells were imaged by the celigo cytometer and GFP quantified at 24 hours post-infection. **E)** DLD-1 cells were infected with 100 VPC EnAd-SA-GFP and subsequently exposed to PMA alongside PKC inhibitors GF-109203X (5 μM) or Gö 6983 (10 μM). Treatments were performed in normal DMEM or Ca^{2+} free DMEM (both supplemented with 2% dialysed Ca^{2+} free FBS) as indicated. Cells were imaged at 24 hours post-infection using Celigo. Significance was assessed by two-way ANOVA. *, $p \leq 0.05$; ** $p \leq 0.01$; *** $p \leq 0.001$; ns, non-significant. Thapsigargin (Tg, 0.1um).

These results suggest that PKC activation by thapsigargin treatment is responsible for the enhancement to virus activity. Due to the complex nature of calcium signalling, and since PKC has been shown to regulate calcium channels, such as store operated calcium channels (Ma et al., 2001) and L-type voltage gated calcium channels (Gutierrez et al., 2019), we wanted to rule out the possibility that PMA was simply imitating the effect of thapsigargin by inducing a rise in cytosolic calcium. To do so we performed the experiment in the absence of extracellular calcium. Even under these conditions, PMA treatment lead to an increase in virus activity (Figure 5.8E). This enhancement to virus

activity conferred by PMA treatment was abrogated by inclusion of PKC inhibitors in the treatment media. These data further support the hypothesis that increased PKC activation is responsible for enhanced virus activity.

The experiments described in this section sometimes involved exposing cells to combinations of two drugs in media free of calcium for a period of 24 hours. Though there were no cytotoxic effects discernible by visual inspection of the cells at the concentrations used, we were concerned that the combination of these insults to the healthy functioning of cells might be adversely affecting their viability and thus confounding our interpretation of the results. In order to assess the viability of the cells after these treatments, we carried out an MTS metabolic assay after having exposed DLD-1 cells to various treatment combinations. We found that none of the treatments significantly negatively affected the viability of the cells at 24h post-treatment (Figure 5.9A, B**).**

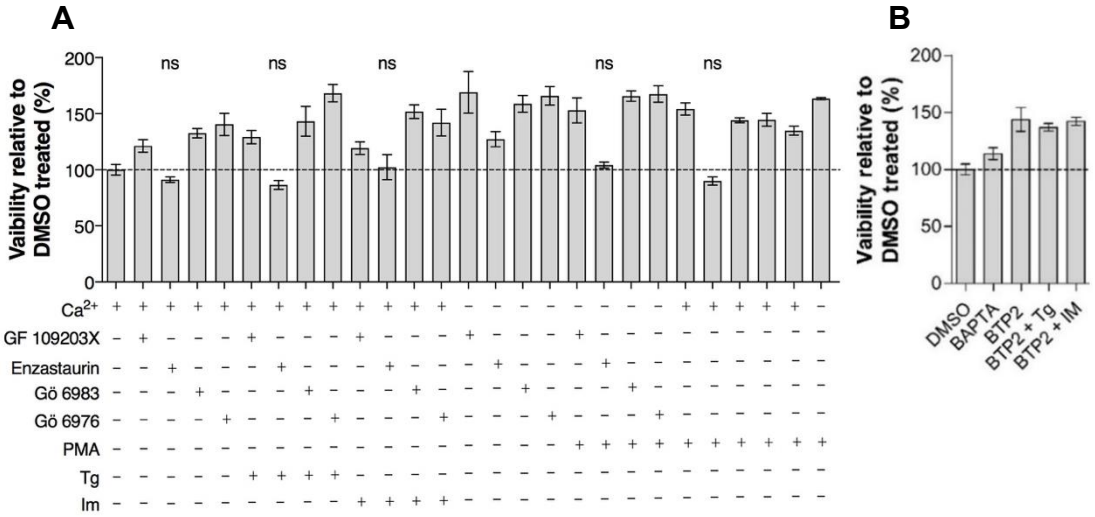


Figure 5.8. Cytotoxicity of drugs used in this study. A, B) DLD-1 cells were treated with drugs for 24 hours before cytotoxicity was assessed via MTS. Significance was assessed by two-way ANOVA. ns, not significant. Ca^{2+}: 1.8 mM, GF-109203X 5 μM, Enzastaurin 10 μM, Gö-6983 10 μM, Gö-6976 5 μM, PMA 5 nM, Tg 0.1 μM, Im 1.25 μM, BAPTA 10 μM, BTP2 5 μM.

5.3.8 Knockdown of PKCα abrogates the enhancing effect of thapsigargin on virus activity.

Our results above all support a model in which thapsigargin and ionomycin induce cytosolic calcium influx to increase E1A expression. Use of PKC inhibitors and activators supported a role for PKC as an intermediary signalling kinase between calcium and E1A upregulation. However, kinase inhibitors such as the ones used in this chapter, whilst useful tools for research, can be misleading due to variable specificity and propensity to inhibit off-target kinases. Moreover, whilst PMA is well-recognised as an inducer of PKC, it also has many other effects on the cell. Genetic knockdown of PKC using siRNA is a far more targeted approach to inhibition of protein function and can also more precisely discriminate between the various isoforms of PKC.

As we suspected the activation of PKC by thapsigargin was due to calcium influx, we chose to knock down a classical PKC isoform, PKCα, due to its expression in many cell lines (Weichert et al., 2003). We transfected DLD-1 cells with siRNAs directed against the PKCα isoform or with a negative control non-target siRNA. Cell lysates were collected at 48 hours post-transfection and total PKCα levels were determined by western blotting. Transfection of the targeted siRNA brought about highly efficient knockdown of PKCα (Figure 5.10A), while a non-target siRNA did not knockdown PKCα levels effectively.

To determine whether of PKCα expression was essential in mediating the enhancing effect of thapsigargin treatment on EnAd replication, cells were infected with 100 VPC of EnAd-SA-GFP at 48 hours post-transfection with PKCα or non-target siRNAs and subsequently exposed to treatment with thapsigargin. Thapsigargin significantly enhanced the proportion of cells displaying expression of GFP only in untransfected cells

or cells transfected with the non-target siRNA. In PKCα knockdown cells, no enhancing effect of thapsigargin on virus activity was observed (Figure 5.10B).

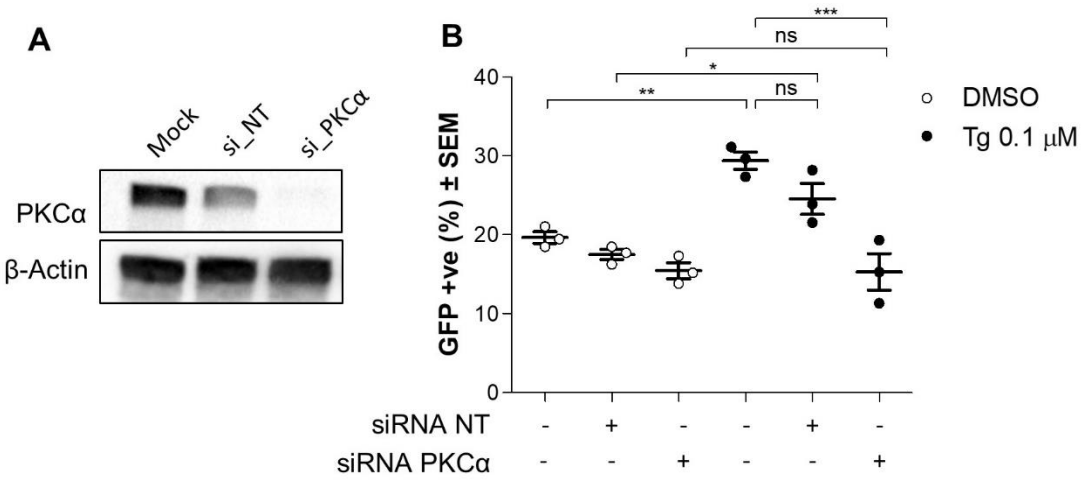


Figure 5.9. Knockdown of PKCα ablates the enhancing effect of thapsigargin. A) Western blot of PKCα protein levels 48 hours after transfection of DLD-1 cells with either siRNAs for the targeted knockdown of PKCα or non-target (NT) control siRNA. **B)** DLD-1 cells were transfected with siRNA targeting PKCα or NT control siRNA. At 48 hours post-transfection, cells were infected with EnAd-SA-GFP (100 VPC), and subsequently treated with either thapsigargin (Tg, 0.1 μM or vehicle control DMSO. At 24 hours post-infection, the proportion of GFP-positive cells was measured by Celigo. Significance was tested for by one-way ANOVA *, $p \leq 0.05$; ** $p \leq 0.01$; *** $p \leq 0.001$; ns, non-significant.

5.4 *Chapter conclusion*

1. Depletion of ER calcium by thapsigargin and ionomycin triggers influx of extracellular calcium through store operated CRAC channels in the plasma membrane.

2. Influx of extracellular calcium enhances E1A expression and therefore virus activity in EnAd infections

3. PKCα mediates calcium influx induced upregulation of E1A expression

5.5 *Chapter discussion*

Calcium signalling is fundamental to life. One of the primary downstream effector of calcium signalling is PKC, which achieves diversification of the signal through numerous isoforms whose functions differ due to the precise subcellular locations in which they are sequestered (Mascia et al., 2012). In this study, we have shown that thapsigargin and ionomycin cause influx of extracellular calcium (Figure 5.1B) by depleting the ER calcium store and activating plasma membrane CRAC store-operated calcium channels (Figure 5.5). We found that this calcium influx was essential for the increase in adenovirus E1A expression we observed upon treatment of cells with either drug (Figure 5.4), and that PKC mediated the signalling between increased cytosolic calcium levels and increased E1A expression (Figures 4.6 and 4.8). Using siRNA knockdown, we showed that it is the PKCα isoform specifically which mediates the effect (Figure 5.10).

Our observation that ionomycin produced a greater rise in cytosolic calcium from intracellular stores fit with the modes of action of the drugs. Ionomycin is an ionophore that directly facilitates depletion of ER calcium by increasing its permeability through the membrane. Numerous other calcium ionophores exist, such as A23187. They are lipid soluble entities that are able to reversibly bind to ions shielding their charge and catalysing their transport across lipid membranes (Bakker et al., 1997). Thapsigargin on the other hand achieves depletion indirectly by blocking the SERCA channels that constantly actively pump calcium up the 10,000-fold gradient into the ER lumen. Therefore, the speed at which calcium is depleted upon thapsigargin treatment depends on the rate at which calcium leaks out of the ER (Treiman et al., 1998). We also observed that EnAd and Ad11p infection increased the cytoplasmic calcium content compared to uninfected cells. These results are supported by previous findings by Dyer et al., who

showed that EnAd caused an increase in cytosolic calcium levels late during infection (Dyer et al., 2017).

Our finding that thapsigargin induces calcium influx by regulation of plasma membrane store-operated channels is supported by previous reports (Takemura et al., 1989; Denys et al., 2004). There are conflicting literature reports about whether thapsigargin increases PKC activation (Schönthal et al., 1991; Denys et al., 2004) as elevation of cytosolic calcium levels alone are sufficient to increase PKC activity regardless of the means. Nevertheless, we have convincingly shown that, at least in DLD-1 cells, PKC is phosphorylated in response to thapsigargin exposure (Figure 5.6A).

During the process of PKC activation, calcium induces translocation of PKC to the plasma membrane where it interacts with lipids such as DAG. These interactions, along with the action of many cofactors and chaperones, direct a highly ordered process of PKC phosphorylation at numerous residues, and of the removal of an auto-inhibitory domain from the catalytic site (Lipp and Reither, 2011). Therefore, whilst phosphorylation of PKC is not a direct readout for activity, it serves as a useful measure to estimate the activation status of PKC. Our data show that thapsigargin does increase phosphorylation of PKC, and that inhibition of PKC activity by both small molecules and genetic knockdown blocks the enhancement to viral activity observed upon thapsigargin treatment. Together these results make a strong case that thapsigargin increases PKCα activity, subsequently driving increased E1A levels. This translates into increased virus replication in the context of EnAd, but not in the context of Ad5.

Previous reports also suggest that PKCα may mediate upregulation of E1A. PMA, a known activator of PKCα (Pany et al., 2012; Wen-Sheng and Jun-Ming, 2005), was found to increase transcription of integrated E1A genes in HEK-293 cells (Carter et al., 1987),

accelerate the onset of adenoviral transcription in HeLa cells (Carter et al., 1984), and accelerate replication of Ad5 (Fisher et al., 1981). Subsequently, a 190 bp region within the E1A enhancer region was identified as responsive to PMA treatment with specific protein-DNA complexes forming due to PMA treatment (Gai and James, 2002). E1A phosphorylation has also been found to increase following PMA treatment (Mirza, 1992), with the authors speculating that PKC might be responsible, though their conclusions were based on the assumption that the protein kinase inhibitor H7 can be used to specifically inhibit PKC. In fact, H7 is a broad-spectrum inhibitor of protein kinases and shows preferential inhibition of numerous other protein kinases over PKC, particularly at the high concentration used in their study. Its use as a PKC inhibitor has since been refuted (Kumahara et al., 1999).

Since PMA has numerous effects on cells, the cited studies do not provide direct evidence for a link between PKC activation and E1A upregulation. It is tempting to postulate that our discovery that the enhancement of PKCα activity upregulates E1A expression explains the link between PMA treatment and accelerated viral kinetics described above. However, further work is needed to confirm whether thapsigargin-induced PKCα activity acts in the exact same manner as PMA treatment.

6 Final discussion

6.1 Overview of this thesis

OVs offer the unique advantage over conventional therapies in that they self-amplify upon reaching their target, allowing a dose escalation *in situ* (Seymour and Fisher, 2016). Some OVs kill their target cell through mechanisms which are independent of the apoptotic pathways usually used by host cells, which are often deregulated in cancers (Li et al., 2013; Dyer et al., 2017). Avoiding apoptosis means that, in principle, OVs are able to spread throughout the tumour infecting neighbouring cells after target cell lysis, creating a pro-inflammatory environment that may stimulate an immunogenic response against the tumour (Weerasinghe and Buja, 2012).

Alongside their ability to bring about direct cell lysis, OVs also provide an opportunity to encode and express therapeutic biologics. This strategy allows for targeted delivery of the biologic to the local tumour microenvironment and dose amplification, thereby minimising off-target effects. This strategy has been effectively employed by Imlygic, which encodes GM-CSF (Andtbacka et al., 2015); however, the scope for arming OVs is much broader, with transgenes ranging from immunomodulators to RNAi expression constructs (Freedman et al., 2017; Shiina et al., 2009). This approach is exciting since it opens the door to an almost limitless number of therapeutic combinations with additive and potentially synergistic anticancer effects (De Gruijl et al., 2015; Hermiston and Kuhn, 2002; Kaur et al., 2009). The arming of OVs is also important because, although the safety record of many OVs has been largely excellent, they often have a lower potency than desired, highlighting a clear need for the development of potentiation strategies.

Our ability to identify and exploit combinations of OVs with either encoded or co-administered drugs depends upon our understanding of their interactions with the host cell. It is now well-established that ER stress and activation of the UPR are tightly associated with the progression of many cancers (Urra et al., 2016). It is also understood that viruses and the UPR have evolved side by side, each manipulating the other to their own ends (Asha et al., 2018; Zhang and Wang, 2012; He et al., 2006; Bhattacharyya, 2014). Some oncolytic therapies have been found to be impeded by induced ER stress (Mahoney et al., 2011) whilst other seem to benefit (Roulstone et al., 2015; Prasad et al., 2014). In some cases, the ER stress caused by a drug is compounded by the ER stress associated with the replication of an oncolytic virus, overwhelming the cell with unresolvable ER stress and forcing it down a pathway to apoptosis (Kelly et al., 2012). In other cases, the induced ER stress and consequent UPR signalling seems to directly enhance replication of the OV within the cancer cell and improve oncolytic killing (Prasad et al., 2014). Though interest in the UPR and ER stress in the context of virotherapy is mounting, it remains an underexplored area of research whose better understanding could underpin important advances in the optimisation of OVs to the benefit of patients.

In this thesis, we have shown that oncolytic adenoviruses induce ER stress to varying degrees, and that the chimeric oncolytic adenovirus Enadenotucirev has a higher propensity to cause ER stress than its parental virus Ad11p or the archetypal adenovirus Ad5. We have also shown that treatment of cancer cells with ER stress-inducing agents thapsigargin or ionomycin greatly enhanced replication of EnAd and Ad11p viruses but not of Ad5 virus. This enhancement seems to be due to an upregulation of the viral E1A gene which is driven by increased activation of PKCα. This signalling pathway is novel and is represented schematically in Figure 6.1.

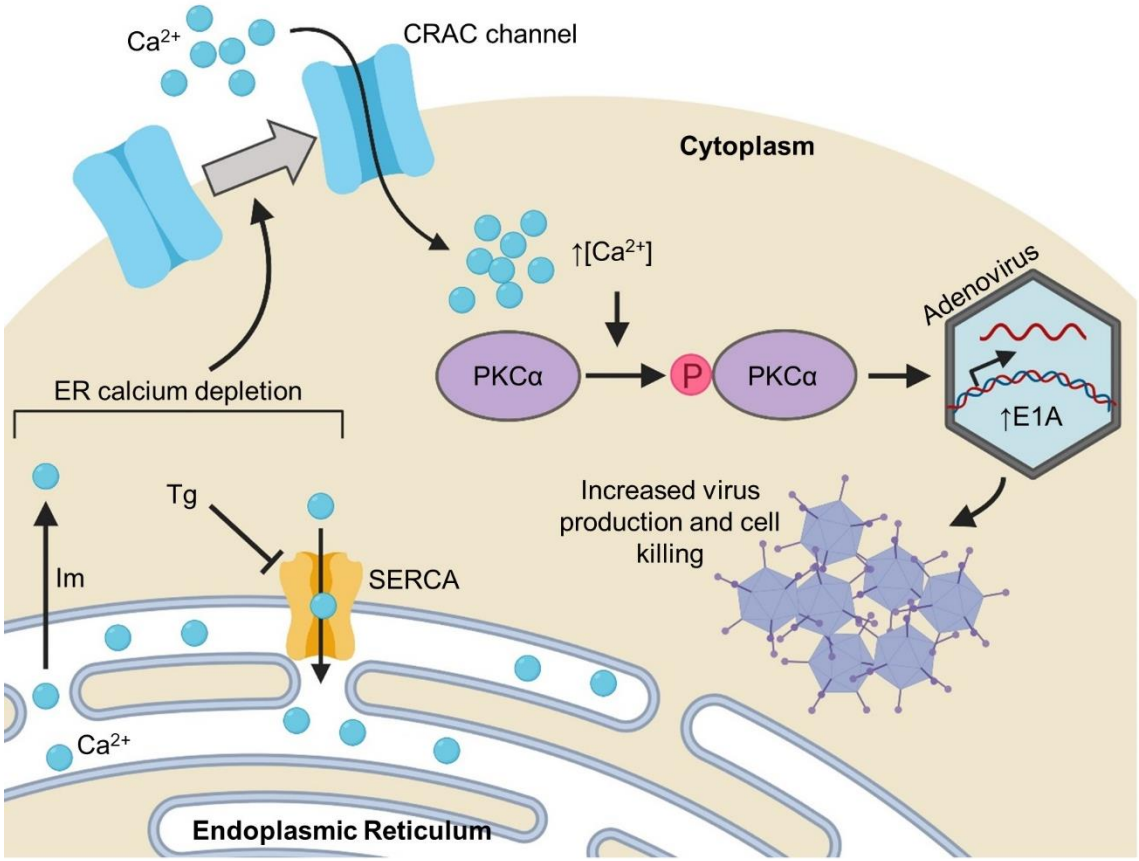


Figure 6.1. Graphical representation of the signalling pathway uncovered in this thesis. Thapsigargin (Tg) blocks uptake of calcium into the ER through inhibition of the sarco/endoplasmic reticulum Ca^{2+} ATPase (SERCA) channels. Ionomycin (Im) treatments aid calcium diffusion across the ER membrane. Both act to deplete the ER calcium store. In response to depletion of ER calcium the store operated calcium release activated channels (CRAC) in the plasma membrane open, allowing influx of extracellular calcium into the cell. A spike in cytosolic calcium levels increases activation and phosphorylation of PKCα. Higher levels of active PKCα stimulate increased transcription of the viral E1A gene, which drives increased infectious virus particle production and cell killing. Image created using Biorender.

6.2 *Adenovirus-induced ER stress*

We developed a method to track induction of ER stress over time by exploiting the XBP1 splicing event that occurs under conditions of ER stress. We chose to use this system for the purpose of tracking ER stress induction over the course of viral infections because, once the stable cell line was generated, it provided an effective way to test numerous

viruses and drugs without lengthy sample preparations or procedures such as those involved in reverse transcription PCR and immunoblotting methods. For this purpose, the system worked well, though inclusion of a degradation tag to the venus protein would have offered better temporal resolution which may have allowed us to discern the dynamics of ER stress induction over time more precisely. Nevertheless, the approach revealed that EnAd powerfully induced ER stress in a dose-dependent manner in A549 cells.

The most intuitive means by which one could imagine a virus inducing ER stress would be a scenario in which the ER lumen is overloaded with viral proteins. However, in the case of adenovirus, only a few proteins, all encoded within the E3 region, are known to interact directly with the ER. These interactions are based on work carried out with group C adenoviruses. E3-19K binds MHC class I molecules and MHC-I-related chain A and B (MICA/B) molecules, sequestering them in the ER (Sester et al., 2013). The adenovirus death protein (ADP or E3-11.6K) is involved in cell lysis but initially localises to the endoplasmic and nuclear membranes (Scaria et al., 1992), and the E3-6.7K protein localises primarily to the ER (Moise et al., 2002). EnAd, on the other hand, lacks these proteins due to a near complete deletion of the E3 region (Figure 1.5) (Kuhn et al., 2008), indicating that interactions with the ER act via a distinct adenovirus protein.

It is not immediately obvious why EnAd would cause ER stress, particularly since it is devoid of most of its E3 proteins including those that localise to the ER, at least in Ad5. A possible means by which ER stress could occur might be by competition for chaperones and other folding proteins. These proteins may be sequestered in the cytoplasm alongside the majority of viral proteins, therefore depleting their presence in the ER. The formation of protein aggregates in the cytosol has been found to inhibit the proteasome and ERAD, and the inhibition of the proteasome in turn has been found to induce ER stress (Leitman

et al., 2013; Obeng et al., 2006). Therefore, these considerations could represent a mechanism by which cytosolic viral proteins may indirectly diminish the protein folding capacity within the ER.

Ad5 induced ER stress to a far lesser extent than did EnAd (Figure 3.7). This could be due to the replication kinetics of EnAd which are inherently faster than those of Ad5 (Dyer et al., 2017). However, with 48 hours being a relatively late time point in the infection of permissive A549 cells, it seems more likely that some difference in the proteins expressed by the viruses accounts for the discrepancy The large E3 region deletion of EnAd leaves it with only three remaining E3 open reading frames, none of which have any described function (Kuhn et al., 2008). It is feasible that any one of these genes of undescribed function might be responsible for the ER stress induction observed in EnAd infections. A previous study by Gros et al. identified an Ad5-based mutant, AdT1, containing a truncation mutation in E3-19K (E3/19K-445A) that redirected the resulting truncated protein to the plasma membrane, and imparted it with a viroporin like function that induced influx of calcium into the cell (Gros et al., 2008). Whilst the authors did not investigate the effect of this virus on the ER stress status of the cell, it seems likely that such mutation would contribute towards ER stress. There is a wide genetic difference between EnAd/Ad11p and Ad5, as well as numerous uncharacterised proteins encoded by EnAd/Ad11p. It is entirely feasible that an ER stress-inducing protein is encoded by EnAd/Ad11p whose function is still to be elucidated.

6.3 *Differences in response of EnAd/Ad11p and Ad5 to ER stress-inducing chemicals*

Previous reports of an enhancing effect of chemically induced ER stress on Ad5 replication in cancer cells (Prasad et al., 2014) lead us to investigate whether the same effect could be observed in the context of EnAd infection. We tested a panel of ER stress-inducing chemicals for their ability to enhance adenovirus activity in cancer cell lines and obtained mixed results. Two of the chemicals, thapsigargin and ionomycin, strongly increased EnAd and Ad11p activity, whilst the other two chemicals, tunicamycin and SubAB had no effect. None of the chemicals had any great effect on Ad5 infection (Figure 3.9.). Thapsigargin and ionomycin brought about a clear upregulation of E1A in EnAd infections, and appeared to upregulate Ad5 E1A levels as well, though less strongly (Figures 3.14 and 3.15). The E3-6.7K protein encoded by Ad5, but not EnAd, contributes towards maintaining ER calcium homeostasis and inhibits the induction of apoptosis induced by high doses of thapsigargin (Moise et al., 2002). Therefore, it is plausible that E3-6.7K expressed by Ad5 changes the cellular response to thapsigargin treatment, which could have an effect on the ability of the virus to respond with enhanced replication to thapsigargin.

We observed that EnAd replication was potentiated by the thapsigargin-driven increase in E1A levels but that Ad5 was not. Though the lack of genetic homology between Ad5 and EnAd makes it difficult to speculate about the reasons for this discrepancy, some insight can be gained from considering their distinct replicative kinetics. The prevailing view of adenovirus DNA replication is based predominantly on studies using the Ad5 serotype. Initiation of DNA replication is dependent on the expression of the E2

transcription unit, consisting of viral genes E2A and E2B, and a further three host factors (De Jong and Van Der Vliet, 1999). The E2 transcription unit is initially controlled by the E2 early promoter, but during the intermediate stages of infection control shifts to the E2 late promoter. It is the E2 early promoter which is regulated by the E1A protein (Horikoshi et al., 1991; Flint and Shenk, 1989; Lee et al., 1991).

Thus, for E1A to drive accelerated onset of viral replication at early stages, E1A must represent a bottleneck to E2 early promoter driven expression of the E2 transcription unit. In turn, expression the E2 transcription unit must represent a bottleneck to viral genome replication at early times. During EnAd and Ad11p infection, this must be the case since elevated levels of E1A at early time points drive an up-regulation of E2B expression and its corollary, enhanced genome replication. However, this is not the case with Ad5, as genome replication is not enhanced despite a thapsigargin treatment-driven increase in levels of E1A (Figures 3.9, 3.11, 3.12 and 3.13). Furthermore, overexpression of plasmid encoded Ad5 E1A did not enhance Ad5 activity in DLD-1 cells either (Figure 3.16). This does not necessarily mean that E2B levels are not raised by increased E1A expression during Ad5 infections, however if they are then some other factor must be limiting viral genome replication. Quantification of early Ad5 transcripts in the presence and absence of thapsigargin treatment would be a logical next experiment to perform in order to clarify this point.

Previous reports suggest that adenovirus replication is not necessarily linearly dependent on enhanced E1A levels (Zheng et al., 2005). Zheng et al found that high levels of E1A expression driven by the strong and constitutive CMV promoter did not always translate to increased replication levels of Ad5 mutant viruses (Zheng et al., 2005). The ability of raised E1A levels to drive higher rates of Ad5 replication was dependent on the cell type and Ad5 variant used. It is also well-established that tumour suppressor signalling

pathways, such as the p53 pathway, which are often deregulated in cancer cells, play an important role in regulating viral replication. Since viral replication is influenced by a number of such variables, it follows that the sensitivity of replication to E1A levels will not be uniform and should depend on both the cell type and the virus used. The interpretation that Ad5 replication is not limited by E1A expression is also supported by previous studies in which Ad5 was found to express E1A in excess for replication, since enhancing E1A expression by replacing the Ad5 E1A promoter enhancer region with a more highly active promoter increased E1A expression levels dramatically but did not affect viral replication (Hitt and Graham, 1990).

As Ad11p and Ad5 are relatively non-homologous (54% homology), differences in their biology should be expected, and extreme caution should be used when extrapolating about one virus from knowledge of the biology of the other. Interestingly it has been reported that Ad11 shows reduced expression of E1A in cells resistant to its replication, however when the E1A promoter region of Ad11 is replaced with that of Ad5, E1A levels are enhanced and concomitantly so is viral replication (Wong et al., 2012).

One way to address this question might be to study the effect with a wider panel of adenoviruses, though given the large differences already apparent between only two subtypes, this would likely be a highly complex task. Clearly, more detailed investigations into the reasons why elevated E1A levels are sufficient to drive enhanced replication of Ad11p and EnAd, but not Ad5, in these cell lines in the context of treatment with the drugs used here are needed before any precise explanation can be described. A systematic quantification of viral transcripts in the presence and absence of thapsigargin treatment would be highly desirable in this regard. It may be particularly salient to identify at which time points each viral transcript appears at detectable levels and to compare the

profile of Ad5 with that of EnAd and Ad11p. This may provide clues as to how the viruses respond differently to the treatments.

6.4 *Mechanism of enhancement of virus replication*

The work constituting this thesis began with the aim of exploring if induction of ER stress could be exploited as a means to potentiate EnAd, as had been encouragingly been reported previously for Ad5 (Prasad et al., 2014). When we found a strong enhancing effect of thapsigargin treatment (Figures 3.9. – 3.13), and a strongly prejudicial effect of IRE1 inhibition (Figure 3.16) on EnAd infection, we initially reasoned that our results concurred with those of Prasad et al. However, more in depth studies revealed that the enhancing effect was due to calcium influx rather that ER stress induction. The failure of IRE1 inhibition to ablate the increases in EnAd E1A transcript levels, the XBP1 splicing patterns generated by the different treatments, and the inability of SubAB or tunicamcyin to enhance Ad5 E1A-Luc or virus reporter protein expression together demonstrated that induction of the UPR was not responsible for the enhancement to virus activity produced by thapsigargin and ionomycin treatments (Figures 3.6, 3.16 and 3.17). Chemical inhibition of the IRE1 and PERK arms of the UPR also failed to block the enhancing effect of thapsigargin treatment on activity of EnAd-SA-GFP (Figure 3.18). Interestingly, the addition of thapsigargin to cells treated with ATF6 inhibitor did increase late gene expression compared to cells without ATF6 inhibition, though we cannot rule out that the trapping and clustering of ATF6 complexes in the ER by Ceapin A7 (Gallagher et al., 2016) may also have downstream negative consequences on viral protein localisation that counteract any potential increases in transgene level driven by thapsigargin treatment. Instead, we found that enhancement is mediated by an influx of extracellular calcium.

It is unclear exactly which stage of the virus replication cycle is affected by the altered calcium flux. Since EnAd and Ad11p differ in E2B, many of the E3 genes, and E4ORF4, but still exhibit similar responses to thapsigargin and ionomycin treatment, it is unlikely that these genes are involved. Here, we can exclude attachment and entry, since the treatments were first added at 2 h post-infection when the majority of viral particles would have already entered the cell (Greber et al., 1997). Though we cannot exclude the possibility that the treatments aid viral endosome escape and delivery of viral genomes to the nucleus, previous work by Greber et al. suggests that calcium depletion in the ER/nuclear lumen by thapsigargin or ionomycin treatment does not affect trafficking of the virus to the nucleus (Greber et al., 1997). However, depletion of calcium stores by ionomycin treatment did block delivery of viral genomes to the nucleus once the virus particles had reached the nuclear envelope. In this study, we observe an *increase* in virus activity following ionomycin treatment, suggesting that delivery of the viral genomes to the nucleus has already taken place by the time the treatments were added at 120 minutes post-infection

We found that E1A and E2B were upregulated by thapsigargin treatment at both the mRNA and protein levels (Figure 3.14). It is important to note that due to the central role the E1A protein plays in driving the expression of the other viral genes, including other early genes, elevated levels of E1A may be sufficient to drive an accelerated onset of viral replication and potentiated virus activity. The enhanced E1A mRNA levels were seen as early as 6 hours p.i. (Figure 3.13), prior to the onset of viral genome replication, thereby excluding the possibility that the enhancing effect was acting directly on DNA replication to increase genome copy number and raise transcript levels. Subsequently higher levels of E2B mRNA levels further support our conclusion that thapsigargin-mediated enhancement occurs at the E1A transcriptional level or earlier.

Calcium has been shown to be important during entry of adenoviral particles (Greber et al., 1997), and some viruses are known to express viroporins to facilitate calcium influx for efficient viral exit and spread (Gonzalez and Carrasco, 2003; Van Kuppeveld et al., 1997). As discussed, the Ad5 variant AdT1 identified by Gros et al. acquired a viroporin like protein through mutation of the E3-19K gene which had the effect of enhancing infection (Gros et al., 2008). The authors observed improved viral spread and plaque formation as a result of better membrane permeabilization or virion release, rather than affecting earlier stages of the virus replication cycle. Indeed, they found that transcript and protein levels remained unaffected in the presence of truncated E3-19K compared to wild-type E3-19K, while in our study, we found major differences in transgene expression directly after infection and in the late phase of virus protein expression. Therefore, we conclude that the effect on transgene expression of UPR-modulating drug treatment (Figure 3.9) acts on an earlier stage in the virus replication cycle than the E3-19K truncation discovered by Gros et al.

Using genetic knockdown, we identified PKCα as the signalling molecule responsible for mediated the enhanced activity of EnAd in response to thapsigargin. The PKC family of serine/threonine kinases regulate many cell functions which are deregulated in cancers, including differentiation, cell growth, survival and cell death (Garg et al., 2014). It also has important consequences for adenovirology. Working with the epidemic keratoconjunctivitis (EKC) causing species D Ad37 virus, Yousuf et al. reported that inhibition of PKC reduced E1A expression (Yousuf et al., 2016). This agrees with our data suggesting that PKC signalling may upregulate E1A expression, though the authors conclude that the up-regulation of E1A levels in their model is due to enhanced viral entry, which as we discuss above, is not the mechanism described in our study.

PKC has numerous downstream cellular targets and its activation will have many effects on the cell, many of which could feasibly modify the intracellular environment in favour of E1A expression and viral replication. For example, one target of PKC is the transcriptional co-activator p300. Like PKC, p300 has been implicated in the expression of genes involved in a diverse number of biological functions (Iyer et al., 2004). PKC has been reported to phosphorylate p300 at serine 89, having an inhibitory effect on its function (Yuan and Gambee, 2000). p300 also interacts with the adenoviral E1A protein, indeed, p300 was first discovered through this interaction - and E1A is thought to repress p300 activity by sequestration through binding (Stein et al., 1990).

Since E1A-directed repression of p300 is clearly important in viral infection, PKC activation by thapsigargin treatment may aid E1A in this repression of p300, thereby potentiating virus activity. The role of p300 could be tested by overexpressing it in cells. In the model described, overexpression of p300 would be expected to reduce the impact of thapsigargin treatment, which could be experimentally determined. We have not generated any data to support such a role for p300, but rather use this as an example to illustrate how signalling interactions linking E1A and PKC might occur to impact viral infection. However, more work is needed in order to elucidate any such complex signalling interaction. This is especially true when considering group B adenovirus biology, since the interactions described above were predominantly discovered by research using Ad5, and the amino acid identity of the Ad5 and Ad11p E1A protein is as low as 35% (Mei et al., 2003).

Though we have found no direct reports from previous studies describing an upregulation effect of PKC activation on adenoviral gene expression, interestingly there may have been indirect reports of the effect. Phorbol esters, such as the PKC activator PMA, were found to increase expression of E1A and E1B genes integrated in HEK-293 or HeLa cells

infected with Ad5 (Carter et al., 1984, 1987), possibly through the interaction of a protein with the adenovirus E1A promoter region (Gal and James, 2001). The similarities between these reports and the observations we have made are noteworthy and, in the cited studies, PMA may have accelerated viral transcription through PKC in the same way as the way we described. However, these studies were carried out with Ad5, and due to the lack of similarity between Ad5 and EnAd in the E1A gene, it is unlikely that the EnAd E1A enhancer region is bound by the same protein as suggested in the report by Gai et al.

Whilst our data convincingly implicate PKCα in the upregulation of E1A in response to thapsigargin treatment, a useful approach to corroborate this finding would be the overexpression of a constitutively active form of PKCα in cells and exploration of its effect on viral infection. However, it would be difficult to control this temporally, which would be necessary to ensure that the additional PKC activity was not affecting virus uptake or endosomal escape. A Tet-on inducible promoter system where the active PKC was only expressed upon addition of doxycyclin after virus entry may be useful to overcome this problem (T. Das et al., 2016). Future work could also include approaches to identify proteins which may bind to the E1A promoter to enhance transcription in response to thapsigargin, for example through electrophoretic mobility shift assays coupled with mass spectrometry. The discovery that PKCα activity potentiates EnAd also raises new possibilities for oncolytic virus design. For example, arming of EnAd with a genetic construct for the expression of a constitutively active form of PKCα could represent an attractive approach. Interestingly, PKCβ overexpression in colorectal cancer HT-29 cells has been reported to have growth inhibitory and anti-tumour effects, suggesting PKCα overexpression from EnAd could have the dual effect of potentiating viral replication whilst also inhibiting tumour growth (Choi et al., 1990).

6.5 *Improving arming of EnAd with shRNA expression constructs*

As we have already discussed, we were able to engineer an EnAd variant virus armed with the ability to knockdown the SERCA2 protein in the cell. We reasoned that the success of this strategy was dependent on a function of the half-life of the target protein and the speed at which the virus replicated and subsequently killed the cell. This meant that we only saw knockdown in SK-OV-3 cells, in which the virus replicates more slowly. However, the engineered virus did not have enhanced replication and cell killing ability compared to the parental EnAd virus, as originally hypothesised. In fact, the engineered viruses were somewhat attenuated, with lower viral genome titres at later time points in both DLD-1 and SK-OV-3 cells. In terms of cell killing, the modified and unmodified viruses caused similar declines in cell index during xCELLigence experiments using DLD-1 cells, the former had slower cell lysis kinetics in SK-OV-3 cells. It would be interesting to assess the replication and cell killing of the viruses in a panel of different additional cell lines to verify that the attenuated killing seen in SK-OV-3 cells by the modified viruses is not specific to this cell line, particularly those already rather resistant to infection. We found no reports in the literature of virally encoded shRNA constructs *per se* having a detrimental effect on viral replication. This could in part be explained by an effect in which the successful knockdown of a target protein enhances replication, which then compensates for the marginally impaired replication of the adenovirus due to insertion of an shRNA construct. However, this possibility can be excluded by comparing the non-target shRNA control encoding virus to the unmodified virus, rather than just comparing the targeted knockdown virus to the non-target control virus, as is the case in many reports.

The shRNA construct was inserted between the E3 region and L5 gene. This site was chosen since it is a non-coding region of the EnAd genome and is located downstream of the promoters that control the expression of viral genes regulating life cycle and capsid assembly (Marino et al., 2017). Indeed, our research group routinely uses this site for the insertion of transgenes (Freedman et al., 2017; Dyer et al., 2019), and it is that site in which the GFP transgenes are inserted in the EnAd-SA-GFP and EnAd-CMV-GFP viruses used in this thesis. Other investigators have used similar locations in the Ad5 genome for the insertion of shRNA constructs and have not reported issues (Motegi et al., 2011; Yoo et al., 2008).

When transcribed, the shRNA sequence will, by its very nature, form strong secondary structure in the form of a hairpin. If transcription from the major late promoter did not terminate before the shRNA construct and its sequence was included in the mRNA produced, the strong secondary structure could conceivably cause problems during processing of the mRNA and during its translation. However, the insertion site for the shRNA cassette is downstream of an AATAAA sequence, a polyadenylation signal sequence which has been associated with the termination of transcription complexes (Logan et al., 1987), downstream of the fibre site and at the end of the major late transcription unit. Therefore, we would not expect the hairpin sequence to be included in the mRNA transcribed from the major late transcription unit. For all these reasons, no problems are or were anticipated with it as a choice for insertion location. Nevertheless, it would be useful to characterise the effect of insertion of shRNA constructs into different sites of the viral genome to optimise this aspect of the design.

6.6 *Concluding remarks*

This thesis aimed to characterise the relationship between ER stress and adenoviral infection and identify strategies which could be employed to potentiate the activity of the oncolytic virus and clinical candidate Enadenotucirev. The approach was built on previous reports of potentially synergistic effects between the induction of ER stress by treatment of cells with small molecules and oncolytic viruses, though there is a distinct gap in the literature regarding group B adenoviruses and ER stress. EnAd and Ad11p were able to induce high levels of ER stress during the replication cycle, but this was not the case for Ad5. Additionally, EnAd and Ad11p experienced an enhancement to parameters of replication when cells were treated with specific ER stress-inducing chemicals that disrupt calcium flux. Again, this did not apply in the context of Ad5. We identified the mechanism of enhancement to replication to be a PKCα-mediated increase in E1A transcription, which was brought about by the activation of PKCα due to calcium influx into the cell in response to calcium depletion in the ER. Though EnAd-encoded shRNAs targeting the SERCA calcium channels did not potentiate EnAd replication, the novel mechanistic understanding of the involvement of PKCα in adenovirus replication opens the door to other potentiation approaches.

With an increasing appreciation of the role of ER stress and UPR signalling, and indeed other forms of cell stress, in both viral and tumour biology, a detailed understanding of these pathways and their interactions will be necessary to effectively optimise oncolytic viruses as therapeutics for the benefit of patients. This work may make a small step in that direction for one particular clinical candidate oncolytic virus but, more importantly, it highlights the opportunities for discovery of synergistic effects through increased understanding of host-virus interactions. More work is clearly needed to elucidate the

nature of these complex signalling networks in the context of oncolytic virotherapy, the results from which will be exciting from both a therapeutic and biological perspective.

7 References

Ahi, Y.S., and S.K. Mittal. 2016. Components of adenovirus genome packaging. *Front. Microbiol.* 7. doi:10.3389/fmicb.2016.01503.

Ahmad, A.S., N. Ormiston-Smith, and P.D. Sasieni. 2015. Trends in the lifetime risk of developing cancer in Great Britain: Comparison of risk for those born from 1930 to 1960. *Br. J. Cancer*. 112:943–947. doi:10.1038/bjc.2014.606.

Alemany, R., and D.T. Curiel. 2001. CAR-binding ablation does not change biodistribution and toxicity of adenoviral vectors. *Gene Ther.* doi:10.1038/sj.gt.3301515.

Andersson, K.B., J.A.K. Birkeland, A.V. Finsen, W.E. Louch, I. Sjaastad, Y. Wang, J. Chen, J.D. Molkentin, K.R. Chien, O.M. Sejersted, and G. Christensen. 2009. Moderate heart dysfunction in mice with inducible cardiomyocyte-specific excision of the Serca2 gene. *J. Mol. Cell. Cardiol.* 47:180–187. doi:10.1016/j.yjmcc.2009.03.013.

Andtbacka, R.H.I., H.L. Kaufman, F. Collichio, T. Amatruda, N. Senzer, J. Chesney, K.A. Delman, L.E. Spitler, I. Puzanov, S.S. Agarwala, M. Milhem, L. Cranmer, B. Curti, K. Lewis, M. Ross, T. Guthrie, G.P. Linette, G.A. Daniels, K. Harrington, M.R. Middleton, W.H. Miller, J.S. Zager, Y. Ye, B. Yao, A. Li, S. Doleman, A. Van Der Walde, J. Gansert, and R.S. Coffin. 2015. Talimogene laherparepvec improves durable response rate in patients with advanced melanoma. *J. Clin. Oncol.* doi:10.1200/JCO.2014.58.3377.

Aparicio, O., N. Razquin, M. Zaratiegui, I. Narvaiza, and P. Fortes. 2006. Adenovirus Virus-Associated RNA Is Processed to Functional Interfering RNAs Involved in

Virus Production. *J. Virol.* 80:1376–1384. doi:10.1128/jvi.80.3.1376-1384.2006.

Asada, T. 1974. Treatment of human cancer with mumps virus. *Cancer*. 34:1907–1928. doi:10.1002/1097-0142(197412)34:6<1907::AID-CNCR2820340609>3.0.CO;2-4.

Asha, K., N. Sharma-Walia, K. Asha, and N. Sharma-Walia. 2018. Virus and tumor microenvironment induced ER stress and unfolded protein response: from complexity to therapeutics. *Oncotarget*. doi:10.18632/oncotarget.25886.

Bagur, R., and G. Hajnóczky. 2017. Intracellular Ca2+ Sensing: Its Role in Calcium Homeostasis and Signaling. *Mol. Cell*. doi:10.1016/j.molcel.2017.05.028.

Bakker, E., P. Bühlmann, and E. Pretsch. 1997. Carrier-based ion-selective electrodes and bulk optodes. 1. General characteristics. *Chem. Rev.* 97:3083–3132. doi:10.1021/cr940394a.

Barøy, T., K. Sørensen, M.M. Lindeberg, and E. Frengen. 2010. shRNA expression constructs designed directly from siRNA oligonucleotide sequences. *Mol. Biotechnol.* 45:116–120. doi:10.1007/s12033-010-9247-8.

Benevento, M., S. Di Palma, J. Snijder, C.L. Moyer, V.S. Reddy, G.R. Nemerow, and A.J.R. Heck. 2014. Adenovirus composition, proteolysis, and disassembly studied by in-depth qualitative and quantitative proteomics. *J. Biol. Chem.* doi:10.1074/jbc.M113.537498.

Bennasser, Y., C. Chable-Bessia, R. Triboulet, D. Gibbings, C. Gwizdek, C. Dargemont, E.J. Kremer, O. Voinnet, and M. Benkirane. 2011. Competition for XPO5 binding between Dicer mRNA, pre-miRNA and viral RNA regulates human Dicer levels. *Nat. Struct. Mol. Biol.* 18:323–327. doi:10.1038/nsmb.1987.

Berget, S.M., C. Moore, and P.A. Sharp. 1977. Spliced segments at the 5’ terminus of

adenovirus 2 late mRNA. *Proc. Natl. Acad. Sci. U. S. A.* 74:3171–3175. doi:10.1073/pnas.74.8.3171.

Berk, A. 1986. Adenovirus Promoters and E1A Transactivation. *Annu. Rev. Genet.* 20:45–79. doi:10.1146/annurev.genet.20.1.45.

Bertolotti, A., Y. Zhang, L.M. Hendershot, H.P. Harding, and D. Ron. 2000. Dynamic interaction of BiP and ER stress transducers in the unfolded-protein response. *Nat. Cell Biol.* 2:326–332. doi:10.1038/35014014.

Bhattacharyya, S. 2014. Can't RIDD off viruses. *Front. Microbiol.* 5. doi:10.3389/fmicb.2014.00292.

Boelens, J., J.P. Jais, B. Vanhoecke, I. Beck, H. Van Melckebeke, J. Philippé, M. Bracke, F. Jardin, J. Brière, K. Leroy, F. Offner, and S. Lust. 2013. ER stress in diffuse large B cell lymphoma: GRP94 is a possible biomarker in germinal center versus activated B-cell type. *Leuk. Res.* 37:3–8. doi:10.1016/j.leukres.2012.08.017.

Bommiasamy, H., S.H. Back, P. Fagone, K. Lee, S. Meshinchi, E. Vink, R. Sriburi, M. Frank, S. Jackowski, R.J. Kaufman, and J.W. Brewer. 2009. ATF6α induces XBP1-independent expansion of the endoplasmic reticulum. *J. Cell Sci.* 122:1626–1636. doi:10.1242/jcs.045625.

Boulanger, P., P. Lemay, G.E. Blair, and W.C. Russell. 1979. Characterization of adenovirus protein IX. *J. Gen. Virol.* 44:783–800. doi:10.1099/0022-1317-44-3-783.

Bozym, R.A., S.A. Morosky, K.S. Kim, S. Cherry, and C.B. Coyne. 2010. Release of intracellular calcium stores facilitates coxsackievirus entry into polarized endothelial cells. *PLoS Pathog.* 6:e1001135. doi:10.1371/journal.ppat.1001135.

Brachtlova, T., and V. van Beusechem. 2018. Unleashing the Full Potential of Oncolytic Adenoviruses against Cancer by Applying RNA Interference: The Force Awakens. *Cells*. 7:228. doi:10.3390/cells7120228.

Brestovitsky, A., R. Sharf, K. Mittelman, and T. Kleinberger. 2011. The adenovirus E4orf4 protein targets PP2A to the ACF chromatin-remodeling factor and induces cell death through regulation of SNF2h-containing complexes. *Nucleic Acids Res.* 39:6414–6427. doi:10.1093/nar/gkr231.

Brini, M., T. Cali, D. Ottolini, and E. Carafoli. 2012. Calcium pumps: Why So many? *Compr. Physiol.* 2:1045–1060. doi:10.1002/cphy.c110034.

Bryant, D.M., A. Datta, A.E. Rodríguez-Fraticelli, J. PeräCurrency Signnen, F. Martín-Belmonte, and K.E. Mostov. 2010. A molecular network for de novo generation of the apical surface and lumen. *Nat. Cell Biol.* 12:1035–1045. doi:10.1038/ncb2106.

Cancer Research UK. 2019. https://www.cancerresearchuk.org/health-professional/cancer-statisticsitle.

Carette, J.E., R.M. Overmeer, F.H.E. Schagen, R. Alemany, O.A. Barski, W.R. Gerritsen, and V.W. Van Beusechem. 2004. Conditionally Replicating Adenoviruses Expressing Short Hairpin RNAs Silence the Expression of a Target Gene in Cancer Cells. *Cancer Res.* 64:2663–2667. doi:10.1158/0008-5472.CAN-03-3530.

Carew, J.S., C.M. Espitia, W. Zhao, K.R. Kelly, M. Coffey, J.W. Freeman, and S.T. Nawrocki. 2013. Reolysin is a novel reovirus-based agent that induces endoplasmic reticular stress-mediated apoptosis in pancreatic cancer. *Cell Death Dis.* 4:e728–e728. doi:10.1038/cddis.2013.259.

Carter, T., C. James, E. Chan, and B. Greene. 1987. Induction of integrated adenovirus

E1A and E1B genes in transformed human cells by phorbol ester tumor promoters. *Cancer Res.* 47:803–808.

Carter, T.H., Z.Z. Milovanovic, L.E. Babiss, and P.B. Fisher. 1984. Accelerated onset of viral transcription in adenovirus-infected HeLa cells treated with the tumor promoter 12-O-tetradecanoyl-phorbol-13-acetate. *Mol. Cell. Biol.* 4:563–566. doi:10.1128/mcb.4.3.563.

Cauet, G., J.M. Strub, E. Leize, E. Wagner, A. Van Dorsselaer, and M. Lusky. 2005. Identification of the glycosylation site of the adenovirus type 5 fiber protein. *Biochemistry*. 44:5453–5460. doi:10.1021/bi047702b.

Cawood, R., H.H. Chen, F. Carroll, M. Bazan-Peregrino, N. Van Rooijen, and L.W. Seymour. 2009. Use of tissue-specific microRNA to control pathology of wild-type adenovirus without attenuation of its ability to kill cancer cells. *PLoS Pathog.* 5:e1000440. doi:10.1371/journal.ppat.1000440.

Cheshenko, N., W. Liu, L.M. Satlin, and B.C. Herold. 2007. Multiple receptor interactions trigger release of membrane and intracellular calcium stores critical for herpes simplex virus entry. *Mol. Biol. Cell*. 18:3119–3130. doi:10.1091/mbc.E07-01-0062.

Chevet, E., C. Hetz, and A. Samali. 2016. Endoplasmic reticulum stress–activated cell reprogramming in oncogenesis. *Cancer Discov.* 5:586–597. doi:10.1158/2159-8290.CD-14-1490.

Chipurupalli, S., E. Kannan, V. Tergaonkar, R. D'andrea, and N. Robinson. 2019. Hypoxia induced ER stress response as an adaptive mechanism in cancer. *Int. J. Mol. Sci.* 20. doi:10.3390/ijms20030749.

Choi, P.M., K.M. Tchou-Wong, and I.B. Weinstein. 1990. Overexpression of protein kinase C in HT29 colon cancer cells causes growth inhibition and tumor suppression. *Mol. Cell. Biol.* 10:4650–4657. doi:10.1128/mcb.10.9.4650.

Chu, L., J. Gu, L. Sun, Q. Qian, C. Qian, and X. Liu. 2008. Oncolytic adenovirus-mediated shRNA against Apollon inhibits tumor cell growth and enhances antitumor effect of 5-fluorouracil. *Gene Ther.* 15:484–494. doi:10.1038/gt.2008.6.

Chuan Yin Liu, M. Schroder, and R.J. Kaufman. 2000. Ligand-independent dimerization activates the stress response kinases IRE1 and PERK in the lumen of the endoplasmic reticulum. *J. Biol. Chem.* 275:24881–24885. doi:10.1074/jbc.M004454200.

Clapham, D.E. 2011. Doi:10.1016/J.Cell.2007.11.028. *Cell*. 131:1–12. doi:10.1016/j.cell.2007.11.028.

Cohen, M.H., G. Williams, J.R. Johnson, J. Duan, J. Gobburu, A. Rahman, K. Benson, J. Leighton, S.K. Kim, R. Wood, M. Rothmann, G. Chen, K. Maung U, A.M. Staten, and R. Pazdur. 2002. Approval summary for imatinib mesylate capsules in the treatment of chronic Myelogenous Leukemia. *Clin. Cancer Res.* 8:935–942.

Conry, R.M., B. Westbrook, S. McKee, and T.G. Norwood. 2018. Talimogene laherparepvec: First in class oncolytic virotherapy. *Hum. Vaccines Immunother.* 14:839–846. doi:10.1080/21645515.2017.1412896.

Corbett, E.F., K. Oikawa, P. Francois, D.C. Tessier, C. Kay, J.J.M. Bergeron, D.Y. Thomas, K.H. Krause, and M. Michalak. 1999. Ca2+ regulation of interactions between endoplasmic reticulum chaperones. *J. Biol. Chem.* 274:6203–6211. doi:10.1074/jbc.274.10.6203.

Crawford-Miksza, L., and D.P. Schnurr. 1996. Analysis of 15 adenovirus hexon proteins reveals the location and structure of seven hypervariable regions containing serotype-specific residues. *J. Virol.* 70:1836–44.

Cullen, B.R. 2002. RNA interference: Antiviral defense and genetic tool. *Nat. Immunol.* doi:10.1038/ni0702-597.

Dales, S., and Y. Chardonnet. 1973. Early events in the interaction of adenoviruses with HeLa cells. IV. Association with microtubules and the nuclear pore complex during vectorial movement of the inoculum. *Virology*. 56:465–483. doi:10.1016/0042-6822(73)90050-0.

Davies, M.P.A., D.L. Barraclough, C. Stewart, K.A. Joyce, R.M. Eccles, R. Barraclough, P.S. Rudland, and D.R. Sibson. 2008. Expression and splicing of the unfolded protein response gene XBP-1 are significantly associated with clinical outcome of endocrine-treated breast cancer. *Int. J. Cancer*. 123:85–88. doi:10.1002/ijc.23479.

Dedkova, E.N., A.A. Sigova, and V.P. Zinchenko. 2000. Mechanism of action of calcium ionophores on intact cells: ionophore-resistant cells. *Membr. Cell Biol.* 13:357–68.

Delie, F., P. Petignat, and M. Cohen. 2012. GRP78 protein expression in ovarian cancer patients and perspectives for a drug-targeting approach. *J. Oncol.* 2012:468615. doi:10.1155/2012/468615.

Deng, J., P.D. Lu, Y. Zhang, D. Scheuner, R.J. Kaufman, N. Sonenberg, H.P. Harding, and D. Ron. 2004. Translational Repression Mediates Activation of Nuclear Factor Kappa B by Phosphorylated Translation Initiation Factor 2. *Mol. Cell. Biol.* 24:10161–10168. doi:10.1128/mcb.24.23.10161-10168.2004.

Denmeade, S.R., C.M. Jakobsen, S. Janssen, S.R. Khan, E.S. Garrett, H. Lilja, S.B.

Christensen, and J.T. Isaacs. 2003. Prostate-specific antigen-activated thapsigargin prodrug as targeted therapy for prostate cancer. *J. Natl. Cancer Inst.* doi:10.1093/jnci/95.13.990.

Denys, A., V. Aires, A. Hichami, and N.A. Khan. 2004. Thapsigargin-stimulated MAP kinase phosphorylation via CRAC channels and PLD activation: Inhibitory action of docosahexaenoic acid. *FEBS Lett.* 564:177–182. doi:10.1016/S0014-5793(04)00361-8.

Déry, M.A., J. Jodoin, J. Ursini-Siegel, O. Aleynikova, C. Ferrario, S. Hassan, M. Basik, and A.C. LeBlanc. 2013. Endoplasmic reticulum stress induces PRNP prion protein gene expression in breast cancer. *Breast Cancer Res.* 15:R22. doi:10.1186/bcr3398.

DeWeese, T.L., H. van der Poel, S. Li, B. Mikhak, R. Drew, M. Goemann, U. Hamper, R. DeJong, N. Detorie, R. Rodriguez, T. Haulk, A.M. DeMarzo, S. Piantadosi, D.C. Yu, Y. Chen, D.R. Henderson, M.A. Carducci, W.G. Nelson, and J.W. Simons. 2001. A phase I trial of CV706, a replication-competent, PSA selective oncolytic adenovirus, for the treatment of locally recurrent prostate cancer following radiation therapy. *Cancer Res.* 61:7464–72.

Do, M.H., P.K. To, Y.S. Cho, S.Y. Kwon, E.C. Hwang, C. Choi, S.H. Cho, S.J. Lee, S. Hemmi, and C. Jung. 2018. Targeting CD46 enhances anti-tumoral activity of adenovirus type 5 for bladder cancer. *Int. J. Mol. Sci.* 19. doi:10.3390/ijms19092694.

Duncan, M.R., S.M. Stanish, and D.C. Cox. 1978. Differential sensitivity of normal and transformed human cells to reovirus infection. *J. Virol.* 28:444–449.

DuRose, J.B., A.B. Tam, and M. Niwa. 2006. Intrinsic capacities of molecular sensors of the unfolded protein response to sense alternate forms of endoplasmic reticulum stress. *Mol. Biol. Cell*. 17:3095–3107. doi:10.1091/mbc.E06-01-0055.

Dyer, A., Y. Di, H. Calderon, S. Illingworth, G. Kueberuwa, A. Tedcastle, P. Jakeman, S.L. Chia, A. Brown, M.A. Silva, D. Barlow, J. Beadle, T. Hermiston, D.J.P. Ferguson, B. Champion, K.D. Fisher, and L.W. Seymour. 2017. Oncolytic Group B Adenovirus Enadenotucirev Mediates Non-apoptotic Cell Death with Membrane Disruption and Release of Inflammatory Mediators. *Mol. Ther. - Oncolytics*. 4:18–30. doi:10.1016/j.omto.2016.11.003.

Dyer, A., B. Schoeps, S. Frost, P. Jakeman, E.M. Scott, J. Freedman, E.J. Jacobus, and L.W. Seymour. 2019. Antagonism of glycolysis and reductive carboxylation of glutamine potentiates activity of oncolytic adenoviruses in cancer cells. *Cancer Res.* 79:331–345. doi:10.1158/0008-5472.CAN-18-1326.

Egan, C., S.T. Bayley, and P.E. Branton. 1989. Binding of the Rb1 protein to E1A products is required for adenovirus transformation. *Oncogene*. 4:383–388.

Engelman, J.A., and J. Settleman. 2008. Acquired resistance to tyrosine kinase inhibitors during cancer therapy. *Curr. Opin. Genet. Dev.* 18:73–79. doi:10.1016/j.gde.2008.01.004.

Fillat, C., M. Carrio, A. Cascante, and B. Sangro. 2006. Suicide Gene Therapy Mediated by the Herpes Simplex Virus Thymidine Kinase Gene / Ganciclovir System: Fifteen Years of Application. *Curr. Gene Ther.* 3:13–26. doi:10.2174/1566523033347426.

Fisher, P.B., C.S. Young, I.B. Weinstein, and T.H. Carter. 1981. Tumor promoters alter the temporal program of adenovirus replication in human cells. *Mol. Cell. Biol.* 1:370–380. doi:10.1128/mcb.1.4.370.

Flint, J., and T. Shenk. 1989. Adenovirus E1A Protein Paradigm Viral Transactivator. *Annu. Rev. Genet.* doi:10.1146/annurev.ge.23.120189.001041.

Frabutt, D.A., B. Wang, S. Riaz, R.C. Schwartz, and Y.-H. Zheng. 2017. Innate Sensing of Influenza A Virus Hemagglutinin Glycoproteins by the Host Endoplasmic Reticulum (ER) Stress Pathway Triggers a Potent Antiviral Response via ER-Associated Protein Degradation. *J. Virol.* 92. doi:10.1128/jvi.01690-17.

Freedman, J.D., J. Hagel, E.M. Scott, I. Psallidas, A. Gupta, L. Spiers, P. Miller, N. Kanellakis, R. Ashfield, K.D. Fisher, M.R. Duffy, and L.W. Seymour. 2017. Oncolytic adenovirus expressing bispecific antibody targets T-cell cytotoxicity in cancer biopsies. *EMBO Mol. Med.* 9:1067–1087. doi:10.15252/emmm.201707567.

Fribley, A., K. Zhang, and R.J. Kaufman. 2009. Regulation of apoptosis by the unfolded protein response. *Methods Mol. Biol.* 559:191–204. doi:10.1007/978-1-60327-017-5_14.

Frisch, S.M., and J.S. Mymryk. 2002. Adenovirus-5 E1A: Paradox and paradigm. *Nat. Rev. Mol. Cell Biol.* doi:10.1038/nrm827.

Fulci, G., L. Breymann, D. Gianni, K. Kurozomi, S.S. Rhee, J. Yu, B. Kaur, D.N. Louis, R. Weissleder, M.A. Caligiuri, and E.A. Chiocca. 2006. Cyclophosphamide enhances glioma virotherapy by inhibiting innate immune responses. *Proc. Natl. Acad. Sci. U. S. A.* 103:12873–12878. doi:10.1073/pnas.0605496103.

Gal, Q., and C.B.L. James. 2001. Identification of a region on the adenovirus E1A gene responsible for induction by phorbol ester tumor promoter. *Vitr. Cell. Dev. Biol. - Anim.* 37:465–470. doi:10.1290/1071-2690(2001)037<0465:IOAROT>2.0.CO;2.

Gallagher, C.M., C. Garri, E.L. Cain, K.K.H. Ang, C.G. Wilson, S. Chen, B.R. Hearn, P. Jaishankar, A. Aranda-Diaz, M.R. Arkin, A.R. Renslo, and P. Walter. 2016. Ceapins are a new class of unfolded protein response inhibitors, selectively targeting the ATF6α branch. *Elife*. 5. doi:10.7554/eLife.11878.

Galluzzi, L., A. Diotallevi, and M. Magnani. 2017. Endoplasmic reticulum stress and unfolded protein response in infection by intracellular parasites. *Futur. Sci. OA*. 3. doi:10.4155/fsoa-2017-0020.

Garcia-Carbonero, R., R. Salazar, I. Duran, I. Osman-Garcia, L. Paz-Ares, J.M. Bozada, V. Boni, C. Blanc, L. Seymour, J. Beadle, S. Alvis, B. Champion, E. Calvo, and K. Fisher. 2017. Phase 1 study of intravenous administration of the chimeric adenovirus enadenotucirev in patients undergoing primary tumor resection. *J. Immunother. Cancer*. 5:71. doi:10.1186/s40425-017-0277-7.

Garg, R., L.G. Benedetti, M.B. Abera, H. Wang, M. Abba, and M.G. Kazanietz. 2014. Protein kinase C and cancer: What we know and what we do not. *Oncogene*. 33:5225–5237. doi:10.1038/onc.2013.524.

Garg, R., M.C. Caino, and M.G. Kazanietz. 2013. Regulation of Transcriptional Networks by PKC Isozymes: Identification of c-Rel as a Key Transcription Factor for PKC-Regulated Genes. *PLoS One*. 8. doi:10.1371/journal.pone.0067319.

GEORGIADES, J., T. ZIELINSKI, A. CICHOLSKA, and E. JORDAN. 1959. Research on the oncolytic effect of APC viruses in cancer of the cervix uteri; preliminary report. *Biul. Inst. Med. Morskiej w Gda??sku*. 10:49–57.

Ghebremedhin, B. 2014. Human adenovirus: Viral pathogen with increasing importance. *Eur. J. Microbiol. Immunol.* 4:26–33. doi:10.1556/eujmi.4.2014.1.2.

Ghosh-Choudhury, G., Y. Haj-Ahmad, and F.L. Graham. 1987. Protein IX, a minor component of the human adenovirus capsid, is essential for the packaging of full length genomes. *EMBO J.* 6:1733–1739. doi:10.1002/j.1460-2075.1987.tb02425.x.

Giaginis, C.T., A.C. Zarros, M.A. Papaefthymiou, A.E. Papadopouli, I.K. Sfiniadakis,

and S.E. Theocharis. 2008. Coxsackievirus and adenovirus receptor expression in human endometrial adenocarcinoma: Possible clinical implications. *World J. Surg. Oncol.* 6:59. doi:10.1186/1477-7819-6-59.

Giering, J.C., D. Grimm, T.A. Storm, and M.A. Kay. 2008. Expression of shRNA from a tissue-specific pol II promoter is an effective and safe RNAi therapeutic. *Mol. Ther.* 16:1630–1636. doi:10.1038/mt.2008.144.

Gonzalez, M.E., and L. Carrasco. 2003. Viroporins. *FEBS Lett.* 552:28–34. doi:10.1016/S0014-5793(03)00780-4.

Görlach, A., P. Klappa, and T. Kietzmann. 2006. The endoplasmic reticulum: Folding, calcium homeostasis, signaling, and redox control. *Antioxidants Redox Signal.* 8:1391–1418. doi:10.1089/ars.2006.8.1391.

de Graaf, J.F., L. de Vor, R.A.M. Fouchier, and B.G. van den Hoogen. 2018. Armed oncolytic viruses: A kick-start for anti-tumor immunity. *Cytokine Growth Factor Rev.* 41:28–39. doi:10.1016/j.cytogfr.2018.03.006.

Greber, U.F., M. Suomalainen, R.P. Stidwill, K. Boucke, M.W. Ebersold, and A. Helenius. 1997. The role of the nuclear pore complex in adenovirus DNA entry. *EMBO J.* 16:5998–6007. doi:10.1093/emboj/16.19.5998.

Greber, U.F., M. Willetts, P. Webster, and A. Helenius. 1993. Stepwise dismantling of adenovirus 2 during entry into cells. *Cell*. 75:477–486. doi:10.1016/0092-8674(93)90382-Z.

Green, N.M., N.G. Wrigley, W.C. Russell, S.R. Martin, and A.D. McLachlan. 1983. Evidence for a repeating cross-beta sheet structure in the adenovirus fibre. *EMBO J.* doi:10.1002/j.1460-2075.1983.tb01592.x.

Gros, A., J. Martínez-Quintanilla, C. Puig, S. Guedan, D.G. Molleví, R. Alemany, and M. Cascallo. 2008. Bioselection of a gain of function mutation that enhances adenovirus 5 release and improves its antitumoral potency. *Cancer Res.* 68:8928–8937. doi:10.1158/0008-5472.CAN-08-1145.

Gros, A., C. Puig, S. Guedan, J.J. Rojas, R. Alemany, and M. Cascallo. 2010. Verapamil enhances the antitumoral efficacy of oncolytic adenoviruses. *Mol. Ther.* doi:10.1038/mt.2010.22.

De Gruijl, T.D., A.B. Janssen, and V.W. Van Beusechem. 2015. Arming oncolytic viruses to leverage antitumor immunity. *Expert Opin. Biol. Ther.* 15:959–971. doi:10.1517/14712598.2015.1044433.

Gunaratne, G.S., Y. Yang, F. Li, T.F. Walseth, and J.S. Marchant. 2018. NAADP-dependent Ca2+ signaling regulates Middle East respiratory syndrome-coronavirus pseudovirus translocation through the endolysosomal system. *Cell Calcium*. 75:30–41. doi:10.1016/j.ceca.2018.08.003.

Gupta, G.P., and J. Massagué. 2006. Cancer Metastasis: Building a Framework. *Cell*. 127:679–695. doi:10.1016/j.cell.2006.11.001.

Gupta, S., B. McGrath, and D.R. Cavener. 2009. PERK regulates the proliferation and development of insulin-secreting beta-cell tumors in the endocrine pancreas of mice. *PLoS One*. 4:e8008. doi:10.1371/journal.pone.0008008.

Gutiérrez, A., C. Contreras, A. Sánchez, and D. Prieto. 2019. Role of phosphatidylinositol 3-kinase (PI3K), mitogen-activated protein kinase (MAPK), and protein kinase C (PKC) in calcium signaling pathways linked to the α 1 -adrenoceptor in resistance arteries. *Front. Physiol.* 10. doi:10.3389/fphys.2019.00055.

Han, D., A.G. Lerner, L. Vande Walle, J.P. Upton, W. Xu, A. Hagen, B.J. Backes, S.A. Oakes, and F.R. Papa. 2009a. IRE1α Kinase Activation Modes Control Alternate Endoribonuclease Outputs to Determine Divergent Cell Fates. *Cell*. 138:562–575. doi:10.1016/j.cell.2009.07.017.

Han, Z., Z. Hong, C. Chen, Q. Gao, D. Luo, Y. Fang, Y. Cao, T. Zhu, X. Jiang, Q. Ma, W. Li, L. Han, D. Wang, G. Xu, S. Wang, L. Meng, J. Zhou, and D. Ma. 2009b. A novel oncolytic adenovirus selectively silences the expression of tumor-associated STAT3 and exhibits potent antitumoral activity. *Carcinogenesis*. 30:2014–2022. doi:10.1093/carcin/bgp249.

Harding, H.P., Y. Zhang, A. Bertolotti, H. Zeng, and D. Ron. 2000. Perk is essential for translational regulation and cell survival during the unfolded protein response. *Mol. Cell*. 5:897–904. doi:10.1016/S1097-2765(00)80330-5.

Harding, H.P., Y. Zhang, and D. Ron. 1999. Protein translation and folding are coupled by an endoplasmic- reticulum-resident kinase. *Nature*. doi:10.1038/16729.

Hastie, E., and V.Z. Grdzelishvili. 2012. Vesicular stomatitis virus as a flexible platform for oncolytic virotherapy against cancer. *J. Gen. Virol.* 93:2529–45. doi:10.1099/vir.0.046672-0.

He, H., M. Liu, Z. Zheng, Y. Liu, J. Xiao, R. Su, C. Hu, J. Li, and S. Li. 2006. Synthesis and analgesic activity evaluation of some agmatine derivatives. *Molecules*. 11:393–402. doi:10.1038/sj.cdd.4401833.

Heise, C., A. Sampson-Johannes, A. Williams, F. McCormick, D.D. Von Hoff, and D.H. Kirn. 1997. ONYX-015, an E1b gene-attenuated adenovirus, causes tumor-specific cytolysis and antitumoral efficacy that can be augmented by standard chemotherapeutic agents. *Nat. Med.* 3:639–645. doi:10.1038/nm0697-639.

Hendrickx, R., N. Stichling, J. Koelen, L. Kuryk, A. Lipiec, and U.F. Greber. 2014. Innate immunity to adenovirus. *Hum. Gene Ther.* 25:265–284. doi:10.1089/hum.2014.001.

Hermiston, T.W., and I. Kuhn. 2002. Armed therapeutic viruses: Strategies and challenges to arming oncolytic viruses with therapeutic genes. *Cancer Gene Ther.* 9:1022–1035. doi:10.1038/sj.cgt.7700542.

Hitt, M.M., and F.L. Graham. 1990. Adenovirus E1A under the control of heterologous promoters: Wide variation in E1A expression levels has little effect on virus replication. *Virology*. 179:667–678. doi:10.1016/0042-6822(90)90134-D.

Hoeben, R.C., and T.G. Uil. 2013. Adenovirus DNA replication. *Cold Spring Harb. Perspect. Biol.* doi:10.1101/cshperspect.a013003.

Hollien, J., and J.S. Weissman. 2006. Decay of endoplasmic reticulum-localized mRNAs during the unfolded protein response. *Science (80-.).* 313:104–107. doi:10.1126/science.1129631.

Horikoshi, N., K. Maguire, A. Kralli, E. Maldonado, D. Reinberg, and R. Weinmann. 1991. Direct interaction between adenovirus E1A protein and the TATA box binding transcription factor IID. *Proc. Natl. Acad. Sci. U. S. A.* doi:10.1073/pnas.88.12.5124.

Horwitz, M.S. 2004. Function of adenovirus E3 proteins and their interactions with immunoregulatory cell proteins. *J. Gene Med.* doi:10.1002/jgm.495.

Hoster, H.A., R.P. Zanes, and E. Von Haam. 1949. Studies in Hodgkin's Syndrome IX. The Association of "Viral" Hepatitis and Hodgkin's Disease (A Preliminary Report). *Cancer Res.* 9:473–480.

Höti, N., W. Chowdhury, J.T. Hsieh, M.D. Sachs, S.E. Lupold, and R. Rodriguez. 2006. Valproic Acid, a Histone Deacetylase Inhibitor, Is an Antagonist for Oncolytic

Adenoviral Gene Therapy. *Mol. Ther.* 14:768–778. doi:10.1016/j.ymthe.2006.07.009.

Höti, N., W.H. Chowdhury, S. Mustafa, J. Ribas, M. Castanares, T. Johnson, M. Liu, S.E. Lupold, and R. Rodriguez. 2010. Armoring CRAds with p21/Waf-1 shRNAs: The next generation of oncolytic adenoviruses. *Cancer Gene Ther.* 17:585–597. doi:10.1038/cgt.2010.15.

Iqbal, N., and N. Iqbal. 2014. Imatinib: A Breakthrough of Targeted Therapy in Cancer. *Chemother. Res. Pract.* 2014:1–9. doi:10.1155/2014/357027.

Isakov, N. 2018. Protein kinase C (PKC) isoforms in cancer, tumor promotion and tumor suppression. *Semin. Cancer Biol.* 48:36–52. doi:10.1016/j.semcancer.2017.04.012.

Iwawaki, T., R. Akai, K. Kohno, and M. Miura. 2004. A transgenic mouse model for monitoring endoplasmic reticulum stress. *Nat. Med.* 10:98–102. doi:10.1038/nm970.

Iyer, N.G., H. Özdag, and C. Caldas. 2004. p300/CBP and cancer. *Oncogene*. 23:4225–4231. doi:10.1038/sj.onc.1207118.

Jafri, M.A., S.A. Ansari, M.H. Alqahtani, and J.W. Shay. 2016. Roles of telomeres and telomerase in cancer, and advances in telomerase-targeted therapies. *Genome Med.* 8. doi:10.1186/s13073-016-0324-x.

Jing, Y., C. Tong, J. Zhang, T. Nakamura, I. Iankov, S.J. Russell, and J.R. Merchan. 2009. Tumor and vascular targeting of a novel oncolytic measles virus retargeted against the urokinase receptor. *Cancer Res.* 69:1459–1468. doi:10.1158/0008-5472.CAN-08-2628.

De Jong, R.N., and P.C. Van Der Vliet. 1999. Mechanism of DNA replication in

eukaryotic cells: Cellular host factors stimulating adenovirus DNA replication. *Gene*. 236:1–12. doi:10.1016/S0378-1119(99)00249-8.

Kalin, S., B. Amstutz, M. Gastaldelli, N. Wolfrum, K. Boucke, M. Havenga, F. DiGennaro, N. Liska, S. Hemmi, and U.F. Greber. 2010. Macropinocytotic Uptake and Infection of Human Epithelial Cells with Species B2 Adenovirus Type 35. *J. Virol.* 84:5336–5350. doi:10.1128/jvi.02494-09.

Kanopka, A., O. Muhlemann, S. Petersen-Mahrt, C. Estmer, C. Ohrmalm, and G. Akusjarvl. 1998. Regulation of adenovirus alternative RNA splicing by dephosphorylation of SR proteins. *Nature*. 393:185–187. doi:10.1038/30277.

Karali, E., S. Bellou, D. Stellas, A. Klinakis, C. Murphy, and T. Fotsis. 2014. VEGF Signals through ATF6 and PERK to Promote Endothelial Cell Survival and Angiogenesis in the Absence of ER Stress. *Mol. Cell*. 54:559–572. doi:10.1016/j.molcel.2014.03.022.

Kaufman, H.L., F.J. Kohlhapp, and A. Zloza. 2015. Oncolytic viruses: A new class of immunotherapy drugs. *Nat. Rev. Drug Discov.* 14:642–662. doi:10.1038/nrd4663.

Kaur, B., T. Cripe, and E. Chiocca. 2009. “Buy One Get One Free”: Armed Viruses for the Treatment of Cancer Cells and their Microenvironment. *Curr. Gene Ther.* 9:341–355. doi:10.2174/156652309789753329.

Keller, B.A., and J.C. Bell. 2016. Oncolytic viruses—immunotherapeutics on the rise. *J. Mol. Med.* 94:979–991. doi:10.1007/s00109-016-1453-9.

Kelly, E., and S.J. Russell. 2007. History of oncolytic viruses: Genesis to genetic engineering. *Mol. Ther.* 15:651–659. doi:10.1038/sj.mt.6300108.

Kelly, E.J., and S.J. Russell. 2009. MicroRNAs and the regulation of vector tropism. *Mol.*

Ther. doi:10.1038/mt.2008.288.

Kelly, K.R., C.M. Espitia, D. Mahalingam, B.O. Oyajobi, M. Coffey, F.J. Giles, J.S. Carew, and S.T. Nawrocki. 2012. Reovirus therapy stimulates endoplasmic reticular stress, NOXA induction, and augments bortezomib-mediated apoptosis in multiple myeloma. *Oncogene*. 31:3023–3038. doi:10.1038/onc.2011.478.

Kim, D.H., and J.J. Rossi. 2008. RNAi mechanisms and applications. *Biotechniques*. 44:613–616. doi:10.2144/000112792.

Kim, S.Y., D. Kang, H.J. Choi, Y. Joo, J.H. Kim, and J.J. Song. 2017. Prime-boost immunization by both DNA vaccine and oncolytic adenovirus expressing GM-CSF and shRNA of TGF-β2 induces anti-tumor immune activation. *Oncotarget*. 8:15858–15877. doi:10.18632/oncotarget.15008.

Kirn, D. 2001. Oncolytic virotherapy for cancer with the adenovirus dl1520 (Onyx-015): Results of Phase I and II trials. *Expert Opin. Biol. Ther.* 1:525–538. doi:10.1517/14712598.1.3.525.

Ko, D., L. Hawkins, and D.C. Yu. 2005. Development of transcriptionally regulated oncolytic adenoviruses. *Oncogene*. 24:7763–7774. doi:10.1038/sj.onc.1209048.

Kozutsumi, Y., M. Segal, K. Normington, M.J. Gething, and J. Sambrook. 1988. The presence of malfolded proteins in the endoplasmic reticulum signals the induction of glucose-regulated proteins. *Nature*. 332:462–464. doi:10.1038/332462a0.

Kuhn, I., P. Harden, M. Bauzon, C. Chartier, J. Nye, S. Thorne, T. Reid, S. Ni, A. Lieber, K. Fisher, L. Seymour, G.M. Rubanyi, R.N. Harkins, and T.W. Hermiston. 2008. Directed evolution generates a novel oncolytic virus for the treatment of colon cancer. *PLoS One*. 3:e2409. doi:10.1371/journal.pone.0002409.

Kumahara, E., T. Ebihara, and D. Saffen. 1999. Protein kinase inhibitor H7 blocks the induction of immediate-early genes zif268 and c-fos by a mechanism unrelated to inhibition of protein kinase C but possibly related to inhibition of phosphorylation of RNA polymerase II. *J. Biol. Chem.* 274:10430–10438. doi:10.1074/jbc.274.15.10430.

Van Kuppeveld, F.J.M., J.G.J. Hoenderop, R.L.L. Smeets, P.H.G.M. Willems, H.B.P.M. Dijkman, J.M.D. Galama, and W.J.G. Melchers. 1997. Coxsackievirus protein 2B modifies endoplasmic reticulum membrane and plasma membrane permeability and facilitates virus release. *EMBO J.* 16:3519–3532. doi:10.1093/emboj/16.12.3519.

Larsen, E.C., J.A. DiGennaro, N. Saito, S. Mehta, D.J. Loegering, J.E. Mazurkiewicz, and M.R. Lennartz. 2000. Differential Requirement for Classic and Novel PKC Isoforms in Respiratory Burst and Phagocytosis in RAW 264.7 Cells. *J. Immunol.* 165:2809–2817. doi:10.4049/jimmunol.165.5.2809.

Lee, K., W. Tirasophon, X. Shen, M. Michalak, R. Prywes, T. Okada, H. Yoshida, K. Mori, and R.J. Kaufman. 2002. IRE1-mediated unconventional mRNA splicing and S2P-mediated ATF6 cleavage merge to regulate XBP1 in signaling the unfolded protein response. *Genes Dev.* doi:10.1101/gad.964702.

Lee, W.S., C.C. Kao, G.O. Bryant, X. Liu, and A.J. Berk. 1991. Adenovirus E1A activation domain binds the basic repeat in the TATA box transcription factor. *Cell*. doi:10.1016/0092-8674(91)90188-5.

Leitman, J., F. Ulrich Hartl, and G.Z. Lederkremer. 2013. Soluble forms of polyQ-expanded huntingtin rather than large aggregates cause endoplasmic reticulum stress. *Nat. Commun.* 4. doi:10.1038/ncomms3753.

Li, G.D., H. Kawashima, A. Ogose, T. Ariizumi, T. Hotta, R. Kuwano, Y. Urata, T.

Fujiwara, and N. Endo. 2013a. Telomelysin shows potent antitumor activity through apoptotic and non-apoptotic cell death in soft tissue sarcoma cells. *Cancer Sci.* 104:1178–1188. doi:10.1111/cas.12208.

Li, H., A. V. Korennykh, S.L. Behrman, and P. Walter. 2010. Mammalian endoplasmic reticulum stress sensor IRE1 signals by dynamic clustering. *Proc. Natl. Acad. Sci. U. S. A.* 107:16113–16118. doi:10.1073/pnas.1010580107.

Li, Z., L. Zhang, Y. Zhao, H. Li, H. Xiao, R. Fu, C. Zhao, H. Wu, and Z. Li. 2013b. Cell-surface GRP78 facilitates colorectal cancer cell migration and invasion. *Int. J. Biochem. Cell Biol.* 45:987–994. doi:10.1016/j.biocel.2013.02.002.

Lichty, B.D., C.J. Breitbach, D.F. Stojdl, and J.C. Bell. 2014. Going viral with cancer immunotherapy. *Nat. Rev. Cancer*. 14:559–567. doi:10.1038/nrc3770.

Lin, J.H., H. Li, D. Yasumura, H.R. Cohen, C. Zhang, B. Panning, K.M. Shokat, M.M. LaVail, and P. Walter. 2007. IRE1 signaling affects cell fate during the unfolded protein response. *Science (80-.).* 318:944–949. doi:10.1126/science.1146361.

Lipp, P., and G. Reither. 2011. Protein kinase C: The “Masters” of calcium and lipid. *Cold Spring Harb. Perspect. Biol.* 3:1–17. doi:10.1101/cshperspect.a004556.

Liu, H., L. Jin, S.B.S. Koh, I. Atanasov, S. Schein, L. Wu, and Z.H. Zhou. 2010. Atomic structure of human adenovirus by Cryo-EM reveals interactions among protein networks. *Science (80-.).* doi:10.1126/science.1187433.

Liu, H., J.H. Naismith, and R.T. Hay. 2003. Adenovirus DNA replication. *Curr. Top. Microbiol. Immunol.* 272:131–164.

Logan, J., E. Falck-Pedersen, J.E. Darnell, and T. Shenk. 1987. A poly(A) addition site and a downstream termination region are required for efficient cessation of

transcription by RNA polymerase II in the mouse beta maj-globin gene. *Proc. Natl. Acad. Sci. U. S. A.* 84:8306–8310. doi:10.1073/pnas.84.23.8306.

Lu, S., and B.R. Cullen. 2004. Adenovirus VA1 Noncoding RNA Can Inhibit Small Interfering RNA and MicroRNA Biogenesis. *J. Virol.* 78:12868–12876. doi:10.1128/jvi.78.23.12868-12876.2004.

Luisoni, S., M. Suomalainen, K. Boucke, L.B. Tanner, M.R. Wenk, X.L. Guan, M. Grzybek, U. Coskun, and U.F. Greber. 2015. Co-option of membrane wounding enables virus penetration into cells. *Cell Host Microbe*. doi:10.1016/j.chom.2015.06.006.

Ma, H., Y. Wu, Y. Dang, J.G. Choi, J. Zhang, and H. Wu. 2014. Pol III promoters to express small RNAs: Delineation of transcription initiation. *Mol. Ther. - Nucleic Acids*. 3:e161. doi:10.1038/mtna.2014.12.

Ma, R., J. Pluznick, P. Kudlacek, and S.C. Sansom. 2001. Protein Kinase C Activates Store-operated Ca2+ Channels in Human Glomerular Mesangial Cells. *J. Biol. Chem.* doi:10.1074/jbc.M011241200.

Machiels, J.P., R. Salazar, S. Rottey, I. Duran, L. Dirix, K. Geboes, C. Wilkinson-Blanc, G. Pover, S. Alvis, B. Champion, K. Fisher, H. McElwaine-Johnn, J. Beadle, and E. Calvo. 2019. A phase 1 dose escalation study of the oncolytic adenovirus enadenotucirev, administered intravenously to patients with epithelial solid tumors (EVOLVE). *J. Immunother. Cancer*. 7:20. doi:10.1186/s40425-019-0510-7.

Machitani, M., F. Sakurai, K. Katayama, M. Tachibana, T. Suzuki, H. Matsui, T. Yamaguchi, and H. Mizuguchi. 2013. Improving adenovirus vector-mediated RNAi efficiency by lacking the expression of virus-associated RNAs. *Virus Res.* 178:357–363. doi:10.1016/j.virusres.2013.09.021.

Machitani, M., F. Sakurai, K. Wakabayashi, M. Tachibana, T. Fujiwara, and H. Mizuguchi. 2017a. Enhanced oncolytic activities of the telomerase-specific replication-competent adenovirus expressing short-hairpin RNA against dicer. *Mol. Cancer Ther.* doi:10.1158/1535-7163.MCT-16-0383.

Machitani, M., F. Sakurai, K. Wakabayashi, K. Takayama, M. Tachibana, and H. Mizuguchi. 2017b. Type I Interferons Impede Short Hairpin RNA-Mediated RNAi via Inhibition of Dicer-Mediated Processing to Small Interfering RNA. *Mol. Ther. - Nucleic Acids*. 6:173–182. doi:10.1016/j.omtn.2016.12.007.

Machitani, M., F. Sakurai, K. Wakabayashi, K. Tomita, M. Tachibana, and H. Mizuguchi. 2016. Dicer functions as an antiviral system against human adenoviruses via cleavage of adenovirus-encoded noncoding RNA. *Sci. Rep.* 6. doi:10.1038/srep27598.

MacTavish, H., J.S. Diallo, B. Huang, M. Stanford, F. Le Boeuf, N. De Silva, J. Cox, J.G. Simmons, T. Guimond, T. Falls, A.J. McCart, H. Atkins, C. Breitbach, D. Kirn, S. Thorne, and J.C. Bell. 2010. Enhancement of vaccinia virus based oncolysis with histone deacetylase inhibitors. *PLoS One*. doi:10.1371/journal.pone.0014462.

Mahoney, D.J., C. Lefebvre, K. Allan, J. Brun, C.A. Sanaei, S. Baird, N. Pearce, S. Grönberg, B. Wilson, M. Prakesh, A. Aman, M. Isaac, A. Mamai, D. Uehling, R. Al-Awar, T. Falls, T. Alain, and D.F. Stojdl. 2011. Virus-Tumor Interactome Screen Reveals ER Stress Response Can Reprogram Resistant Cancers for Oncolytic Virus-Triggered Caspase-2 Cell Death. *Cancer Cell*. 20:443–456. doi:10.1016/J.CCR.2011.09.005.

Mansour, M., P. Palese, and D. Zamarin. 2011. Oncolytic Specificity of Newcastle Disease Virus Is Mediated by Selectivity for Apoptosis-Resistant Cells. *J. Virol.*

85:6015–6023. doi:10.1128/jvi.01537-10.

Marciniak, S.J., C.Y. Yun, S. Oyadomari, I. Novoa, Y. Zhang, R. Jungreis, K. Nagata, H.P. Harding, and D. Ron. 2004. CHOP induces death by promoting protein synthesis and oxidation in the stressed endoplasmic reticulum. *Genes Dev.* 18:3066–3077. doi:10.1101/gad.1250704.

Marcu, M.G., M. Doyle, A. Bertolotti, D. Ron, L. Hendershot, and L. Neckers. 2002. Heat Shock Protein 90 Modulates the Unfolded Protein Response by Stabilizing IRE1 . *Mol. Cell. Biol.* 22:8506–8513. doi:10.1128/mcb.22.24.8506-8513.2002.

Marengo, B., C. de Ciucis, R. Ricciarelli, M.A. Pronzato, U.M. Marinari, and C. Domenicotti. 2011. Protein kinase C: An attractive target for cancer therapy. *Cancers (Basel).* doi:10.3390/cancers3010531.

Marino, N., S. Illingworth, P. Kodialbail, A. Patel, H. Calderon, R. Lear, K.D. Fisher, B.R. Champion, and A.C.N. Brown. 2017. Development of a versatile oncolytic virus platform for local intra-tumoural expression of therapeutic transgenes. *PLoS One*. 12:e0177810. doi:10.1371/journal.pone.0177810.

Martin, M.E., and A.J. Berk. 1998. Adenovirus E1B 55K represses p53 activation in vitro. *J. Virol.* 72:3146–54.

Martin, V., R. Bredoux, E. Corvazier, R. Van Gorp, T. Kovàcs, P. Gélébart, and J. Enouf. 2002. Three novel sarco/endoplasmic reticulum Ca 2+-ATPase (SERCA) 3 isoforms: Expression, regulation, and function of the members of the SERCA3 family. *J. Biol. Chem.* 277:24442–24452. doi:10.1074/jbc.M202011200.

Mascia, F., M. Denning, R. Kopan, and S.H. Yuspa. 2012. The black box illuminated: Signals and signaling. *J. Invest. Dermatol.* 132:811–819. doi:10.1038/jid.2011.406.

Masouleh, B.K., H. Geng, C. Hurtz, L.N. Chan, A.C. Logan, M.S. Chang, C. Huang, S. Swaminathan, H. Sun, E. Paietta, A.M. Melnick, P. Koeffler, and M. Müschen. 2014. Mechanistic rationale for targeting the unfolded protein response in pre-B acute lymphoblastic leukemia. *Proc. Natl. Acad. Sci. U. S. A.* 111:E2219-28. doi:10.1073/pnas.1400958111.

Mathews, M.B., and T. Shenk. 1991. Adenovirus virus-associated RNA and translation control. *J. Virol.* 65:5657–62.

McKenna, S.A., I. Kim, C.W. Liu, and J.D. Puglisi. 2006. Uncoupling of RNA Binding and PKR Kinase Activation by Viral Inhibitor RNAs. *J. Mol. Biol.* 358:1270–1285. doi:10.1016/j.jmb.2006.03.003.

Medghalchi, S., R. Padmanabhan, and G. Ketner. 1997. Early region 4 modulates adenovirus DNA replication by two genetically separable mechanisms. *Virology*. 236:8–17. doi:10.1006/viro.1997.8737.

Mei, Y.F., J. Skog, K. Lindman, and G. Wadell. 2003. Comparative analysis of the genome organization of human adenovirus 11, a member of the human adenovirus species B, and the commonly used human adenovirus 5 vector, a member of species C. *J. Gen. Virol.* 84:2061–2071. doi:10.1099/vir.0.19178-0.

Mei, Y.F., and G. Wadell. 1992. The nucleotide sequence of adenovirus type 11 early 3 region: Comparison of genome type Ad11p and Ad11a. *Virology*. 191:125–133. doi:10.1016/0042-6822(92)90173-M.

Meier, O., and U.F. Greber. 2003. Adenovirus endocytosis. *J. Gene Med.* 5:451–462. doi:10.1002/jgm.409.

Mendez, A.S., J. Alfaro, M.A. Morales-Soto, A.C. Dar, E. McCullagh, K. Gotthardt, H.

Li, D. Acosta-Alvear, C. Sidrauski, A. V. Korennykh, S. Bernales, K.M. Shokat, and P. Walter. 2015. Endoplasmic reticulum stress-independent activation of unfolded protein response kinases by a small molecule ATP-mimic. *Elife*. 4. doi:10.7554/eLife.05434.

Miller, A., L. Suksanpaisan, S. Naik, R. Nace, M. Federspiel, K.W. Peng, and S.J. Russell. 2014. Reporter gene imaging identifies intratumoral infection voids as a critical barrier to systemic oncolytic virus efficacy. *Mol. Ther. - Oncolytics*. 1:14005. doi:10.1038/mto.2014.5.

Miller, C., and H.P. Koeffler. 1993. P53 mutations in human cancer. *Leukemia*. 7:49 LP – 53. doi:10.1126/science.1905840.

Mirza, A. 1992. Stimulation of adenovirus early gene expression by phorbol ester: Its possible mechanism. *Virology*. 190:645–653. doi:10.1016/0042-6822(92)90902-2.

Miyazawa, N., R.G. Crystal, and P.L. Leopold. 2001. Adenovirus Serotype 7 Retention in a Late Endosomal Compartment prior to Cytosol Escape Is Modulated by Fiber Protein. *J. Virol.* doi:10.1128/jvi.75.3.1387-1400.2001.

Moise, A.R., J.R. Grant, T.Z. Vitalis, and W.A. Jefferies. 2002. Adenovirus E3-6.7K Maintains Calcium Homeostasis and Prevents Apoptosis and Arachidonic Acid Release. *J. Virol.* doi:10.1128/jvi.76.4.1578-1587.2002.

Molin, M., L. Bouakaz, S. Berenjian, and G. Akusjärvi. 2002. Unscheduled expression of capsid protein IIIa results in defects in adenovirus major late mRNA and protein expression. *Virus Res.* 83:197–206. doi:10.1016/S0168-1702(01)00443-9.

Montell, C., E.F. Fisher, M.H. Caruthers, and A.J. Berk. 1982. Resolving the functions of overlapping viral genes by site-specific mutagenesis at a mRNA splice site.

Nature. 295:380–384. doi:10.1038/295380a0.

Moore, C.B., E.H. Guthrie, M.T. Huang, and D.J. Taxman. 2010. Short Hairpin RNA (shRNA). *Methods Mol Biol.* 629:141–158. doi:10.1007/978-1-60761-657-3.

Morgan, A.J., L.C. Davis, S.K.T.Y. Wagner, A.M. Lewis, J. Parrington, G.C. Churchill, and A. Galione. 2013. Bidirectional Ca2+ signaling occurs between the endoplasmic reticulum and acidic organelles. *J. Cell Biol.* 200:789–805. doi:10.1083/jcb.201204078.

Morgan, A.J., and R. Jacob. 1994. Ionomycin enhances Ca2+ influx by stimulating store-regulated cation entry and not by a direct action at the plasma membrane. *Biochem. J.* 300 (Pt 3):665–72.

Motegi, Y., K. Katayama, F. Sakurai, T. Kato, T. Yamaguchi, H. Matsui, M. Takahashi, K. Kawabata, and H. Mizuguchi. 2011. An effective gene-knockdown using multiple shRNA-expressing adenovirus vectors. *J. Control. Release*. doi:10.1016/j.jconrel.2011.04.009.

Mujcic, H., A. Nagelkerke, K.M.A. Rouschop, S. Chung, N. Chaudary, P.N. Span, B. Clarke, M. Milosevic, J. Sykes, R.P. Hill, M. Koritzinsky, and B.G. Wouters. 2013. Hypoxic activation of the PERK/eIF2α arm of the unfolded protein response promotes metastasis through induction of LAMP3. *Clin. Cancer Res.* 19:6126–6137. doi:10.1158/1078-0432.CCR-13-0526.

Murray, S., C.L. Nilsson, J.T. Hare, M.R. Emmett, A. Korostelev, H. Ongley, A.G. Marshall, and M.S. Chapman. 2006. Characterization of the Capsid Protein Glycosylation of Adeno-Associated Virus Type 2 by High-Resolution Mass Spectrometry. *J. Virol.* 80:6171–6176. doi:10.1128/jvi.02417-05.

Nakano, M.Y., K. Boucke, M. Suomalainen, R.P. Stidwill, and U.F. Greber. 2000. The First Step of Adenovirus Type 2 Disassembly Occurs at the Cell Surface, Independently of Endocytosis and Escape to the Cytosol. *J. Virol.* 74:7085–7095. doi:10.1128/jvi.74.15.7085-7095.2000.

Nemerow, G.R. 2002. Biology of Adenovirus Cell Entry. *In* Adenoviral Vectors for Gene Therapy. 19–38.

Nemerow, G.R., and P.L. Stewart. 2016. Insights into adenovirus uncoating from interactions with integrins and mediators of host immunity. *Viruses*. 8. doi:10.3390/v8120337.

Newton, A.C. 1995. Protein kinase C: Structure, function, and regulation. *J. Biol. Chem.* 270:28495–28498. doi:10.1074/jbc.270.48.28495.

Niehans, G.A., D.L. Cherwitz, N.A. Staley, D.J. Knapp, and A.P. Dalmasso. 1996. Human carcinomas variably express the complement inhibitory proteins CD46 (membrane cofactor protein), CD55 (decay-accelerating factor), and CD59 (protectin). *Am. J. Pathol.*

O'Shea, C., K. Klupsch, S. Choi, B. Bagus, C. Soria, J. Shen, F. McCormick, and D. Stokoe. 2005a. Adenoviral proteins mimic nutrient/growth signals to activate the mTOR pathway for viral replication. *EMBO J.* doi:10.1038/sj.emboj.7600597.

O'Shea, C.C., S. Choi, F. McCormick, and D. Stokoe. 2005b. Adenovirus overrides cellular checkpoints for protein translation. *Cell Cycle*. 4:883–888. doi:10.4161/cc.4.7.1791.

O'Shea, C.C., L. Johnson, B. Bagus, S. Choi, C. Nicholas, A. Shen, L. Boyle, K. Pandey, C. Soria, J. Kunich, Y. Shen, G. Habets, D. Ginzinger, and F. McCormick. 2004.

Late viral RNA export, rather than p53 inactivation, determines ONYX-015 tumor selectivity. *Cancer Cell*. 6:611–623. doi:10.1016/j.ccr.2004.11.012.

Obbard, D.J., K.H.J. Gordon, A.H. Buck, and F.M. Jiggins. 2009. The evolution of RNAi as a defence against viruses and transposable elements. *Philos. Trans. R. Soc. B Biol. Sci.* 364:99–115. doi:10.1098/rstb.2008.0168.

Obeng, E.A., L.M. Carlson, D.M. Gutman, W.J. Harrington, K.P. Lee, and L.H. Boise. 2006. Proteasome inhibitors induce a terminal unfolded protein response in multiple myeloma cells. *Blood*. 107:4907–4916. doi:10.1182/blood-2005-08-3531.

Oikawa, D., Y. Kimata, K. Kohno, and T. Iwawaki. 2009. Activation of mammalian IRE1α upon ER stress depends on dissociation of BiP rather than on direct interaction with unfolded proteins. *Exp. Cell Res.* 315:2496–2504. doi:10.1016/j.yexcr.2009.06.009.

Okegawa, T., R.C. Pong, Y. Li, J.M. Bergelson, A.I. Sagalowsky, and J.T. Hsieh. 2001. The mechanism of the growth-inhibitory effect of coxsackie and adenovirus receptor (CAR) on human bladder cancer: A functional analysis of car protein structure. *Cancer Res.* 61:6592–6600.

Pahl, H.L., M. Sester, H.G. Burgert, and P.A. Baeuerle. 1996a. Activation of transcription factor NF-kappaB by the adenovirus E3/19K protein requires its ER retention. *J. Cell Biol.* 132:511–22.

Pahl, H.L., M. Sester, H.G. Burgert, and P.A. Baeuerle. 1996b. Activation of transcription factor NF-kappaB by the adenovirus E3/19K protein requires its ER retention. *J. Cell Biol.* 132:511–22. doi:10.1083/jcb.132.4.511.

Palam, L.R., T.D. Baird, and R.C. Wek. 2011. Phosphorylation of eIF2 facilitates

ribosomal bypass of an inhibitory upstream ORF to enhance CHOP translation. *J. Biol. Chem.* 286:10939–10949. doi:10.1074/jbc.M110.216093.

Pany, S., A. Majhi, and J. Das. 2012. PKC Activation by Resveratrol Derivatives with Unsaturated Aliphatic Chain. *PLoS One*. 7. doi:10.1371/journal.pone.0052888.

Park, G.T., and K.C. Choi. 2016. Advanced new strategies for metastatic cancer treatment by therapeutic stem cells and oncolytic virotherapy. *Oncotarget*. 7:58684–58695. doi:10.18632/oncotarget.11017.

Patel, S., and R. Docampo. 2010. Acidic calcium stores open for business: Expanding the potential for intracellular Ca2+ signaling. *Trends Cell Biol.* 20:277–286. doi:10.1016/j.tcb.2010.02.003.

Paul Thomas, G., and M.B. Mathews. 1980. DNA replication and the early to late transition in adenovirus infection. *Cell*. 22:523–533. doi:10.1016/0092-8674(80)90362-1.

Peña, J., and E. Harris. 2011. Dengue virus modulates the unfolded protein response in a time-dependent manner. *J. Biol. Chem.* 286:14226–14236. doi:10.1074/jbc.M111.222703.

Pereira, E.R., K. Frudd, W. Awad, and L.M. Hendershot. 2014. Endoplasmic Reticulum (ER) stress and Hypoxia response pathways interact to Potentiate Hypoxia-inducible Factor 1 (HIF-1) Transcriptional activity on targets like Vascular Endothelial Growth Factor (VEGF). *J. Biol. Chem.* 289:3352–3364. doi:10.1074/jbc.M113.507194.

Pesonen, S., I. Diaconu, L. Kangasniemi, T. Ranki, A. Kanerva, S.K. Pesonen, U. Gerdemann, A.M. Leen, K. Kairemo, M. Oksanen, E. Haavisto, S.-L. Holm, A.

Karioja-Kallio, S. Kauppinen, K.P.L. Partanen, L. Laasonen, T. Joensuu, T. Alanko, V. Cerullo, and A. Hemminki. 2012. Oncolytic Immunotherapy of Advanced Solid Tumors with a CD40L-Expressing Replicating Adenovirus: Assessment of Safety and Immunologic Responses in Patients. *Cancer Res.* 72:1621–1631. doi:10.1158/0008-5472.CAN-11-3001.

Van Petegem, F. 2012. Ryanodine receptors: Structure and function. *J. Biol. Chem.* 287:31624–31632. doi:10.1074/jbc.R112.349068.

Phillips, M., J. Stuart, R. Rodríguez Stewart, J. Berry, B. Mainou, and K. Boehme. 2018. Current understanding of reovirus oncolysis mechanisms. *Oncolytic Virotherapy*. Volume 7:53–63. doi:10.2147/ov.s143808.

Prakriya, M. 2009. The molecular physiology of CRAC channels. *Immunol. Rev.* 231:88–98. doi:10.1111/j.1600-065X.2009.00820.x.

Prasad, V., M. Suomalainen, M. Pennauer, A. Yakimovich, V. Andriasyan, S. Hemmi, and U.F. Greber. 2014. Chemical induction of unfolded protein response enhances cancer cell killing through lytic virus infection. *J. Virol.* 88:13086–98. doi:10.1128/JVI.02156-14.

Prostko, C.R., J.N. Dholakia, M.A. Brostrom, and C.O. Brostrom. 1995. Activation of the double-stranded RNA-regulated protein kinase by depletion of endoplasmic reticular calcium stores. *J. Biol. Chem.* 270:6211–6215. doi:10.1074/jbc.270.11.6211.

Raja, J., J.M. Ludwig, S.N. Gettinger, K.A. Schalper, and H.S. Kim. 2018. Oncolytic virus immunotherapy: Future prospects for oncology 11 Medical and Health Sciences 1107 Immunology 11 Medical and Health Sciences 1112 Oncology and Carcinogenesis. *J. Immunother. Cancer*. 6. doi:10.1186/s40425-018-0458-z.

Ramesh, N., Y. Ge, D.L. Ennist, M. Zhu, M. Mina, S. Ganesh, P.S. Reddy, D.C. Yu, and P. Working. 2006. CG0070, a conditionally replicating granulocyte macrophage colony-stimulating factor - Armed oncolytic adenovirus for the treatment of bladder cancer. *Clin. Cancer Res.* 12:305–313. doi:10.1158/1078-0432.CCR-05-1059.

Ramke, M., J.Y. Lee, D.W. Dyer, D. Seto, J. Rajaiya, and J. Chodosh. 2017. The 5′UTR in human adenoviruses: Leader diversity in late gene expression. *Sci. Rep.* 7. doi:10.1038/s41598-017-00747-y.

Rodriguez, R., E.R. Schuur, H.Y. Lim, G.A. Henderson, J.W. Simons, and D.R. Henderson. 1997. Prostate attenuated replication competent adenovirus (ARCA) CN706: a selective cytotoxic for prostate-specific antigen-positive prostate cancer cells. *Cancer Res.* 57:2559–63.

Ron, D., and P. Walter. 2007. Signal integration in the endoplasmic reticulum unfolded protein response. *Nat. Rev. Mol. Cell Biol.* 8:519–529. doi:10.1038/nrm2199.

Ronco, V., D.M. Potenza, F. Denti, S. Vullo, G. Gagliano, M. Tognolina, G. Guerra, P. Pinton, A.A. Genazzani, L. Mapelli, D. Lim, and F. Moccia. 2015. A novel Ca2+-mediated cross-talk between endoplasmic reticulum and acidic organelles: Implications for NAADP-dependent Ca2+ signalling. *Cell Calcium*. 57:89–100. doi:10.1016/j.ceca.2015.01.001.

Rothmann, T., A. Hengstermann, N.J. Whitaker, M. Scheffner, and H. zur Hausen. 1998. Replication of ONYX-015, a potential anticancer adenovirus, is independent of p53 status in tumor cells. *J. Virol.* 72:9470–8.

Roulstone, V., M. Pedersen, J. Kyula, D. Mansfield, A.A. Khan, G. Mcentee, M. Wilkinson, E. Karapanagiotou, M. Coffey, R. Marais, A. Jebar, F. Errington-Mais, A. Melcher, R. Vile, H. Pandha, M. Mclaughlin, and K.J. Harrington. 2015. BRAF-

and MEK-targeted small molecule inhibitors exert enhanced antimelanoma effects in combination with oncolytic reovirus through ER stress. *Mol. Ther.* 23:931–942. doi:10.1038/mt.2015.15.

Rowe, W.P., R.J. Huebner, L.K. Gilmore, R.H. Parrott, and T.G. Ward. 1953. Isolation of a Cytopathogenic Agent from Human Adenoids Undergoing Spontaneous Degeneration in Tissue Culture. *Proc. Soc. Exp. Biol. Med.* 84:570–573. doi:10.3181/00379727-84-20714.

Ruggiano, A., O. Foresti, and P. Carvalho. 2014. ER-associated degradation: Protein quality control and beyond. *J. Cell Biol.* 204:869–879. doi:10.1083/jcb.201312042.

Russell, S.J., K.-W. Peng, and J.C. Bell. 2012. Oncolytic virotherapy. *Nat. Biotechnol.* 30:658–70. doi:10.1038/nbt.2287.

Rux, J.J., and R.M. Burnett. 2004. Review: Adenovirus Structure. *Hum. Gene Ther.* 1176:1167–1176. doi:10.1089/hum.2004.15.1167.

Sachs, M.D., K.A. Rauen, M. Ramamurthy, J.L. Dodson, A.M. De Marzo, M.J. Putzi, M.P. Schoenberg, and R. Rodriguez. 2002. Integrin αv and coxsackie adenovirus receptor expression in clinical bladder cancer. *Urology*. 60:531–536. doi:10.1016/S0090-4295(02)01748-X.

Sakurai, Y., A.A. Kolokoltsov, C.C. Chen, M.W. Tidwell, W.E. Bauta, N. Klugbauer, C. Grimm, C. Wahl-Schott, M. Biel, and R.A. Davey. 2015. Two-pore channels control Ebola virus host cell entry and are drug targets for disease treatment. *Science (80-.).* doi:10.1126/science.1258758.

San Martín, C. 2012. Latest Insights on Adenovirus Structure and Assembly. *Viruses*. doi:10.3390/v4050847.

Scaria, A., A.E. Tollefson, S.K. Saha, and W.S.M. Wold. 1992. The E3-11.6K protein of adenovirus is an asn-glycosylated integral membrane protein that localizes to the nuclear membrane. *Virology*. 191:743–753. doi:10.1016/0042-6822(92)90250-S.

Schönthal, A., J. Sugarman, J.H. Brown, M.R. Hanley, and J.R. Feramisco. 1991. Regulation of c-fos and c-jun protooncogene expression by the Ca2+-ATPase inhibitor thapsigargin. *Proc. Natl. Acad. Sci. U. S. A.* 88:7096–7100. doi:10.1073/pnas.88.16.7096.

Scott, E.M., E.J. Jacobus, B. Lyons, S. Frost, J.D. Freedman, A. Dyer, H. Khalique, W.K. Taverner, A. Carr, B.R. Champion, K.D. Fisher, L.W. Seymour, and M.R. Duffy. 2019. Bi- and tri-valent T cell engagers deplete tumour-associated macrophages in cancer patient samples. *J. Immunother. Cancer*. 7:320. doi:10.1186/s40425-019-0807-6.

Selman, M., P. Ou, C. Rousso, A. Bergeron, R. Krishnan, L. Pikor, A. Chen, B.A. Keller, C. Ilkow, J.C. Bell, and J.S. Diallo. 2018. Dimethyl fumarate potentiates oncolytic virotherapy through NF-B inhibition. *Sci. Transl. Med.* 10. doi:10.1126/scitranslmed.aao1613.

Senzer, N.N., H.L. Kaufman, T. Amatruda, M. Nemunaitis, T. Reid, G. Daniels, R. Gonzalez, J. Glaspy, E. Whitman, K. Harrington, H. Goldsweig, T. Marshall, C. Love, R. Coffin, and J.J. Nemunaitis. 2009. Phase II clinical trial of a granulocyte-macrophage colony-stimulating factor-encoding, second-generation oncolytic herpesvirus in patients with unresectable metastatic melanoma. *J. Clin. Oncol.* 27:5763–5771. doi:10.1200/JCO.2009.24.3675.

Sester, M., Z. Ruszics, E. Mackley, and H.-G. Burgert. 2013. The Transmembrane Domain of the Adenovirus E3/19K Protein Acts as an Endoplasmic Reticulum

Retention Signal and Contributes to Intracellular Sequestration of Major Histocompatibility Complex Class I Molecules. *J. Virol.* 87:6104–6117. doi:10.1128/jvi.03391-12.

Seymour, L.W., and K.D. Fisher. 2016. Oncolytic viruses: Finally delivering. *Br. J. Cancer*. 114:357–361. doi:10.1038/bjc.2015.481.

Shang, J., and M.A. Lehrman. 2004. Discordance of UPR signaling by ATF6 and Ire1p-XBP1 with levels of target transcripts. *Biochem. Biophys. Res. Commun.* 317:390–396. doi:10.1016/j.bbrc.2004.03.058.

Shayakhmetov, D.M., Z.-Y. Li, V. Ternovoi, A. Gaggar, H. Gharwan, and A. Lieber. 2003. The Interaction between the Fiber Knob Domain and the Cellular Attachment Receptor Determines the Intracellular Trafficking Route of Adenoviruses. *J. Virol.* 77:3712–3723. doi:10.1128/jvi.77.6.3712-3723.2003.

Shiina, M., M.D. Lacher, C. Christian, and W.M. Korn. 2009. RNA interference-mediated knockdown of p21 WAF1 enhances anti-tumor cell activity of oncolytic adenoviruses. *Cancer Gene Ther.* doi:10.1038/cgt.2009.29.

Shortridge, K.F., and F. Biddle. 1970. The proteins of adenovirus type 5. *Arch. Gesamte Virusforsch.* 29:1–24. doi:10.1007/BF01253875.

Sieczkarski, S.B., and G.R. Whittaker. 2005. Viral entry. *Curr. Top. Microbiol. Immunol.* 285:1–23.

Signas, C., G. Akusjarvi, and U. Pettersson. 1985. Adenovirus 3 fiber polypeptide gene: Implications for the structure of the fiber protein. *J. Virol.* 53:672–678.

Singh, P.K., J. Doley, G. Ravi Kumar, A.P. Sahoo, and A.K. Tiwari. 2012. Oncolytic viruses & their specific targeting to tumour cells. *Indian J. Med. Res.* 136:571–584.

Small, E.J., M.A. Carducci, J.M. Burke, R. Rodriguez, L. Fong, L. van Ummersen, D.C. Yu, J. Aimi, D. Ando, P. Working, D. Kirn, and G. Wilding. 2006. A Phase I Trial of Intravenous CG7870, a Replication-Selective, Prostate-Specific Antigen-Targeted Oncolytic Adenovirus, for the Treatment of Hormone-Refractory, Metastatic Prostate Cancer. *Mol. Ther.* 14:107–117. doi:10.1016/j.ymthe.2006.02.011.

Smith, K.D., J.J. Mezhir, K. Bickenbach, J. Veerapong, J. Charron, M.C. Posner, B. Roizman, and R.R. Weichselbaum. 2006. Activated MEK Suppresses Activation of PKR and Enables Efficient Replication and In Vivo Oncolysis by 134.5 Mutants of Herpes Simplex Virus 1. *J. Virol.* 80:1110–1120. doi:10.1128/jvi.80.3.1110-1120.2006.

Smittenaar, C.R., K.A. Petersen, K. Stewart, and N. Moitt. 2016. Cancer incidence and mortality projections in the UK until 2035. *Br. J. Cancer*. 115:1147–1155. doi:10.1038/bjc.2016.304.

Southam, C.M., and A.E. Moore. 1952. Clinical studies of viruses as antineoplastic agents, with particular reference to egypt 101 virus. *Cancer*. 5:1025–1034. doi:10.1002/1097-0142(195209)5:5<1025::AID-CNCR2820050518>3.0.CO;2-Q.

Spurgeon, M.E., and D.A. Ornelles. 2009. The Adenovirus E1B 55-Kilodalton and E4 Open Reading Frame 6 Proteins Limit Phosphorylation of eIF2 during the Late Phase of Infection. *J. Virol.* 83:9970–9982. doi:10.1128/jvi.01113-09.

Stamey, T.A., N. Yang, A.R. Hay, J.E. McNeal, F.S. Freiha, and E. Redwine. 1987. Prostate-Specific Antigen as a Serum Marker for Adenocarcinoma of the Prostate. *N. Engl. J. Med.* 317:909–916. doi:10.1056/NEJM198710083171501.

Stein, R.W., M. Corrigan, P. Yaciuk, J. Whelan, and E. Moran. 1990. Analysis of E1A-

mediated growth regulation functions: Binding of the 300-kilodalton cellular product correlates with E1A enhancer repression function and DNA synthesis-inducing activity. *J. Virol.* 64:4421–4427.

Steinberg, S.F. 2008. Structural basis of protein kinase C isoform function. *Physiol. Rev.* 88:1341–1378. doi:10.1152/physrev.00034.2007.

Steinkamp, J.A., and C.C. Stewart. 1986. Dual-laser, differential fluorescence correction method for reducing cellular background autofluorescence. *Cytometry*. 7:566–574. doi:10.1002/cyto.990070611.

Stevenson, S.C., M. Rollence, B. White, L. Weaver, and A. McClelland. 1995. Human adenovirus serotypes 3 and 5 bind to two different cellular receptors via the fiber head domain. *J. Virol.* 69:2850–7.

Stewart, P.L., R.M. Burnett, M. Cyrklaff, and S.D. Fuller. 1991. Image reconstruction reveals the complex molecular organization of adenovirus. *Cell*. doi:10.1016/0092-8674(91)90578-M.

Stone, D., A. Furthmann, V. Sandig, and A. Lieber. 2003. The complete nucleotide sequence, genome organization, and origin of human adenovirus type 11. *Virology*. 309:152–165. doi:10.1016/S0042-6822(02)00085-5.

Strong, J.E., M.C. Coffey, D. Tang, P. Sabinin, and P.W.K. Lee. 1998. The molecular basis of viral oncolysis: Usurpation of the Ras signaling pathway by reovirus. *EMBO J.* 17:3351–3362. doi:10.1093/emboj/17.12.3351.

Strong, J.E., D. Tang, and P.W.K. Lee. 1993. Evidence That the Epidermal Growth Factor Receptor on Host Cells Confers Reovirus Infection Efficiency. *Virology*. 197:405–411. doi:10.1006/viro.1993.1602.

Strunze, S., M.F. Engelke, I.H. Wang, D. Puntener, K. Boucke, S. Schleich, M. Way, P. Schoenenberger, C.J. Burckhardt, and U.F. Greber. 2011. Kinesin-1-mediated capsid disassembly and disruption of the nuclear pore complex promote virus infection. *Cell Host Microbe*. doi:10.1016/j.chom.2011.08.010.

Su, R., Z. Li, H. Li, H. Song, C. Bao, J. Wei, and L. Cheng. 2010. Grp78 promotes the invasion of hepatocellular carcinoma. *BMC Cancer*. 10:20. doi:10.1186/1471-2407-10-20.

Suomalainen, M., S. Luisoni, K. Boucke, S. Bianchi, D.A. Engel, and U.F. Greber. 2013. A Direct and Versatile Assay Measuring Membrane Penetration of Adenovirus in Single Cells. *J. Virol.* doi:10.1128/jvi.01833-13.

Suomalainen, M., M.Y. Nakano, S. Keller, K. Boucke, R.P. Stidwill, and U.F. Greber. 1999. Microtubule-dependent plus- and minus end-directed motilities are competing processes for nuclear targeting of adenovirus. *J. Cell Biol.* 144:657–672. doi:10.1083/jcb.144.4.657.

Svoboda, P. 2014. Renaissance of mammalian endogenous RNAi. *FEBS Lett.* 588:2550–2556. doi:10.1016/j.febslet.2014.05.030.

T. Das, A., L. Tenenbaum, and B. Berkhout. 2016. Tet-On Systems For Doxycycline-inducible Gene Expression. *Curr. Gene Ther.* 16:156–167. doi:10.2174/1566523216666160524144041.

Takemura, H., A.R. Hughes, O. Thastrup, and J.W. Putney. 1989. Activation of calcium entry by the tumor promoter thapsigargin in parotid acinar cells. Evidence that an intracellular calcium pool, and not an inositol phosphate, regulates calcium fluxes at the plasma membrane. *J. Biol. Chem.* 264:12266–12271.

Tan, G., H. Kasuya, T.T. Sahin, K. Yamamura, Z. Wu, Y. Koide, Y. Hotta, T. Shikano, S. Yamada, A. Kanzaki, T. Fujii, H. Sugimoto, S. Nomoto, Y. Nishikawa, M. Tanaka, N. Tsurumaru, T. Kuwahara, S. Fukuda, T. Ichinose, T. Kikumori, S. Takeda, A. Nakao, and Y. Kodera. 2015. Combination therapy of oncolytic herpes simplex virus HF10 and bevacizumab against experimental model of human breast carcinoma xenograft. *Int. J. Cancer*. 136:1718–1730. doi:10.1002/ijc.29163.

Taverner, W.K., E.J. Jacobus, J. Christianson, B. Champion, A.W. Paton, J.C. Paton, W. Su, R. Cawood, L.W. Seymour, and J. Lei-Rossmann. 2019. Calcium influx caused by ER stress inducers enhances oncolytic adenovirus Enadenotucirev replication and killing through PKCα activation. *Mol. Ther. - Oncolytics*. doi:10.1016/J.OMTO.2019.09.003.

Thimmappaya, B., C. Weinberger, R.J. Schneider, and T. Shenk. 1982. Adenovirus VAI RNA is required for efficient translation of viral mRNAs at late times after infection. *Cell*. 31:543–551. doi:10.1016/0092-8674(82)90310-5.

Thorsteinsson, L., G.M. O'Dowd, P.M. Harrington, and P.M. Johnson. 1998. The complement regulatory proteins CD46 and CD59, but not CD55, are highly expressed by glandular epithelium of human breast and colorectal tumour tissues. *APMIS*. 106:869–78.

Tian, P., M.K. Estes, Y. Hu, J.M. Ball, C.Q. Zeng, and W.P. Schilling. 1995. The rotavirus nonstructural glycoprotein NSP4 mobilizes Ca2+ from the endoplasmic reticulum. *J. Virol.* 69:5763–72.

Tigges, M.A., and H.J. Raskas. 1984. Splice junctions in adenovirus 2 early region 4 mRNAs: Multiple splice sites produce 18 to 24 RNAs. *J. Virol.*

Tollefson, A.E., A. Scaria, T.W. Hermiston, J.S. Ryerse, L.J. Wold, and W.S. Wold.

1996. The adenovirus death protein (E3-11.6K) is required at very late stages of infection for efficient cell lysis and release of adenovirus from infected cells. *J. Virol.* 70:2296–306.

Treiman, M., C. Caspersen, and S.B. Christensen. 1998. A tool coming of age: Thapsigargin as an inhibitor of sarco-endoplasmic reticulum Ca2+-ATPases. *Trends Pharmacol. Sci.* 19:131–135. doi:10.1016/S0165-6147(98)01184-5.

Tseng, Y.Z.C.C., Y.L. Tsai, X. Fu, R. Schiff, and A.S. Lee. 2013. Cancer cells resistant to therapy promote cell surface relocalization of GRP78 which complexes with PI3K and enhances PI(3,4,5)P3 production. *PLoS One*. 8:e80071. doi:10.1371/journal.pone.0080071.

Twigger, K., V. Roulstone, J. Kyula, E.M. Karapanagiotou, K.N. Syrigos, R. Morgan, C. White, S. Bhide, G. Nuovo, M. Coffey, B. Thompson, A. Jebar, F. Errington, A.A. Melcher, R.G. Vile, H.S. Pandha, and K.J. Harrington. 2012. Reovirus exerts potent oncolytic effects in head and neck cancer cell lines that are independent of signalling in the EGFR pathway. *BMC Cancer*. 12. doi:10.1186/1471-2407-12-368.

Twumasi-Boateng, K., J.L. Pettigrew, Y.Y.E. Kwok, J.C. Bell, and B.H. Nelson. 2018. Oncolytic viruses as engineering platforms for combination immunotherapy. *Nat. Rev. Cancer*. 18:419–432. doi:10.1038/s41568-018-0009-4.

Uchida, H., H. Hamada, K. Nakano, H. Kwon, H. Tahara, J.B. Cohen, and J.C. Glorioso. 2018. Oncolytic Herpes Simplex Virus Vectors Fully Retargeted to Tumor-Associated Antigens. *Curr. Cancer Drug Targets*. 18:162–170. doi:10.2174/1568009617666170206105855.

Upton, J.P., L. Wang, D. Han, E.S. Wang, N.E. Huskey, L. Lim, M. Truitt, M.T. McManus, D. Ruggero, A. Goga, F.R. Papa, and S.A. Oakes. 2012. IRE1α cleaves

select microRNAs during ER stress to derepress translation of proapoptotic caspase-2. *Science (80-.).* 338:818–822. doi:10.1126/science.1226191.

Urra, H., E. Dufey, T. Avril, E. Chevet, and C. Hetz. 2016. Endoplasmic Reticulum Stress and the Hallmarks of Cancer. *Trends in Cancer*. 2:252–262. doi:10.1016/j.trecan.2016.03.007.

Valentine, R.C., and H.G. Pereira. 1965. Antigens and structure of the adenovirus. *J. Mol. Biol.* 13:13–20. doi:10.1016/S0022-2836(65)80076-6.

Vangheluwe, P., L. Raeymaekers, L. Dode, and F. Wuytack. 2005. Modulating sarco(endo)plasmic reticulum Ca2+ ATPase 2 (SERCA2) activity: Cell biological implications. *Cell Calcium*. 38:291–302. doi:10.1016/j.ceca.2005.06.033.

Vattem, K.M., and R.C. Wek. 2004. Reinitiation involving upstream ORFs regulates ATF4 mRNA translation in mammalian cells. *Proc. Natl. Acad. Sci. U. S. A.* 101:11269–11274. doi:10.1073/pnas.0400541101.

Vellinga, J., S. Van der Heijdt, and R.C. Hoeben. 2005. The adenovirus capsid: Major progress in minor proteins. *J. Gen. Virol.* doi:10.1099/vir.0.80877-0.

Wang, H., Z.Y. Li, Y. Liu, J. Persson, I. Beyer, T. Möller, D. Koyuncu, M.R. Drescher, R. Strauss, X.B. Zhang, J.K. Wahl, N. Urban, C. Drescher, A. Hemminki, P. Fender, and A. Lieber. 2011. Desmoglein 2 is a receptor for adenovirus serotypes 3, 7, 11 and 14. *Nat. Med.* 17:96–104. doi:10.1038/nm.2270.

Wang, M., and R.J. Kaufman. 2014. The impact of the endoplasmic reticulum protein-folding environment on cancer development. *Nat. Rev. Cancer*. doi:10.1038/nrc3800.

Wang, Y., G.N. Alam, Y. Ning, F. Visioli, Z. Dong, J.E. Nör, and P.J. Polverini. 2012.

The unfolded protein response induces the angiogenic switch in human tumor cells through the PERK/ATF4 pathway. *Cancer Res.* 72:5396–5406. doi:10.1158/0008-5472.CAN-12-0474.

Weerasinghe, P., and L.M. Buja. 2012. Oncosis: An important non-apoptotic mode of cell death. *Exp. Mol. Pathol.* 93:302–308. doi:10.1016/j.yexmp.2012.09.018.

Weichert, W., V. Gekeler, C. Denkert, M. Dietel, and S. Hauptmann. 2003. Protein kinase C isoform expression in ovarian carcinoma correlates with indicators of poor prognosis. *Int. J. Oncol.* doi:10.3892/ijo.23.3.633.

Weitzman, M.D. 2005. Functions of the adenovirus E4 proteins and their impact on viral vectors. *Front. Biosci.* 10:1106–1117. doi:10.2741/1604.

Wen-Sheng, W., and H. Jun-Ming. 2005. Activation of protein kinase C alpha is required for TPA-triggered ERK (MAPK) signaling and growth inhibition of human hepatoma cell HepG2. *J. Biomed. Sci.* doi:10.1007/s11373-005-1210-5.

Whyte, P., K.J. Buchkovich, J.M. Horowitz, S.H. Friend, M. Raybuck, R.A. Weinberg, and E. Harlow. 1988. Association between an oncogene and an anti-oncogene: the adenovirus E1A proteins bind to the retinoblastoma gene product. *Nature*. doi:10.1038/334124a0.

Wickham, T.J., E.J. Filardo, D.A. Cheresh, and G.R. Nemerow. 1994. Integrin αvβ5 selectively promotes adenovirus mediated cell membrane permeabilization. *J. Cell Biol.* 127:257–264. doi:10.1083/jcb.127.1.257.

Wiethoff, C.M., H. Wodrich, L. Gerace, and G.R. Nemerow. 2005. Adenovirus Protein VI Mediates Membrane Disruption following Capsid Disassembly. *J. Virol.* 79:1992–2000. doi:10.1128/jvi.79.4.1992-2000.2005.

Williams, B.R.G. 1999. PKR; A sentinel kinase for cellular stress. *Oncogene*. 18:6112–6120. doi:10.1038/sj.onc.1203127.

Wilson-Rawls, J., S.L. Deutscher, and W.S.M. Wold. 1994. The Signal-Anchor Domain of Adenovirus E3-6.7K, a Type III Integral Membrane Protein, Can Direct Adenovirus E3-gp19K, a Type I Integral Membrane Protein, into the Membrane of the Endoplasmic Reticulum. *Virology*. 201:66–76. doi:10.1006/viro.1994.1266.

Wold, W.S.M., and M.G. Ison. 2013. Adenovirus. *In* Fields Virology 6th Edition. Lippincott, Williams & Wilkins. 1732–1767.

Wold, W.S.M., and K. Toth. 2013. Adenovirus vectors for gene therapy, vaccination and cancer gene therapy. *Curr. Gene Ther.* 13:421–33.

Wong, H.H., G. Jiang, R. Gangeswaran, P. Wang, J. Wang, M. Yuan, H. Wang, V. Bhakta, H. Müller, N.R. Lemoine, and Y. Wang. 2012. Modification of the early gene enhancer-promoter improves the oncolytic potency of adenovirus 11. *Mol. Ther.* 20:306–316. doi:10.1038/mt.2011.242.

Workenhe, S.T., and K.L. Mossman. 2014. Oncolytic virotherapy and immunogenic cancer cell death: Sharpening the sword for improved cancer treatment strategies. *Mol. Ther.* 22:251–256. doi:10.1038/mt.2013.220.

Wu, W., J.L. Booth, K.M. Coggeshall, and J.P. Metcalf. 2006. Calcium-dependent viral internalization is required for adenovirus type 7 induction of IL-8 protein. *Virology*. 355:18–29. doi:10.1016/j.virol.2006.07.001.

Wunder, T., K. Schmid, D. Wicklein, P. Groitl, T. Dobner, T. Lange, M. Anders, and U. Schumacher. 2013. Expression of the coxsackie adenovirus receptor in neuroendocrine lung cancers and its implications for oncolytic adenoviral infection.

Cancer Gene Ther. 20:25–32. doi:10.1038/cgt.2012.80.

Xia, H., Q. Mao, H.L. Paulson, and B.L. Davidson. 2002. Sirna-mediated gene silencing in vitro and in vivo. *Nat. Biotechnol.* 20:1006–1010. doi:10.1038/nbt739.

Yadav, R.K., S.-W. Chae, H.-R. Kim, and H.J. Chae. 2014. Endoplasmic Reticulum Stress and Cancer. *J. Cancer Prev.* 19:75–88. doi:10.15430/JCP.2014.19.2.75.

Ye, J., R.B. Rawson, R. Komuro, X. Chen, U.P. Davé, R. Prywes, M.S. Brown, and J.L. Goldstein. 2000. ER stress induces cleavage of membrane-bound ATF6 by the same proteases that process SREBPs. *Mol. Cell*. 6:1355–1364. doi:10.1016/S1097-2765(00)00133-7.

Yoo, J.Y., B.S. Hurwitz, C. Bolyard, J.-G. Yu, J. Zhang, K. Selvendiran, K.S. Rath, S. He, Z. Bailey, D. Eaves, T.P. Cripe, D.S. Parris, M.A. Caligiuri, J. Yu, M. Old, and B. Kaur. 2014. Bortezomib-induced unfolded protein response increases oncolytic HSV-1 replication resulting in synergistic antitumor effects. *Clin. Cancer Res.* 20:3787–98. doi:10.1158/1078-0432.CCR-14-0553.

Yoo, J.Y., J.H. Kim, J. Kim, J.H. Huang, S.N. Zhang, Y.A. Kang, H. Kim, and C.O. Yun. 2008. Short hairpin RNA-expressing oncolytic adenovirus-mediated inhibition of IL-8: Effects on antiangiogenesis and tumor growth inhibition. *Gene Ther.* 15:635–651. doi:10.1038/gt.2008.3.

Yoo, J.Y., J.H. Kim, Y.G. Kwon, E.C. Kim, N.K. Kim, H.J. Choi, and C.O. Yun. 2007. VEGF-specific short hairpin RNA-expressing oncolytic adenovirus elicits potent inhibition of angiogenesis and tumor growth. *Mol. Ther.* doi:10.1038/sj.mt.6300023.

Yoshida, H., T. Matsui, A. Yamamoto, T. Okada, and K. Mori. 2001. XBP1 mRNA is induced by ATF6 and spliced by IRE1 in response to ER stress to produce a highly

active transcription factor. *Cell*. doi:10.1016/S0092-8674(01)00611-0.

Yousuf, M.A., J.S. Lee, X. Zhou, M. Ramke, J.Y. Lee, J. Chodosh, and J. Rajaiya. 2016. Protein Kinase C Signaling in Adenoviral Infection. *Biochemistry*. 55:5938–5946. doi:10.1021/acs.biochem.6b00858.

Yuan, L.W., and J.E. Gambee. 2000. Phosphorylation of p300 at serine 89 by protein kinase C. *J. Biol. Chem.* 275:40946–40951. doi:10.1074/jbc.M007832200.

Zeng, Y., X. Cai, and B.R. Cullen. 2005. Use of RNA polymerase II to transcribe artificial microRNAs. *Methods Enzymol.* 392:371–380. doi:10.1016/S0076-6879(04)92022-8.

Zhang, L., and A. Wang. 2012. Virus-induced ER stress and the unfolded protein response. *Front. Plant Sci.* doi:10.3389/fpls.2012.00293.

Zhang, Y., and J.M. Bergelson. 2005. Adenovirus Receptors. *J. Virol.* 79:12125–12131. doi:10.1128/jvi.79.19.12125-12131.2005.

Zhang, Y.A., J. Nemunaitis, S.K. Samuel, P. Chen, Y. Shen, and A.W. Tong. 2006. Antitumor activity of an oncolytic adenovirus-delivered oncogene small interfering RNA. *Cancer Res.* 66:9736–9743. doi:10.1158/0008-5472.CAN-06-1617.

Zhao, Y., H. Ogawa, S.I. Yonekura, H. Mitsuhashi, S. Mitsuhashi, I. Nishino, C. Toyoshima, and S. Ishiura. 2015. Functional analysis of SERCA1b, a highly expressed SERCA1 variant in myotonic dystrophy type 1 muscle. *Biochim. Biophys. Acta - Mol. Basis Dis.* 1852:2042–2047. doi:10.1016/j.bbadis.2015.07.006.

Zheng, X., X.-M. Rao, C. Snodgrass, M. Wang, Y. Dong, K.M. Mcmasters, and H.S. Zhou. 2005. Adenoviral E1a expression levels affect virus-selective replication in human cancer cells. *Cancer Biol. Ther.* 4:1255–1262. doi:10.4161/cbt.4.11.2137.

Zhou, Y., S. Xue, and J.J. Yang. 2013. Calcium and Viruses. *In* Encyclopedia of Metalloproteins. 415–424.

Zuker, M. 2003. Mfold web server for nucleic acid folding and hybridization prediction. *Nucleic Acids Res.* 31:3406–3415. doi:10.1093/nar/gkg595.

8 Appendices

8.1 *Materials*

TFB1: 30 mM KC2H3O2, 100 mM RbCl, 10 mM CaCl2·2H2O, 50 mM MnCl2·4H2O, 15% v/v glycerol. pH adjusted to 5.8 using 0.2 M acetic acid. In water, filter sterilised.

TFB2: 10 mM MOPS, 10 mM RbCl, 75 mM CaCl2·2H2O, 15% v/v glycerol. pH adjusted to 6.6 using 5 M KOH. In water, filter sterilised.

TAE: 1 mM EDTA, 40 mM Tris-Acetate.

CsCl ρ = 1.32 - 32.0g CsCl, 6.8 mL of 0.5 M Tris-HCl, pH 7.9, 61.2 mL distilled water.

CsCl ρ = 1.45 - 20.5g CsCl, 2.9 mL 0.5 M Tris-HCl, pH 7.2, 28.5 mL distilled water.

40% glycerol: 40 g glycerol, 2 mL of 0.5 M Tris-HCl pH 7.9, 0.5 mL of 0.2 M EDTA pH 8.0, made up to 100 mL distilled water.

Running buffer: 25 mM Tris base, 190 mM glycinem 0.1% SDS, pH adjusted to 8.3

Transfer buffer: 25 mM Tris base, 190 mM glycine, 10% methanol, pH adjusted to 8.3

MACS buffer: In PBS, 0.5% BSA and 2 mM EDTA.

8.2 *Recombinant adenovirus*

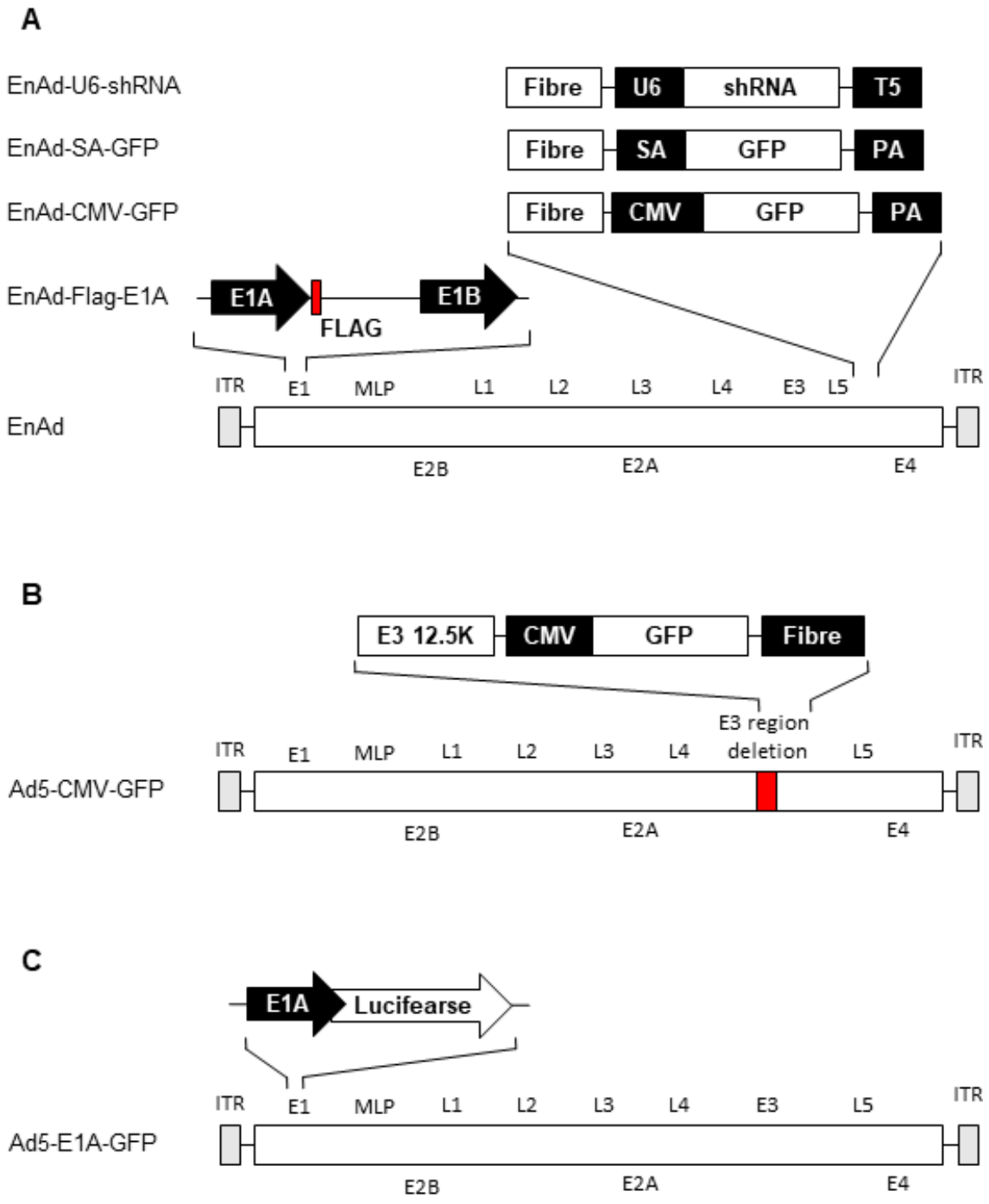


Figure 8.1. Recombinant adenoviral genomes are represented schematically.

Table 8.1 recombinant viruses used in this thesis

Recombinant Virus	Parental virus	Insertion	Insertion site	Deletion
EnAd-U6-NT	EnAd	Non target shRNA driven by U6 promoter	Between the fibre sequence and the E4 transcription unit	None
EnAd-U6-s1748	EnAd	Anti-SERCA shRNA driven by U6 promoter	Between the fibre sequence and the E4 transcription unit	None
EnAd-SA-GFP	EnAd	GFP coding sequence downstream of splice acceptor sequence	Between the fibre sequence and the E4 transcription unit	None
EnAd-CMV-GFP	EnAd	GFP coding sequence driven by CMV promoter	Between the fibre sequence and the E4 transcription unit	None
EnAd-FLAG-E1A	EnAd	E1A replaced with Flag tagged E1A sequence	E1A	None
Ad5-CMV-GFP	Ad5	GFP coding sequence driven by CMV promoter	Downstream of the E3 12.5K ORF	Deletion of E3 ORFs, only 12.5K ORF remaining
Ad5-E1A-Luc	Ad5	E1A protein coding sequence replaced with E1A-luciferase fusion protein		None

8.3 *DNA sequences*

U6 promoter sequence:

GAGGGCCTATTTCCCATGATTCCTTCATATTTGCATATACGATACAAGGCTG

TTAGAGAGATAATTGGAATTAATTTGACTGTAAACACAAAGATATTAGTAC

AAAATACGTGACGTAGAAAGTAATAATTTCTTGGGTAGTTTGCAGTTTTAAA

ATTATGTTTTAAAATGGACTATCATATGCTTACCGTAACTTGAAAGTATTTC

GATTTCTTGGCTTTATATATCTTGTGGAAAGGACGAAACACCGGAA

shRNA s1748:

CAACTGGAGTTAACACCGATTCCACACCAATCGGTGTTAACTCCAGTTGTTT

TT

shRNA NT:

AATCCTAAGGTTAAGTCGCCCTCGCTCGAGCGAGGGCGACTTAACCTTAGG

ATTTTT